QUEEN MARY UNIVERSITY OF LONDON

PHD THESIS

THESIS SUBMITTED IN PARTIAL FULFILMENT OF THE REQUIREMENTS FOR THE DEGREE OF DOCTOR OF PHILOSOPHY

THE EFFECT OF SOCIAL ISOLATION ON THE IMMUNE SYSTEM

ALICE LAURA HAMILTON

CENTRE FOR BIOCHEMICAL PHARMACOLOGY,

WILLIAM HARVEY RESEARCH INSTITUTE,

BARTS AND THE LONDON SCHOOL OF MEDICINE AND DENTISTRY,

QUEEN MARY UNIVERSITY OF LONDON

Statement of Originality

I, Alice Laura Hamilton, confirm that the research included within this thesis is my own work or that where it has been carried out in collaboration with, or supported by others, that this is duly acknowledged below, and my contribution indicated. Previously published material is also acknowledged below.

I attest that I have exercised reasonable care to ensure that the work is original and does not to the best of my knowledge break any UK law, infringe any third party's copyright or other Intellectual Property Right, or contain any confidential material.

I accept that the College has the right to use plagiarism detection software to check the electronic version of the thesis.

I confirm that this thesis has not been previously submitted for the award of a degree by this or any other university.

Signature:

Date: 03.09.19

Collaborations and Publications

Collaborations

Raffaella Rizzo and Dr Samuel Brod did the RNA extraction from whole blood for the microarray. The initial microarray service was undertaken by Dr Mark Kristiansen (Genomics Facility, Department of Child Health, University College London) with data analysis being carried out by Dr Masahiro Ono (Faculty of Natural Sciences, Department of Life Sciences, Imperial College London).

The primers used for the initial testing of the bacteria within the faeces were kindly donated by Dr Ezra Aksoy (Biochemical Pharmacology, William Harvey Research Institute, Queen Mary University of London). The next generation sequencing and subsequent analysis of the faecal microbiota was carried out by Dr Adele Costabile (Health Sciences Research Centre, University of Roehampton).

Professor Qingzhong Xiao (Clinical Pharmacology, William Harvey Research Institute, Queen Mary University of London) provided the initial *ApoE*$^{-/-}$ breeders and gave advice both on experimental design and breeding of the mice. Dr Pasquale Maffia and Lucy McShane (Institute of Infection, Immunity and Inflammation, University of Glasgow) gave expertise on experimental design of the atherosclerosis experiments and carried out quantification of the plaque in the aortic sinus.

Publications

Pietro Ghezzi, Luciano Floridi, Diana Boraschi, Antonio Cuadrado, Gina Manda, Snezana Levic, Fulvio D'Acquisto, **Alice Hamilton**, Toby J. Athersuch, and Liza Selley. Oxidative Stress and Inflammation Induced by Environmental and Psychological Stressors: A Biomarker Perspective. *Antioxidant and Redox Signalling.* **28**, (2017).

Acknowledgements

I would like to thank the British Heart Foundation for the funding throughout the duration of my 4-year doctoral training program for without this, all that follows would not be possible.

I would like to express my gratitude and heartfelt indebtedness to my supervisor, Professor Fulvio D'Acquisto, for his ceaseless guidance, expertise, insights and training, as well as for the freedom to take this project in the directions I wished. Beyond the project, I would like to thank him for his support and encouragement and for sparking in me the love of research and science that is needed for this career. Next, I would like to thank Dr Dianne Cooper for her excellent supervision, endless encouragement and positivity throughout my PhD. I am also thankful to Professor Mauro Perretti and Dr Lucy Norling for both adopting and welcoming me into their research groups as well as imparting their expertise and knowledge on to me. I would also like to express my gratitude to Dr Maffia, University of Glasgow, for all his guidance and advice on my atherosclerosis experiments and for giving me the opportunity to visit his laboratory in order to learn new techniques. Thank you, to Dr Samuel Brod for his guidance with initial experiments and for mentoring me and answering all my questions even after he left the lab.

Thank you to all of Biochemical Pharmacology, particularly those in the Cooper-Norling group, and all those on the British Heart Foundation 4-year doctoral training programme at the WHRI for being so welcoming, supportive, encouraging and for all the fun times. Whilst I have made many friendships over my PhD, I would particularly like to thank Sarah Turner, Kelly Woods, Vivek Maharaj and Kama Zion for their endless support, encouragement, banter and true friendship.

I would like to thank my father, John Hamilton, for allowing me the freedom to choose my own path and for all the encouragement, without this I would have given up a long time ago. Thank you to my brother, Colin Hamilton, for understanding how hard PhDs can be and for all the advice and support. Finally, I am grateful to my Grandad, Dr Samuel Lyle, for inspiring me to pursue a career in science and for answering my questions ever since.

In Memory of my Mother

Helen Hamilton

who always encouraged me to be the best scientist I could be.

Abstract

A person's social network size and quality of life can affect the body at three levels: behavioural, psychological and physiological. A socially isolated person is more likely to have a poor diet, suffer from depression and have increased blood pressure, all of which are risk factors for chronic inflammatory diseases. This thesis aimed to understand how social isolation affects the immune system in the acute inflammatory setting, sepsis, and in the chronic inflammatory setting, atherosclerosis.

CD-1 mice subjected to 2 weeks of social isolation had increased food intake without increased weight gain, a finding that was accompanied by an increased number of smaller adipocytes suggesting socially isolated mice have increased thermogenesis to maintain body temperature. Social isolation profoundly altered the microbiota to one that is pro-inflammatory. Microarray analysis of whole blood revealed a unique transcriptional fingerprint for social isolation.

After 2 weeks of social isolation, mice were given *E.coli* induced sepsis and found to have enhanced bacterial clearance. Toll-like receptor signalling pathways in peritoneal macrophages revealed that genes involved in fighting bacterial infections were upregulated. Social isolation was neither beneficial nor detrimental during viral sepsis.

ApoE$^{-/-}$ mice underwent social isolation for a 4-week period. Mice subjected to social isolation maintained a consistent calorie intake both on the Western diet and standard diet whilst socially housed mice increased their calorie intake on the Western diet probably as a result of leptin resistance. Social isolation did not increase atherosclerotic burden but increased necrosis in the atherosclerotic plaque suggesting that social isolation might increase risk of plaque rupture.

This thesis demonstrated for the first time that just 2-4 weeks of social isolation causes profound immunological and metabolic changes in the body which might account in part for the increased risk of chronic inflammatory diseases seen in socially isolated people.

Abbreviations List

AC	Adenylate cyclase
AgRP	Agouti-related peptide
ALT	Alanine aminotransferase
ApoE	Apolipoprotein E
ARC	Arcuate nucleus
AST	Alanine transaminase
Bach2	BTB Domain and CNC Homolog 2
BAT	Brown adipose tissue
BMI	Body mass index
cAMP	Cyclic adenosine monophosphate
CCL	Chemokine ligand
CD	Cluster of differentiation
CD55	Complement decay accelerating factor 55
cDNA	Complimentary DNA
CFU	Colony forming unit
CLP	Cecal ligation puncture
CRP	C-reactive protein
Csf2	Colony stimulating factor 2
Ctla2b	Cytotoxic T lymphocyte-associated protein 2β
CTRA	Conserved transcriptional response to adversity
CVD	Cardiovascular disease
CXCL	Chemokine c-x-c motif legend
DAMPs	Danger associated molecular pathogens

DC	Dendritic cell
Dennd5b	DENN domain containing 5B
DNA	Deoxyribonucleic acid
Dnah8	Dynein axonemal heavy chain 8
E.coli	*Escherichia coli*
EDTA	Ethylenediaminetetraacetic acid
EE	Environmentally enriched
ELISA	Enzyme linked substrate assay
EPICII	The Extended Prevalence in Infection in Intensive Care Study II
ETC	Electron transport chain
FACS	Fluorescence-activated cell sorting
FFA	Free fatty acid
FH	Familial hypercholesterolemia
GABA	Gamma-aminobutyric acid
GAPDH	Glyceraldehyde 3-phosphate dehydrogenase
Gdpd3	Glycerophosphodiester Phosphodiesterase Domain Containing 3
GF	Germ free
Glb1	Galactosidase beta 1
Gm6445	Predicted gene 6445
Gm6793	Predicted gene 6793
H & E	Haematoxylin and eosin
Hist1h2bg	Histone cluster 1 h2b family member g
Hist1h2bc	Histone H2B type 1 c
Hist1h4k	Histone H4 type 1 k
Hist1h2bf	Histone H2B type 1 F

HLA	Human leukocyte antigen
HRP	Horse radish peroxidase
IBD	Inflammatory Bowel Disease
ICAM-1	Intracellular adhesion molecule-1
ICU	Intensive care unit
Ifi214	Interferon activated gene 214 protein
IFN	Interferon
Ig	Immunoglobulin
Igkv10-96	Immunoglobulin kappa variable 10-96
IKK	Inhibitor of nuclear factor kappa-B kinase
IL	Interleukin
I.p.	Intraperitoneal
IRAK	Interleukin-1 receptor-associated kinase
IRF	Interferon regulatory factor
KC	Keratinocyte-derived chemokine
Laptm4b	Lysosomal transmembrane protein 4β
LB	Lysogeny broth
LDL	Low density lipoprotein
Ldlr	Low density lipoprotein receptor
Lepr-b	Leptin receptor long form
LFA-1	Lymphocyte function-associated antigen-1
Lpgat1	Lysophosphatidylglycerol acyltransferase 1
LPM	Large peritoneal macrophage
LPS	Lipopolysaccharide

M1	Classically activated macrophages
M2	Alternatively activated macrophages
MCP-1	Monocyte chemoattractant protein-1
M-CSF	Macrophage colony-stimulating factor
MetS	Metabolic syndrome
MFI	Mean fluorescence intensity
MHCII	Major histocompatibility complex class II
MI	Myocardial infarction
Mir467e	MicroRNA 467e
Mir512	MicroRNA 512
Mir5104	MicroRNA 5104
MMP	Matrix metalloproteinase
mRNA	Messenger ribonucleic acid
MyD88	Myeloid differentiation primary response 88
NE	Norepinephrine
NETs	Neutrophil extracellular traps
NFκB	Nuclear factor kappa-light-chain-enhancer of activated B cells
NGS	Next generation sequencing
NK	Natural killer
NLR	Neutrophil:lymphocyte ratio
NLRs	Nucleotide-binding oligomerisation domain receptors
NO	Nitric oxide
NOD	Nucleotide binding oligomerization domain containing 2
NOS2	Nitric oxide synthase 2
NPY	Neuropeptide Y

OAS	Oligoadenylate synthetase
OCT	Optimum cutting temperature
OR	Odds ratio
oxLDL	Oxidised low-density lipoprotein
PAD	Peripheral artery disease
PAMPS	Pattern associated molecular pathogens
PAR1	Protease-activated receptor 1
PBS	Phosphate buffer saline
PCoA	Principal coordinates analysis
PCR	Polymerase chain reaction
PECAM-1	Platelet endothelial cell adhesion molecule-1
PFA	Paraformaldehyde
PKA	Protein kinase A
PLF	Peritoneal lavage fluid
Poly (I:C)	Polyinosinic-polycytidylic acid
PRRs	Pathogen recognition receptors
PSI	Perceived social isolation
PTSD	Post-traumatic stress disorder
qSOFA	Quick sepsis-related organ failure assessment
RA	Rheumatoid Arthritis
Rab	Ras-related protein
Rhoj	Ras homolog j
RNA	Ribonucleic acid
Rnu37b	U73B small nuclear RNA
ROS	Reactive oxygen species

RT-PCR	Real time polymerase chain reaction
SAPSII	Simplified acute physiology score II
SBP	Systolic blood pressure
Sclc30a4	Solute carrier family 30 member 4
SH	Socially housed
SI	Socially isolated
Slamf1	Signalling lymphocytic activation molecule 1
SMC	Smooth muscle cell
Snord93	Small nucleolar RNA, C/D box 93
SNS	Sympathetic nervous system
SOCS3	Suppressor of cytokine signalling 3
SPF	Specific pathogen free
T2D	Type 2 diabetes
TAK1	Transforming growth factor beta-activated kinase 1
TBK1	TANK-binding kinase 1
TBS	Tris-buffer saline
TCR	T cell receptor
Th	T helper
TIRAP	TIR Domain Containing Adaptor Protein
TLRs	Toll-like receptors
TNF	Tumour necrosis factor
TRAF6	Tumour necrosis factor receptor associated factor 6
TRAM	Trif-related adaptor molecule
T_{reg}	Regulatory T cells

TRIF	TIR-domain adaptor inducing interferon-β
UCLA	University of California, Los Angles
UCP-1	Uncoupling protein-1
VAT	Visceral adipose tissue
VCAM-1	Vascular cell adhesion molecule-1
VLDL	Very low-density lipoprotein
WAT	White adipose tissue
WT	Wild type
Xaf1	XIAP associated factor 1
Zfp729a	Zinc finger protein 729a
Zfp992	Zinc finger protein 992

TABLE OF CONTENTS

TABLE OF FIGURES

TABLE OF TABLES

Chapter 1

Introduction

1.1 The Vascular and the Immune System: Generalities and Key Players

The inflammatory response that follows infection begins when pathogen associated molecular patterns (PAMPS), conserved structures in pathogens e.g. lipopolysaccharide (LPS), are recognised by pathogen recognition receptors (PRRs) such as toll-like receptors (TLRs) and nucleotide-binding oligomerisation domain receptors (NLRs). Activation of TLRs and NLRs leads to the activation of the nuclear factor kappa-light-chain-enhancer of activated B cells (NFκB) pathway which promotes the release of the pro-inflammatory mediators such as tumour necrosis factor (TNF)-α and interleukin (IL)-1β. These pro-inflammatory molecules cause damage to the endothelium resulting in the release of danger associated molecular patterns (DAMPs), which interact with PRRs to cause further inflammation. The goal of this response is to deliver leukocytes to the site of infection[1].

Leukocytes, primarily neutrophils, can undergo extravasation to allow them to home to inflamed tissues from the postcapillary venules. During inflammation, P-selectin and E-selectin are induced on the surface of the endothelial cells by inflammatory mediators including histamine and TNF-α. The selectins can then transiently interact with sialyl $Lewis^X$ on the leukocytes in a process known as rolling. Intracellular adhesion molecule-1 (ICAM-1), is induced on the endothelial cell surface by inflammatory mediators such as TNF-α and IL-1β[2]. During tight binding ICAM-1 binds leukocytes *via* interactions with the integrin lymphocyte function-associated antigen-1 (LFA-1) and macrophage-1 antigen thus immobilising the leukocyte[3]. Prior to transmigration of the leukocyte across

the endothelial cell layer, it must re-arrange its cytoskeleton allowing it to spread out across the endothelial cells and extend its pseudopodia into the gaps between endothelial cells[2,4]. Transmigration can then occur by interactions with several adhesion molecules including platelet endothelial cell adhesion molecule-1 (PECAM-1), which effectively push the leukocyte through the endothelial cell wall[5]. Leukocytes are then homed to the site of infection by a chemoattractant gradient[2]. This process is summarised in **Figure 1.1**[6].

When the immune response does not resolve then chronic inflammation occurs, which is a more adaptive mediated response such as that seen in atherosclerosis. During chronic inflammation, prolonged activation of the endothelial cells causes the release of reactive oxygen species (ROS), which cause further injury to both the endothelium and smooth muscle cells (SMCs), as well as promoting clotting[7,8]. This leads to endothelial dysfunction as a result of injury to the endothelium and this is where the endothelium of the artery produces less endothelium derived relaxation factors such as nitric oxide (NO), whilst increasing the production of endothelium derived contraction factors such as endothelin[9,10]. Increased pro-inflammatory cytokines such as TNF-α and IL-1 are produced at this stage causing increased permeability of the vasculature[11]. Endothelial dysfunction results in the upregulation of adhesion molecules such as ICAM-1, vascular cellular adhesion molecule-1 (VCAM-1) and E-selectin, which cause the recruitment of immune cells thus promoting further inflammation[12]. The scavenger receptors found on macrophages allow for the uptake of the antigens and presentation of them to T cells *via* major histocompatibility complex II (MHCII) receptor on macrophages and the T cell receptor upon the T cells[13]. For example, scavenger receptor A-I can detect modified lipoproteins, both gram-positive and gram-negative bacteria and apoptotic cells[14]. The majority of T cells will differentiate into T helper (Th)1 cells, which secrete interferon

(IFN)-γ and TNF-α which can cause macrophages to become classically activated (M1). M1 macrophages further contribute to the damage of the vessel wall by releasing more pro-inflammatory cytokines. Less commonly, the T cells may differentiate into Th2 cells, which release the cytokines IL-4 and IL-13 causing macrophages to become polarised into alternatively activated macrophages (M2). This bias towards M1 macrophage production contributes to a highly pro-inflammatory environment[13].

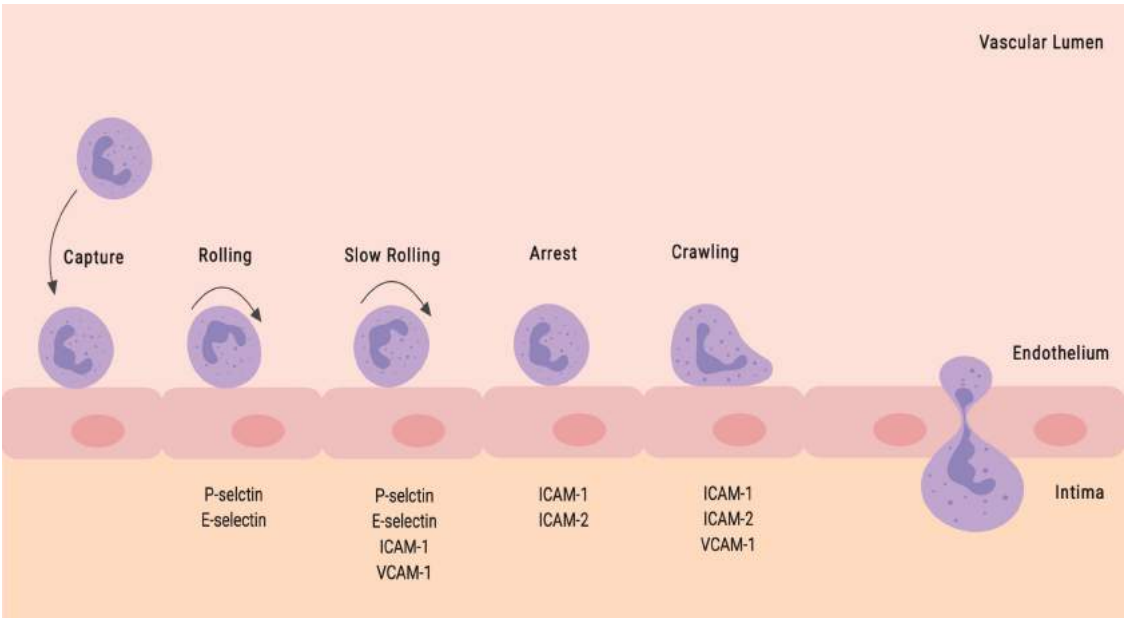

Figure 1.1: Summary of Leukocyte Extravasation. Pro-inflammatory stimuli trigger leukocyte adhesion to the endothelium by inducing adhesion molecules such as E-selectin on the endothelium. Transient interactions between the leukocyte and the endothelium occur during the rolling phase. Chemokines induce intergrins on the cell surface of the leukocytes. The leukocyte undergoes arrest where the leukocyte stops rolling due to interactions with integrins on the endothelium. Prior to transmigration the leukocyte undergoes crawling and begins to rearrange its cytoskeleton for migration through the endothelium allowing the pseudopodia to extend into the endothelial cells. Interactions with adhesion molecules allow for the transmigration of the leukocyte through the endothelial cell wall. Image created on Biorender.

1.2 Sepsis: The Uncontrolled Acute Inflammatory Response

Sepsis is the leading cause of deaths in intensive care units (ICU)s worldwide and is defined according to the Third International Consensus Sepsis-3 as 'a life-threatening organ dysfunction due to a dysregulated host response to infection'[15]. The quick sepsis-related organ failure assessment (qSOFA) score is used by clinicians to assess whether a patient might be suffering from sepsis (**Table 1**). A score of greater than 2 on the qSOFA should prompt investigation for infection and this is indicative of poor outcome and prolonged ICU stays[15]. In the United Kingdom, 100,000 people will suffer from sepsis each year with 44,000 of those dying[16]. Very little is known about why some patients survive sepsis and others do not, with clinical trials in this field consistently failing[17].

Table 1: qSOFA Diagnostic Criteria for Sepsis-Related Organ Dysfunction.

Symptom	Criteria
Respiratory rate	≥22 breaths/minute
Systolic blood pressure (SBP)	≤100 mmHg
Altered mental status	Glasgow coma scale <15

1.2.1 Aetiology

The most common cause of sepsis is from a respiratory tract infection with this accounting for about 60% of all patients. Other less common sites of infection include the abdomen (20%), bloodstream (15%) and the renal/genitourinary system (14%)[18]. According to the Extended Prevalence of Infection and Intensive Care Study II (EPICII), about 70% of all sepsis patients will test positive for microbiology with the majority of these being accounted for by gram-negative (gram -) bacteria (62%). Other less common causes include gram-positive (gram +) bacteria (47%) and fungal infections (19%). In Europe, the most common gram-positive bacteria is *Staphylococcus aureus* (20%) and

the two main gram-negative organisms found are *Pseudomonas* species (17%) and *Escherichia coli* (*E.coli,* 17%)[18]. *Pseudomonas* species has been shown to be independently associated with increased mortality rates[19].

1.2.2 Epidemiology

Incidence of sepsis has a bimodal age distribution with the highest incidence of mortality being in infants and the elderly with risk beginning to increase after 50-60 years of age[20]. Women are less likely to develop sepsis and to be admitted to the ICU than men with some studies suggesting better prognosis in women[21–23]. One study looking at risk of sepsis after pneumonia, found that this disparity in survival may in part be due to elevated pro-inflammatory cytokines and lower levels of coagulation factors in men. The same study found in females that higher levels of anti-inflammatory cytokines were correlated with better prognosis[24]. Genetic variations can affect a person's susceptibility to certain types of infection and thus sepsis, with the most robust variations being found in TLR4 and TNF-β. One such mutation is *TLR4* Asp299Gly allele which was found to be about 45% more prevalent in patients who had gram-negative bacterial infections[25]. Studies have identified that *TNF-β252A* variations were associated with increased susceptibility to shock and increased TNF-β serum levels. It is thought that this variant might be found in as many as 65% of non-survivors[26,27].

1.2.3 Pathophysiology

Sepsis is characterised by a dysregulated response of the immune system, initially by a pro-inflammatory response and later by an anti-inflammatory phase. Patients that die during the first 72 hours, the initial inflammatory phase, die as a result of multiple organ failure, whilst those that die after this time die as a result of secondary infections[1,28].

The initial pro-inflammatory stages of sepsis involve the activation of TLRs and NLRs thus promoting inflammation. DAMPs interact with PRRs to cause further inflammation[1]. During bacterial infection one of the main TLRs, TLR4 can become activated upon detection of PAMPs such as LPS. Upon activation, TLR4 can either signal in a myeloid differentiation primary response 88 (MyD88)-dependent or MyD88 independent manner to launch an in immune response (**Figure 1.2**). The MyD88-dependent pathway is primarily involved in the early NF-κB response, which involves the production of pro-inflammatory cytokines including TNF-α, IL-6 and IL-1β[29]. Conversely, the MyD88-independent pathway signals *via* TRIF-related adaptor molecule (TRAM) and TIR-domain containing adaptor inducing interferon-β (TRIF) to cause the late NF-κB response, which leads to the production of type 1 IFNs and chemokines including chemokine (c-x-c) motif ligand (CXCL)10[30]. It is thought that oscillating TNF-α may be responsible for inducing the late NF-κB response[31]. IL-6, IL-1β and TNF-α cytokines peak around 2 hours after LPS stimulation as an early response to infection, whereas IFNs peak later around 6-8 hours[32,33].

When infection is detected, both leukocytes and platelets adhere to the endothelial surface and the leukocytes then migrate to the site of infection[1]. Protease-activated receptor 1 (PAR1) interacts with both thrombin and matrix metalloproteinase (MMP)1 to damage the stability of the endothelial wall, which can lead to tissue oedema as well as reduced microvascular perfusion. The activated endothelium contributes to the release of pro-inflammatory mediators[34]. Additionally, PAMPS such as LPS can induce macrophages to upregulate tissue factor which in turn leads to upregulation of fibrinogen and factor V, thus promoting coagulation. This can lead to disseminated intravascular coagulation[35]. Vascular inflammation and coagulation promote neutrophils to release

neutrophil extracellular traps (NETs), which can capture pathogens. However, the presence of NETs can be detrimental as they act as a scaffold for platelet aggregation and entrapment, once again promoting hypercoagulation[36]. Thus, it is not surprising that high levels of NETs have been associated with organ dysfunction[37].

It has been documented that during the later stages of sepsis, patients have an anti-inflammatory response where lymphocytes have been shown to fail to produce cytokines[38]. Macrophages, neutrophils and dendritic cells (DCs) are all known to undergo increased apoptosis during sepsis, which may account in part for the failure of adequate cytokine function[39]. Cluster of differentiation (CD)4^+ and $CD8^+$ T cells were also found to be depleted in the spleens from ICU sepsis patients, with $CD4^+$ numbers primarily being low as a result of apoptosis[40]. Sepsis patients have also been shown to have increased proportions of regulatory T (T_{reg}) cells, which inhibit monocyte, neutrophil and effector T cell function leading to further immunosuppressive effects[41]. DCs, monocytes and macrophages in this stage are characterised by reduced expression of human leukocyte antigen (HLA)-DR. This reduction in HLA-DR results in DCs releasing increased IL-10, whilst the monocytes and macrophages undergo immunoparalysis whereby they have reduced capacity to release pro-inflammatory cytokines upon stimulation[42]. Epigenetic changes can also occur, for example, activation of oxidative phosphorylation during the pro-inflammatory stage of sepsis can cause a decrease in intracellular levels of acetyl coenzyme A, which results in less histone acetylation leading to inhibition of gene transcription and immunoparalysis[43]. It is during the anti-inflammatory phase of sepsis that viruses such as cytomegalovirus viremia and herpes simplex virus are reactivated, and there is evidence that the reactivation of cytomegalovirus viremia is in fact predictive of fungal infection and thus 90 day mortality[44]. The presence of lymphopenia four days post-diagnosis is linked to secondary

bacterial infections and thus predicts both 28 day and 1 year mortality[45]. Interestingly, patients who have high levels of IL-6 at discharge have increased risk of diseases such as cancer and cardiovascular disease (CVD), as well as repeated infections[46].

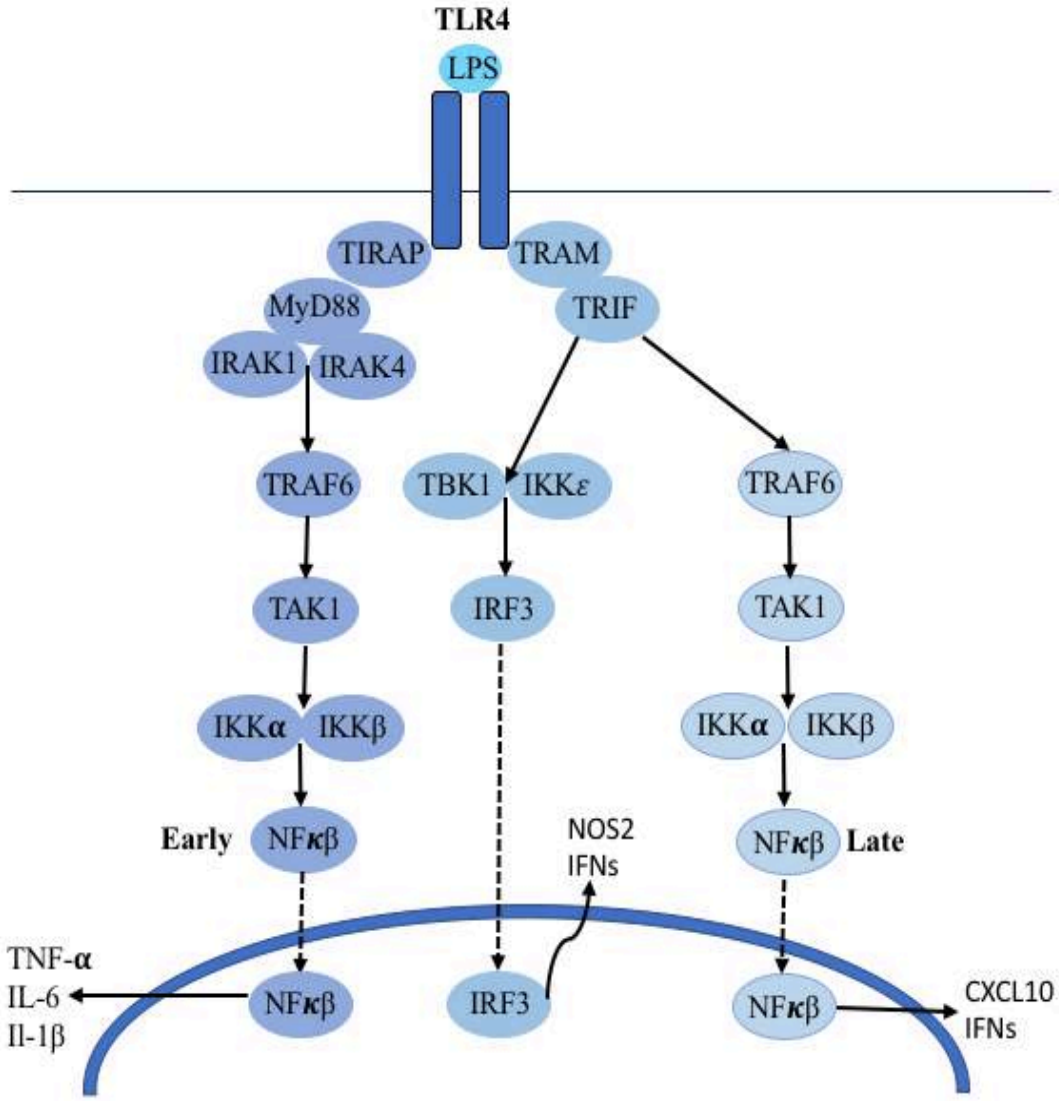

Figure 1.2: The Early and Late NFκB Response During TLR4 Activation. Upon activation by LPS, TLR4 can signal either through the MyD88 pathway to induce the early NFκB response (left pathway) or through TRAM and TRIF (right pathway) to induce the late NFκB response. Activation of the early NFκB response causes pro-inflammatory cytokines such as TNF-α, IL-6 and IL-1β to be produced. Activation of the late NFκB response causes the production of CXCL10 and IFNs. The TRAM-TRIF pathway can also cause IRF3 to translocate to the nucleus and cause the transcription of NOS2 and IFNs. See abbreviations list for all abbreviations used in this figure.

1.3 Atherosclerosis: The Chronic Vascular Inflammatory State

CVD is the most common cause of premature death worldwide accounting for an estimated 17.7 million deaths worldwide every year[47]. Atherosclerosis is a disease that affects both the large and medium arteries and is characterised by the presence of the following:

1. Endothelial dysfunction
2. Accumulation of lipid, cholesterol and calcium in the intima of the artery
3. Vascular inflammation which leads to the formation of plaque in the vasculature.

If the plaque ruptures, it can lead to either an acute myocardial infarction (MI) or a stroke, depending on whether the coronary artery or the carotid artery respectively[48].

1.3.1 Aetiology

Atherosclerosis is considered to have a complex aetiology comprised of genetic, non-modifiable, and environmental, modifiable, risk factors. One such non-modifiable risk factor is gender as CVD tends to present earlier in men than in women, with men <60 years old having a greater than 4-fold higher risk of MI or unheralded coronary heart disease[49]. Another genetic factor is familial hypercholesterolemia (FH) is estimated to affect as many as 34 million people worldwide. Sufferers exhibit abnormally high levels of low density lipoprotein (LDL) as they cannot clear LDL due to genetic mutations being found in the low density lipoprotein receptor (LDLR). This puts them at increased risk of developing premature atherosclerosis and CVD[50]. One study found that 93% of the patients in the study with FH had established CVD and 69% of all patients at time of death had suffered from a MI[51].

The American Heart Association identifies 7 key modifiable factors known as 'Life's Simple 7' to reduce risk of CVD: blood pressure, physical activity, weight, diet, cholesterol, smoking status and blood glucose. It is interesting to note for the specific focus of this thesis, that most of the modifiable factors here listed are often summarised under 'changes in lifestyle'[52]. Even more strikingly, lifestyle has been often linked to social and economic status, thus providing a further dimension to the complex scenario that contributes to CVD[53].

An ideal blood pressure to prevent CVD is considered to be ≤120/80 mmHg[54]. Hypertension, blood pressure ≥140/90 mmHg, is thought to be responsible for around 45% of all CVD related deaths and 51% of deaths from strokes[55]. To reduce the risk of CVD a person should aim to do around 150 minutes of moderate or 75 minutes of vigorous exercise per week[54]. Studies have shown that there is an inverse graded association between physical activity and coronary heart disease, with men who have >23 hours per week of sedentary lifestyle behaviours having 64% greater chance of dying from CVD[56,57]. Similarly, being obese, body mass index (BMI) >30kg/m^2, has been shown in the Framingham heart study to increase the risk of CVD by about 2-fold, whilst a BMI of 25kg/m^2 is considered to be ideal for reducing the risk of CVD[54,58]. Non-surprisingly, having a diet that promotes obesity i.e. one high in fat, sugar and salt promotes CVD whilst the Mediterranean diet has been shown to be inversely related to CVD[59]. There is a positive correlation between increasing serum cholesterol and CVD with ideal cholesterol levels being <170 mg/dl[54,60]. Smoking is estimated to cause 140,000 premature deaths each year in the United States from CVD but this risk can be attenuated by never smoking or having quit smoking for 12 months[54,61]. Fasting glucose levels are positively correlated with risk of atherosclerosis related CVD[62]. Therefore, it is not surprising that people who suffer from type 2 diabetes (T2D) are 2x more likely to

have a MI than those who have normal glucose levels, with ideal glucose levels being below 100mg/dl[54,63].

1.3.2 Pathophysiology

The first stage of atherosclerosis begins with endothelial dysfunction which is the result of chronic inflammation and oxidative stress[8,64]. LPS derived from *E.coli* has been shown to be proatherogenic in animal studies and is localised in human atherosclerotic plaque, suggesting it can act *via* TLR4 to promote endothelial dysfunction by exacerbating inflammation and oxidative stress[65,66]. During this stage, the vasculature becomes more permeable and more prone to clotting[7,8,11]. Adhesion molecules, promoting leukocyte recruitment are upregulated with ICAM-1 and VCAM-1 levels having been shown to be correlated to intima-medial thickness, a biomarker of atherosclerosis, in T2D patients[12]

As the endothelial cells become increasingly more permeable as a result of ROS injury, LDL begins to enter into the intima of the artery where it binds to proteoglycans in the extracellular matrix, thus trapping it[67]. The ROS released during endothelial dysfunction and from the resident tissue macrophages can oxidise the LDL forming oxidised-LDL (oxLDL),which further exacerbates the pro-inflammatory environment by promoting the release of pro-inflammatory cytokines from the endothelium and SMCs[68]. Vascular segments with disturbed oscillatory flow, such as that seen in artery bifurcations, which are sites prone to atherogenesis, have upregulated levels of VCAM-1 allowing monocytes to bind to the endothelium[69]. The presence of pro-inflammatory cytokines results in the endothelium upregulating adhesion molecules thus allowing monocytes and to a lesser extent T cells to bind to the endothelium of the vessel[70].

Once the monocytes enter into the intima of the artery, they are stimulated by macrophage colony- simulation factor (M-CSF) which is released from both the

endothelial and SMCs. M-CSF promotes the differentiation of monocytes into macrophages and the upregulation of scavenger receptors on their surface[71]. Foam cells are formed when the macrophages have taken up so much oxLDL that they can no longer clear it effectively. A fatty streak is formed when there is an accumulation of foam cells in the vessel[71]. The scavenger receptors allow for the uptake of the oxLDL and allow the macrophages to present this to T cells *via* the MHCII receptor on macrophages and the T cell receptor (TCR) upon the T cells. The majority of T cells will differentiate into Th1 cells which secrete IFN-γ and TNF-α which can cause macrophages to become classically activated. M1 macrophages further contribute to the damage of the vessel wall by releasing more pro-inflammatory cytokines. Less commonly, the T cells may differentiate into Th2 cells which release the cytokines IL-4 and IL-13 causing alternative activation of macrophages. M2 macrophages are involved in the production of collagen (**Figure 1.3**)[13].

The presence of DAMPs including heat-shock protein 60 cause the production of pro-inflammatory cytokines such as IL-2, which causes T cell proliferation[72]. SMCs and endothelial cells begin to proliferate in response to endothelial injury as a result of aberrant inflammation. This requires remodelling of the extracellular matrix causing collagen to become deposited[73].

In the later stages of the disease, the fibrous cap's integrity may become compromised. An unstable plaque is one that has a thin fibrous cap, decreased T_{reg} numbers and increased DCs[42,73]. This occurs when there is an imbalance in the amount of collagen and elastin being made, essential components of the smooth muscle layer, and the degradation of the cell wall. This imbalance is a result of elevated MMP activity. In unstable plaques, MMP-1 and MMP-3 have been found to cleave collagen and MMP-9

and MMP-12 cleave elastin, all of which are essential components of a stable plaque[74–76]. Conversely, a stable plaque tends to be larger in size and has a thick fibrous cap. If a plaque ruptures, thrombus formation may occur blocking the artery and depending upon whether this happens in the coronary artery or the carotid artery, this can lead to either acute MI or a stroke[68].

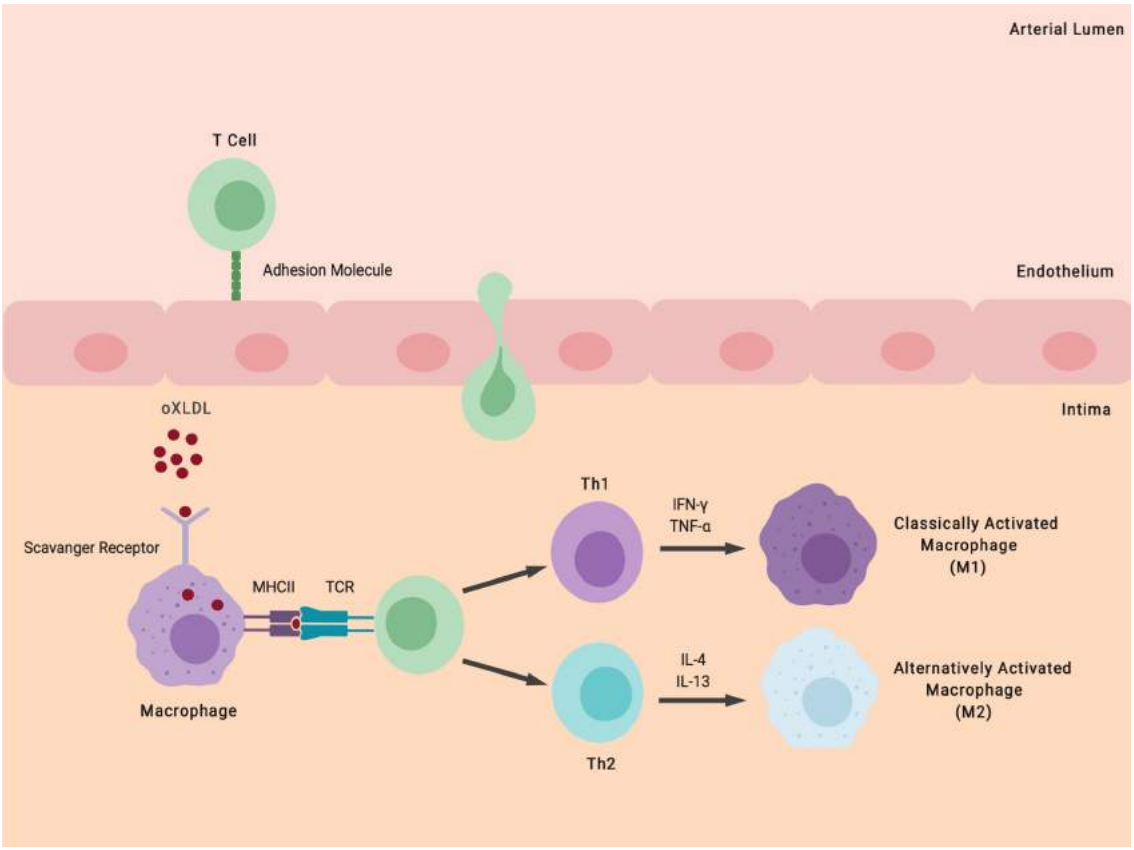

Figure 1.3: Macrophage and T Cell Interactions During Atherosclerosis. T cells bind to adhesion molecules on the endothelium of the lumen before undergoing diapedesis to enter into the intima of the artery. Scavenger receptors upon the macrophages detect and uptake oXLDL. Major histocompatibility complex II (MHCII) upon the macrophages interacts with the T cell receptor (TCR) on the T cell allowing the antigen, oXLDL, to be presented to the T cell. Primarily the T cells will differentiate into Th1 cells which will release pro-inflammatory cytokines such as IFN-γ and TNF-α which are responsible for causing macrophages to become classically activated. Classically activated macrophages promote inflammation by release of pro-inflammatory cytokines and thus promote tissue damage. Alternatively, the T cells may differentiate into Th2 cells, which release IL-4 and IL-13 to cause macrophages to become alternatively activated. Alternatively activated macrophages are involved in the production of collagen and thus the formation of the fibrous cap upon the plaque. Image created on Biorender.

1.4 Microbiota: A Missing Link Between the Immune and Neuronal Systems

The human microbiota is estimated to consist of 100 trillion microorganisms. Predominately the human microbiota consists of bacteria, but fungi, parasites and viruses are also found within the oral-gastrointestinal tract, albeit in much lower concentrations. The main bacterial phyla found in the colon of healthy adults are Bacteroidetes and Firmicutes whilst Actinobacteria, Proteobacteria and Verrucomicrobia phyla are found in smaller quantities[77]. Some of the main roles of the microbiota for the host include aiding digestion, production of vitamins and contributing to the immune response[78].

A commonly used mouse model for elucidating the role of specific bacteria is germ-free (GF) mice. GF mice are bred in isolated conditions resulting in the complete absence of microbes. They can be colonised by a specific known microbe allowing for the generation of gnotobiotic animals[79]. GF mice also have an altered gut with there being fewer goblet cells, a thinner mucus layer, impaired brush border differentiation, reduced villus thickness and lower serotonin production despite increased numbers of enterochromaffin cells[80–83]. Thus, where GF mice are used for studies it is very important to consider the possibility that there are most likely physiological consequences of this model. It is important to note that GF mice have been found to have an altered immune system[79]. For example, there is evidence to suggest that in GF mice myeloid cell populations are broadly decreased, common lymphoid progenitors are reduced in the bone marrow and DC priming is impaired in GF mice compared to normal mice[80,84].

Disruptions in the commensal relationship between the host and the microbiota are thought to contribute to the development of some diseases such as irritable bowel disease and have been demonstrated to occur in obesity, atherosclerosis and T2D[85–89]. Emerging evidence suggests that the composition of the microbiota may also be involved in social

and affective behaviours as well as in mental illnesses[90–92]. It is essential to note that changes in the microbiota are often correlative to diseases or behaviour rather than causative, and the mechanisms underlying such correlations in most cases remains elusive. There are two main areas proposed that mechanistically could be attributed to disease: **1.** small molecule production and **2.** modulation of the host immune response[93]. For example, trimethylamine N-oxide is a small molecule produced as a result of microbial metabolism of choline and carnitine and has been found in murine models to be both proatherogenic and prothrombotic in nature[94,95]. In IBD high levels of the Enterobacteriaceae species are seen and as the Enterobacteriaceae species has highly endotoxic LPS on its outer membranes, this induces high levels of inflammation by the suppression of T_{reg} cells and the activation of effector T_H cells in the gut and it has also been demonstrated to cause colitis development in mice[96]. In order to elucidate causality versus correlation, more mechanistic studies are needed.

When the microbiota is discussed, the anthropogenic labels of 'good' or 'bad' are often assigned to describe individual species of bacteria or shifts in the phyla that are associated with changes in health[97]. However, this is a highly simplified view. For example, *Salmonella typhimurium* is considered to be an intestinal pathogen and thus 'bad'[98]. Rao *et al* (2017) demonstrated that the *Salmonella typhimurium* effector, known as the *Salmonella* leucine rich repeat protein, negatively regulated virulence and promoted survival of the host. Host survival was promoted by inhibition of the infection-induced host response, to induce the vagus nerve dependent hypothalamic anorexic feeding program. In this study, when IL-1β is not inhibited, the anorexic response occurred which lead to increased dissemination of the intestine and increased pathogen virulence at the expense of the pathogen's transmission to a new host. This study has demonstrated that microbes such as *Salmonella typhimurium* have evolved over time to have anti-virulence

strategies that inhibit sickness-induced anorexia in order to promote host survival and pathogen transmission[99]. In other words, *Salmonella typhimurium* is not as 'bad' for the body as it has the potential to be, as it actively reduces its virulence to promote host survival and thus its own transmission.

1.4.1 Brain-Gut Interactions

The importance of brain-gut interactions was demonstrated by investigating the role of microbiota on the development of the brain and behaviour, by comparing specific pathogen free (SPF) mice, who only had commensal bacteria, to GF mice. SPF mice had normal morphological development and maturation of grey matter and white matter in the brain, demonstrated by better spatial learning and contextual memory in behavioural tests compared to GF mice. This highlights that commensal bacteria are imperative for the normal development and maturation of the brain, which will have implications in locomotion and cognitive function[100].

The gut microbes and the brain interact with each other through the vagus nerve. Subdiaphragmatic vagal deafferentation in rats was shown to reduce anxiety and increase expression of auditory cued fear conditioning, which was associated with changes in noradrenaline and gamma-aminobutyric acid (GABA), neurotransmitter, in the limbic system[101]. One example of this is that after mice had ingested *Lactobacillus rhamnosus* they exhibited reduced depression and anxiety related behaviour, which was mediated by vagus nerve stimulation thus altering the levels of GABA expression in the brain[102]. Taken together these two studies demonstrate that the gut is involved in depression, anxiety and learned fear responses.

Acute psychological stress has been shown to increase the small intestinal permeability in humans *via* mast cell activation, as a result of increased corticotropin releasing factor

from the paraventricular nucleus in the hypothalumus[103–105]. Chronic stress over a period of 10 days was found to increase serum corticosterone levels as well as increase the number of mucosal mast cells by 3-fold[105]. Increased intestinal permeability leads to the activation of the immune system as a result of food-derived, microbial, bacterial and parasitic antigens being recognised by the immune system. Interestingly, in patients with chronic depression there is increased immunoglobulin (Ig)A and IgM responses against gut commensals, suggesting a leaky gut[106].

The microbiota is responsible for the production of short-chain fatty acids including butyrate and propionate, which in animal models has been shown to affect the release of the gut hormones gastroinhibitory peptide and peptide YY, both satiety hormones, thus reducing appetite and food intake[107]. Mice fed a high fat diet were found to have increased Proteobacteria and dysbiosis of the gut microbiota. These changes were associated with suppressed brain-derived neurotrophic factor, increased NFκB and microglial activation in the hippocampus and increased macrophages, DCs and TNF-α levels in the colon[108]. Such changes have been described in the literature as previously being associated with depression[109–111].

1.5 Personality, Emotional State and Social Status in Disease

It is well documented that acute infections induce sickness behaviour which is characterised by anhedonia, lethargy, social withdrawal and anorexic behaviour[112]. The main proinflammatory cytokines involved in the induction of sickness behaviour are IL-1β and TNF-α as peripheral administration of LPS induces food reduction and withdrawal from the physical and social environment[113]. IL-1 has a key role in mediating sickness behaviour in the brain inducing fatigue, depression social exploration and during infection[114]. Administration of IL-1β alone at either the periphery or the left ventricle of the brain induces fever, hypothalamic pituitary adrenal axis activation and depression[115]. However, the role of such sickness behaviours in the host defence remains largely unknown. Interestingly, nutritional supplementation was extremely detrimental during bacterial sepsis and it was determined that glucose was the constituent of food that conferred this increased mortality[116]. In contrast, glucose inhibition is lethal in influenza infection and thus nutritional supplementation is protective during viral sepsis[116]. It was this observation that inflammation could lead to changes in behaviour that led to investigations as to whether similar changes in the immune system could be seen as a consequence of social status and/or emotional wellbeing and whether such changes could account for the increased prevalence of chronic inflammatory diseases seen in those with poor status or emotional wellbeing[112,117–119].

As briefly mentioned before, studies are increasingly showing that a person's emotional wellbeing can in fact influence their risk, severity and outcome in a number of chronic diseases including vascular diseases[117–119]. Social connections play a key role in emotional wellbeing and therefore, it is not surprising that they control several aspects of human health. A person who has poor social connections is more likely to exhibit negative behavioural choices and suffer from psychological dysfunctions that can lead to

physiological dysfunctions. The interaction between changes in behaviour, psychology and physiology results in a vicious cycle being formed, which can ultimately lead to increased risk of morbidity and mortality (**Figure 1.4**). For example, if a person does not have a good social status they are more likely to be stressed, have a poor diet and to have increased blood pressure, which in turn puts them at increased risk of suffering from CVD as all the factors aforementioned are well known risk factors for this disease[120].

1.5.1 The Microbiota and Social Interactions

As discussed earlier there is a clear link between the microbiota and the brain thus it is not surprising that there is emerging evidence that sociability and social network might have an effect on the microbiome[121–125] In chimpanzees, frequent social interaction was found to promote microbial diversity within the microbiome and changes in the microbiome could be passed down to different generations by further social interaction[121]. In red lemurs, individual sociality was negatively associated with microbial diversity, whilst the group size that the red lemurs were part of did not affect microbial diversity. However, the red lemurs' position within the social network predicted gut microbial composition[122]. Interestingly, in baboons, the types of bacteria that were found to be affected by social interactions and network size were primarily found to be anaerobic and non-spore-forming[123]. *Lactobacillus reuteri* is thought to have a role in normal social interaction, as in multiple murine models of autism spectrum disorder, *Lactobacillus reuteri* was able to rescue the induction of social interaction synaptic plasticity in the ventral tegmental area of the brain[126]. Rats subjected to social isolation were found to have increases in Actinobacteria and decreases in the class Clostridia compared to controls[125]. In married individuals who reported close relationships, higher levels of gut microbial diversity was reported compared to single people, suggesting that human interactions especially close and sustained interactions

influence the gut microbiota[124]. There is a need for further investigations in humans to determine whether social isolation and loneliness have an effect on the microbiota.

1.5.2 The Effect of Personality, Lifestyle and Mental Illness on the Immune System

There is new evidence emerging that suggests a person's personality may affect their prognosis and risk of disease *via* changes in both inflammation and oxidative stress levels. Some psychologists believe that there are four main personality types (Type A, B, C and D) that people can have depending on their dominate personality traits. People who are thought to have a Type A personality are ambitious, competitive, practical, impatient and aggressive, whilst in contrast people who exhibit a Type B personality tend to be relaxed, cheerful, patient and procrastinators[127]. Those individuals who tend to be systemic, thoughtful, sensitive, cautious and critical are thought to have a Type C personality[128]. Type D personality refers to the 'distressed' personality trait which is characterised by the presence of the following dominant personality traits: negativity, pessimism, depression and social inhibition[129]. For example, Type D personality is characterised by both a pessimistic outlook on life and social inhibition and heart failure patients with this personality were found to have increased serum levels of xanthine oxidase as well as having decreased serum levels of heat shock protein 70 contributing to oxidative stress and thus poor prognosis[130]. People with an optimistic outlook in life have been found to have lower levels of IL-6 and higher levels of the antioxidant molecules known as the carotenoids thus suggesting that optimism may be able to attenuate oxidative stress[131].

The practice of meditation, has been shown to be potentially atheroprotective as it increases NO production, which is essential for normal endothelial function as well as

lowering serum lipid peroxidation[132,133]. Moreover, patients with T2D who practice yoga were found to have improved glycaemic control, lower BMI, lower levels of malondialdehyde and an increase in the antioxidants glutathione and vitamin C[134]. There is a need for larger, better powered studies in this area to investigate whether treatments such as meditation and yoga may be beneficial in the prevention and progression of chronic diseases.

Mental disorders have also been associated with changes in both oxidative stress and inflammation levels, with emerging evidence that these can to some degree be predictive of response to pharmacological treatments and symptoms[135]. Patients suffering from depression have elevated inflammation including increased IL-1, TNF-α, IL-6 and C-reactive protein (CRP) levels[136]. In fact, there is evidence to suggest that some pharmacological treatments for depression such as selective serotonin reuptake inhibitors can reduce levels of inflammatory markers in serum back to that seen in non-depressed people and that this decrease in inflammation was correlated with lower clinical depression scores[137]. Depression causes a decrease in total antioxidant activity, and the lower this activity is the more likely that pharmacological interventions will fail[138]. Suicidal thoughts during depression have been correlated with increased NO levels[139,140]. Similarly, post-traumatic stress disorder (PTSD) has been associated with increased plasma pro-inflammatory cytokines including IL-17 and IL-6 and this is accompanied by increased numbers of Th1 and Th17 cells in the blood[141–143]. Women with anxiety disorders have been shown to have increased superoxide anion production as a result of an increased respiratory burst accompanied by increased TNF-α and IL-2 release[144].

Social isolation and loneliness in humans increases the risk of premature mortality and a number of chronic diseases (**Figure 1.4**)[119,120,145]. Conversely, those who have stronger

relationships appear to have decreased mortality[146]. There is evidence to show that loneliness can double the risk of Alzheimer's disease and cause more rapid cognitive decline[147]. Social isolation and loneliness are both correlated with depressive symptoms, which in-turn is a risk factor for CVD[148,149]. Loneliness in the elderly was found to cause a 12.3% decline in activities of daily living, which would also be a risk factor for CVD[150]. Similarly, results from a Swiss based survey found that those who were lonely were significantly less likely to be physically active (odds ratio [OR] 1.20). It was also found that those who were lonely were significantly less likely to adhere to guidelines on fruit and vegetable consumption (OR 1.21) and were significantly more likely to be current smokers (OR 1.13)[151]. It is clear that loneliness is closely linked to a number of lifestyle choices, thus it is unsurprising that people who are lonely are more likely to suffer from metabolic syndrome (MetS), which places them at increased risk of CVD[152].

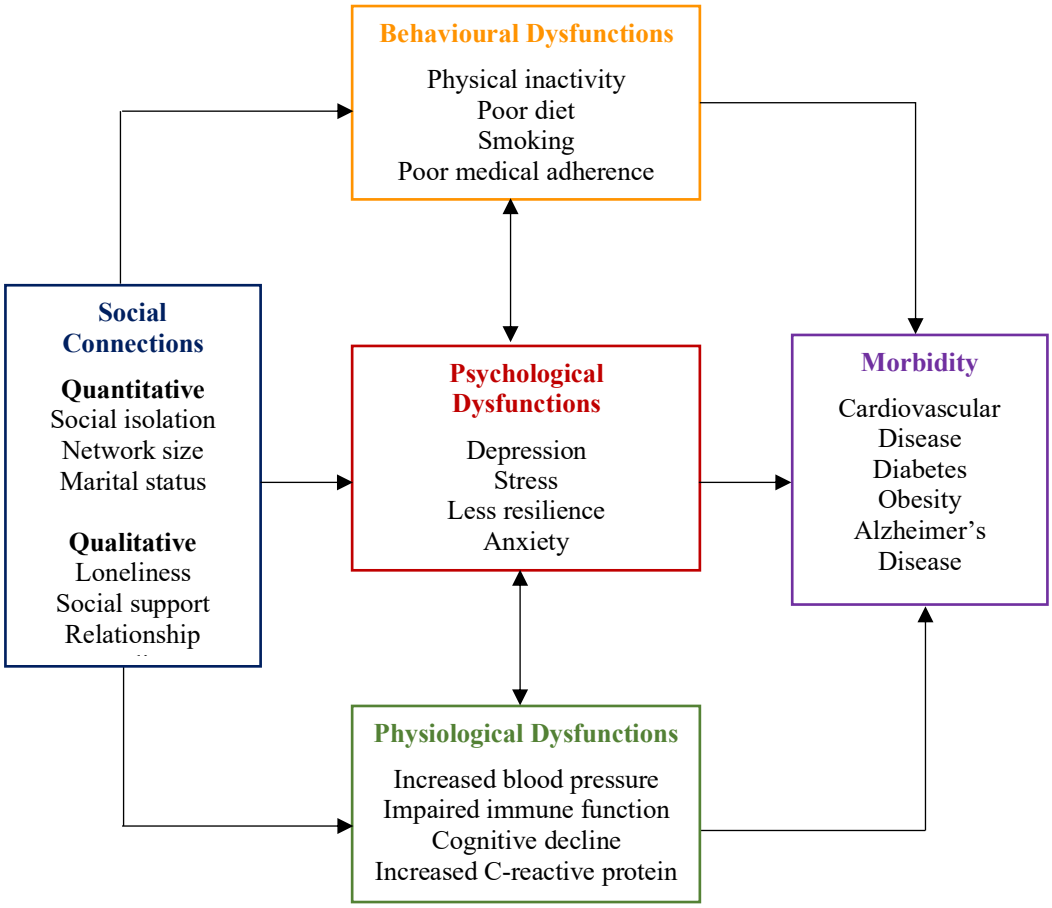

Figure 1.4: The Link between Social Connections and Disease. Both the size and quality of a person's social network can affect their wellbeing at three different levels: behavioural, psychological and physiological. Having poor social connections negatively affects the behavioural, psychological and physiological factors and each of these factors can interact with each other to further exacerbate the problem. A vicious cycle is then formed, which, if not broken can lead to a number of morbidities including CVD and thus increased risk of mortality.

1.5.3 Gene Signature and Molecular Mechanisms Modulated by Social Status

Studies in female macaques have shown that hierarchy, a form of social status, can alter immune system signalling. Those females who were considered to be low ranked were found to have upregulation of *MYD88*, leading to upregulation of the genes involved in the early NFκB pro-inflammatory response leading to enhanced IL-6 and TNF-α production. Since low ranked females have enhanced expression of the genes involved in the early NFκB response, this suggests that they may have a primed bacterial response. In contrast, high ranking females were found to exhibit upregulation of *TRIF* mediated signaling promoting the release of antiviral cytokines such as IFN-γ[153].

Environmental enrichment is classically described as a complex environment that is comprised of both inanimate and social stimulation[154]. Environmentally enriched (EE) mice were found to have a higher basal neutrophil to lymphocyte ratio (NLR). During infection, EE mice were found to have increased neutrophil and macrophage recruitment to the site of infection, as well as enhanced bacterial clearance due to increased ROS production during phagocytosis[155]. Environmental enrichment has been shown to be beneficial in a number of neurological diseases, with one study finding that the exosomes released from EE mice's immune cells reduced oxidative stress and promoted myelin content in cultured slices of the brain[156]. Similarly, environmental enrichment was also beneficial in a humanised murine model of Alzheimer's disease, where EE mice were found to have normalized extracellular levels of chemokine ligand (CCL)3, TNF-α and CCL4, as well as preventing inflammation related changes to microglial structure[157].

This risk of increased disease burden associated with social isolation and loneliness, may be in part due to changes in the immune system. Studies in humans who had high levels of loneliness, have found that their leukocytes had a unique gene expression pattern,

whereby 131 genes were found to be downregulated and a further 78 genes were found to be upregulated. Steve Cole, coined this phenomenon as the conserved transcriptional response to adversity (CTRA). The CTRA response can be summarised as follows (**Figure 1.5**):

- Upregulation of pro-inflammatory cytokines involved in bacterial responses e.g. IL-1β, IL-6, TNF and IL-8;
- Downregulation of antiviral genes involved IFN type 1 responses e.g. oligoadenylate synthetase (OAS);
- Downregulation of IgG1 antibody synthesis[158].

Perceived social isolation (PSI) is a term coined to describe the difference in the amount of social interaction a person had and how much they desire. In people, who were considered to have high levels of PSI, it was found that the CTRA response was most predominate in antigen presenting cells, especially monocytes and DCs. The CTRA response is also seen to a lesser extent in B cells[159].

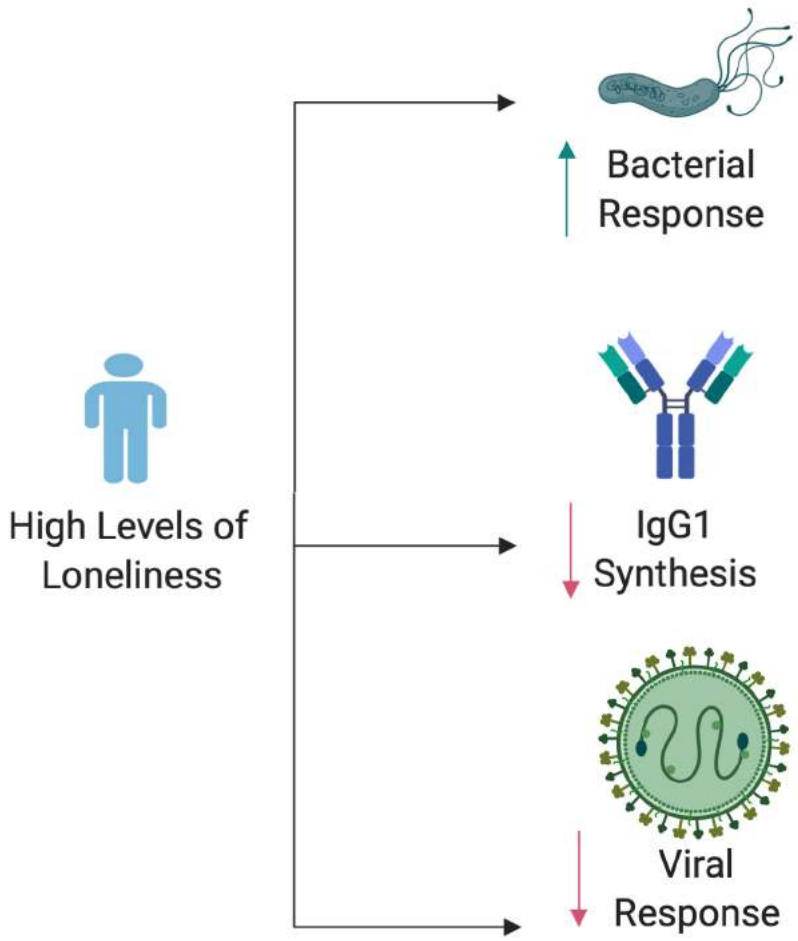

Figure 1.5: Summary of the Conserved Transcriptional Response to Adversity. High levels of loneliness causes the upregulation of genes involved in the bacterial response and the downregulation of the genes involved in the synthesis of IgG1 antibodies and in the viral response. Image created on Biorender.

1.6 Social Isolation and Loneliness

Whilst social isolation and loneliness are often used interchangeably, they in fact have distinct meanings. Social isolation is an objective term coined to quantitatively describe the absence or near-absence of social relationships, based upon network size and diversity, as well as how often social contact occurs[148]. Loneliness refers to a subjective feeling that occurs when a person does not have the quantity and quality of social relationships that they desire. It is important to note that social isolation is not always associated with loneliness and that a person can feel lonely despite having numerous social connections[160].

1.6.1 Epidemiology

Both loneliness and social isolation are becoming increasingly more common with the Jo Cox Commission on Loneliness identifying that between 2016-2017 about 5% of adults in England considered themselves to 'often' or 'always' feel lonely[160]. However, frequently feeling lonely is not a unique problem to the UK as it is reported worldwide. The prevalence of loneliness differs across the world with the most comprehensive information being found for Europe, where on average, 7.9% of adults 'often' or 'always' feel lonely (**Table 2**)[161–163]. Within Europe the percentage of adults reporting 'often' or 'always' feeling lonely differs from being around 3-4% in the Scandinavian countries, to ~10% in Italy, Poland and France[161]. In comparison, to the United States of America (22%) and Australia (27.6%), Europe (7.9%) has considerably lower % of adults reporting 'often' or 'always' feeling lonely[161,162,164,165]. Japan (9.0%) and New Zealand (3.6%) have similar levels of loneliness to that seen in individual countries across Europe[161,163,165]. It is not clear why such differences in the prevalence of loneliness are seen worldwide but it is likely to be in part due to cultural and lifestyle.

It is estimated that loneliness costs employers in the UK £2.5 billion per year and it is in fact estimated that lack of social connections could be as damaging to health as smoking 15 cigarettes per day, thus highlighting a growing problem[160,166]. It is important to note that both the prevalence and cost of loneliness is likely to be underestimated due to the stigma that surrounds admitting being lonely.

Whilst loneliness is often perceived to be associated with the elderly, the Jo Cox Commission on Loneliness highlighted that young adults, aged 16-24, more frequently reported loneliness compared to older age groups, and this was confirmed by the Loneliness experiment, a large scale self-reported study across multiple countries[160,167]. The commission found that loneliness is more common in women than in men. The three highest risk groups for loneliness are as follows: **1.** young renters in areas where there is little sense of community and trust, **2.** unmarried middle-aged people suffering from chronic health conditions and **3.** unmarried older homeowners with chronic conditions[160]. Those who have a poor social status, i.e. those who have low income and low levels of education, are at increased risk of feeling lonely[168,169]. Unsurprisingly, living alone has been shown in numerous studies to be a risk factor for loneliness[160,170,171].

Table 2: Prevalence of Loneliness Worldwide.

	Always Lonely (% of Population)
Europe[161]	7.9
Northern Europe[161]	5.2
Denmark	3.0
Finland	4.0
Western Europe[161]	6.6
France	10.0
Ireland	5.0
Southern Europe[161]	8.9
Italy	10.0
Eastern Europe[161]	10.8
Poland	10.0
Oceania	
Australia[162]	27.6
New Zealand[163]	3.6
United States of America[164,165]	22.0
Asia	
Japan[165]	9.0

1.6.2 Assessing Loneliness and Social Isolation

Loneliness is commonly assessed using the University of California, Los Angeles (UCLA) Loneliness Scale[160]. The UCLA Loneliness Scale is used in about 80% of all research published to identify loneliness and is a 20-item scale where subjects are asked for each item on the scale if they 'often', 'sometimes', 'rarely' or 'never' feel that way, with each of the options carrying a score from 4 to 1 from 'often' to 'never'. Higher overall scores indicate higher degrees of loneliness. Examples of statements used in the UCLA Loneliness Scale include 'I am no longer close to anyone' and 'I feel completely alone'[172,173].

As mentioned previously social isolation is a quantitative measure of the number of social connections a person has. In order to determine the number and the quality of connections a person has, a series of questions are asked that determine the frequency of contact with family, frequency of contact with friends and relatives, emotional support levels and social network support levels. Participants have the option to choose an answer from a predetermined set of answers with examples being 'every day, most days, few days' and 'never' or 'yes and no'. Example questions include 'How often in the previous two weeks have you spent time together with family?' and 'Do you have anyone with whom you can discuss intimate and personal matters?'[174].

1.7 Aims and Hypothesis

Longitudinal studies have shown that social isolation and loneliness have been linked to increased premature mortality[119,145]. However, very little is known about the underlying mechanisms that result in this increased premature mortality. Loneliness has been shown to alter leukocytes' gene expression into a more pro-inflammatory profile, which could contribute to the increased prevalence of chronic diseases, including CVD in people who are lonely[118,175]. Therefore, this thesis focuses on how social isolation affects the immune system in both acute and chronic inflammatory models.

Hypothesis:

'Social isolation has a unique and discreet pathway of influencing the immune system, thus affecting the severity of acute and chronic models of inflammation.'

Aims:

1. To determine the effects of social isolation on the general health status and immune repertoire of CD-1 mice;
2. To examine whether social isolation can affect the immune system and thus survival, during extreme vascular dysfunction such as that seen in sepsis;
3. To determine whether social isolation affects the metabolic and biochemical phenotype of *ApoE*$^{-/-}$ mice;
4. To investigate whether social isolation affects the incidence and severity of atherosclerosis in *ApoE*$^{-/-}$ mice;
5. To establish whether social isolation can affect the immune system during experimental atherosclerosis.

Chapter 2
Basal Effects of Social Isolation

2.1 Introduction

Social isolation and loneliness have been implicated as a risk factor for a number of chronic inflammatory diseases, including MetS, T2D and CVD[152,176,177]. However, there are very few studies that try to characterise whether social isolation itself, rather than its associated behavioural and lifestyle changes, alters the physiology, the microbiome and the immune system of humans.

Both social isolation and loneliness are risk factors for MetS, T2D and CVD suggesting that poor social status can alter metabolism[152,177,178]. It has been discovered that long-term social isolation results in changes in appetite, whereby social isolation results in reduced food intake and increased plasma leptin, the satiety hormone[179]. In contrast, women with high levels of loneliness were found to have increased postprandial levels of ghrelin, the hunger hormone[180]. Social exclusion from a task has been shown to cause increases in plasma glucose levels in comparison to individuals who participated in a task[181]. Long-term social isolation in rodents has been shown to increase adiposity[182,183].

Emerging evidence suggests that the immune system can be influenced by the quality and quantity of social interactions[184–186]. Social isolation has been shown to be related to increased CRP, fibrinogen and inflammation index scores, with this effect being more pronounced in males than females[187]. Long-term social isolation in rats was found to reduce IL-10, both in the blood and hippocampus, compared to social housing[185]. Loneliness has been found to lower natural killer (NK) cell activity and to cause higher antibody titres in response to herpes simplex virus and Epstein Barr virus[186,188]. In lonely individuals, after an acute stress task, it was revealed that there was an increase in NK

cells and fibrinogen compared to non-lonely individuals[184]. Loneliness and small social network size in college students was predictive of a poor antibody response to the influenza vaccine[189].

It has been suggested by a number of studies that there is an altered microbiome in people with mental illnesses and/or in chronic inflammatory diseases, which are both closely associated with social isolation[90,91,190]. Depression has been linked to lower levels of the Firmicute genera *Dialister* and *Coprococcus*. In contrast, there was a clear association between increased levels of *Faecalibacterium*, which produces butyrate, a known anti-depressant, and increased indicators of a higher quality of life[191]. In females, there is emerging evidence to suggest an inverse relationship between anxiety scores and *Bifidobacterium,* whilst in males an inverse relationship was identified between *Lactobacillus* and depression scores[192]. Additionally, a study has shown that those individuals who suffer from PTSD have decreased abundance of the Actinobacteria, Lentisphaerae and Verrucomicrobia compared to trauma exposed controls[193]. Studies have shown that individuals who are considered to have low bacterial diversity in their guts tend to have increased adiposity, dyslipidaemia, insulin resistance and more pro-inflammatory bacteria[194].

Increasingly, it is becoming clear that the environment, social status and loneliness can alter gene expression. Short-term changes in the environment, such as EE for 2 weeks, can result in transcriptional changes in whole blood, whereby 13 genes were found to be differentially expressed[195]. Low rank marquee monkeys' leukocytes were shown to have upregulation of gene expression for the *MyD88* signalling pathway whilst high rank marquees' leukocytes had upregulation of the genes involved in the *TRIF* signalling pathway upon LPS stimulation[153]. Recently, a genome-wide association study revealed

that there are 15 genomic loci that are associated with increased susceptibility to loneliness[196]. Additionally, high levels of PSI have been demonstrated to induce a set of changes in transcriptional changes in gene expression, known as CTRA, in antigen presenting cells[175].

2.1.1 Specific Aims

This chapter aimed to address the following objectives:

1. To determine whether weight gain and nutritional intake were altered in response to short-term social isolation in CD-1 mice and if social isolation affected these parameters in a sex dependent manner;
2. To establish whether short-term social isolation in CD-1 mice causes changes in the faecal microbiota;
3. To investigate whether short-term social isolation in CD-1 mice alters whole blood cellularity and biochemical markers of inflammation;
4. To investigate TLR expression and signalling profile in basal peritoneal macrophages after short-term social isolation in CD-1 mice;
5. To elucidate the transcriptional fingerprint of short-term social isolation in the whole blood of CD-1 mice.

2.2 Methods

2.2.1 Animal Husbandry

All animals were housed in individually ventilated enclosures with standard food and water being provided *ad libitum* and with a 12-hour light-dark cycle. All experiments undertaken were approved and performed according to the guidelines of the Ethical Committee for the Use of Animals, Bart's and The London School of Medicine and Dentistry and the Home Office Regulations Act 1986 (Prof. D'Acquisto, PPL. 70/8714).

2.2.2 Modelling Social Isolation

Social isolated (SI) cages were set up based upon the protocol used by *Liu et al* (2012) using standard cages (W x D x H:193x 419x 179x mm, Allentown) with 1 mouse per cage[197]. As controls, socially housed (SH) cages were set up using standard cages with 4/5 mice that had been weaned together (**Figure 2.1**). Regardless of housing type each cage included: 2 strips of nesting material and sawdust bedding up to 5cm in depth. Cages were cleaned once a week and only one researcher was allowed to handle the mice.

For basal studies, in house bred CD-1 male or female mice at 5-6 weeks of age were assigned to either social isolation or social housing for a period of 2 weeks as this is the minimum period of time for changes in gene expression to be seen[155,198]. Mice were fed standard chow for the duration of these studies (**Figure 2.2**).

SH SI

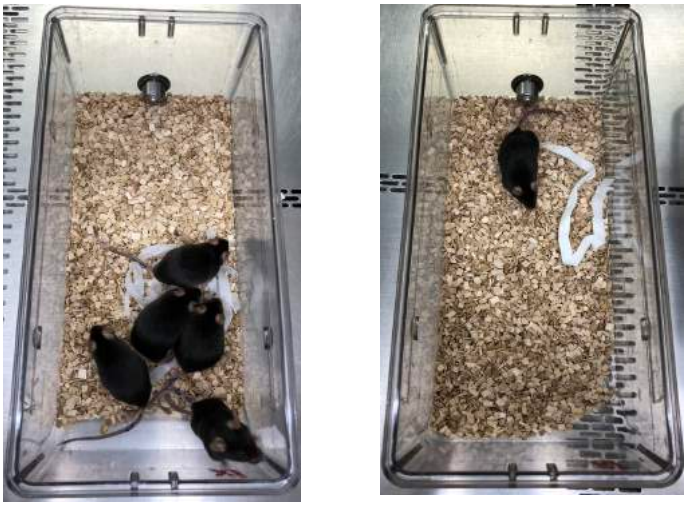

Figure 2.1: Set up of Different Housing Conditions. a) social housing: 4/5x mice weaned together in standard size cage (W x D x H: 193mm x 419mm x 179mm, Allentown), 2 strips of nesting material and sawdust bedding up to 5cm in depth **b)** 1x mouse in standard size cage (W x D x H:193x 419x 179x mm, Allentown), 2x strips of nesting material and sawdust bedding up to 5cm in depth.

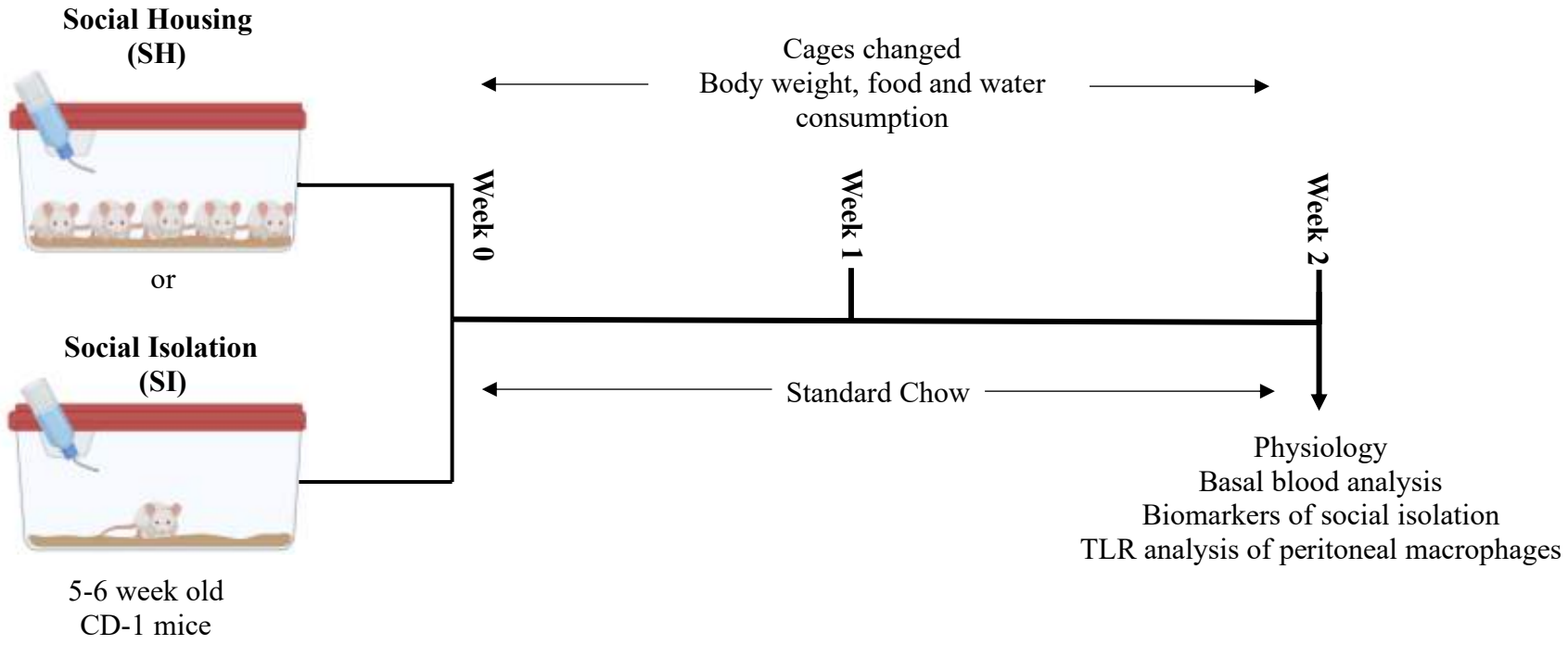

Figure 2.2: Basal CD-1 Study Overview. CD-1 mice at 5-6 weeks of age were randomly assigned to either social housing (4-5x mice per cage) or social isolation (1x mouse per cage) for a period of 2 weeks during which time the mice were fed the standard chow. Throughout the study cages were changed on a weekly basis at which time the mice were weighed. Food and water consumption were assessed every 2-3 days. After 2 weeks, mice were sacrificed, and four main parameters were assessed: metabolic physiology, basal blood analysis, biomarkers of social isolation and TLR analysis of peritoneal macrophages. Image created on Biorender.

2.2.3 Weight Gain and Nutritional Intake

During the period of social housing or social isolation food and water was monitored and replenished as needed every 2-3 days. Mice were weighed once a week during cage changing to assess weight gain over the study.

2.2.4 Cardiac Puncture

Mice were anesthetised in a chamber using isoflurane at setting 4 and once the mice were sufficiently under, an individual mouse was scruffed and the 1ml syringe (25G 5/8" needle) containing 0.1ml of 2% heparin (Leo Pharma, **cat.** 009876-04) was placed into the heart just under the armpit at a perpendicular angle. The plunger was pulled back slowly to collect the blood and the needle was moved as required. Mice were sacrificed by CO_2 asphyxiation.

2.2.5 Plasma Leptin

Satiety levels were measured at the end of the social isolation period in CD-1 mice *via* quantification of leptin in plasma using a precoated murine leptin enzyme linked substrate assay (ELISA) kit (Thermofisher, **cat.** KMC2281). Plasma was isolated from whole blood collected at the end of the social isolation period by centrifuging samples for 5 minutes at 10,000 *g*. The ELISA was carried out according to manufacturer's instructions. In brief, before plasma was used, it was spun down for a further 3 minutes at 10,000 *g* and samples were diluted at 1:5 and 1:10 with standard dilution buffer prior to being loaded onto the ELISA plate, where they bound to the antigen. After 2 hours incubation, biotin conjugate was added and incubated for 1 hour. Streptavidin-horseradish peroxidise (HRP) was added and the plate was incubated for 30 minutes before stabilised chromatin was added and after ~15 minutes, stop solution was added.

The ELISA plate was read at 450nm and the equation of the standard curve was used to extrapolate the concentration of leptin in each sample.

2.2.6 Visceral Adipose Tissue

Mice were sprayed with ethanol prior to a small incision being made in the middle of the abdomen and the skin was gently pulled back. Visceral adipose tissue (VAT) was used, as adipocytes tend to be large in size thus aiding counting and sizing of individual adipocytes. The VAT is located in the abdominal area and was removed by gently pulling it with forceps. Once removed the VAT was weighed and placed in 4% paraformaldehyde (PFA) overnight.

After remaining in 4% PFA overnight half of the adipose tissue was placed in 70% ethanol in preparation for haematoxylin and eosin stain (H&E) staining. Adipose tissue was stained and mounted by Barts Cancer Institute Pathology Services. Three field images per adipose slide were taken at 20x zoom using a Nikon Eclipse TE300 microscope. The adipocytes were counted, and their individual areas were measured across the three field images using Image J.

2.2.7 Faecal Boli

In order to assess the effect of social isolation on the microbiome, faecal boli were collected after 1 week and again at 2 weeks of social isolation. Approximately, 5x faecal boli were taken per mouse at each of these time points. Faecal boli were frozen at -20°C.

Deoxyribonucleic acid (DNA) was extracted from a single faecal boli, as determined by a calibration curve, using a PowerFecal DNA Isolation Kit (Mo Bio Laboratories Inc., **cat.** 12830-50) and following the manufacturer's instructions. In brief, samples were thawed and prepared in solution C1, containing SDS to promote the breakdown of fatty

acids and lipids, prior to being lysed in lysis buffer at 4°C. Once lysed, an Inhibitor Removal Technology buffer was added and the DNA was bound to the Eppendorf. The solution was transferred to a spin column and the DNA was washed prior to elution. DNA concentration and quality were assessed using the Nanodrop 1000.

Primers used were custom made by Sigma and are listed in **Table 3**. All samples were loaded in triplicate and run on the BioRad CFX Connect Real Time Polymerase Chain Reaction (RT-PCR) machine according to primer annealing temperatures. Genes of interest were normalised to Universal 16s and analysed using the $\Delta\Delta C_T$ method of analysis to calculate the fold change.

Due to technical difficulties with the RT-PCR, frozen faecal boli (3x per housing group) was given to Dr Adele Costabile at the University of Roehampton for next generation sequencing (NGS). Total bacterial DNA was extracted from 200mg of faecal sample using QIAamp DNA Stool Mini Kit (QIAGEN, **cat.** 51504) following the manufacturer's instructions. The DNA samples were resuspended in 100µl of TE buffer and treated with 2µl of DNase-free RNase (10 mg/ml) at 37°C for 15 min. Proteins were removed by treatment with 15µl of proteinase K at 70°C for 10 min. DNA was subsequently purified using QIAamp Mini Spin columns. Final DNA concentration was quantified by using NanoDrop ND-1000.

For NGS analysis, the V3-V4 region of the 16S rRNA gene was amplified by PCR in 50µl final volume mix containing 25ng of microbial DNA, 2X KAPA HiFi HotStart ReadyMix (Roche, **cat.** KK2601), and 200 nmol/l of S-D-Bact-0341-b-S-17/S-D-Bact-0785-a-A-21 primers carrying Illumina overhang adapter sequences. Amplification was performed using a Biometra Thermocycler T Gradient ThermoBlock according to the settings shown in **Table 4**.

The Agencourt AMPure XP magnetic bead-based clean-up system (Beckman Coulter, **cat.** A63881) was used for purification of the 460 base pair amplicons and these were then used to prepare indexed libraries by use of a limited-cycle PCR (Nextera Technology). Libraries were purified and successively pooled at 4nM, denatured and diluted to 6pmol/l. Samples were sequenced on Illumina MiSeq platform using a 2×300 base pair paired end protocol, according to the manufacturer's instructions.

Principal Coordinates Analysis (PCoA) was conducted to explore and visualize similarities among samples. The weighted UniFrac metric, a quantitative and phylogenetic metric was used to highlight differences among samples taking in to account the most abundant species[199]. PCoA analysis was displayed using the Vegan package in R (https://www.r-project.org/)[200], while cluster analysis was performed using Made 4[201]. Genera superimposition to the PCoA graph was conducted using the function envifit of Vegan.

Table 3: Primer Information for Microbiota Analysis.

Primer	Sequence 5' to 3'	Annealing Temperature (°C)
Universal 16s	**Forward:** ACT CCT ACG GGA GGC AGC AGT	64.0
	Reverse: ATT ACC GCG GCT GCT GG	70.7
Hepaticus	**Forward:** GCA TTT GAA ACT GTT ACT CTG	56.5
	Reverse: CTG TTT TCA AGC TCC CC	58.3
Lactobacillus	**Forward:** AGC AGT AGG GAA TCT TCC ACA	62.6
	Reverse: CAC CGC TAC ACA TGG AG	58.7
Heliobacter	**Forward:** GGT CGC CTT CGC AAT GAG TA	67.3
	Reverse: CTT AAC CAT AGA ACT GCA TTT GAA ACT AC	64.0
Robacterios	**Forward:** ATG GCT GTC GTC AGC TCG T	66.2
	Reverse: CCT ACT TCT TTT GCA ACC CAC TC	64.7
Murine norovirus 1	**Forward:** GCG TAA TAC GAC TCA CTA T	60.3
	Reverse: GCT TTT GGC CTC ACC TCT G	60.4
Bacteroides	**Forward:** AAG GCC ATC TGC TAC CCC TA	64.6
	Reverse: GGA CGG AGT TGA CGT GAG TT	64.3
Clostridiales	**Forward:** CCC ACA CTC CAG AGT AAC AGT	60.7
	Reverse: CCC ACA CTC CAG AGT AAC AGT	60.5

Table 4: Thermocycler Settings

Step	Time	Temperature (°C)
Activation	3 minutes	95
3 Step Cycling:		
Denaturation	30 seconds	95
Annealing (25x)	30 seconds	55
Extension	30 seconds	72
Final extension	5 minutes	72

2.2.8 Whole Blood Cellularity

Cardiac puncture was carried out at the end of the 2 weeks as previously described. Total leukocyte counts and the percentage of lymphocytes, monocytes and neutrophils were analysed in whole blood on an IDEXX Procyte Dx® Haematological analyser (IDEXX Ltd, West Sussex).

2.2.9 Plasma Cytokines

Plasma was isolated from whole blood as previously described. IL-6, TNF-α and IFN-γ concentrations were determined *via* multiplex assay (Labospace Ltd., Milan).

2.2.10 Biochemical Parameters

Cardiac puncture was carried out as previously. Plasma was generated from whole blood as previously described. 1x aliquot of plasma was sent to MRC Harwell for the following biochemical tests, which were run on Beckman Coulter AU680 Clinical Chemistry Analyser: glucose, alanine transaminase (AST), alanine aminotransferase (ALT) and creatinine.

2.2.11 Whole Blood Microarray

After 2 weeks of social isolation or social housing, whole blood was collected *via* cardiac puncture using 3.2% citrate. 150µl of collected blood was stored in RNAprotect Animal Blood Tubes (Qiagen, **cat.** 76544) and this was allowed to sit at room temperature for 2 hours to allow the blood to lyse.

Total ribonucleic acid (RNA) was extracted from whole blood from SI and SH mice (n=3 per housing group) using the RNeasy Protect Animal Blood Kit (Qiagen, **cat.** 73224) and following the manufacturer's instructions. In brief, the RNAprotect Animal Blood Tubes were centrifuged for 3 minutes at 10,000 *g* and the supernatant was removed. The pellet

was washed with RNAse-free water before resuspension in Buffer RSB. Samples were then digested in Buffer RBT with proteinase K and homogenised by centrifugation through the QIAshredder column. Ethanol was added, and the RNA was bound to the RNeasy MinElute column. DNA was digested, and the samples were washed with Buffer RW1 and Buffer RPE. Total RNA was eluted in 25µl of Buffer REB and was quantified and assessed for purity using the Nanodrop 1000.

Extracted RNA was hybridised at UCL genomics using the GeneChip Fluidics Station 450 to Affymetrix Mouse Gene 1.0 ST array chips by use of standard Affymetrix protocols. Robust multiarray average was used to normalise the data using Affy (Bioconductor software). Genes were excluded if they did not have an Entrez ID or if their gene expression was less than 100 by non-logged value. Limma, Bioconductor software, was used to apply T-statistics to the data. Differentially expressed genes were identified if they had both a fold change greater than 2 or if the non-adjusted P value was <0.05.

2.2.12 Validation of Microarray Genes

After careful consideration and taking into account known immunological function, and availability of primers and antibodies the following 4 genes were selected to be confirmed at a protein and messenger ribonucleic acid (mRNA) level: complement decay accelerating factor 55 (*cd55*)*, cd52, BTB Domain and CNC homolog 2* (*bach2*) and *XIAP associated factor 1*(*xaf1*).

After 2 weeks of social isolation or social housing whole blood was collected *via* cardiac puncture using 3.2% citrate as an anticoagulant, as there is some evidence that heparin interferes with RT-PCR[202]. 150µl of collected blood was stored in RNeasy Protect Animal Blood Tubes and this sat at room temperature for 2 hours to allow the blood to

lyse. After 2 hours, RNA was extracted using the RNeasy Protect Animal Blood Kit and following the manufacturer's instructions as described previously. RNA was quantified using the Nanodrop 1000.

Complementary DNA (cDNA) synthesis was carried out, by adding 10µl of RNA to 1µl of 0.5µg/µl OLIGO dT primers (Promega, **cat.** C110A) and 1µl of RNase free water. Samples were incubated at 70°C for 10 minutes and placed on ice to cool for 5 minutes. After the 5-minute period, 8µl of a mastermix containing 4µl of AMV reverse transcriptase 5x buffer (Promega, **cat.** M515A), 1µl of RNAsin (Promega, **cat.** N211A), 1µl of RNase free water, 1µl of 10mM dnTP mix (Promega, **cat.** C114B) and 1µl of AMV reverse transcriptase (Promega, **cat.** M5101A) was added and samples were incubated at 42°C for 60 minutes and 10 minutes at 70°C. Samples were cooled to 4°C on ice before being stored at -20°C.

The following was added to 2µl of cDNA to prepare the samples for RT-PCR:

- 20µl of SYBR green mastermix (Applied Bioscience, **cat.** 4309155)
- 4µl of primer for the gene of interest or housekeeping gene
- 14µl of RNase free water

Primers used were as follows: *glyceraldehyde 3-phosphate dehydrogenase (GAPDH)* (Qiagen, **cat.** QT01658692)*, cd55* (Qiagen, **cat.** QT00133994)*, cd52* (Qiagen, **cat.** QT00255339)**,** *bach2* (Qiagen, **cat.** QT0254459) and *xaf1* (Qiagen, **cat.** QT01545033). All samples were loaded in triplicate and run on the BioRad CFX Connect RT-PCR machine using the settings shown in **Table 5**. Genes of interest were normalised to the

house keeping gene, *GAPDH*, and analysed using the $\Delta\Delta C_T$ method of analysis to calculate the fold change.

Table 5: RT-PCR Settings.

Step	Time	Temperature (°C)
Activation	15 minutes	95
3 Step Cycling:		
Denaturation	15 seconds	94
Annealing (40x)	30 seconds	55
Extension	30 seconds	72

2.2.13 *Ex Vivo* Analysis of Peritoneal Macrophages

In order to determine which, if any, TLR pathways were changed after a 2-week period of social isolation in CD-1 mice, peritoneal lavage fluid (PLF) was collected from the mice (n=3 per housing group) by washing the peritoneal cavity with 0.3M ethylenediaminetetraacetic acid (EDTA). Collected PLF was spun down at 264 *g* for 5 minutes at 4°C. The supernatant was removed, and the pellet resuspended in 200µl RNA*later*™ Stabilization Solution (ThermoFisher Scientific, **cat.** AM7020). A Qiagen RNAeasy Mini Kit (Qiagen, **cat.** 74104) was used to extract the RNA according to manufacturer's instructions. In brief, RNA*later*™ Stabilization Solution was removed and the peritoneal macrophage cells were lysed and homogenised. Ethanol was added, and total RNA was bound to the RNAeasy spin column and this was washed 3x before being eluted in 25µl of RNase-free water. Total RNA was quantified using the Nanodrop 1000.

cDNA synthesis was carried out on the 3 samples from each group that had the highest RNA concentrations using the RT^2 First Strand Kit and by following the manufacturer's

instructions. In brief, samples were incubated with genomic DNA elimination mix before being added to the reverse-transcription mix and RNase-free water was added.

Samples were loaded individually onto RT^2 Profiler PCR Array: Mouse Toll-Like Receptor Signalling Pathway Kit plates (Qiagen, **cat.** PAMM-018ZD-6) and were run according to the manufacture's settings on BioRad CFX Connect RT-PCR machine using RT^2 SYBR Green qPCR Mastermix. The fold change was analysed using the $\Delta\Delta C_T$ method of analysis.

2.2.14 Statistics

Significance was tested using the statistical analysis specified in each figure legend on GraphPad Prism 8 (GraphPad Software Inc, USA).

2.3 Results

2.3.1 Weight Change and Nutritional Intake

Weight and nutritional intake were assessed to give an indication of any gross changes in the physiology of the mice. During the 2-week period of social isolation, SI mice weighed significantly less than SH mice (**Figure 2.3a**). SI mice consistently consumed significantly more food than the SH controls (**Figure 2.3b**). Additionally, there was no significant difference in water intake between the housing groups (**Figure 2.3c**). Weight change was assessed over the 2-week period of social isolation to determine whether social isolation would alter female physiology in a different manner to males. Similarly, to male CD-1 mice, SI female mice showed a consistent trend towards gaining less weight compared to SH female mice (**Figure 2.4**). Since food intake was higher in SI mice, satiety was assessed by measuring leptin, the satiety hormone, in plasma from male CD-1 mice. SI mice had a trend towards lower plasma leptin levels than SH mice (**Figure 2.5**).

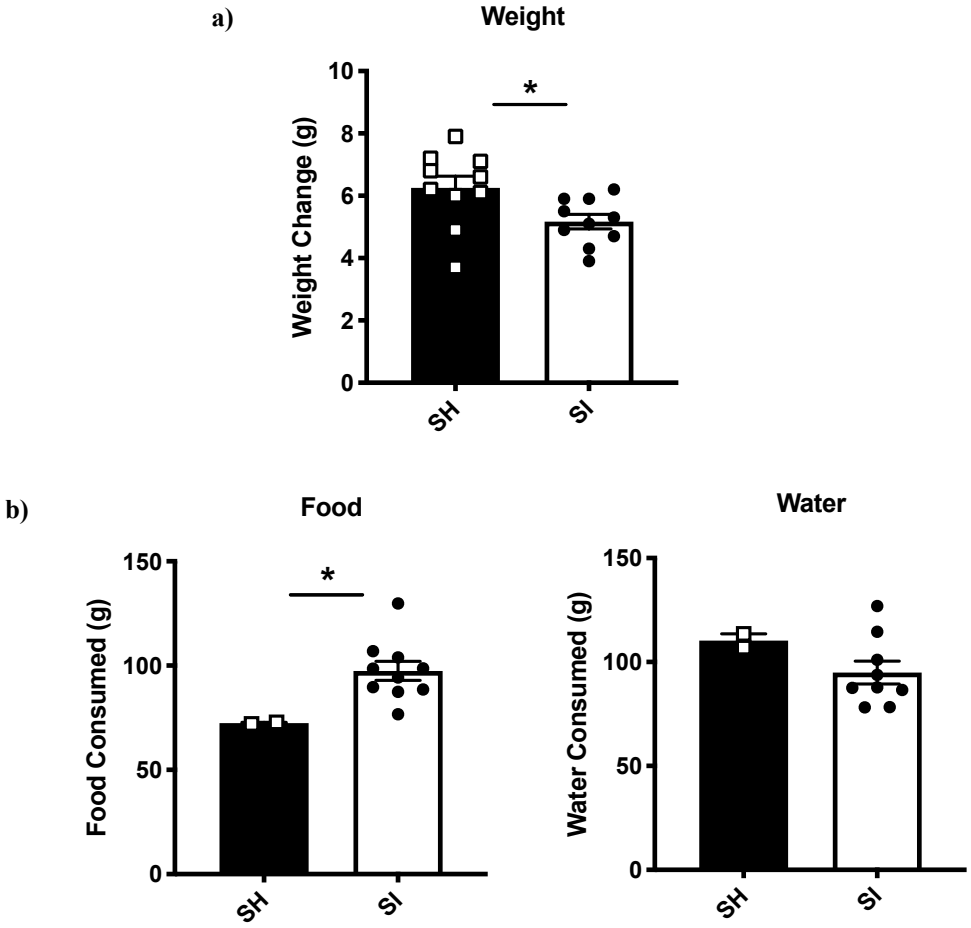

Figure 2.3: Weight and Nutritional Intake in Male CD-1 Mice. The following physiological parameters were assessed: **a)** weight change, **b)** food and water intake over the period of 2 weeks of social housing or social isolation. Each bar shows mean ± SEM of n=10 mice with each symbol representing n=1 mouse for weight change or n=1 cage for food and water intake. Significance was determined when * $p<0.05$ was gained using an unpaired parametric T-test.

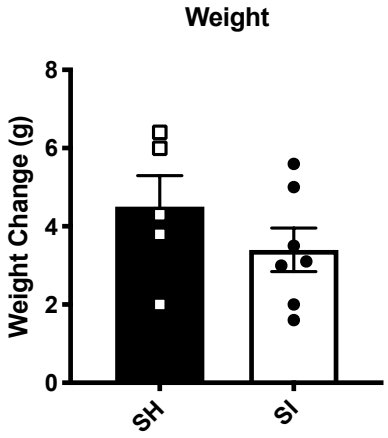

Figure 2.4: Weight Change During Social Isolation in Female CD-1 Mice. Weight change was assessed over the period of 2 weeks of social housing or social isolation. Each bar shows mean ± SEM of n=5-7 mice from a single experiment with each symbol representing a single mouse. Significance was assessed by an unpaired T-test where $p<0.05$.

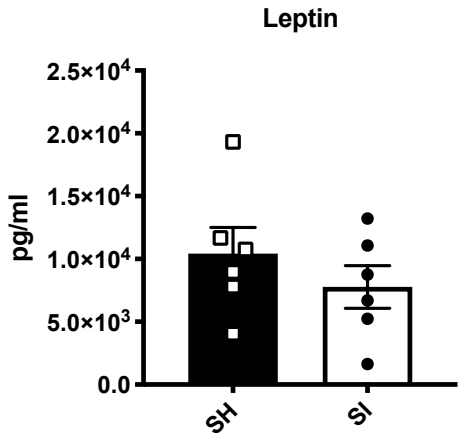

Figure 2.5: Plasma Leptin Levels in Male CD-1 Mice. Plasma leptin levels were quantified after 2 weeks social isolation or social housing *via* ELISA. Values are expressed as mean ± SEM of n=6 mice per housing group with each symbol being representative of a single mouse. Significance was assessed by an unpaired T-test where $p<0.05$.

2.3.2 Visceral Adipose Tissue

Since social isolation has been linked to changes in adipose tissue, particularly increased adiposity, VAT was assessed to determine whether there were any changes in the adipocyte number and size, that might be indicative of metabolic changes[179,183]. Representative images of H & E stained VAT after 2 weeks of social isolation or social housing show that SI mice have increased numbers of smaller adipocytes and SH mice have fewer larger adipocytes present (**Figure 2.6**).

VAT accounted for ~2% of overall body weight in both housing groups (**Figure 2.7a**). VAT was taken from CD-1 mice after 2 weeks of social isolation or social housing. VAT underwent H & E staining to allow for the number of adipocytes to be counted and their area sized, as this can be an initial indication of whether changes in energy expenditure and metabolism had occurred. There was a trend towards increased numbers of adipocytes present in the VAT from SI mice compared to SH mice (**Figure 2.7b**). The adipocytes from VAT showed a trend towards being smaller in SI CD-1 mice compared to SH CD-1 mice (**Figure 2.7c**, p=0.06).

a) **SH Adipocyte Count**= 33

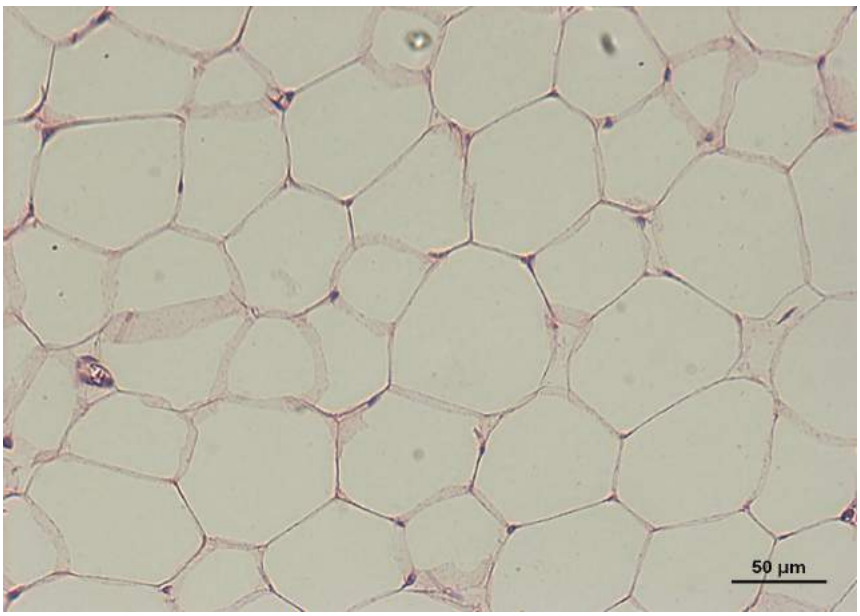

b) **SI Adipocyte Count**= 60

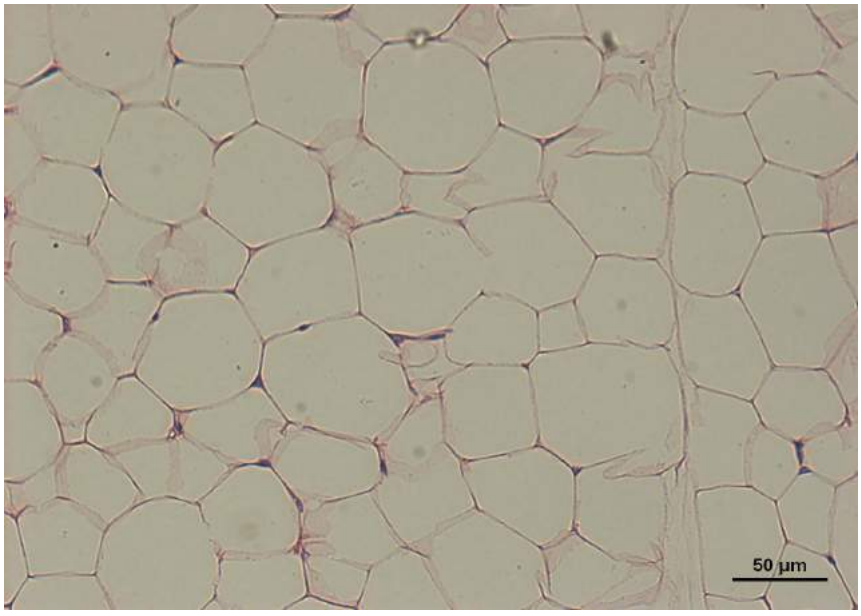

Figure 2.6: Representative CD-1 H&E Stained VAT Images. Representative images of H & E stained VAT at 20x magnification from **a)** SH and **b)** SI CD-1 mice. VAT was taken from n=4-6 mice per housing group. Scale bars are representative of 50µm.

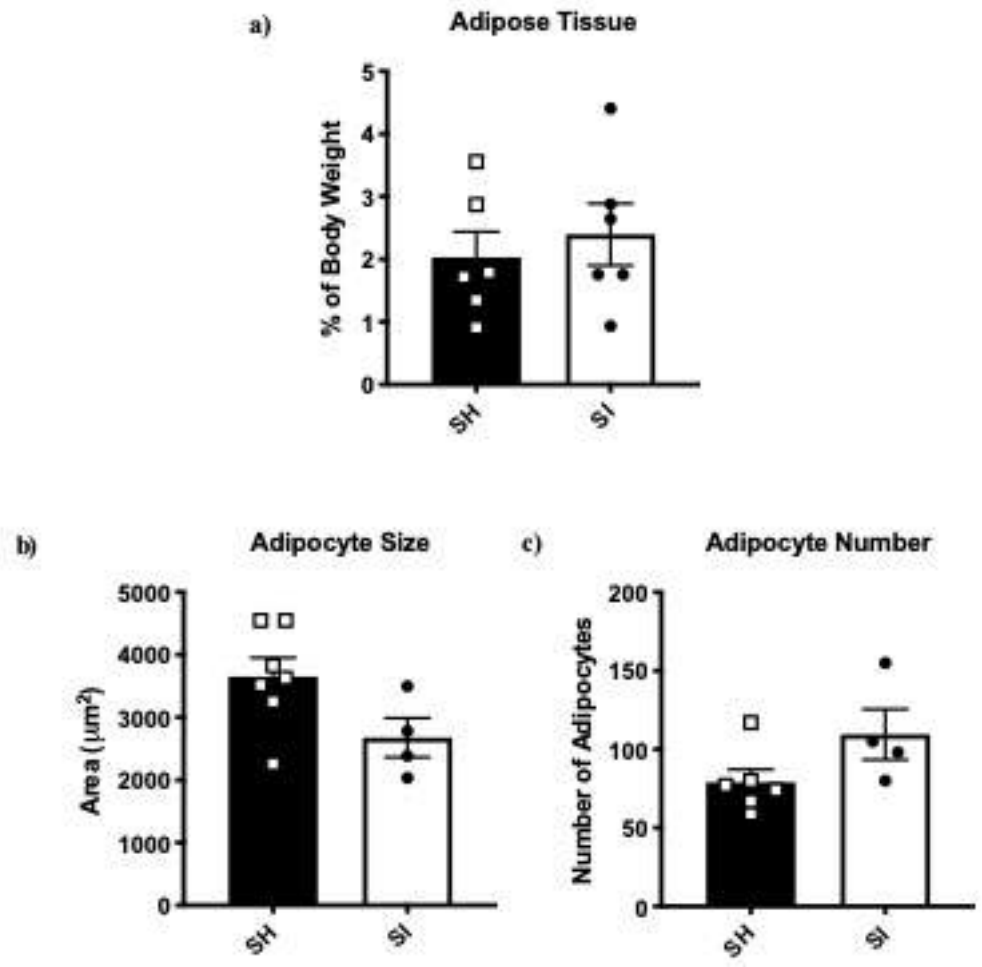

Figure 2.7: VAT Characteristics. VAT was weighed and stained with H & E. The following characteristics were assessed: **a)** VAT as a % of body weight, **b)** adipocyte count and **c)** adipocyte area. Data is shown as the mean value per housing group where n=4-6 mice and each individual symbol is representative of 1x individual mouse. 2x SI mice did not have adipocyte size and number calculated due to problems with sectioning the tissue for staining. Significance was assessed by an unpaired T-test where $p<0.05$.

2.3.3 Faecal Boli Bacterial Analysis

The microbiota composition of SI mice compared to SH mice was characterised in the faecal boli of male CD-1 mice, as it is well known that negative emotions, such as anxiety and the environment, can alter the microbiota[203,204]. After 2 weeks of social isolation, there was a relative increase in the Bacteroidetes classes of bacteria and a decrease in the Firmicutes classes compared to those mice who were subjected to social housing (**Figure 2.8**).

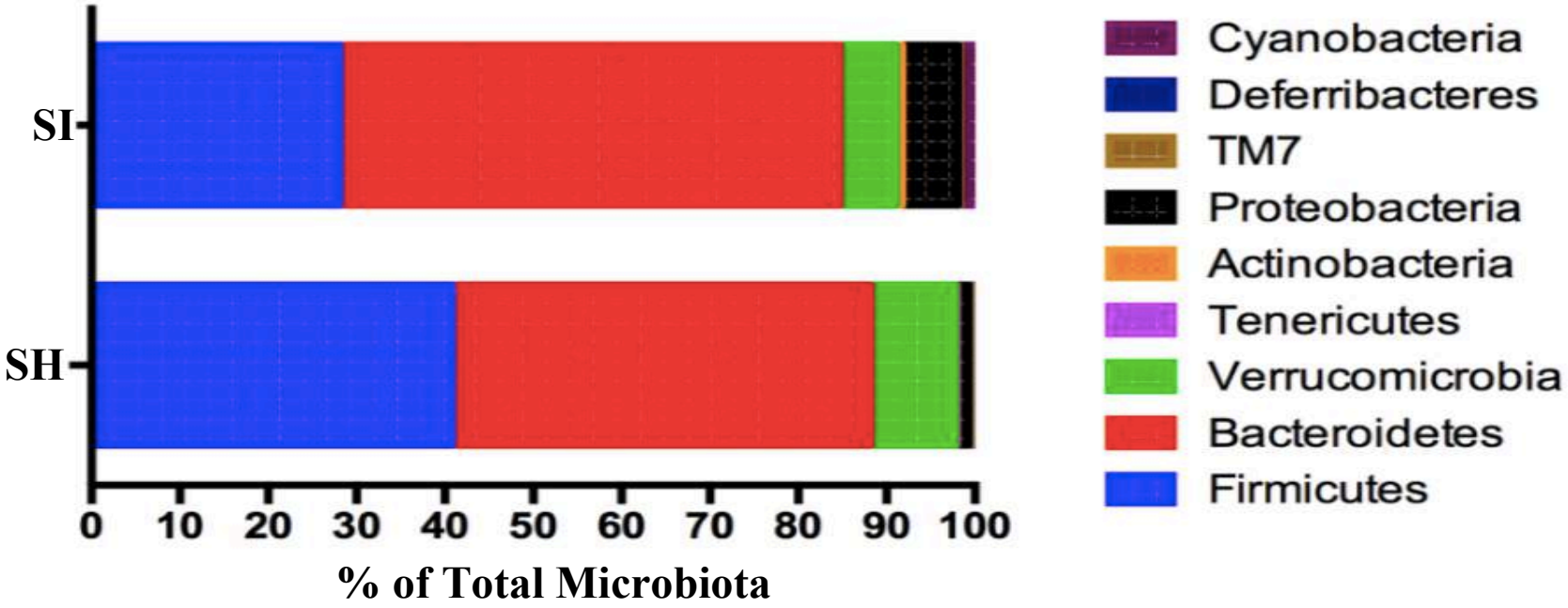

Figure 2.8: Microbiota Composition in Male CD-1 Mice. Faecal boli were pooled from n=4-5 mice and the microbiota taxonomies were expressed in **a)** SI and **b)** SH mice. Taxonomies are presented as a % of the total microbiota present.

2.3.4 Peripheral Blood Analysis in CD-1 Mice

In order, to determine whether the immune system is changed as a basal effect of social isolation, the immune cell profile and levels of inflammation were assessed. After 2 weeks of social isolation or social housing, whole blood was analysed to give the total leukocyte count and the subtypes of leukocytes present, since previous studies on environmental enrichment have shown a differences in whole blood immune cell profile[195]. SI mice and SH mice had similar numbers of leukocytes present, in their whole blood (**Figure 2.9a**). There was a similar number of lymphocytes between the housing groups (**Figure 2.9b**). The number of neutrophils were significantly lower in SI mice compared to SH mice (**Figure 2.9c**). The NLR was significantly lower in SI mice compared to SH mice (**Figure 2.9d**). There was a trend towards slightly lower numbers of monocytes present in SI mice compared to SH mice (**Figure 2.9e)**.

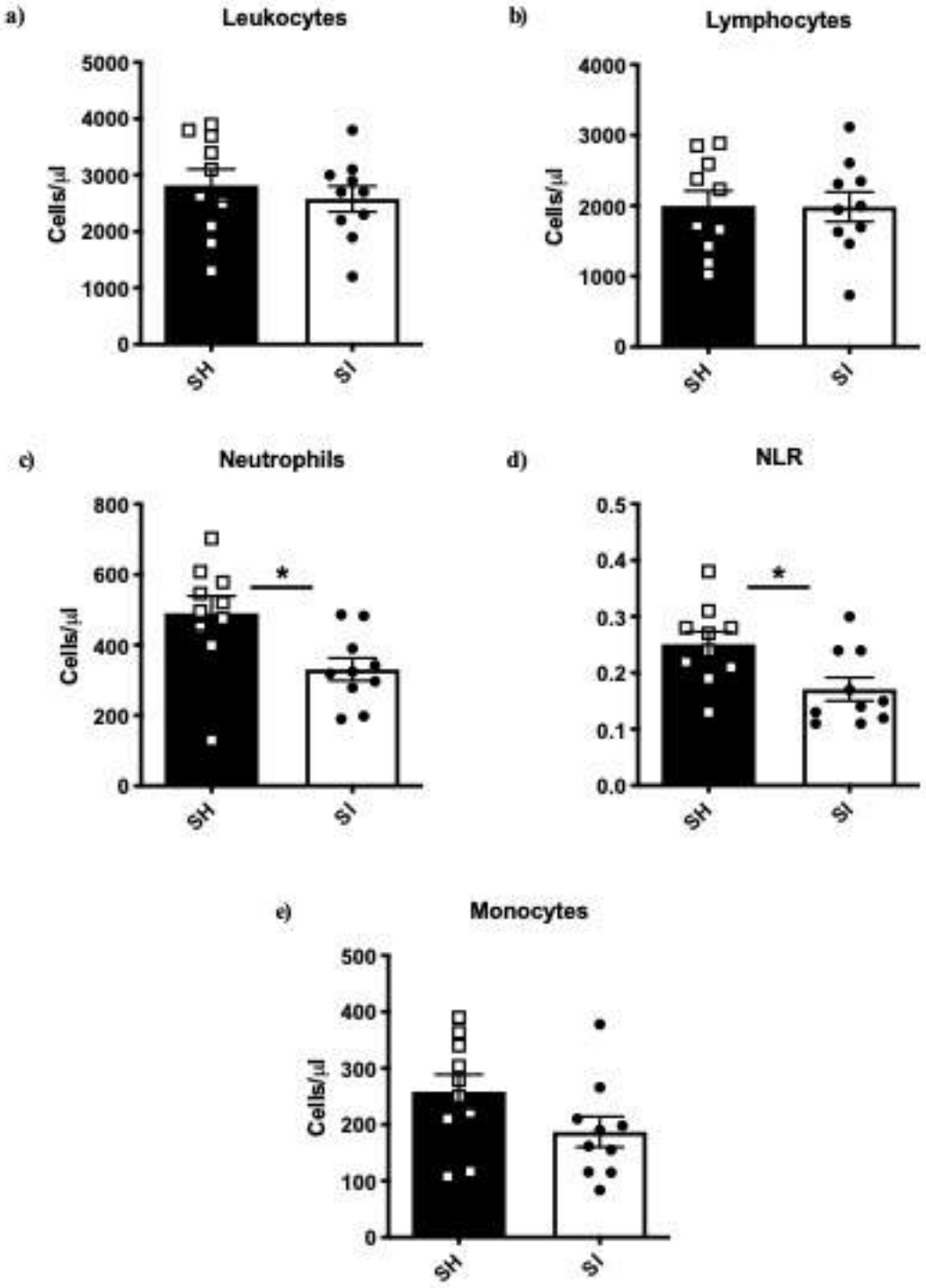

Figure 2.9: Immune Cell Numbers and Profile in CD-1 Male Mice. Basal immune cell response was assessed after 2 weeks social isolation or social housing: **a)** total leukocyte count**, b)** lymphocyte count, **c)** neutrophil count, **d)** NLR and **e)** monocyte count. Each bar shows mean ± SEM of n=10 mice with each symbol representing n=1 mouse. Significance was determined when *$p<0.05$ was gained using an unpaired parametric T-test.

2.3.5 Plasma Cytokines in CD-1 Mice

In order to assess basal inflammation TNF-α, IL-6 and IFN-γ concentrations were measured in plasma after 2 weeks of either social isolation or social housing. However, in basal plasma, TNF-α, IL-6 and IFN-γ concentrations were too low to be accurately detected by the multiplex assay hence the data is not shown.

2.3.6 Biochemical Parameters

To assess whether SI mice had different levels of organ damage the following biochemical markers were assessed: AST, ALT, creatinine and glucose were measured in basal plasma (MRC Harwell). AST and ALT are markers of liver function and damage and it was seen that AST levels were significantly higher in SI mice compared to SH mice, whilst similar levels of ALT were seen between the housing groups (**Figure 2.10a**). Creatinine, which is a marker of kidney function, was not significantly changed between SI and SH mice (**Figure 2.10b**). Plasma glucose levels were found to be significantly higher in SI mice compared to SH mice (**Figure 2.10c**).

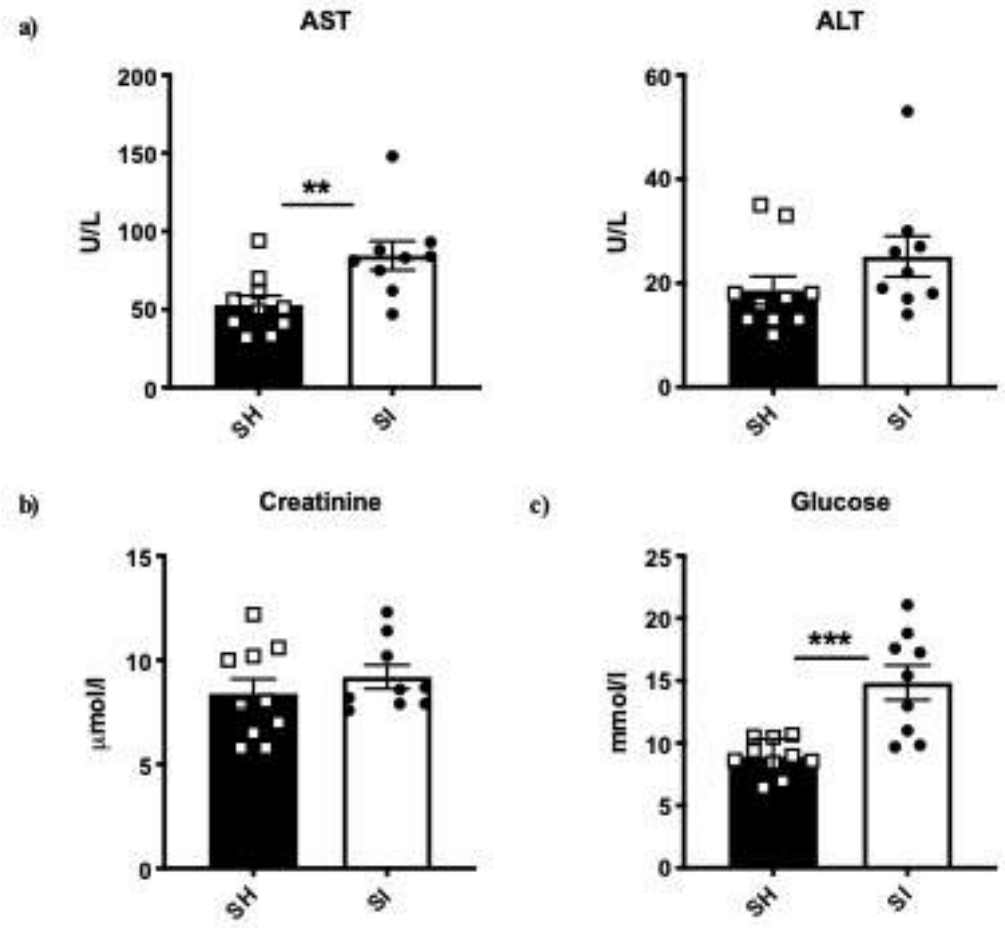

Figure 2.10: Basal Biochemical Parameters. The following biochemical parameters were analysed: **a)** AST (left), ALT (right) **b)** creatinine and **c)** glucose**.** Data shown as mean per housing group ± SEM with n=9-10 mice and symbols are representative of a single mouse. Significance was determined when **p<0.01 and ***p<0.005 as determined by use of an unpaired parametric T-test.

2.3.7 *Ex Vivo* TLR Analysis of Peritoneal Macrophages

TLR signalling was assessed in peritoneal macrophages to see whether social isolation would induce a similar response to that seen in low ranking monkeys, whereby downregulation of the viral response genes and upregulation of the bacterial response genes occurs[153].

To investigate whether social isolation could alter basal gene expression in immune cells TLR signalling pathway genes, 84 in total, were assessed *via* RT^2-PCR profiling array in peritoneal macrophages. The majority of the genes with the largest fold change were involved in MyD88 signalling (**Figure 2.11**).

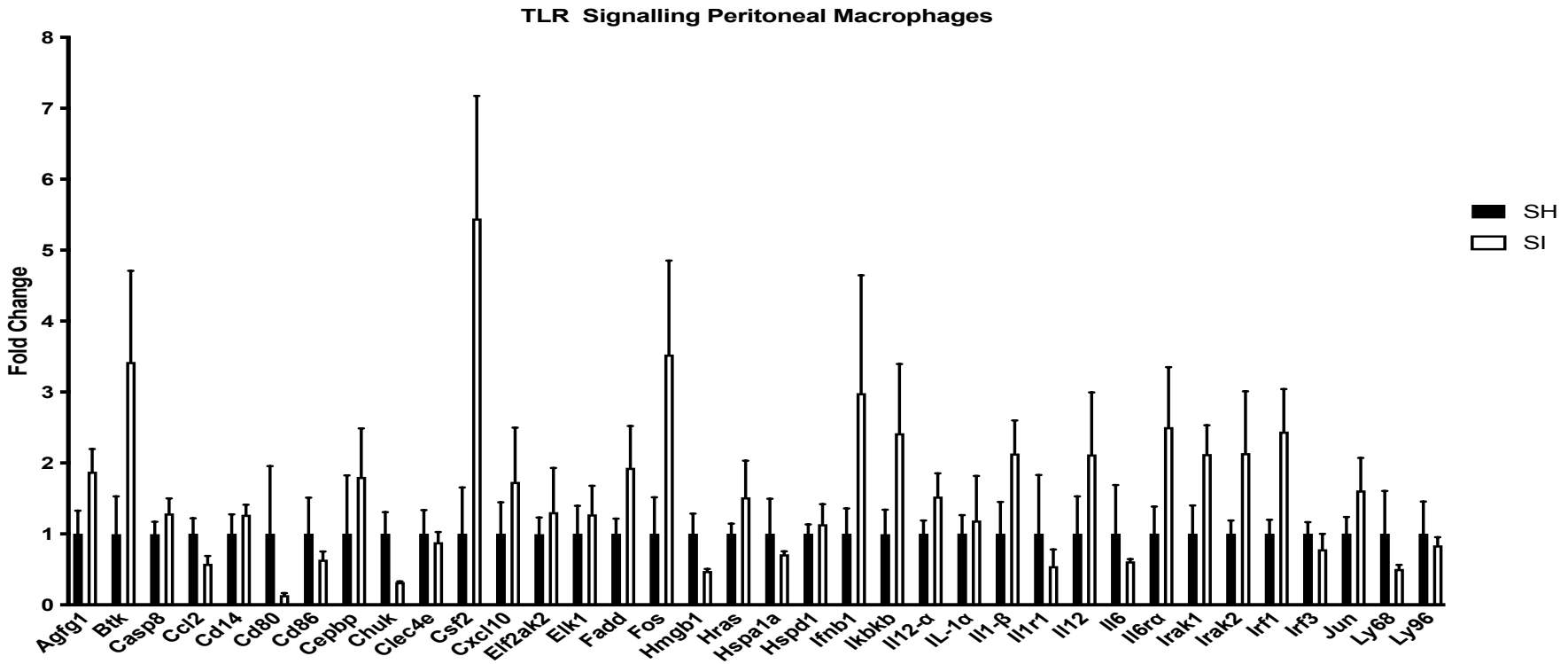

Figure 2.11a: TLR Signalling Gene Expression in Basal Peritoneal Macrophages. Fold gene expression of TLR signalling genes normalised to β2-Microglobulin in social isolation *vs* social housing. Each bar shows mean ± SEM of n=3 mice. Significance was assessed by use of multiple T-tests corrected for by the Holm-Sidak method.

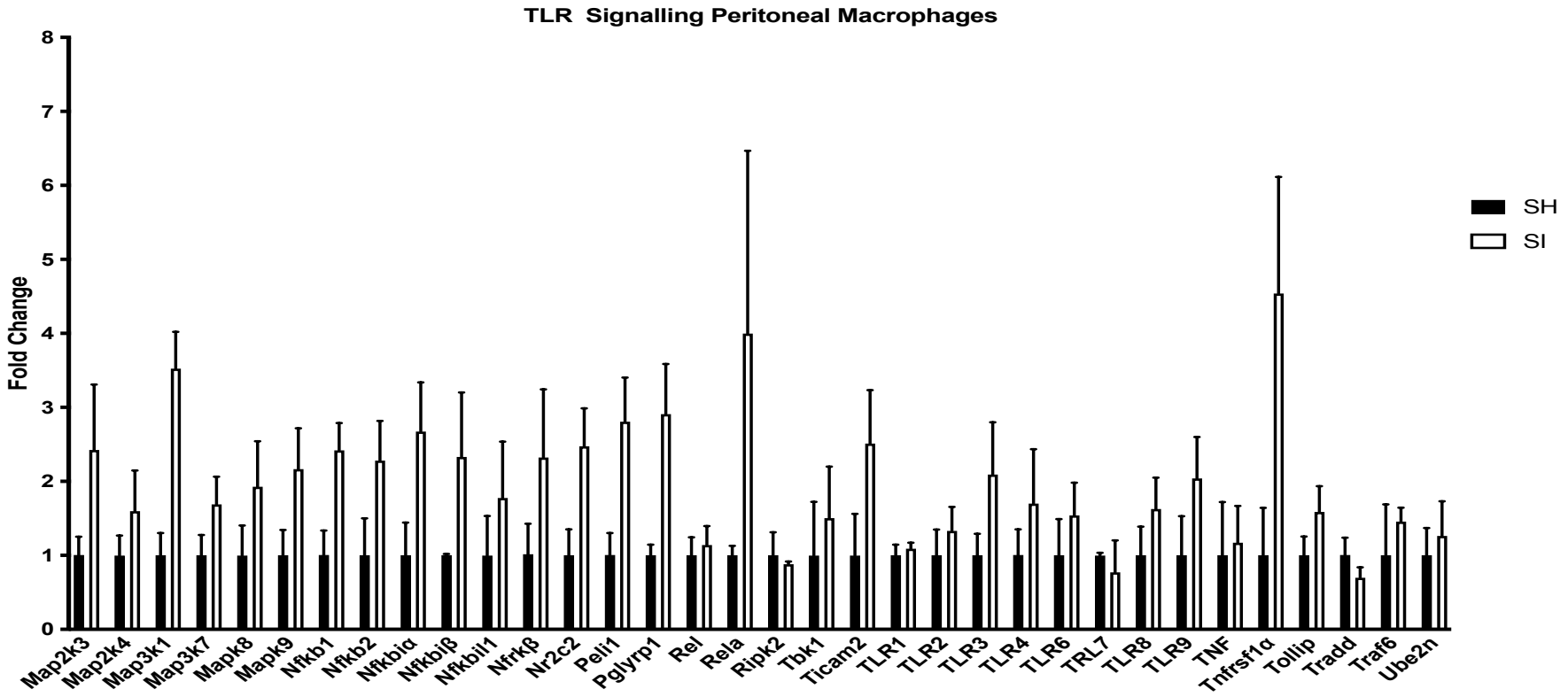

Figure 2.11b: TLR Signalling Gene Expression in Basal Peritoneal Macrophages. Fold gene expression of TLR signalling genes normalised to β2-Microglobulin in social isolation *vs* social housing. Each bar shows mean ± SEM of n=3 mice. Significance was assessed by use of multiple T-tests corrected for by Holm-Sidak method.

2.3.8 Whole Blood Microarray Analysis for Potential Biomarkers of Social Isolation

In order, to identify the potential mechanisms for the observed altered immune response and to find potential biomarkers of social isolation, microarray analysis was carried out on basal blood from SI and SH mice at the end of the 2-week period. Microarray analysis of whole blood at a basal level showed that SI mice have a unique transcriptional fingerprint whereby 26 genes where upregulated (fold change >2 or a non-adjusted $p<0.05$) and 10 genes were downregulated (fold change <2 or a non-adjusted $p<0.05$) (**Figure 2.12**). The differentially expressed genes and their functions if known are listed in (**Table 6**).

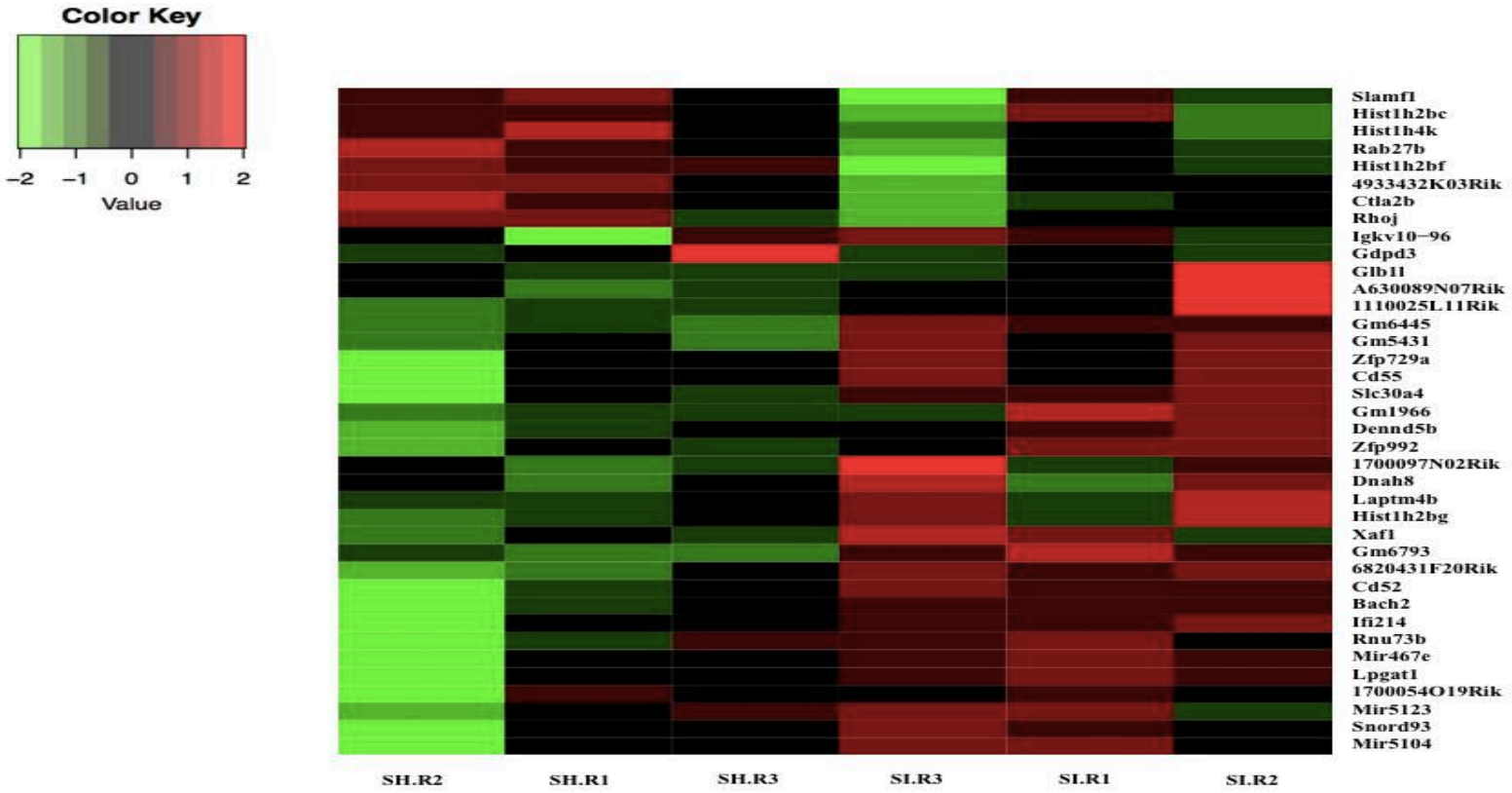

Figure 2.12: Gene Expression in Whole Blood from SI and SH Mice. Microarray analysis was done on RNA extracted from blood in SI *versus* SH mice where n=3 mice per housing group. Bright green represents the most downregulated genes whilst bright red the most upregulated genes.

Table 6: Differentially Expressed Genes in SI Whole Blood.

Gene	Codes	Function	Role in Immune System to Inflammation Related Diseases	Log Fold Change	Non-adjusted P Value
Upregulated Gene During Social Isolation					
Glb1	Galactosidase beta 1	Involved in lysosomal storage[205]	High levels are associated with cellular senescence[1].	1.272	0.00991
Zfp729a	Zinc finger protein 729a	N/A	N/A	1.220	0.00029
Cd55	Complement decay accelerating factor	GPI bound membrane protein involved in inhibition of complement[2]	Inhibits the activation of complement by affecting the C3 and C5 convertases needed for the classic and the alternative pathways. Some evidence it suppresses T cell immunity[206,207]. Nucleotide binding oligomerization domain containing 2 (NOD2) suppresses CD55 on neutrophils thus enhancing production of C5a during polymicrobial sepsis[208].	1.059	0.00048
Slc30a4 or ZnT4	Solute carrier family 30 member 4	Intracellular Zn^{2+} transporter[209].	IL-4 stimulation of M2 macrophages causes metallothionein 3 and SLC30A4 to promote Zn^{2+} storage and thus allow	1.040	0.00029

			pathogens to exploit the Zn^{2+} in order to survive[209].		
Dennd5b	DENN domain containing 5B	Ras associated protein (Rab)39 guanine nucleotide exchange factor – involved in membrane trafficking[210].	N/A	1.030	0.00053
Zfp992	Zinc finger protein 992	N/A	N/A	1.192	0.00014
Dnah8	Dynein axonemal heavy chain 8	Regulates androgen receptor proliferation and transcriptional activity[211].	May influence the tissue biology of adipocytes during obesity by regulating inflammation especially IL-6 and IL-1β[212].	1.459	0.00611
Laptm4b	Lysosomal transmembrane protein 4β	Needed for the formation of autolysosomes *via* aiding the fusion of lysosomes with autophagosomes[213].	Allele variation is associated with increased risk of a number of cancers including breast, liver, ovarian and gastric. Associated with metastasis in breast cancer and ovarian cancer and thus poorer prognosis[214–217]. Interacts with ceramide in late endosomes to aid its removal thus regulating sphingolipid-mediated cell death[218].	1.836	0.00059

			Involved in the recruitment of the LAT1-4F2hc Leu transporter to lysosomes allowing for Leucine to be taken up into the cells thus promoting mTORC1 activation which in turn leads to autophagy[219]. Upregulated in sepsis patients[220].		
Hist1h2bg	Histone cluster 1 h2b family member g	Key component of the nucleosome where it is essential for transcriptional regulation, DNA repair, DNA replication and chromosomal stability[221].	Modified in schizophrenia[221].	1.222	0.0044
Xaf1	XIAP-associated factor 1	Tumour suppressor gene involved in sensitizing death of cells[222]. Needed for KIF1Bβ-mediated apoptosis and acts as a molecular switch for p53 promoting apoptosis as	Interacts with TNF-α to enhance apoptosis by activation of the mitochondrial pathway and cytochrome C release[225].	1.380	0.00018

		opposed to cell cycle arrest[223–225].			
Cd52	Cluster of differentiation factor 52	Antigen expressed on the cell surface of B and T lymphocytes, monocytes and NK cells[226].	Involved in the activation of complement and is targeted by antibodies in the treatment of chronic lymphocytic leukaemia, RA and multiple sclerosis amongst other diseases[226]. Upregulated in the prefrontal cortex in response to pain in mice[227].	1.044	0.00044
Bach2	BTB domain and CNC homolog 2	Transcription factor involved in adaptive immune cell differentiation[228].	Promotes T cell effector memory by reducing the availability of activator protein-1 thus limiting the expression of TCR driven[228]. Promotes antibody class switching in B cells by repression of plasma cell regulatory genes[229]. Mediates antiapoptotic and anti-oxidative properties during treatment with Bortezomib in Mantle cell lymphoma[230].	1.048	$5.00x10^{-4}$

Ifi214	Interferon activated gene 214 protein	N/A	N/A	1.379	0.00037
Rnu73b	U73B small nuclear RNA	N/A	N/A	1.052	0.00146
A630089N07Rik	N/A	N/A	N/A	1.189	0.00204
1110025L11Rik	N/A	N/A	N/A	1.033	0.00056
1700097N02Rik	N/A	N/A	N/A	1.470	0.00029
6820431F20Rik	N/A	N/A	N/A	1.530	1.00×10^{-5}
1700054O19Rik	N/A	N/A	N/A	1.091	0.00041
Mir467e	MicroRNA 467e	N/A	N/A	1.142	0.00027
Mir5123	MicroRNA 512	N/A	N/A	1.068	0.01302
Mir5104	MicroRNA 5104	N/A	N/A	1.215	0.00051
Gm6445	Predicted gene 6445	N/A	N/A	1.034	7.00×10^{-5}
Igkv10-96	Immunoglobulin kappa variable 10-96.	Makes up part of the kappa variable region of immunoglobulins[231].	N/A	1.073	0.04822
Gm6793	Predicted gene 6793	N/A	N/A	1.104	6.00×10^{-5}
Lpgat1	Lysophosphatidylglycerol Acyltransferase 1	Catalyses the reacylation of lysophisphatidylglycerol to phosphatidylglycerol, an important membrane	Thought to be associated with obesity by influencing BMI in Pima Indians[233]. Some variants have been shown to be associated with lower levels of steric acid[234].	1.007	0.00118

		phospholipid precursor for cardiolipin which is a component of the inner mitochondrial membrane[232].			
Snord93	Small nucleolar RNA, C/D box 93	N/A	N/A	1.183	0.00297
Downregulated Genes During Social Isolation					
Slamf1	Signalling lymphocytic activation molecule 1	Acts as a microbial sensor for gram negative bacteria e.g. *E.coli*[235].	Regulates bacterial phagosome functions in macrophages by the recruitment of the Vps34 proteins needed for regulation of NADPH oxidase 2 and membrane fusion[235].	-1.042	0.00206
Hist1h2bc	Histone H2B type 1 c	Key component of the nucleosome where it is essential to transcriptional regulation, DNA repair, DNA replication and chromosomal stability[221].	N/A	-1.159	0.0085

Hist1h4k	Histone H4 type 1 k	Key component of the nucleosome where it is essential to transcriptional regulation, DNA repair, DNA replication and chromosomal stability[221].	N/A	-1.538	$8.00x10^{-5}$
Hist1h2bf	Histone H2B type 1 F	Key component of the nucleosome where it is essential to transcriptional regulation, DNA repair, DNA replication and chromosomal stability[221].	N/A	-1.192	0.00013
Rab27b	RAB27B	Membrane bound proteins with roles in vesicular trafficking and is particularly involved in the distribution of	Regulates neutrophil azurophilic granule exocytosis and is involved in the exosome secretion pathway[236]. Regulates neutrophil chemotaxis by regulating primary granule exocytosis[237]. Regulates the	-1.018	0.00051

		secretory granules near the plasma membrane[236].	department where nicotinamide adenine dinucleotide phosphate oxidase is stored in activated macrophages[238].		
Ctla2b	Cytotoxic T lymphocyte-associated protein 2β	Novel cysteine proteinase inhibitor[239].	Expressed in T cells and mast cells. Induced by IL-4 during T2 polarisation[240,241]. Upregulated during chronic stress in the hippocampus of mice[242].	-1.006	0.00063
Rhoj	Ras homolog J	Rho GTPase involved in the following: endocytic pathway, differentiation of adipocytes, endothelial motility and focal adhesion[243].	Hypomethylation linked to discoid rash in SLE and is thought to promote apoptosis[244]. Upregulated in response to infection in zebrafish[245].	-1.070	0.03066
Gdpd3	Glycerophosphodiester Phosphodiesterase Domain Containing 3	Lysophospholipase[246].	Potential marker of memory T cells[247].	-1.957	0.01235
4933432Ko3Rik	N/A	N/A	N/A	-1.182	0.00014

2.3.9 Validation of Microarray Genes

The microarray genes were confirmed at a transcriptional level in whole blood using RT-PCR to ensure they were true biomarkers of social isolation. *cd52*, *cd55* and *bach2* were significantly upregulated in SI mice compared to SH mice **(Figure 2.13**). *Xaf1* had a trend towards a higher fold change in SI mice compared to SH mice **(Figure 2.13c**).

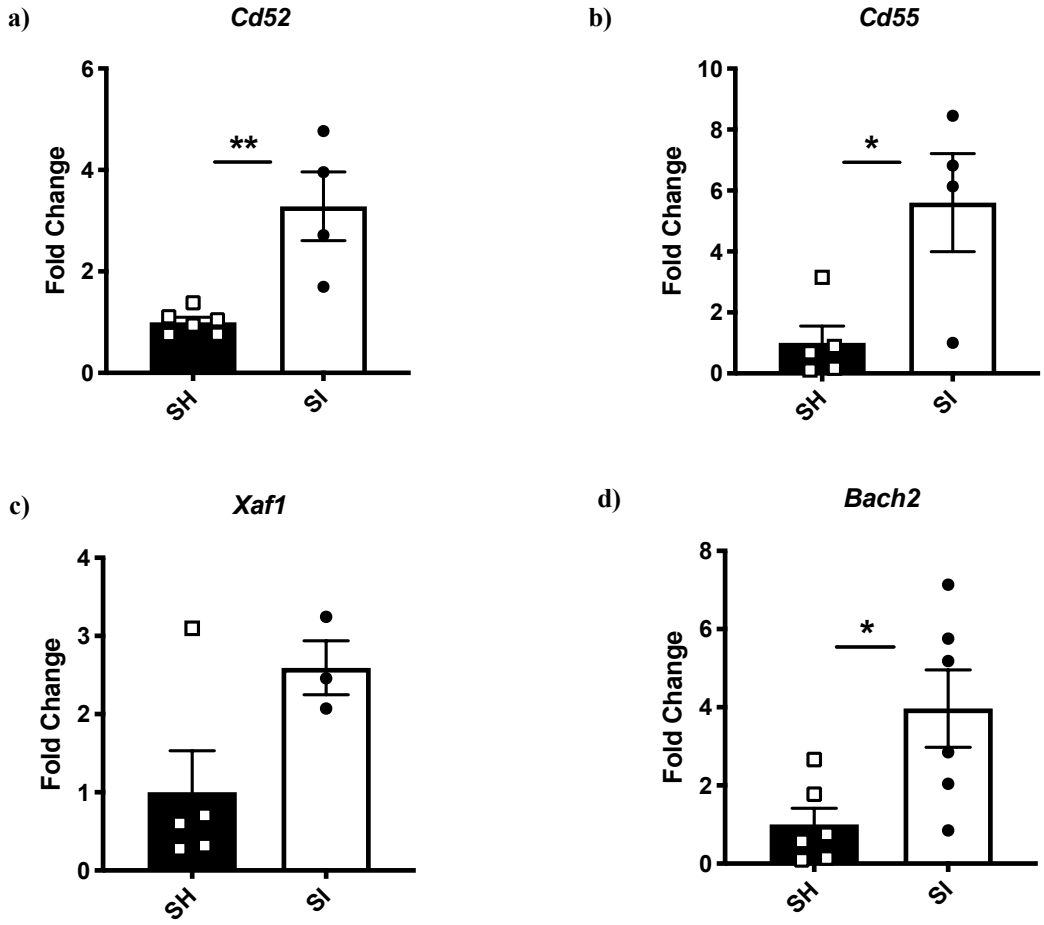

Figure 2.13: Validation of Microarray Genes in Male CD-1 Mice. Fold change was calculated for the following genes by RT-PCR to confirm microarray data. The following genes were tested: **a)** *cd52*, **b)** *cd55*, **c)** *xaf1* and **d)** *bach2*. Data points are representative of a single mouse where n=3-6 mice per housing group and bars representing the mean ± SEM. Mice were excluded if the ct value for the gene of interest was above 35. Significance was determined when p*<0.05 and **p<0.01 as assessed by an unpaired parametric T-test.

2.4 Discussion

This chapter aimed to assess the basal effects of social isolation. It was demonstrated that SI mice have increased food intake but do not gain as much weight over the period of 2 weeks. Social isolation was shown to alter the NLR and to upregulate the MyD88 pathway in peritoneal macrophages. Microarray analysis revealed that short-term social isolation caused a unique transcriptional fingerprint to be seen in whole blood. Microbiota analysis of faecal boli showed that the microbiome is altered after social isolation.

SI CD-1 mice were found to not put on as much weight as SH mice despite eating more over the 2-week period of social isolation. This differs from studies carried out in C57BL/6 mice that underwent social isolation for either 3 weeks or 8 weeks where SI mice were found to have similar weights to SH mice whilst having lower food intake[248,249]. It is possible that if the time period of social isolation was extended, that SI mice might weigh the same as the SH mice. However, one study using CD-1 mice to investigate the effect of social isolation on weight over a period of 42 days found similar results whereby SI mice consistently weighed 2-3% less than SH mice suggesting that this finding could be strain dependent[250]. Mice are known to be sociable creatures who huddle together for warmth and it is known that huddling can increase metabolic efficiency by 40–65%[251,252]. In the absence of huddling, it is possible that the increased food intake seen accompanied by little weight gain in SI mice is the result of increased energy demand to fulfil the need for increased thermogenesis to maintain body temperature. Interestingly, it has been reported that female mice are more likely to huddle for warmth, have enhanced BAT thermogenesis, and were warmer in the absence of littermates compared to males, suggesting this effect may be potentiated in female mice[251]. Sociability is known to play a role in thermoregulation. For example, in

macaques, the social behaviour of grooming was predictive of huddle size, whereby those individuals who were more sociable had a greater huddle size which is suggestive of reduced energy expenditure and exposure to the environment, potentially explaining how sociality affects survival[252]. Additionally, studies have shown that the wood chippings in cages are not sufficient to aid mice in terms of insulation[253,254]. Since mice are normally housed at an ambient temperature of 20-24°C which is below their lower critical temperature, estimated to be ~30°C, this raised the question of whether or not SI mice were cold as they could not huddle for warmth[254] .

Leptin, the hormone of satiety, was measured in plasma to determine whether social isolation could alter appetite, with the expectation that it would be lower in SI mice as they eat more[255]. Plasma leptin concentrations were found to be among the normal range, 1-20ng/ml, in both housing groups although concentrations showed a trend towards being decreased in those mice subjected to social isolation compared to controls[256]. This disagrees with previous studies investigating social isolation in C57BL/6 mice, where serum leptin levels were increased accompanied by decreased food intake[182]. However, social stress and chronic social defeat have been shown to decrease leptin levels[257,258]. The majority of studies investigating the effects of both acute and long-term periods of cold, such as that hypothesised to occur in SI mice, showed that leptin levels decrease[259–261]. Further appetite hormones such as ghrelin should be tested to better understand whether appetite is affected by social isolation.

VAT was found to account for a similar % weight between the housing groups used in this study. This is in contrast to the literature where VAT accounts for a higher % of body weight in those rodents who were subjected to social isolation. However, this difference might be accounted for by the longer period of social isolation, 7-8 weeks, used in these

studies compared to the shorter 2 weeks used in this study[182,183]. Interestingly, the size of adipocytes showed a trend towards having a smaller area in SI VAT compared to SH VAT, despite similar adipocyte counts being present. Adipocytes store excess triglycerides and the more triglycerides they store, the more hypertrophic they become, thus smaller adipocytes would be suggestive of more energy being expended. There are two possible reasons why more energy would be being expended: increased thermogenic demand due to absence of littermates to huddle with, or increased locomotion[262,263]. Locomotion was not tested in these studies, but the concept of increased thermogenic demand is discussed in **Chapter 4**. There is contrasting findings in the literature with regards to social isolation and locomotor activity with some studies finding no change in locomotor activity and others finding increased locomotor activity[179,263].

Plasma glucose levels were found to be significantly higher in SI mice compared to SH mice, which is in concordance with a study carried out in humans where social exclusion was found to be associated with higher blood glucose levels[264]. Similarly, a study has shown that CD-1 mice subjected to chronic social defeat model, were found to have hyperglycaemia, glucose level >8.83mmol/l. Interestingly, this change appeared to be independent of insulin sensitivity, which was unaffected, in the chronic social defeat model. Since SI mice in our study had an average glucose level of 14.85mmol/l, this suggests that social stress can increase the risk of hyperglycaemia[265]. The increased plasma glucose seen in SI mice is interesting since there is evidence to suggest that social isolation increases risk of T2D and this implies that the increased risk cannot be accounted for alone by diet and sedentary lifestyle alone[177].

Leptin is a satiety hormone so the trend towards lower leptin levels in SI mice partially facilitates increased food intake seen in SI mice and therefore, might account for the

increased glucose levels seen in SI mice. However, it is important to note that leptin, as well as supressing appetite, also contributes to glucose uptake into the skeletal muscle and BAT[266,267]. Thus, the lower levels of leptin seen in SI mice would suggest less glucose is being taken up into the skeletal muscle and BAT, causing there to be higher circulating levels of glucose as measured in the plasma of SI mice. However, since the difference in leptin levels is neither significant nor very large, it is unlikely to account completely for such a profound change in plasma glucose level in SI mice.

Another factor that might account for the increased glucose levels seen in SI mice, could be their increased food intake. Ideally, to avoid any differences in plasma glucose being the result of food intake, mice would be fasted, but this was not possible as the protocol required to carry out this was not on the group's Home Office Project License[268]. To minimise this samples were taken in the morning during the light cycle, since mice consume 2/3rd of their food during the night due to their nocturnal nature[269,270]. Similarly, plasma glucose in non-fasted mice follows a circadian rhythm, whereby plasma glucose is lowest in the night and increases during the light period. It is for this reason that, where possible, blood for glucose testing was taken first thing in the morning to give as close as possible reading to what would be seen in the fasted state as glucose uptake primarily occurs in the dark cycle[271,272]. It is unlikely that differences in food intake could completely account for the increased plasma glucose levels as the samples were taken in the light cycle. Due to the nature of social housing, it is impossible to know how much food each individual mouse actually consumes, as food intake is measured per cage and an average calculated to gain an estimated food intake/mouse. If the exact food intake was known in each SH mouse this could be checked against their individual plasma glucose values to see if there is any significant correlation between food intake and

plasma glucose, which might help to determine the likelihood of whether food intake could be accounting for the increased plasma glucose levels seen in SI mice.

AST concentration was demonstrated to be higher in the plasma from SI mice compared to SH mice. AST is traditionally thought of as a marker for liver function, although it is not as specific as ALT, as it is also found in cardiac and skeletal muscle, brain, pancreas, lungs, erythrocytes and leukocytes[273]. This suggests that SI mice have higher levels of generalised basal inflammation, since ALT, a specific marker for liver function, and creatinine, a marker of kidney function, did not differ between housing groups.

There were no differences in the number of leukocytes and lymphocytes present. Although there was no significant difference, there was a definite decrease in circulating monocytes. The number of neutrophils and the NLR was significantly lower in SI mice compared to SH mice. The NLR is considered to be a marker of subclinical inflammation, whereby high NLR scores are indicative of poor prognosis in cancer and sepsis, premature mortality, CHD and heart failure[274–277]. Therefore, this finding of a lower NLR in SI mice compared to SH mice is somewhat surprising, since those individuals who have high levels of social isolation or loneliness are at increased risk of chronic inflammatory diseases and premature mortality[119,147,176,177]. One possible reason why such a finding might occur, is that in non-lonely people, as cortisol levels increase so does the NLR ratio, but such a response is blunted in individuals who are lonely[278].

TLR pathway analysis of basal peritoneal macrophages revealed that one of the largest gene expression changes was *colony stimulating factor 2* (*csf2*). Csf2 stimulates the production of macrophages and granulocytes as well as promoting survival[279,280]. Additionally, Csf2 primes macrophages towards a more activated pro-inflammatory state, thus it would be interesting to profile the cell types in the peritoneal cavity at

baseline[281]. Csf2 levels increase upon infection and have been implicated in inflammatory diseases including arthritis and atherosclerosis[282,283]. Recombinant Csf2 was tried in clinical trials as a way of treating neutropenia and leukopenia during the immunosuppressive stage of sepsis, with initial results showing improved outcomes[284–286]. It should be noted that due to a small n number (n=3 per housing group), more pronounced differences may be present than shown here. Although not significant, there was a trend towards the *MYD88* pathway genes being higher in basal peritoneal macrophages from SI mice compared to SH mice. This is not surprising since studies looking at social status in macaques and humans demonstrated those with low status had enrichment of the *MYD88* pathway genes at the expense of the *TRIF* pathway genes i.e. a primed bacterial response[153].

Initial studies, comparing the microbiota in faeces from SI CD-1 mice to SH CD-1 mice, showed a change in the types of bacterial phyla, which is not surprising since there is emerging evidence that shifts in microbiota have been shown to be involved in a number of mental illnesses including depression and anxiety disorders[91,287,288]. For example, patients with generalised anxiety disorder had reduced microbial richness and diversity, accompanied by short-chain fatty acid-producing bacteria, whilst patients with depression were found to have a lower % of Firmicutes composition in the microbiota and altered microbial metabolite production[91,287,288].The most notable shift was seen in the proportions of the Bacteroidetes and the Firmicutes phyla in SI CD-1 mice compared to SH CD-1 mice. SI CD-1 mice have a lower Firmicutes:Bacteriodetes ratio compared to SH CD-1 mice. There is some debate about whether the Firmicutes:Bacteriodetes ratio is correlated to BMI, with some studies showing a higher Firmicutes:Bacteriodetes ratio being correlated to increasing BMI, whilst other studies reported seeing no change in the ratio[190,289–291]. Therefore, it is possible that the shift in microbiota seen in SI mice could

partially account for the lower weight gain seen in SI mice. Additionally, the lower % of firmicutes composition of the microbiota seen in SI mice, has been potentially linked to depression in humans[288].

A higher proportion of the microbiota in SI CD-1 mice was attributed to the Proteobacteria phylum. There are studies indicating that members of the Proteobacteria phylum might be involved in microbiota dysbiosis and thus be implicated in metabolic diseases such as T2D[88]. It is possible that over a prolonged period of time, such a shift could account for the increased incidence of the aforementioned diseases in people who are lonely or isolated[152,292–294]. Actinobacteria was present only in the faeces from SI CD-1 mice but not SH CD-1 mice, whereas the Tenericutes phylum was only seen in SH CD-1 mice. This result was also seen in mice subjected to chronic social defeat stress for 10 minutes each day for a period of 10 days[295]. This suggests that social stress might account for this shift in microbiota composition. Additionally, it has been noted that rheumatoid arthritis (RA) patients have increased prevalence of Actinobacteria in their gut, which would suggest SI mice might be more susceptible to RA[296]. This suggests that an increase in Actinobacteria accompanied by a decrease in Tenericutes in murine faeces, might have the potential to be a biomarker of social stress.

The Verrucomicrobia phylum accounted for a lower % of the microbiota seen in faeces in SI CD-1 mice compared to SH CD-1 mice. This phylum has been proposed to be a biomarker of microbiota health, as it has been seen to become more prevalent during remission in inflammatory bowel disease (IBD)[297]. Similarly, the TM7 phylum was unique to SI CD-1 mice. TM7 has been associated with inflammatory mucosal diseases such as periodontitis and IBD where it is thought to alter the local environment to promote a more pro-inflammatory microbiota[298,299]. It is possible that longer periods of

social isolation would cause a further increase in the % of microbiota by the TM7 phylum resulting in the promotion of inflammation, which may account for the increased prevalence of inflammatory disease in SI people[120,147]. Cyanobacteria was only detectable in the faeces from SI CD-1 mice. This is perhaps not surprising, since faeces from SI CD-1 mice had a much more potent smell compared to that of SH CD-1 mice that could be potentially accounted for by the increase in cyanobacteria present, which are well known reducers of sulphate[300].

These findings suggest that just 2 weeks of social isolation can alter the proportions and numbers of different bacteria phyla present in the faeces. Interestingly, our findings concur with that found in a small scale study looking at faecal microbiota from patients with major depressive disorder, where the Bacteroidetes, Proteobacteria and Actinobacteria phyla were increased whilst the Firmicutes phylum was decreased[90]. This highlights a close link between emotional wellbeing and the microbiota. Currently, the majority of the changes seen in the phyla present in the faeces would suggest that social isolation promotes the presence of inflammation. However, what is not as clear is what the long-term effects of social isolation might have on the microbiota present in the faeces. Since mice are coprophagic animals, it is possible that the SH mice could influence their microbiota by the consumption of other mice's faeces, an issue that could be overcome by the use of metabolic cages[301]. Additionally, further work is needed to determine which classes within each of the phyla have been altered by social isolation, to better understand how changes in the microbiota may predispose the body to inflammation and/or chronic diseases.

Since people who were identified with having high levels of perceived loneliness have been shown to have a unique gene expression pattern known as CTRA and show other

potential immunological biomarkers of loneliness (IL-6, CRP and fibrinogen), it was investigated whether social isolation would cause changes in gene expression[175,184,302,303]. Additionally, since EE mice, the polar opposite model to social isolation, have their own unique gene expression pattern, it was thought that SI mice would have the opposite effect on the same gene expression[155]. As of yet there have been no studies that have looked at the immunogenotype of social isolation in mice and in order to attempt to do this, microarray analysis was performed on RNA from whole blood from SI and SH mice. To this end, whole blood microarray analysis was carried out and 36 genes were found to be differentially expressed, 26 upregulated and 10 downregulated, with the majority of these having immunological functions or promoting apoptosis. In the polar opposite model, environmental enrichment, 8 genes were upregulated and 5 were downregulated in the blood, with the differentially expressed genes having roles in metabolism and regulation of the immune system. Interestingly, apart from *RhoJ*, which was upregulated in EE mice and downregulated in SI mice, both paradigms have their own unique gene expression pattern, suggesting that each emotion and environment will have its own unique expression pattern[155]. Four of the most immunologically interesting genes were chosen for confirmation by RT-PCR: *cd55*, *cd52*, *xaf1*, and *bach2.* With the exception of *xaf1*, which only showed a trend towards being upregulated in SI mice, all the other chosen genes were significantly upregulated confirming the microarray data.

The main role of the CD55, a surface membrane protein, is to inhibit the activation of complement by affecting the C3 and C5 convertases involved in both the classical and the alternative pathways[207]. CD55 protects neuronal cells against chemical hypoxic-induced injury *via* reduction in cell death and apoptosis and partially protects against neuroinflamamtion[304]**.** Interestingly, there is evidence to suggest that *cd55* expression is suppressed on neutrophils by NOD2-mediated signals during polymicrobial sepsis, thus

promoting C5a production. C5a has been linked to multiple organ failure, dysfunctional coagulation and cardiomyopathy[208]. There is evidence to suggest that CD55 may be implicated in atherosclerosis, as *cd55* deficiency in *ApoE*$^{-/-}$ mice was found to increase C3a production, leading to increased adiposity, altered lipid handling, as well as atheroprotection[305]. Since SI mice have elevated *cd55* levels this would suggest that they would also have increased plaque.

CD52 is a glycoprotein found on the surface of mature lymphocytes, monocytes and NK cells. It is currently targeted by antibodies in the treatment of RA and chronic lymphocytic leukaemia[226]. Interestingly, it has been found to be upregulated in the prefrontal cortex during pain[227]. CD52 is involved in apoptosis of cells by inhibition of TLR activation of NFκB[306]. This is interesting as apoptosis, in contrast to necrosis, does not promote a pro-inflammatory immune response, as apoptotic cells normally keep their membrane integrity preventing the release of DAMPs. In fact, apoptosis can promote macrophages to release anti-inflammatory cytokines, such as IL-10, thus having higher levels of *cd52* may be beneficial in promoting resolution of inflammation during chronic inflammatory diseases, such as atherosclerosis[307].

Bach2 is a transcription factor that is involved in adaptive immune cell differentiation. More specifically Bach2 promotes T cell effector memory and antibody class switching in B cells[228,229]. Interestingly, *Bach2* was found to have the highest fold change in peripheral blood mononuclear cells in patients suffering from peripheral artery disease (PAD) compared to healthy controls. As PAD is caused by the accumulation of fatty deposits in the leg, it is possible that Bach2 may play a role in the pathogenesis of atherosclerosis, although to elucidate its exact role in vascular disease, further studies

looking at downstream markers are needed[308]. Bach2 has also been shown to promote apoptosis during oxidative stress in cancer[230,309].

Xaf1 is a tumour suppressor gene, which is essential for KIF1Bβ-mediated apoptosis and it acts as a molecular switch for p53, promoting apoptosis as opposed to cell cycle arrest[223–225]. *Xaf1* gene expression has been found to be decreased in blood at the onset of sepsis shock and recovered to normal levels within 48 hours in patients with a low Simplified Acute Physiology Score II (SAPSII) score, whilst recovery of Xaf1 was delayed in those with high SAPSII scores[310].

These results show that just 2 weeks of social isolation can induce a unique transcriptional fingerprint in mice. The majority of the genes significantly changed were involved in the differentiation of immune cells and the promotion of apoptosis, suggesting social isolation primes the immune system ready for infection and promotes a more anti-inflammatory phenotype for cell death. These unique genes could potentially be used as biomarkers of social isolation after further validation in animal and human models, allowing for a more personalised approach to the treatment of patients with inflammatory diseases.

In conclusion, short-term social isolation exerts its effects on weight and nutritional intake, biochemical, immunological and whole blood transcriptional phenotype of mice. It was demonstrated that SI mice eat more but have reduced weight gain and that there was a shift in the microbiota towards groups of bacteria associated with chronic inflammatory diseases and stress. It was established that SI mice had increased concentrations of the biochemical markers of organ function, AST and glucose. Social isolation was found to induce changes in the immune system, with a decreased NLR being demonstrated compared to SH mice, and SI mice having upregulation of the TLR

signalling involved in bacterial clearance. Finally, at the transcriptional level it was found that social isolation caused upregulation of 26 genes and down regulation of 10 genes in whole blood, with those upregulated genes primarily being involved in the immune system and apoptosis. Taken together these results elucidated that just 2 weeks of social isolation is enough to cause profound changes in the body.

Chapter 3
Social Isolation and Sepsis

3.1 Introduction

Sepsis is a life-threatening acute inflammatory disease that is characterised by the presence of severe organ dysfunction, in response to a dysregulated response by the host to infection[15]. The initial stage of sepsis is driven by an innate immune response to an infectious stimulus, most commonly bacteria, followed by an immunosuppressive stage[1,28]. Despite a wealth of clinical trials and research studies aiming to reduce the mortality of sepsis patients, very little is known about why sepsis remains the leading cause of death in ICUs worldwide and why some patient's survive, whilst others do not[17,20].

Socioeconomic status refers to the class or group a person belongs to with the three main factors defining it being their occupation, education and income[311]. There is increasing evidence to suggest that socioeconomic status can affect risk of sepsis and prognosis. In a Danish population, it was demonstrated that those people with a lower socioeconomic status were at increased risk of having *Staphylococcus aureus* bacteraemia, bacteria in the blood, which can be a precursor to sepsis[312]. Patients who have a low personal income have a higher risk of dying both at 30 days (35%) and 180 days (25%) after discharge from the hospital. Furthermore, patients who had a low educational background and low income were seen to have a trend towards readmission to the hospital after discharge[313]. In a population based study, it was shown that higher scores of perceived stress were associated with increased incidence of sepsis at 1 year and 10 years[314]. In the United States, the counties with strong levels of clustered sepsis were found to be predominately in the South and once again have low income and education, but were also found to be

predominately composed of black race people, high unemployment rates and elderly people[315,316].

3.1.1 Specific Aims

This study had the following aims:

1. To investigate the effects of social isolation on the acute immune system;
2. To understand whether social isolation has a differential response to LPS and polyinosinic-polycytidylic acid (poly (I:C)) induced sepsis;
3. To determine the effects of social isolation on the immune system using an *E.coli* induced model of sepsis.

3.2 Methods

3.2.1 Animal Husbandry

All animals were housed in individually ventilated enclosures with standard food and water being provided *ad libitum* and with a 12-hour light-dark cycle. All experiments undertaken were approved and performed according to the guidelines of the Ethical Committee for the Use of Animals, Bart's and The London School of Medicine and Dentistry and the Home Office Regulations Act 1986 (Prof. D'Acquisto, PPL. 70/8714).

3.2.2 Modelling Social Isolation in CD-1 Mice

As previously described, in house bred 5-week-old male or female CD-1 mice weighing between 20-25g were used. Mice were randomly assigned to either social isolation or social housing for a period of 2 weeks before the induction of sepsis. As CD-1 mice are outbred and have been shown to be suitable for experiments involving sociability, they were chosen over C57BL/6 mice, as they have greater genetic diversity and are more representative of the human population[317].

3.2.3 LPS Induced Sepsis

Sepsis was induced in male CD-1 mice *via* intraperitoneal (i.p.) injection of 15mg/kg of *E.coli 0111:B4* LPS (Sigma-Aldrich, **cat.** 297-473-0) resuspended in PBS. Mice were left for 4 hours and cardiac puncture was done as previously described (**Figure 3.1**)[318].

In order to collect the PLF by peritoneal lavage, the fur of the mouse was sprayed with ethanol and a small horizontal incision on the abdominal fur was made and the fur was pulled back to reveal the abdominal cavity. The needle of a 2.5ml syringe (25G 1" needle) filled with 3mM EDTA and a little air in it was inserted into the peritoneal cavity. 2.5ml of 3mM EDTA was slowly injected into the peritoneal cavity and the mouse was gently

shaken to loosen the cells. A small cut was made, and a Pasteur pipette was used to take up the PLF (~2 ml).

PLF was spun down at 264 *g* for 5 minutes and the supernatant removed. PLF supernatant was sent to Labospace Ltd. (Milan) for measuring the concentration of IL-6, TNF-α and keratinocyte-derived chemokine (KC) by multiplex assays.

Whole blood was sent to IDEXX laboratories for whole blood profiling using IDEXX Procyte Dx® Haematological analysis. Remaining blood was spun down at 10,000*g* and the plasma collected. In order, to measure the severity of sepsis, 1x aliquot of plasma was sent to IDEXX laboratories for the following biochemical tests: AST, ALT and creatinine. IL-6, TNF-α, monocyte chemoattractant protein-1 (MCP-1) and IFN-γ concentrations were determined in plasma *via* multiplex assay (Labsopace Ltd., Milan).

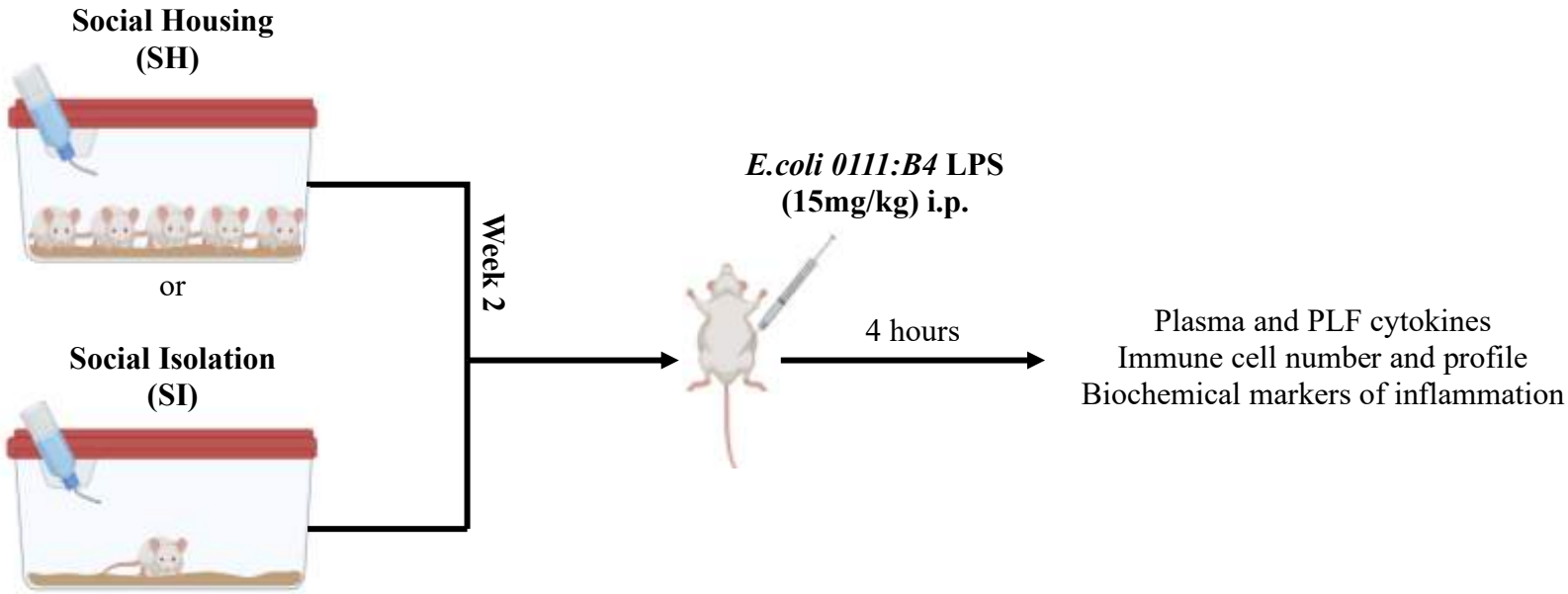

Figure 3.1: LPS Sepsis Study Overview. CD-1 mice were randomly assigned to either social housing or social isolation for a period of 2 weeks as previously described. After 2 weeks, mice were injected i.p. with LPS (15mg/kg) and sacrificed at 4 hours. Three main parameters were assessed: plasma and PLF cytokines, immune cell number and profile and biochemical markers of inflammation. Image created on Biorender.

3.2.4 *E.coli* Induced Sepsis

The *E.coli* model of sepsis confers an advantage over the LPS model of sepsis as it allows the ability of the immune cells to clear infection to be assessed. As the *E.coli* model uses live bacteria, the ability of the immune cells to deal with infection can be assessed by bacterial clearance. This is not possible with the LPS model as it is a TLR4 stimulant that is derived from gram-negative bacteria and cannot be killed by the immune system, although it can trigger cytokine release (**Figure 3.2**). Thus, the *E.coli* model of sepsis was used to assess the functionality of the immune response to a bacterial challenge.

Male and female mice were used as controversy exists surrounding whether there is a sexual dimorphism in susceptibility to sepsis and in survival, with some studies finding that women have better clinical outcomes and lower mortality, whilst others found this not to be the case[319–323]. Mice were weighed prior to the induction of bacterial sepsis and just before sacrifice to give an objective indication of how physically sick the mice were. In order to model bacterial sepsis, male or female CD-1 mice were given *E.coli* serotype 06:K2:H1 [ATCC®19138™] at a dose of $1x10^7$ colony forming unit (CFU) by i.p. injection and were left for a period of 6 hours (**Figure 3.3**).[324].

After 6 hours, the mice were observed and recorded *via* video to assess sickness behaviours: piloerection, huddling, fever and cloudy eyes. Mice were then anesthetised using isoflurane and cardiac puncture was performed as previously described with around 0.4ml of blood being collected due to hypercoagulation as a result of the sepsis. To give an indication of the local response to infection peritoneal lavage was carried out as previously described.

Since studies in female macaques suggest social isolation primes the immune response for bacterial infection, bacterial clearance was assessed to see whether social isolation

would have any functional effects on the immune system[153]. For males, blood and PLF was diluted 1:1,000 in sterile PBS. For females, blood was diluted in sterile PBS at a 1:10,000 dilution and PLF was diluted 1:50,000 in sterile PBS. 50µl of diluted blood and diluted PLF was pipetted and spread evenly on a lysogeny broth (LB) plate. LB plates were incubated overnight at 37°C. In the morning, the bacteria colonies were counted, and CFU/ml was calculated using the following equation:

$$CFU/ml = \frac{number\ of\ colonies\ per\ ml\ of\ agar}{total\ dilution\ factor}$$

Remaining blood was spun down at 10,000*g* and the plasma collected. In order, to measure the severity of sepsis 1x aliquot of plasma was sent to MRC Harwell for glucose, AST, ALT and creatinine measurement using a Beckman Coulter AU680 clinical chemistry analyser.

For ELISAs, 2x aliquots of plasma were used in order to measure the concentration of the following cytokines: IL-6 (1:10 and 1:50) (Invitrogen, **cat.** 88-7064-77) and TNF-α (1:100) (Invitrogen, **cat.** 88-7234-77). In brief, high affinity binding 96-well plates were coated with 1x capture antibody in coating buffer and were incubated overnight at 4°C. Plates were blocked with ELISA/ELISASPOT diluent (1X) and incubated at room temperature for 1 hour. Samples were loaded to bind the antigen and the plate was incubated at room temperature for 2 hours. Detection antibody (1X) was added and the plate was incubated at room temperature for 1 hour. Avidin-HRP was added and the plate was incubated at room temperature for 30 minutes. 1X 3,3′,5,5′-Tetramethylbenzidine solution was added and the plate was incubated for ~10-15 minutes at which point stop solution was added and the plate was read at 450nm. The equation of the standard curve was used to calculate the concentration of each cytokine in each sample.

PLF samples were centrifuged for 5 minutes at 264 *g* and the supernatant removed and stored at -80°C. The pelleted leukocyte cells were resuspended in 200µl of residual volume. Cells were then washed in FACS buffer and blocked with 50µl of CD16/CD32 FcγIIR–blocking antibody (clone 93; eBioscience, **cat.** 14-0161-82) in fluorescence-activated cell sorting (FACS) buffer. After 30 minutes, the block was washed off and the cells were stained with 50µl of Anti-Mouse CD11b FITC (eBioscience, **cat.** 11-0112-82), Anti-Mouse Ly6G (eBioscience, **cat.** 17-9668-82) and Anti-Mouse F4/80 PE (eBioscience, **cat.**12-4801-82) in FACS buffer for 30 minutes at 4°C. Cells were then washed and fixed in 4% PFA and were acquired on a LSRFortessa flow cytometer (Becton Dickson). Analysis was carried out using FlowJo 7.0 software (Tree Star).

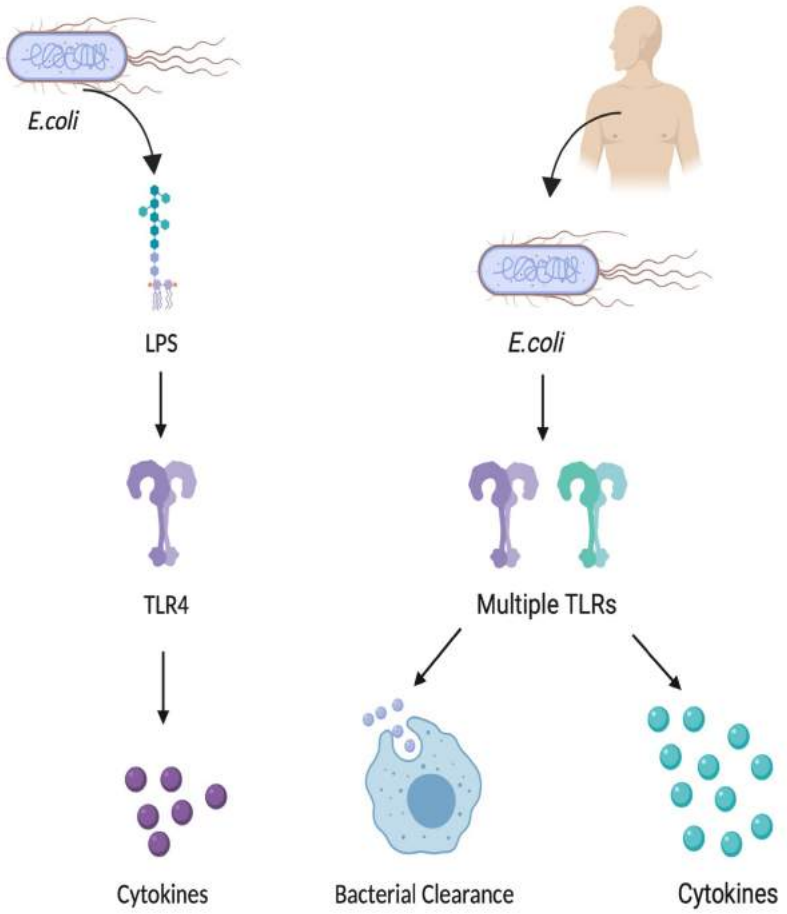

Figure 3.2: Comparison of LPS and *E.coli* Sepsis Models. LPS is found on the outer membrane of gram-negative bacteria such as *E.coli*. LPS induced sepsis results in the activation of the TLR4 pathway thus causing cytokine production. *E.coli* is found in the human body as a commensal bacteria and during infection in its pathogenic form. In contrast to LPS, use of live bacteria such as *E.coli* serotype 06:H2:K1 to induce sepsis causes the activation of multiple TLRs leading to cytokine production. Additionally, the use of live *E.coli* allows for the assessment of the functional ability of immune cells to clear the live bacteria.

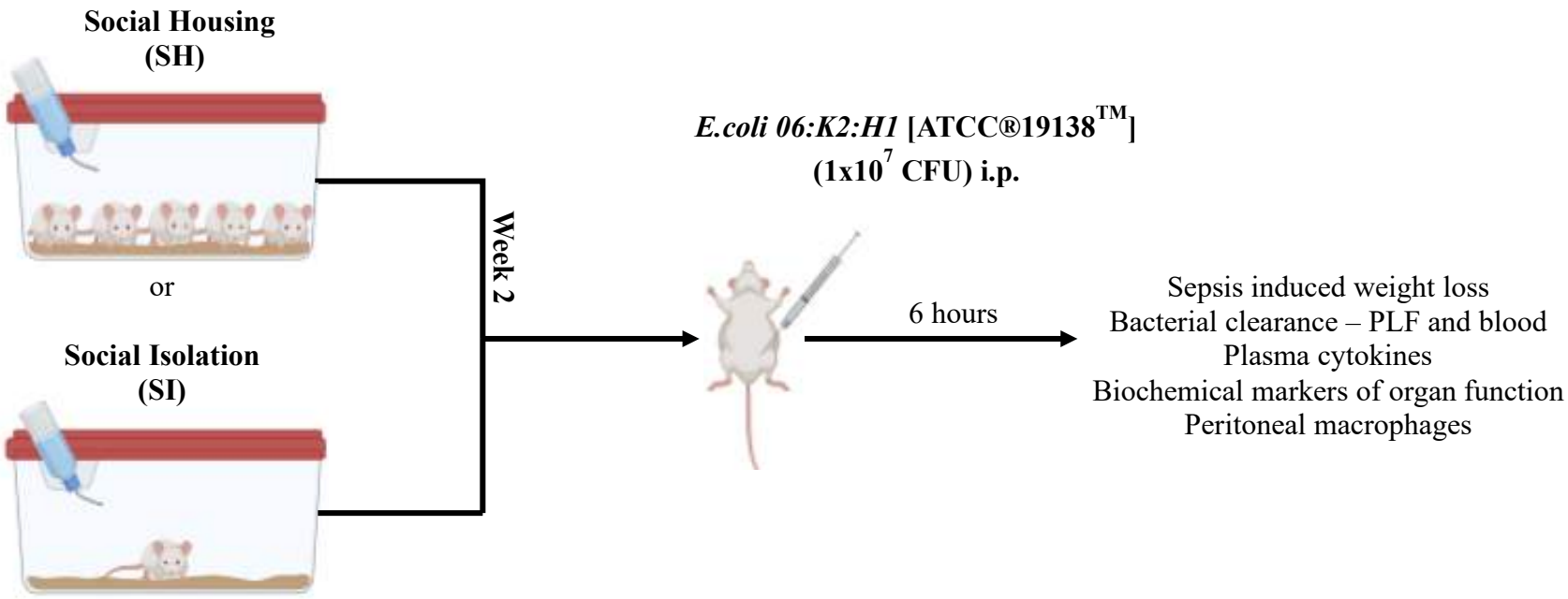

Figure 3.3: *E.coli* Sepsis Study Overview. CD-1 mice were randomly assigned to either social housing or social isolation for a period of 2 weeks as previously described. After 2 weeks, mice were injected i.p. with *E.coli 06:K2:H1* ($1x10^7$ CFU) and sacrificed at 6 hours. The following parameters were assessed: sepsis induced weight loss, bacterial clearance in PLF and blood, plasma cytokines, biochemical markers of organ function and peritoneal macrophages. Image created on Biorender.

3.2.5 Poly(I:C) Induced Sepsis

The balance of expression of *MyD88* and *IRF3* has been shown to be regulated by social connections, as both people and female macaques who respectively have high levels of PSI or low social rank have downregulation of *IRF3* and the subsequent viral response, and upregulation of *MyD88* and the subsequent bacterial response[153,325]. In order to test whether this would also be true in SI mice, as they had shown an enhanced response to bacterial infection, viral sepsis was modelled.

In order to test for sexual dimorphism during viral sepsis both male and female CD-1 mice were used. After 2 weeks of social isolation or social housing CD-1 mice were injected i.p. with 12mg/kg of poly (I:C) (Sigma, **cat.** P1530-25MG), a synthetic TLR3 stimulator[326]. After 6 hours, the mice were observed and recorded *via* video to assess sickness behaviours: piloerection, huddling, fever and cloudy eyes (**Figure 3.4**). Mice were then anesthetised using isoflurane and cardiac puncture was performed with ~0.8ml of blood.

Blood was spun down at 10,000 *g* and the plasma collected. In order, to measure the severity of sepsis, plasma AST, ALT and creatinine concentrations were assessed as described previously for *E.coli* induced sepsis.

3.2.6 Statistics

Significance was tested using the statistical analysis specified in each figure legend on GraphPad Prism 8 (GraphPad Software Inc, USA).

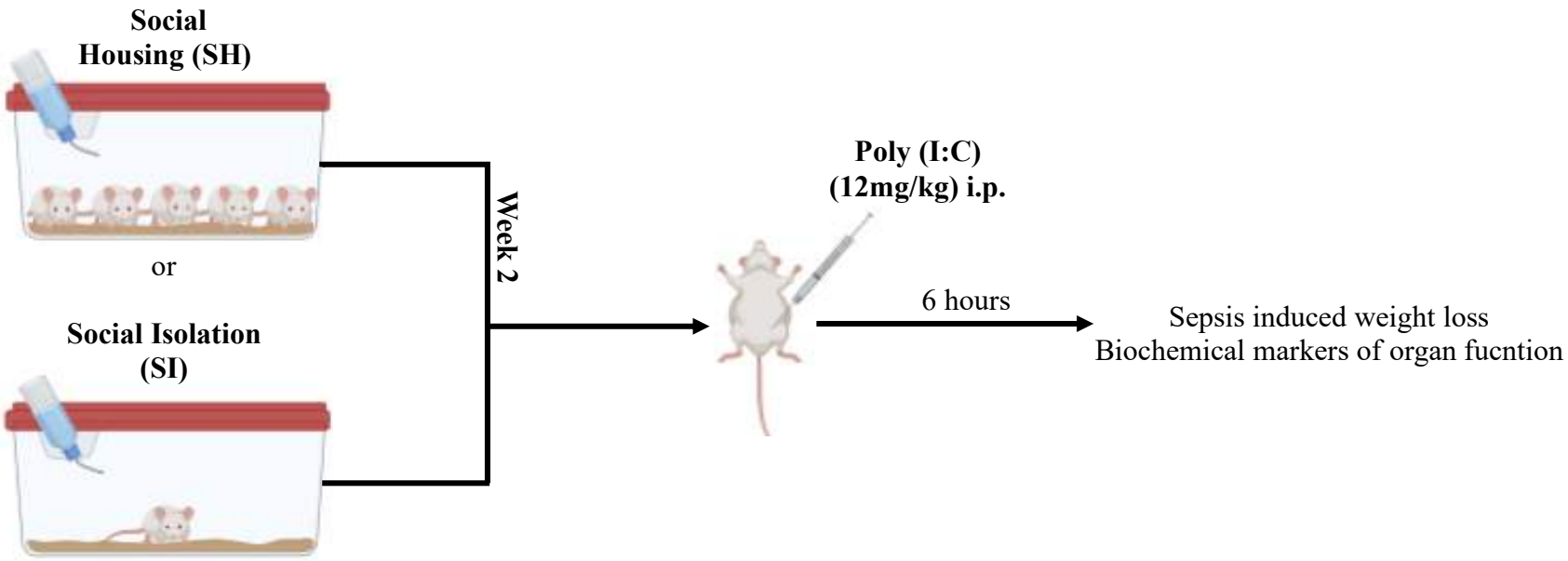

Figure 3.4: Poly (I:C) Sepsis Study Overview. CD-1 mice were randomly assigned to either social housing or social isolation for a period of 2 weeks as previously described. After 2 weeks, mice were injected i.p. with poly (I:C) (12 mg/kg) and sacrificed at 6 hours. The following parameters were assessed: sepsis induced weight loss and biochemical markers of organ function. Image created Biorender.

3.3 Results

3.3.1 LPS Induced Sepsis

LPS, a TLR4 ligand, induced sepsis was used as an initial means to test the immune response to infection after social isolation. In order to determine whether inflammation was altered systemically or locally, cytokine levels were measured in the plasma and in the PLF respectively, 4 hours post-induction of LPS sepsis. The early NFκB-dependent cytokines, TNF-α and IL-6, were significantly higher in the plasma of SI mice in comparison to SH mice, whilst the late NFκB response in plasma, MCP-1 and IFN-γ, showed a trend towards being higher in SI mice (**Figure 3.5**). Both the early NFκB response, TNF-α and IL-6, and the late NFκB response, MCP-1 and KC, in PLF showed a trend towards being higher in SI mice as opposed to SH mice (**Figure 3.6**).

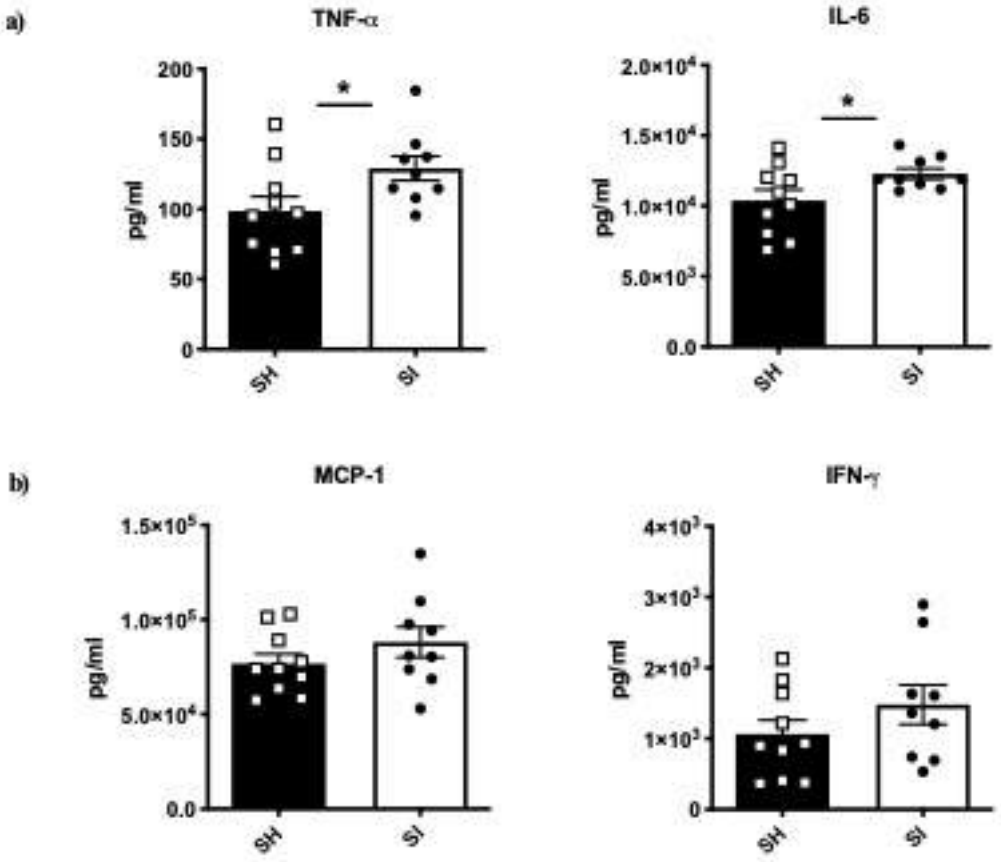

Figure 3.5: Plasma Cytokines - LPS. The following cytokines were measured in plasma: **a)** TNF-α and IL-6 (early NFκB response) and **b)** MCP-1 and IFN-γ (late NFκB response) *via* multiplex assay. Data shown as mean ± SEM where n=9-10 mice per housing group and data points represent a single mouse. Significance was determined when *$p<0.05$ was gained using an unpaired parametric T-test.

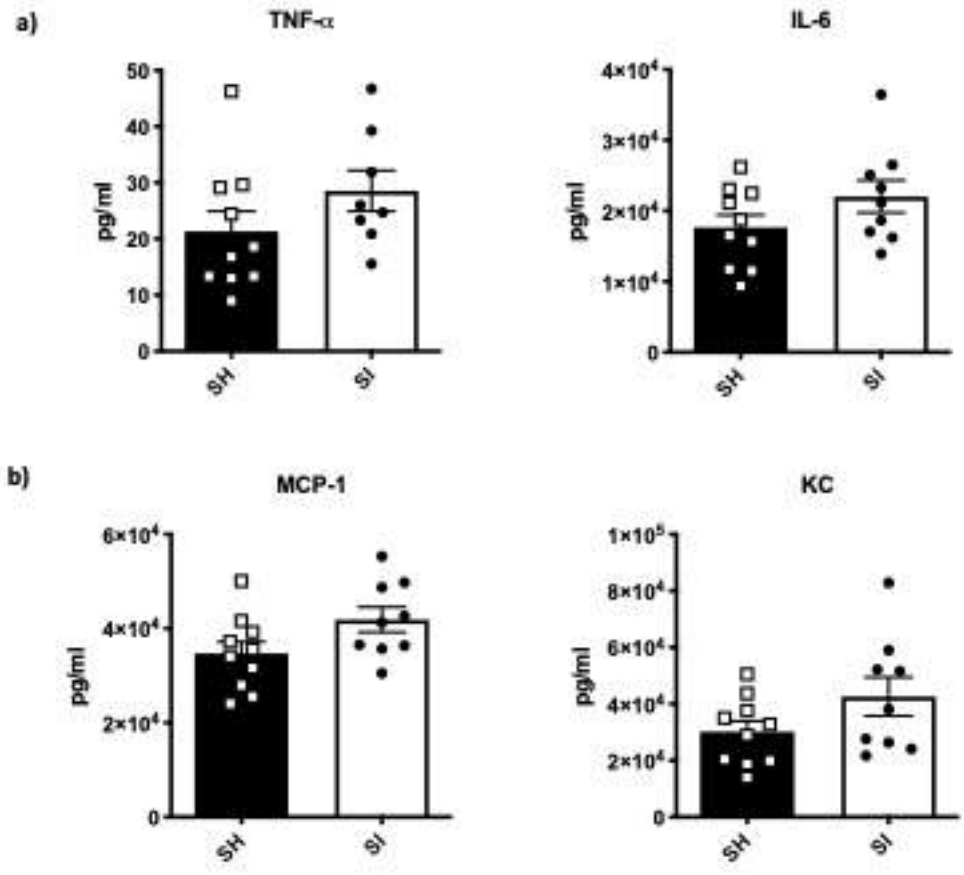

Figure 3.6: Peritoneal Lavage Fluid Cytokines - LPS. The following cytokines were measured in PLF: **a)** TNF-α and IL-6 (early NFκB response) and **b)** MCP-1 and KC (late NFκB response) *via* multiplex assay. Data shown as mean ± SEM where n=9-10 mice per housing group and symbols represent a single mouse. Significance was determined when $p<0.05$ was gained using an unpaired parametric T-test.

Whole blood cellularity was assessed 4 hours post-sepsis to give an indication of whether social isolation effects the number or type of immune cells present and thus, may have an effect on their ability to fight an immune challenge. The number of leukocytes was similar between both housing groups (**Figure 3.7a**). In addition, the relative % of lymphocytes and neutrophils between housing groups were similar (**Figure 3.7b and d**). Monocytes showed a trend towards being lower in SI mice (**Figure 3.7c**). It should be noted that due to low leukocyte counts in some mice it was not always possible to detect the subtypes of leukocytes present.

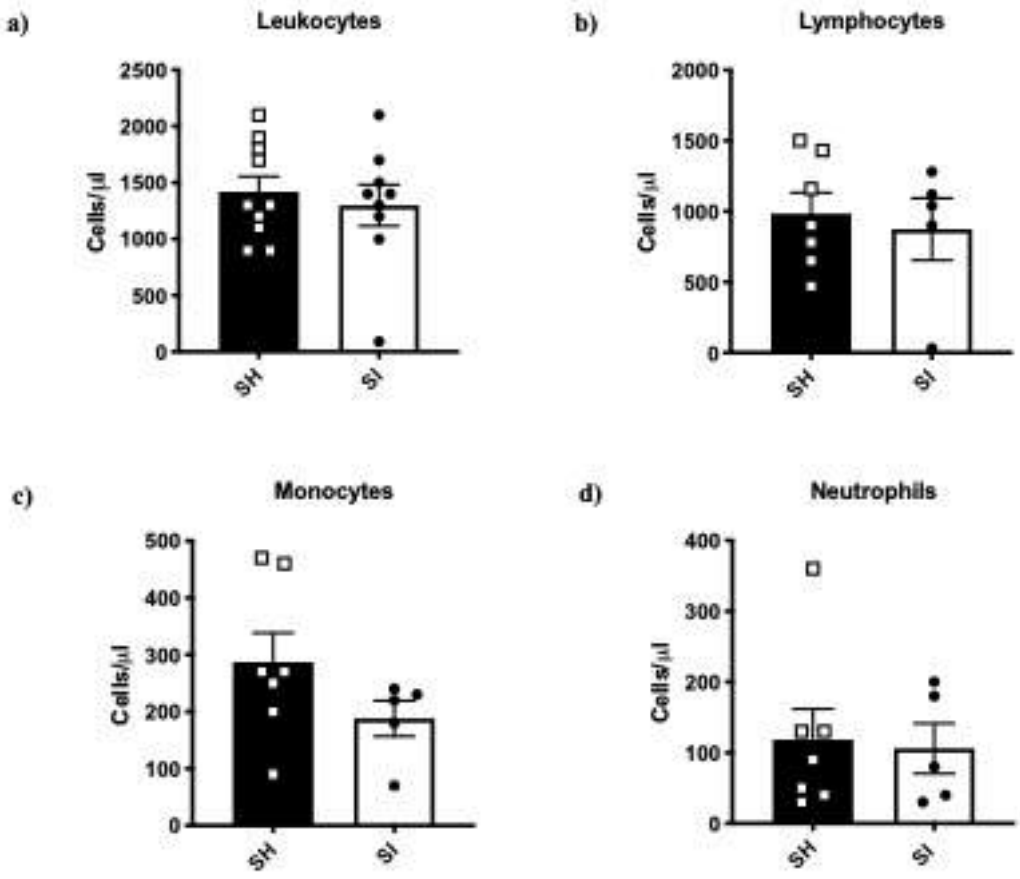

Figure 3.7: Immune Cell Numbers and Profile. Immune cell response was assessed after 4 hours post-induction of LPS sepsis: **a)** total leukocyte count**, b)** lymphocyte count **c)** monocyte count **d)** neutrophil count. Each bar shows mean ± SEM of n=5-10 mice from with each symbol representing a single mouse. Significance was determined when $p<0.05$ was gained using an unpaired parametric T-test.

As a measure of as organ damage biochemical markers of liver (AST and ALT) and kidney function (creatinine) were measured 4 hours post-induction of LPS induced sepsis. AST concentrations showed a trend towards being slightly lower in SI mice compared to SH mice, whilst ALT levels were similar in SI mice compared to SH mice (**Figure 3.8a**). Creatinine levels were similar between housing groups (**Figure 3.8b**).

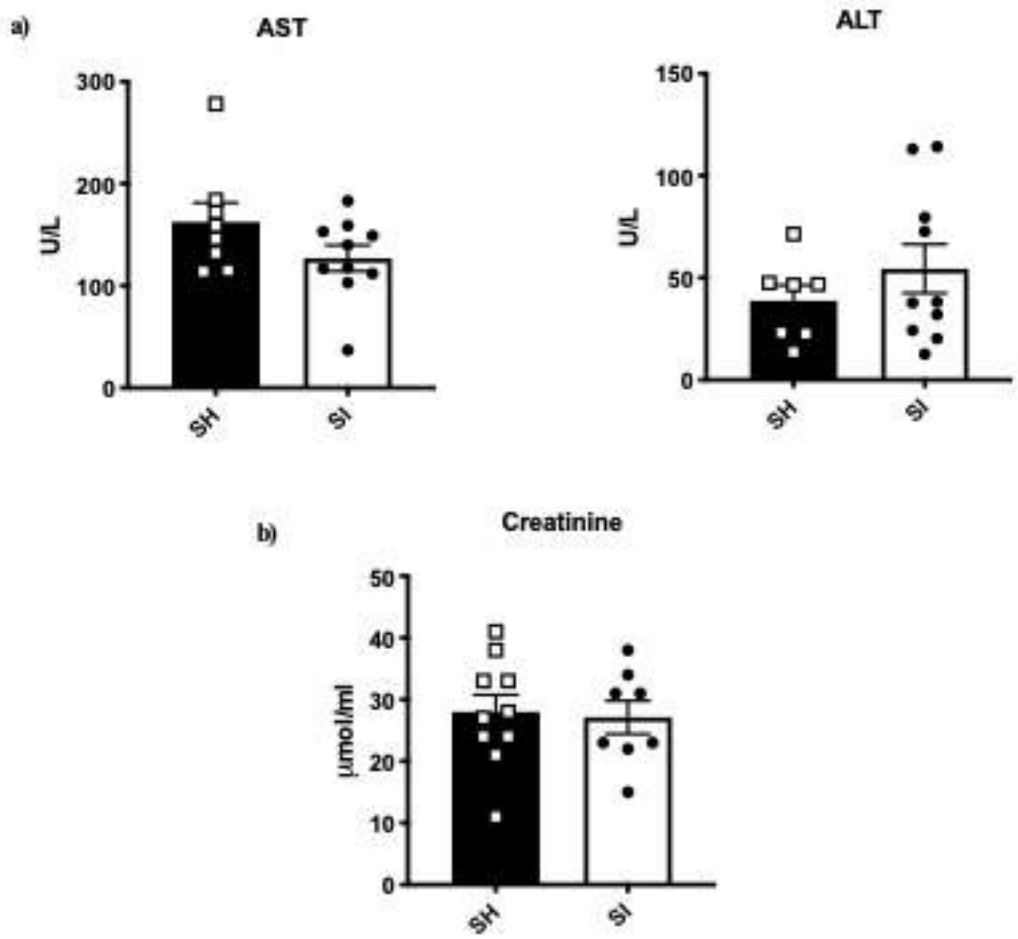

Figure 3.8: Biochemical Markers of Liver and Kidney Function. Markers of liver function: **a**) AST and ALT and the marker of kidney function, **b**) creatinine were measured in plasma 4 hours post-LPS sepsis induction. Data shown as mean ± SEM where each symbol represents a single mouse and n=7-10 mice per housing group. Mice were excluded if values were below the range of accurate detection of the assay. Significance was determined when $p<0.05$ was gained using an unpaired parametric T-test.

3.3.2 *E.coli* Induced Sepsis

Since social isolation in the LPS model of sepsis showed increased early NFκB cytokines (IL-6 and TNF-α) levels in plasma and an absence of changes in the levels of the late NFκB cytokines in both plasma and PLF, this suggested that social isolation does not exert its effects on the immune system in an indiscriminate manner. Therefore, a live strain of bacteria, *E.coli 06:K2:H1*, was given *via* i.p. injection at a dose of $1x10^7$ CFU in order to induce sepsis in the mice and to allow for any functional changes in the immune response and bacterial clearance to be elucidated (**Figure 3.2**). The effect of sex was also assessed as the immune response is known to differ between males and females as there is some evidence to suggest that sexual dimorphism occurs during sepsis[319–323,327].

Initially, sepsis severity was assessed to give an indication of whether or not the changes in environment could affect sepsis severity. Upon observation throughout the experiment, SH mice (left) showed visual signs of ill-health. The SH mice exhibited the classical signs of sickness, (huddled together, piloerection of the fur, orbital tightening and ear tightening) whereas the SI mice (right) did not display such signs of discomfort and were moving around the cage throughout (**Figure 3.9a**). To assess sepsis severity objectively, mice were weighed before and after the induction of sepsis to allow for sepsis induced weight loss to be calculated. Weight loss was significantly lower in SI male mice and showed a trend towards being lower in female SI mice compared to SH mice (**Figure 3.9b)**.

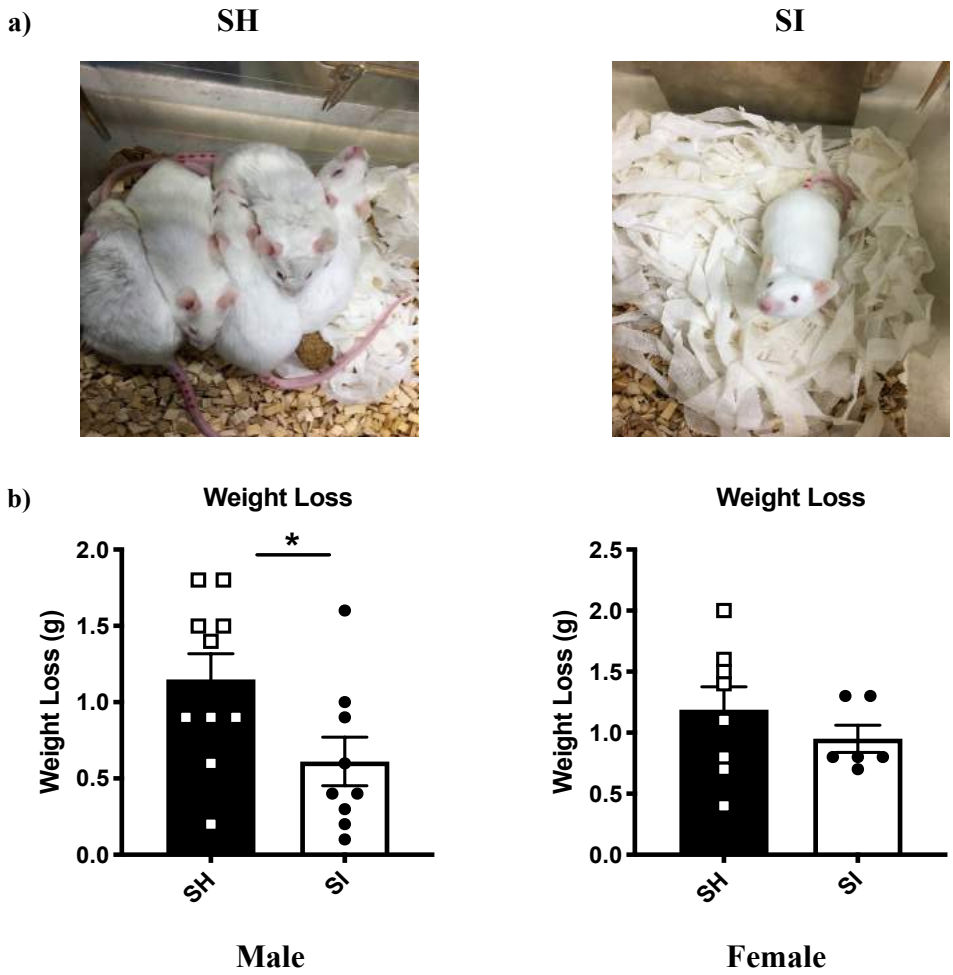

Figure 3.9: Sepsis Severity. a) Representative images illustrating the severity of sepsis in SH (left) and SI (right) male mice 6 hours post-sepsis and **b)** weight loss over the 6-hour period of sepsis in male (left) and female (right) mice. Data shown as mean ± SEM where n=6-10 mice per housing group and data points represent a single mouse. Significance was determined where *$p<0.05$ was gained using an unpaired parametric T-test.

Bacterial clearance was assessed as a measure of how sick the mice were and of how well their immune system was functioning. In SI males, there was significantly less bacteria systemically, blood, and locally, PLF, compared to SH male mice (**Figure 3.10a**). In females, SI mice had significantly less bacteria in the blood and a trend towards lower bacteria in the PLF compared to SH mice (**Figure 3.10b)**.

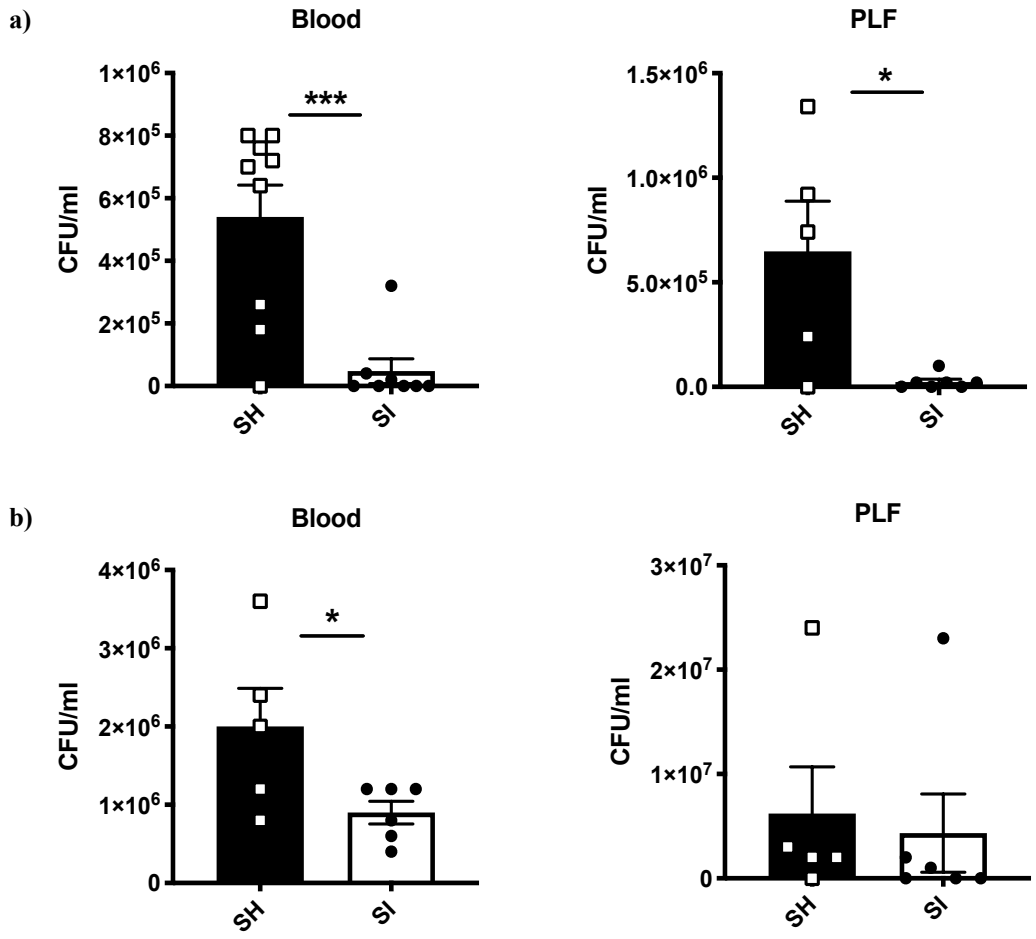

Figure 3.10: Bacterial Clearance in Blood and Peritoneal Lavage Fluid. To assess bacterial clearance, blood and PLF (left to right) were taken after 6 hours: **a)** male CD-1 was plated at a 1:1,000 dilution and **b)** female CD-1 was plated at 1:10,000 dilution for blood and 1:50,000 dilution for PLF before being cultured overnight and colonies were counted in order to calculate CFU. Data shown as mean ± SEM where each symbol represents an individual mouse and n=5-10 mice per housing group. Significance was determined using an unpaired parametric T-test where $p<0.05$* and $p<0.001$***.

Plasma cytokines were measured 6 hours post-sepsis induction in order to assess systemic inflammation, particularly with regards to understanding whether social isolation alters the MyD88/TRIF balance and thus the early and the late NFκB cytokine response (**Figure 1.5**). The early NFκB cytokines, TNF-α and IL-6, were found at lower concentrations in the plasma of SI mice compared to SH mice, with IL-6 being significantly lower in SI mice at the 6-hour time point (**Figure 3.11**). The late NFκB interferon, IFN-γ, was non-detectable in plasma at the 6-hour time point in both housing groups in male CD-1 mice (data not shown). Cytokines (TNF-α and IL-6) were too low to accurately quantify in plasma from female SI mice (data not shown).

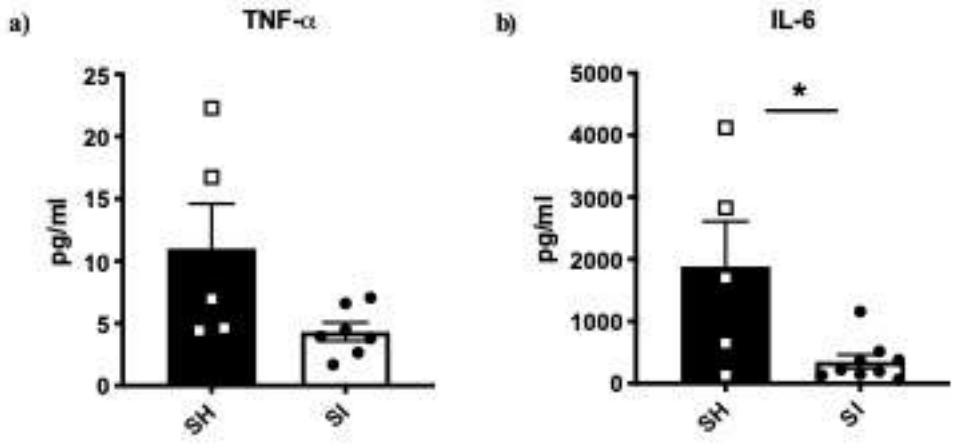

Figure 3.11: Plasma Cytokines - Males. a) TNF-α and **b**) IL-6 were measured in plasma *via* ELISA at 6 hours post-*E.coli* induced sepsis. Data shown as mean± SEM where n=5-8 mice per housing group with each symbol represents an individual mouse. Significance was determined when * $p<0.05$ was gained using an unpaired parametric T-test.

As a measure of systemic inflammation and sepsis severity, biochemical markers of organ function were assessed. Liver function was assessed by measuring AST and ALT in the plasma of CD-1 mice 6 hours post-sepsis. AST was significantly lower in male SI mice compared to SH mice and ALT showed a similar non-significant trend (**Figure 3.12**). AST and ALT levels were similar in female mice between the housing groups (**Figure 3.13**). Kidney function was assessed at the 6-hour time point by measuring creatinine levels in plasma and was found at similar levels between the two housing groups in both males and females (**Figure 3.12-13**). Glucose levels were measured in plasma at the 6-hour time point and were found to be at similar levels between housing groups in both male and female mice (**Figure 3.12-13**).

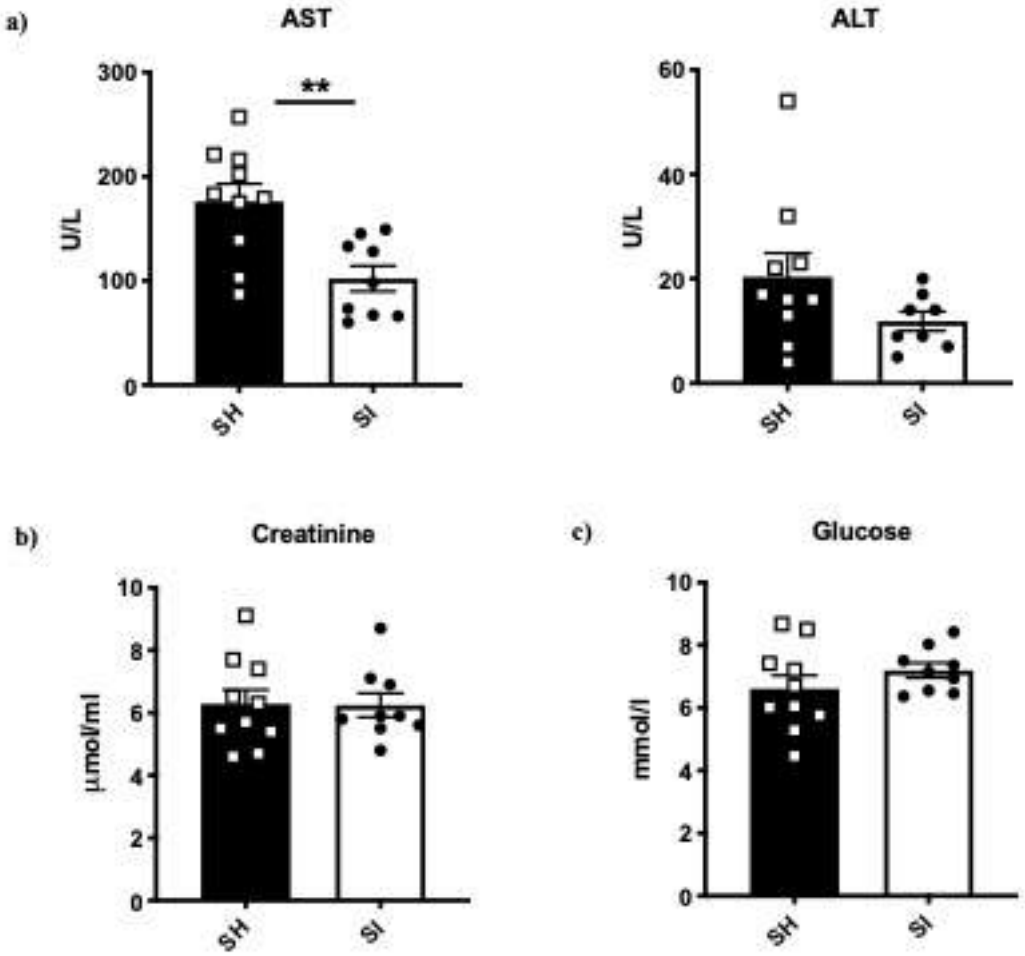

Figure 3.12: Biochemical Markers of Organ Function in Males. Plasma concentrations of **a)** AST and ALT, **b)** creatinine and **c)** glucose were measured. Data shown as mean± SEM where each symbol represents a single mouse where n=8-10 mice per housing group. Significance was determined when **p<0.01 was gained using an unpaired parametric T-test.

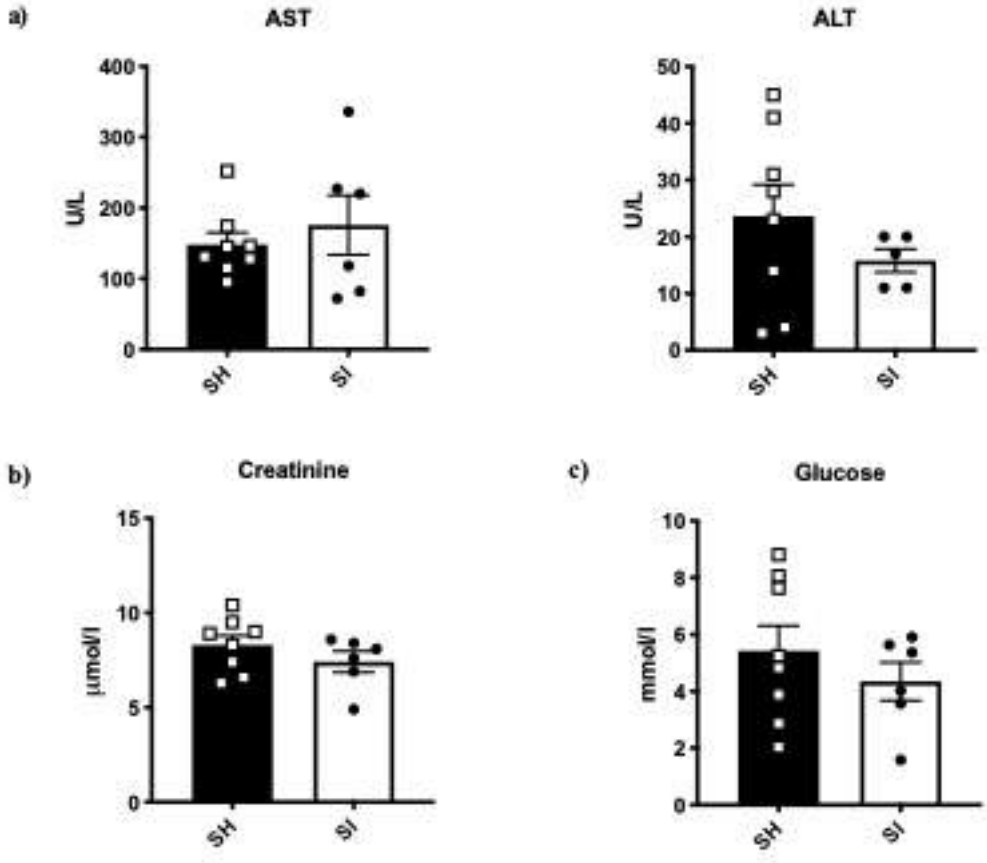

Figure 3.13: Biochemical Markers of Organ Function in Females. Plasma concentrations of **a)** AST and ALT, **b)** creatinine and **c)** glucose were measured. Data shown as mean per housing group ± SEM where n=6-7 mice per housing group with each symbol representing a single mouse. Significance was assessed by use of an unpaired parametric T-test where $p<0.05$.

In order to determine the immune cell types in the PLF 6 hours post-sepsis, flow cytometry was carried out on the PLF. After excluding doublets, leukocytes ($CD45^+$ cells) were gated for and the % of PLF cells that were leukocytes was shown on the pseudocolour plot (**Figure 3.14**). Myeloid cells were identified by gating on the leukocyte population for CD11b and the % of leukocytes that were identified to be myeloid cells was shown on the pseudocolour plot (**Figure 3.14**). From the myeloid cell population, macrophages ($F4/80^+$ cells) and neutrophils ($Ly6G^+$ cells) were gated upon and shown as a % of myeloid cells (**Figure 3.14**).

The % of leukocytes accounted for by macrophages and neutrophils was quantified in the peritoneal cavity of male SI and SH mice 6 hours post-induction of to determine if this might account for lower bacteria in SI mice post-sepsis. Representative pseudocolour plots for SH and SI mice showing the number of macrophages and neutrophils are shown in **Figure 3.15a** and **Figure 3.15b** respectively. Macrophages accounted for a significantly higher % of the total leukocytes accounted for in SI mice compared to SH mice (**Figure 3.15c**). Neutrophils accounted for a significantly lower % of the total leukocytes accounted for in SI mice compared to SH mice (**Figure 3.15d**).

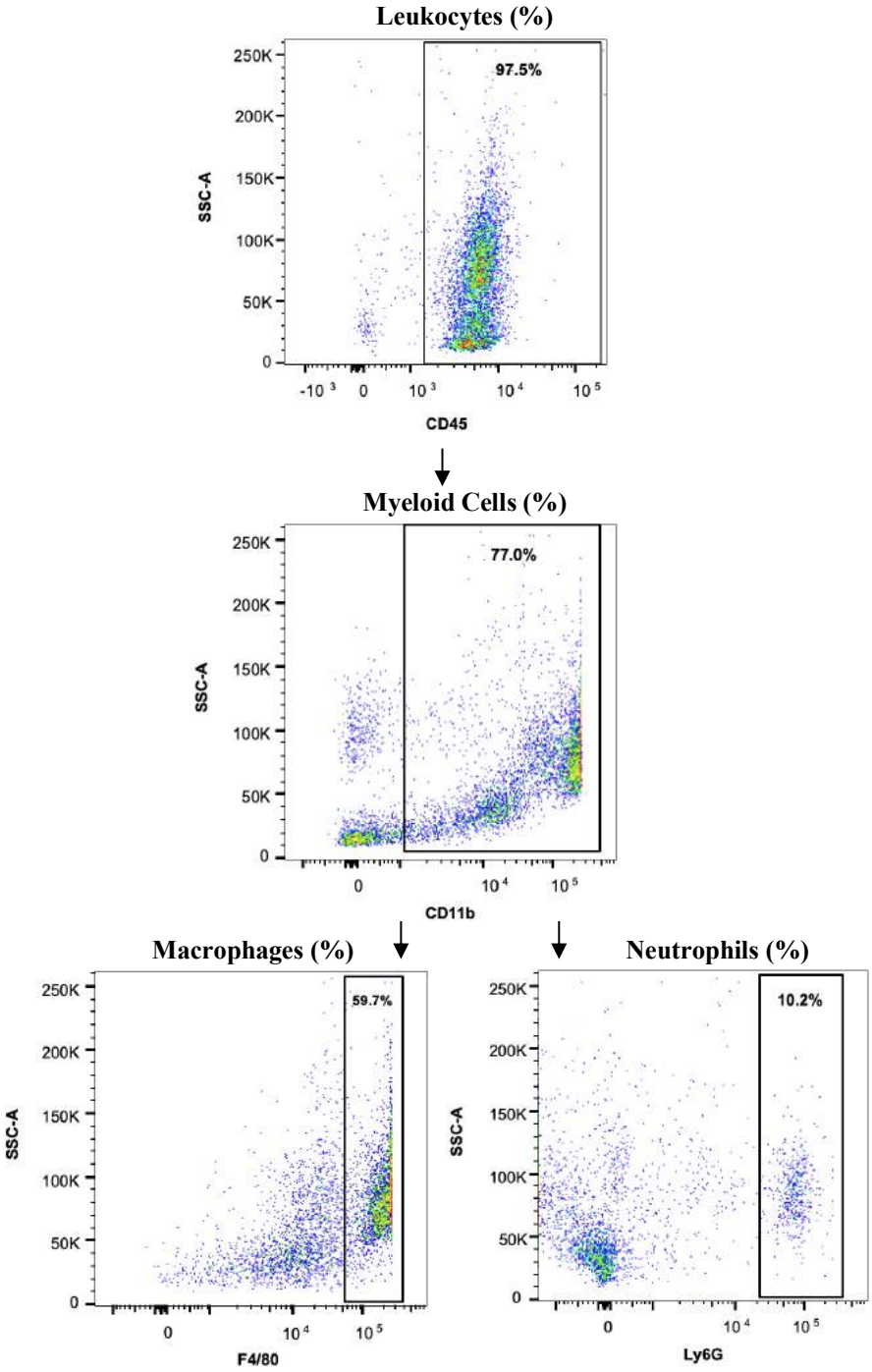

Figure 3.14: Representative Gating Strategy for PLF Immune Cells - 6 Hours. Leukocytes were gated upon using CD45 as a marker and shown on the pseudocolour plot as a % of total events. From the leukocyte cell population, myeloid cells were identified by use of the CD11b marker and were shown on the pseudocolour plot as a % of leukocytes. From the myeloid cell population, macrophages were gated on by use of the F4/80 marker and were shown on the pseudocolour plot as a % of myeloid cells. Similarly, using Ly6G and gating on the myeloid positive cells the % of myeloid cells accounted for by neutrophils was shown.

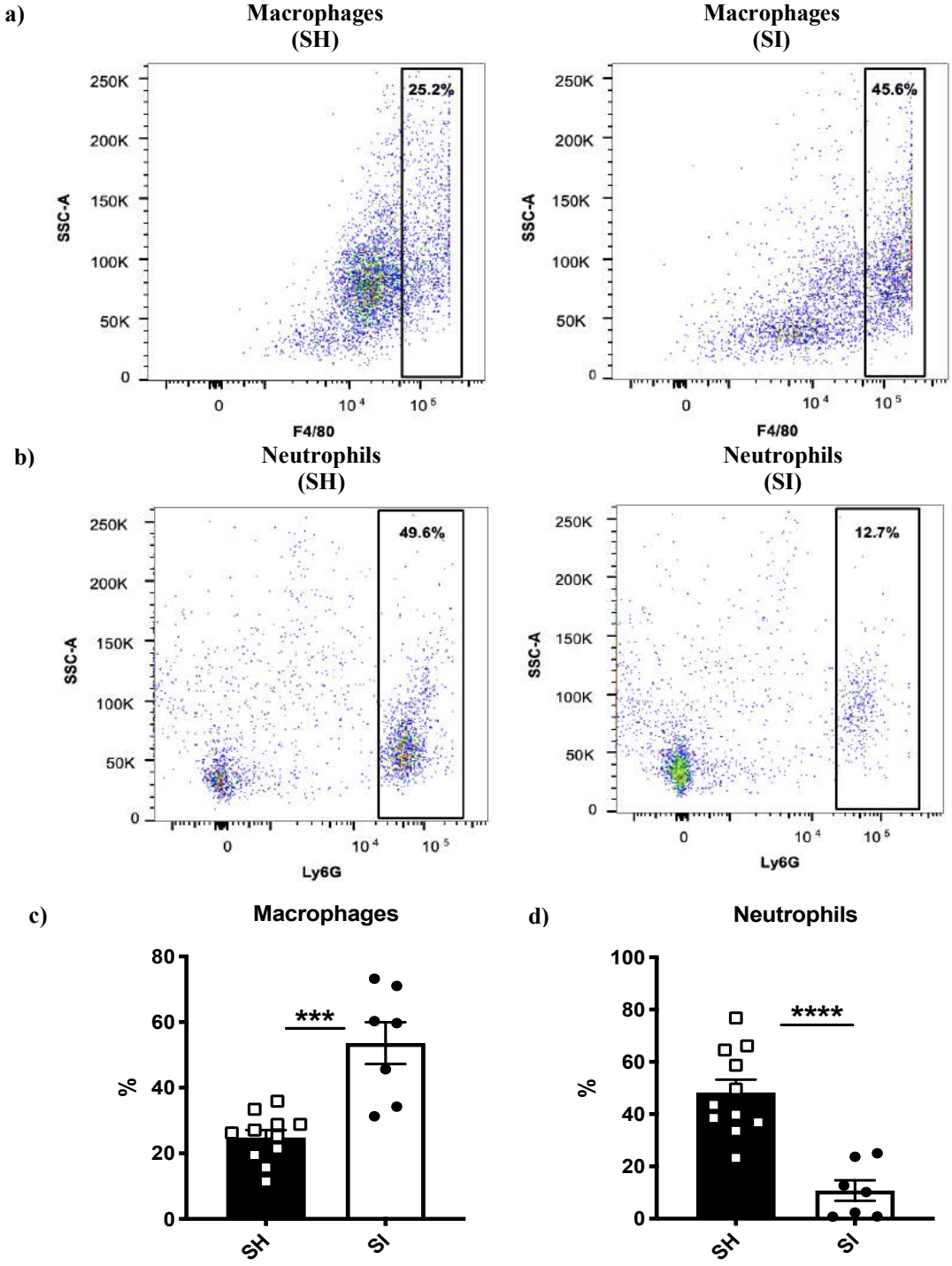

Figure 3.15: Peritoneal Macrophages and Neutrophils at 6 Hours - Males. **a)** representative pseudocolour plots for macrophages, **b)** representative pseudocolour plots for neutrophils, **c)** % of macrophages in PLF and **d)** % of neutrophils in PLF. Data shown as mean± SEM with n=7-10 mice per housing group. Each symbol represents an individual mouse. p=0.0001*** and p<0.0001**** as determined by use of an unpaired parametric T-test.

3.3.3 Poly (I:C) Induced Sepsis

It is known that those individuals who have high levels of PSI have downregulation of *TRIF* and the genes involved in the viral response, and upregulation of *MyD88* and thus the genes involved in the bacterial response (**Figure 1.5**)[159]. Testing the effect of social isolation on the immune system at a functional level revealed that SI mice had enhanced bacterial clearance compared to SH mice during *E.coli* sepsis, thus suggesting that SI mice have a primed bacterial response. Therefore, poly (I:C), TLR3 ligand, was given at a dose of 12mg/kg to induce viral sepsis in these mice thus testing whether the immune response to viral infections would be blunted as the literature suggests[159].

To objectively assess sepsis severity, weight loss was measured during the 6-hour period of sepsis with male SI mice losing ~0.16g less than male SH mice (**Figure 3.16a**). Similarly, female mice lost ~0.32g less than female SH mice (**Figure 3.16b**).

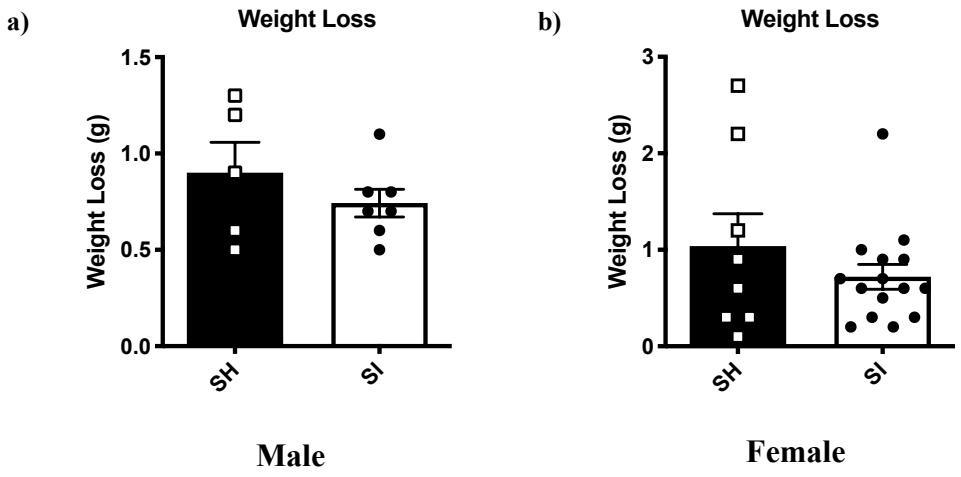

Figure 3.16: Weight Loss During Poly (I:C) Induced Sepsis. Weight loss was calculated over the 6-hour period in **a)** male and **b)** female SH and SI mice. Data shown as mean ± SEM where n=5-7 male mice and n=8-15 female mice per housing group where each symbol represents an individual mouse. Significance was determined when $p<0.05$ was gained using an unpaired parametric T-test.

Systemic inflammation was assessed by measuring biochemical markers of both liver and kidney function. Liver function was assessed by measuring AST and ALT in the plasma of CD-1 mice 6 hours post-poly (I:C) induced sepsis. AST and ALT concentrations in plasma showed a trend toward being lower in SI male mice compared to SH mice (**Figure 3.17a**). In males, kidney function was assessed at the 6-hour time point by measuring creatinine levels in plasma and was found at similar levels between the two housing groups (**Figure 3.17b**). In females AST and ALT concentrations were similar between the housing groups (**Figure 3.18a**). Plasma creatinine concentration was similar between housing groups (**Figure 3.18b**).

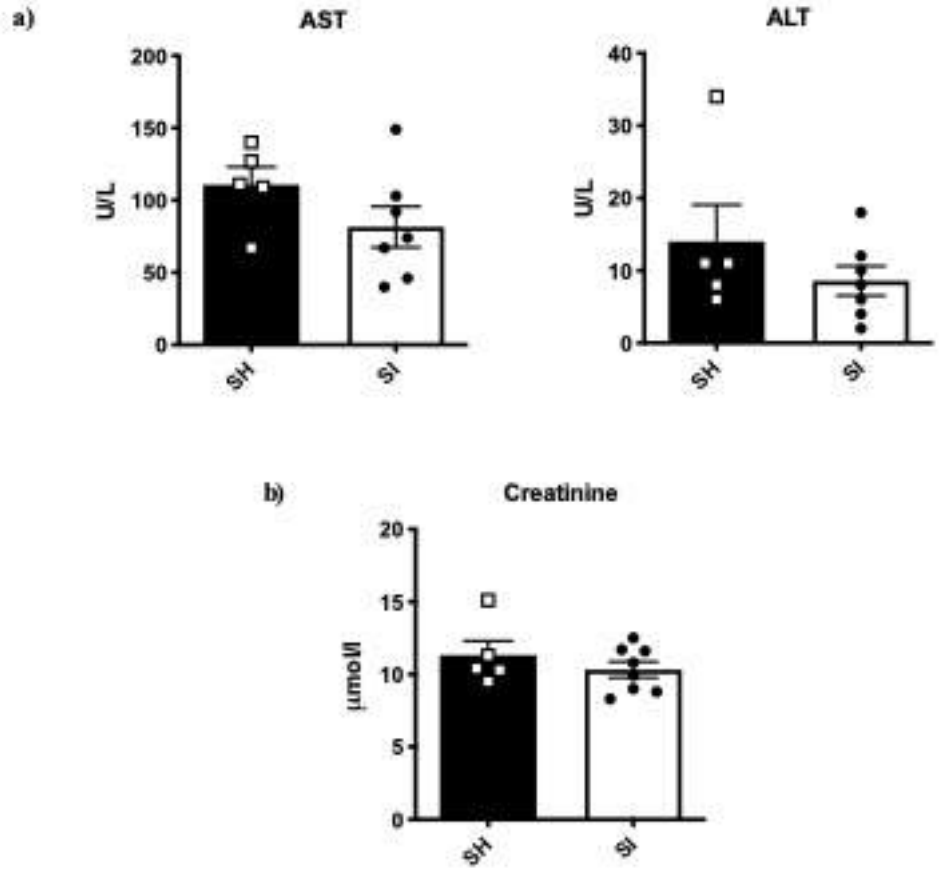

Figure 3.17: Biochemical Markers of Liver and Kidney Function in Males. The following biochemical parameters were analysed **a)** AST and ALT and **b)** creatinine. Data shown as mean ± SEM where n=5-8 mice per housing group and each symbol represents a single mouse. Significance was assessed by use of an unpaired parametric T-test where $p<0.05$.

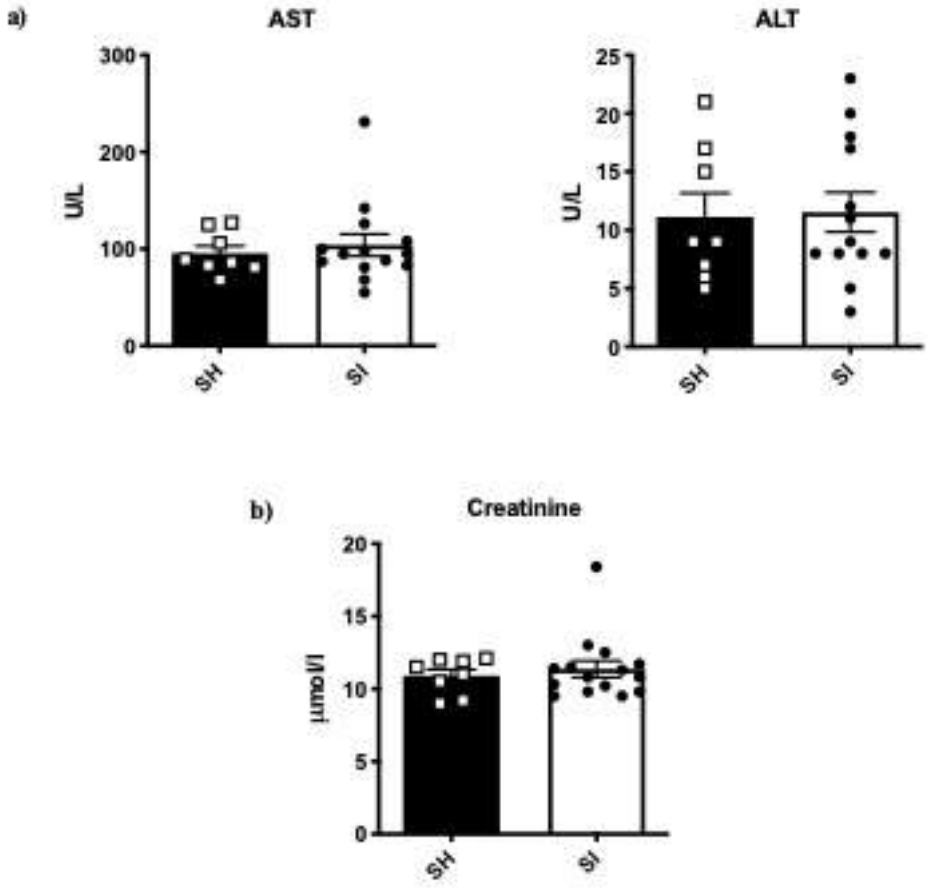

Figure 3.18: Biochemical Markers of Liver and Kidney Function in Females. The following biochemical parameters were analysed **a)** AST and ALT and **b)** creatinine. Data shown as mean ± SEM where n=8-15 mice per housing group where each symbol represents a single mouse. Significance was determined when $p<0.05$ was gained using an unpaired parametric T-test.

3.4 Discussion

This set of studies aimed to assess the effect of social isolation in the acute inflammatory setting of bacterial and viral sepsis. Three models of sepsis were utilised: LPS, *E.coli* and poly (I:C). The main finding of this chapter was that SI mice have increased bacterial clearance and reduced inflammatory markers following *E.coli* induced sepsis compared to SH mice. LPS induced sepsis illustrated that SI mice have an increased cytokine response compared to SH mice. In contrast, there was no difference in the weight loss and inflammatory markers assessed between housing groups in the poly (I:C) model of sepsis. Taken together these findings are indicative of a primed bacterial response in those mice that underwent social isolation without affecting the viral response.

Initially, an LPS model of sepsis was used to compare the immune response in SI to SH mice. At the 4-hour time point, it was demonstrated that plasma TNF-α and IL-6 were significantly higher in SI mice compared to SH mice whilst MCP-1 and IFN-γ were found at similar levels in plasma. This is in concordance with studies in humans who have high levels of perceived loneliness, where their leukocytes, especially monocytes, have upregulation of the genes encoding the pro-inflammatory cytokines involved in bacterial responses (IL-6 and TNF-α)[158]. There were no differences in the concentrations of cytokines found in the PLF suggesting that social isolation exerts its effects primarily at the systemic level as opposed to locally. Despite changes in cytokine levels in the plasma, whole blood cellularity was similar between the two housing groups which suggests that the immune cells present have the transcriptional changes seen by Cole *et al* (2007) in humans with high levels of perceived loneliness[158].

As demonstrated earlier, basal level SI mice compared to SH mice had a significantly lower NLR, a subclinical marker of inflammation. High NLR scores are associated with

poor prognosis during bacterial infection suggesting that SI mice would have some degree of protection during bacterial sepsis[274,275]. As social isolation in the LPS model of sepsis showed an increase in the early NFκB cytokines, IL-6 and TNF-α, levels in plasma but an absence of changes in the late NFκB cytokines or in PLF, this suggests that social isolation does not exert its effects on the immune system in an indiscriminate manner.

As social isolation seemed to effect only some aspects of the immune system, the second model of sepsis that was utilised was the live *E.coli* model, which allowed the functional effects of the immune system during social isolation to be elucidated. During, *E.coli* induced sepsis both male and female SI CD-1 mice were found to lose less weight and appeared to be physically less sick compared to SH CD-1 mice, although this effect was more pronounced in males than females. Ideally, mice would have been assessed according to the murine sepsis score, which scores mice for appearance, level of consciousness, activity, response to stimulus, appearance of eyes, respiration rate and respiration quality. In retrospect, SH CD-1 mice in particular displayed many of the markers of high sepsis severity according to the murine sepsis score, including only moving when provoked, piloerection of the far, eyes half closed and cloudy[328].

Weight loss is most commonly monitored in the cecal ligation puncture (CLP) model, a more long-term sepsis model, on a daily basis and in this model, mice typically lose about ~1g of weight over the 24-hour period which is attributed to both the stress of surgery and the initial infection[329]. Similarly, in the live *E.coli* model of sepsis used here the SH mice lose ~1g in weight but over a much shorter 6-hour time period, as a pilot study at 12 hours resulted in high mortality of 60% in the SH group (data not shown). However, in the faecal slurry model of sepsis, where homogenised faeces are injected by i.p.,

weight loss is not seen at the 1 day mark[328]. In a study that used a slightly higher dose of *E.coli* ($1.5x10^7$ CFU) at the 1 day time point, mice had lost ~5% of their body weight whilst at the 6-hour time point, the SH mice in our study had lost ~3.4% of their body weight, thus suggesting that if the model had been continued a similar weight loss as this study would have occurred[330]. The main benefit of this model of the live *E.coli* model of sepsis is that it can induce severe sepsis without the need for surgery. As SI mice lost less weight over the 6-hour time period, this suggests that they have some protection against *E.coli* induced sepsis.

SI mice lost less weight over the 6-hour time period compared to SH mice and it is likely that the weight loss seen during *E.coli* induced sepsis is due to water loss, as such a profound weight loss over this period of time is otherwise unlikely. There are two main routes whereby this water loss could occur *via* fever and diarrhoea and urine. However, to objectively and accurately quantify whether there was a change in temperature over the 6-hour time period that may indicate a fever, radiotelemetry probes would have to be used, which requires surgery and thus induces stress[329]. In order to assess the differences in water loss *via* diarrhoea and urine, metabolic cages could be used which requires mice to be individually housed but this would be a confounding factor in a study of this nature[331,332].

In the live *E.coli* model of sepsis, the expression of plasma cytokines at 6 hours suggests that SI mice might have a primed bacterial response, as the early NFκB cytokines, IL-6 and TNF-α, which are involved in the bacterial immune response were lower in SI mice compared to SH mice. In contrast, IFN-γ levels which are associated with the late NFκB response, antiviral response, were undetectable at this time point[158]. The lower cytokine levels in SI mice suggest that a primed bacterial response allows for bacteria to be cleared

both systemically and locally more effectively, thus reducing levels of inflammatory cytokines. This primed bacterial response was confirmed by the bacteria counts in the blood and PLF which were significantly lower in SI male mice compared to male SH mice, whilst in females only the blood had significantly lower bacteria. Although SI mice in both sexes had enhanced bacteria clearance, it is interesting to note that female mice needed their blood and PLF diluted at a much higher dilution to see clear colonies. This suggests that there is sexual dimorphism in the ability to clear bacterial infection during sepsis. Although controversial in humans, the literature has reported sexual dimorphism in terms of clinical outcomes and mortality. However, in contrast to what is seen here, most studies report that females have better clinical outcomes and mortality[319–323]. Interestingly, the finding of the reduced bacteria in SI mice after a bacterial challenge has also been documented in a wound healing model, where it has been reported that SI mice had less bacteria in their wounds at the end of the study, even after being challenged with additional bacteria in the wound, suggesting enhanced bacterial clearance[333].

In male SI CD-1 mice there were significantly more F4/80$^+$ CD11b$^+$ macrophages in the PLF, which are known to be large peritoneal macrophages (LPMs)[334]. LPMs are able to undergo phagocytosis and release NO under LPS stimulation, so it is likely that the increased presence in the peritoneal cavity contributes to the lower bacterial counts seen in the PLF of SI mice and thus minimising the spread of bacteria systemically[335]. Additionally, unstimulated peritoneal macrophages from SI mice had a trend towards higher levels of *Csf2* gene expression. This suggests that during a bacterial infection they would be primed to further recruit more macrophages to the site of infection, conferring an advantage for clearance of the bacterial infection. Initially, during infection neutrophils predominate but as time goes on, macrophages become the main innate immune cells present[336]. The presence of less neutrophils in the peritoneal cavity of SI

mice suggests that the aforementioned switch in immune cell proportion has occurred at an earlier stage in SI mice compared to SH mice, once again suggesting that SI mice have a primed response to bacterial infections.

In terms, of biochemical markers of organ function AST was lower in male SI mice compared to male SH mice whilst ALT, creatinine and glucose remained similar between the housing groups. However, there was no difference in female mice between housing groups in the aforementioned biochemical biomarkers of organ function. The lower AST concentrations seen in the plasma of male SI mice suggests that less organ damage has occurred. It is possible at later time points, more profound differences in the biochemical markers of organ damage would be seen. However, in the faecal slurry model of sepsis it has been shown that AST and ALT peak at 6 hours, suggesting that this might also be the case in the *E.coli* induced sepsis model[328]. In order to gain a clear indication of severity of infection in the organs, it would be pertinent to assess bacteria levels in the organs and this would also give an indication of potential long-term survival of the mice[328].

In order, to determine whether SI mice had an enhanced ability to clear all infections, the viral mimic poly (I:C) was used to induce sepsis. However, the protective effect, attenuated weight loss and lower inflammatory markers, seen in SI mice during the live *E.coli* model of sepsis was not as pronounced in the poly (I:C) model of sepsis. Similarly to the literature, the mice in all groups lost about 2-3% of their body weight at the 6-hour time point showing that the model was effective at inducing sickness[326]. Poly (I:C) is a viral mimic that activates TLR3 and whilst social isolation is clearly beneficial during bacterial sepsis, it appears to be neither beneficial nor detrimental to the immune response during a viral challenge. At the transcriptional level, macaques with low social

status have enhanced gene expression *MyD88* and genes involved in the bacterial response, and reduced gene expression of *TRIF* and genes involved in the viral response[153,158]. However, this study only investigated the immune response at a transcriptional level, so it is possible that the changes do not translate into significant differences in sepsis severity and biomarkers of inflammation after a viral challenge. Since peak inflammation in this model occurs at 3 hours, if AST, ALT and creatinine had been measured at 3 hours instead of 6 hours, differences might have be seen between the housing groups[326]. In order to get a clearer indication of the effect of social isolation on the viral response, cytokine levels would have to be measured.

In conclusion, it was demonstrated that SI mice that were challenged with LPS at 4 hours exhibited TNF-α and IL-6 concentrations that were significantly higher in the plasma compared to SH mice, despite whole blood profile and biochemical markers of inflammation being similar between the two groups. Interestingly, it was demonstrated that SI mice subjected to *E.coli* induced sepsis exhibited less weight loss over the 6-hour period and had enhanced bacterial clearance, both systemically and locally, compared to SH mice. Additionally, it was demonstrated at the 6-hour time point that SI mice had lower levels of inflammatory markers and plasma cytokines suggesting that the infection was cleared quicker. In contrast to the benefits of social isolation seen in *E.coli* induced sepsis, SI mice given poly(I:C) induced sepsis at 6 hours did not exhibit any significant differences in weight loss over the time period or in biochemical markers of inflammation. Collectively, the data suggests that social isolation in mice primed the immune system for a bacterial response without any profound effect on the viral response.

Chapter 4

Social Isolation and Thermogenesis

4.1 Introduction

SI mice were shown to consume more food than SH mice, despite this SI mice did not weigh significantly more than SH mice. It was hypothesised that SI mice might have increased thermogenesis due to an absence of other mice to huddle with to keep warm, thus requiring increased energy input in the form of food intake[251,337]. Therefore, it was proposed that a potential difference in temperature of the mice might cause the SI mice to undergo browning of the adipose tissue.

Energy balance within the body can be summarised by the equation: $\mathbf{E_S = E_I - E_O}$ where E_S refers to energy stored in the system, E_I is energy intake and E_O is the rate of energy output from the system. Energy input can increase as a result of food and water intake, whilst energy outputs include: **1.** basal metabolic rate - energy needed by the body at rest at neutral temperature, **2.** thermal effect of food - energy needed to breakdown and absorb food, **3.** adaptive thermogenesis – production of extra heat during the cold and **4.** physical activity. Excess energy is stored in the adipose tissue[338].

Adipose tissue, more commonly known as fat, is an endocrine tissue comprised of adipocytes, lipid filled cells, a collagen matrix, fibroblasts, blood vessels and immune cells. There are two types of adipose tissue: white adipose tissue (WAT) and brown adipose tissue (BAT). WAT's main function is to store energy in the form of triglycerides, whilst conversely, BAT's role is to dissipate heat in response to cold. White adipocytes secrete hormones such as leptin, the satiety hormone, and are comprised of a large lipid droplet as well as a few mitochondria. Conversely, brown adipocytes have high mitochondrial density accompanied by numerous small lipid droplets[339]. Until

recently, it was assumed that only infants but not adult's possess BAT, but there is now evidence to support the idea that adults do in fact have BAT located in the following areas: supraclavicular, cervical, axillary and paravertebral[340]. BAT depots can also be found in mice in the following areas: interscapular, subscapular and cervical[339].

Mice that are housed at thermoneutral temperatures (30-33°C) as opposed to being housed at standard temperatures (22°C), have an altered immune response and metabolism[341–344]. For example, WT mice housed in thermoneutral conditions had increased levels of plasma cytokines and increased expression of macrophage infiltration genes in the adipose tissue and atherosclerosis was induced when mice were fed the Western diet[341]. Thermoneutrality has also been demonstrated to suppress monocyte egress from the bone marrow into the blood stream[343]. There is also evidence to show that the environment one lives in can affect how much adipose tissue is present and overall satiety. In particular, cold environments and enriched environments are able to induce metabolic changes in the adipose tissue that cause increased energy expenditure[259,345,346]. These changes may be useful in treating obesity and its associated metabolic diseases.

Browning of the adipose tissue refers to adipocytes that have WAT characteristics but are moving towards a set of characteristics more similar to that seen in brown adipocytes, with such adipocytes being referred to as beige or brite. Beige adipocytes have a medium density of mitochondria with a few to many lipid droplets[339]. Their role is to generate heat in order to maintain body temperature[339]. The most well documented cause of browning of the adipose tissue is thought to be prolonged exposure to cold[346]. During cold temperatures the sympathetic nervous system (SNS) becomes increasingly activated, thus causing increased norepinephrine (NE) production. The NE produced can

bind to the β3-adrenergic receptors on the cell membrane, thus activating the G-coupled protein $G\alpha_s$ and this induces the production of cyclic adenosine monophosphate (cAMP) by adenylate cyclase (AC). cAMP activates protein kinase A (PKA), which then phosphorylates lipases activating them. Activation of lipases causes lipolysis to occur leading to free fatty acid production, which can activate uncoupling protein-1 (UCP-1) in the mitochondria, causing uncoupling of the electron transport chain (ETC) resulting in heat being released (**Figure 4.1**)[347].

There has been some suggestions that browning of adipose tissue *via* either environmental or pharmacological mechanisms could be used to increase metabolic rate and cause reduction of weight during obesity[348]. Intermittent cold exposure in mice was found to improve metabolic rate two-fold, increase food intake and activate browning of the adipose tissue. These mice were not found to have any changes in overall body weight or adipose tissue weight but were found to have improved glucose homeostasis[260]. Leptin levels were found to be decreased in plasma in women following acute cold exposure, further suggesting cold can affect satiety[259].

Environmental enrichment, which involves placing mice in a complex and stimulating environment is the polar opposite experimental paradigm to social isolation. EE mice are leaner than controls and have upregulation of the BAT specific marker *Prdm16*, as well as genes involved in thermogenesis and β-adrenergic signalling. Within the WAT there were areas of adipose tissue that display the morphological features of BAT, with associated characteristic high UCP-1 levels. EE mice had elevated brain-derived neurotrophic factor in the hypothalamus, which lead to increased sympathoneural modulation of WAT, thus causing browning of the tissue and increased energy dissipation, which in turn was protective against diet-induced obesity[345].

However, not all browning of the adipose tissue is beneficial. Cold is associated with high cardiovascular risk, with persistent cold in *ApoE*$^{-/-}$ and *Ldlr*$^{-/-}$ mice significantly increasing plasma levels of LDL remnants, thus leading to accelerated atherosclerotic development. Atherosclerotic plaques that formed in mice subjected to prolonged cold had higher levels of both microvessels and inflammatory cells present in the plaque, which is indicative of plaque instability. Deletion of UCP-1 completely protected the mice from accelerated plaque development, suggesting that browning of the adipose tissue may be detrimental during CVD[349]. When mice are placed under thermoneutral temperatures (30°C), there is accelerated onset of macrophage related inflammation in the perivascular adipose tissue, which causes the BAT depots to take on a more WAT phenotype. This is accompanied by preferential recruitment of monocytes to the atherosclerotic lesions, thus increasing vessel wall inflammation and potentiating atherosclerosis in these mice[342]. Browning of the adipose tissue has also been observed in hypermetabolic conditions such as those seen in post-burn patients and in cancer patients, where it has a deleterious effect by driving cachexia *via* enhanced lipolysis[350,351].

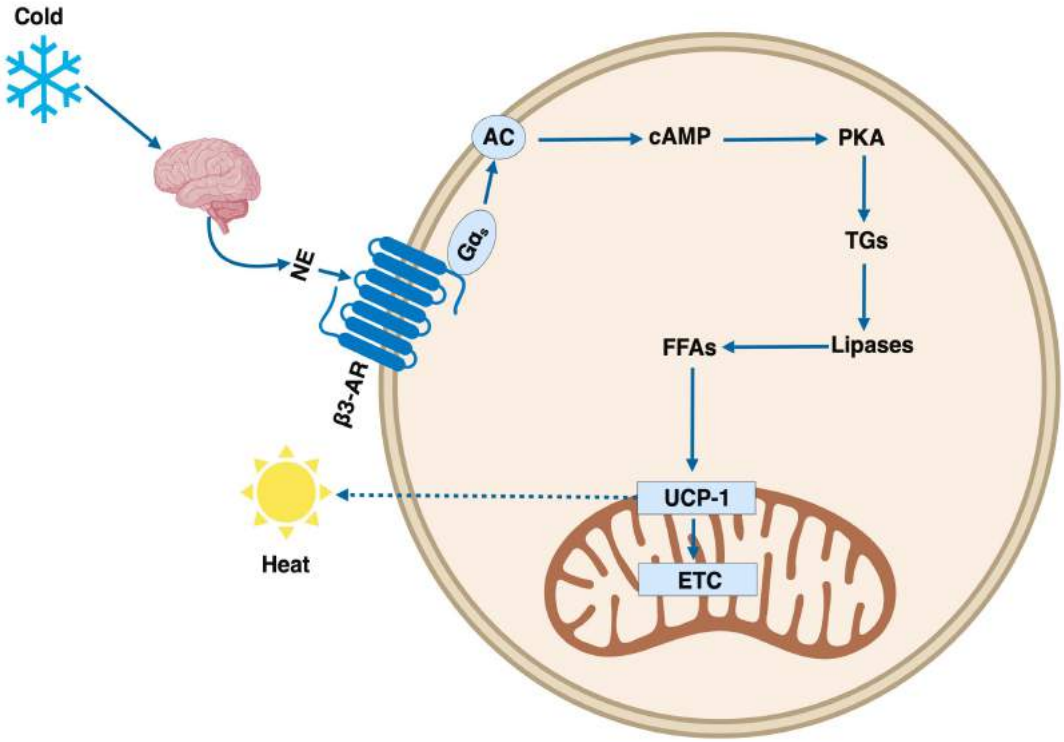

Figure 4.1: Browning of Adipose Tissue *via* Prolonged Cold Exposure. Prolonged cold exposure activates the SNS and increases NE production. NE binds to the β3-adrenergic receptors on the cell membrane activating the $G\alpha_s$, which activates AC to induce cAMP. cAMP activates PKA, which then phosphorylates lipases activating them. Activation of lipases causes lipolysis to occur, leading to free fatty acid (FFA) production, which can activate UCP-1 in the mitochondria causing uncoupling of the ETC resulting in heat being released. Image created with Biorender.

4.1.1 Chapter Aims

This study had the following aims:

1. To characterise the morphology and number of adipocytes in inguinal adipose tissue after social isolation;
2. To explore whether browning of the adipose tissue occurs during social isolation;
3. To determine whether the presence of an artificial nest would be able to reverse the metabolic and immunological changes seen during social isolation.

4.2 Methods

4.2.1 Animal Husbandry

All animals were housed in individually ventilated enclosures with standard food and water being provided *ad libitum* and with a 12-hour light-dark cycle. All experiments undertaken were approved and performed according to the guidelines of the Ethical Committee for the Use of Animals, Bart's and The London School of Medicine and Dentistry and the Home Office Regulations Act 1986 (Prof. D'Acquisto, PPL. 70/8714).

4.2.2 Modelling Social Isolation

To address whether the mice were cold, CD-1 male or female mice were either SI with or without an artificial nest for a period of 2 weeks (**Figure 4.2**). Cages were set up as follows:

- **Social housing:** 5x CD-1 mice weaned together in standard size cage (W x D x H:193x 419x 179x mm, Allentown), 2x strips of nesting material and sawdust bedding up to 5cm in depth (**Figure 2.1**).
- **Social isolation:** 1x CD-1 mouse in standard size cage (W x D x H:193x 419x 179x mm, Allentown), 2x strips of nesting material and sawdust bedding up to 5cm in depth (**Figure 2.1**).
- **Social isolation and artificial nest:** 1x CD-1 mouse in standard size cage (W x D x H:193x 419x 179x mm, Allentown), 2x strips of nesting material, sawdust bedding up to 5cm in depth and 1x artificial nest (Amazon UK, **seller.** Travelinwind) (**Figure 4.3**).

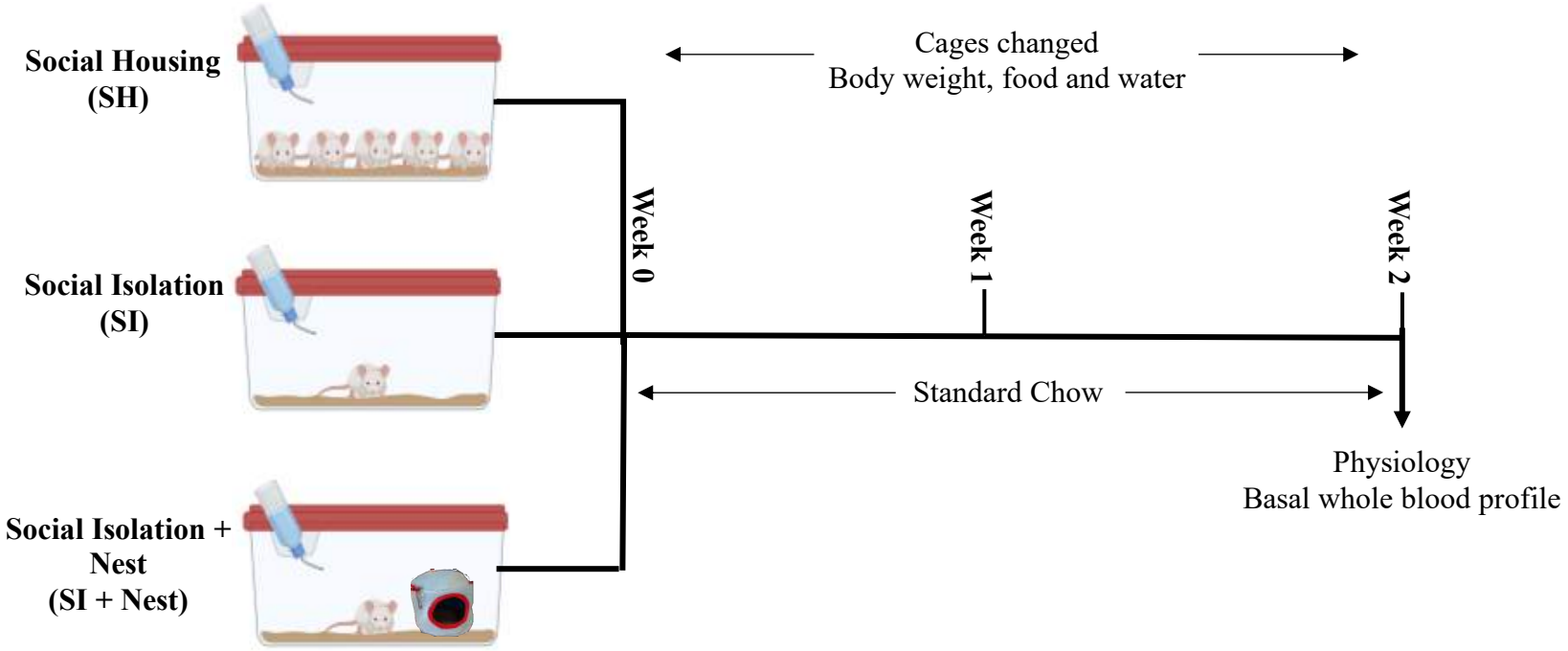

Figure 4.2: Thermogenisis CD-1 Study Overview. CD-1 mice at 5-6 weeks of age were randomly assigned to social housing (5x mice per cage) or social isolation (1x mouse per cage) or social isolation + nest (1x mouse per cage and a nest) for a period of 2 weeks, during which time the mice were fed the standard chow. Throughout the study cages were changed on a weekly basis at which time the mice were weighed. Food and water consumption and tail temperature were assessed every 2-3 days. After 2 weeks, mice were sacrificed, and two main parameters were assessed: physiology and whole blood profile.

Figure 4.3: Cage Setup for Social Isolation with Artificial Nest. Cages were set up to include: 1x CD-1 mouse with 2 strips of nesting material, sawdust bedding up to 5cm in depth and 1x artificial nest.

4.2.3 Weight Gain and Nutritional Intake

Weight was monitored on a weekly basis when cages were changed. Food and water consumption were monitored every 2-3 days and replenished as needed.

4.2.4 Temperature

During the period of social isolation, mice in all housing groups had their tail temperatures measured every 2-3 days *via* an infrared thermometer to minimise stress (Amazon UK, **seller.** Aimshine).

4.2.5 Plasma Leptin Concentration

Plasma was generated as previously described. Satiety levels were measured at the end of the social isolation period in CD-1 mice *via* quantification of leptin in plasma using a precoated murine leptin ELISA kit (Thermofisher, **cat.** KMC2281) as previously described.

4.2.6 Adipocyte Counting and Size

After the period of social isolation or social housing was complete, mice underwent cardiac puncture and were sacrificed as previously described with PLF and blood being collected as stated before. Inguinal adipose tissue, was harvested as there is less variability in the amount of adipose tissue present and it is known to be affected by cold[352]. Adipose tissue was removed by gently pulling the adipose tissue located just above the leg with forceps. This was then placed in 4% PFA overnight.

Inguinal adipose tissue underwent H&E staining and imaging as previously described for VAT. Adipocyte number and area were quantified using Image J as previously described for VAT.

4.2.7 UCP-1 Immunohistochemistry

WAT and interscapular BAT was collected from the mice by use of forceps and once removed was placed in 4% PFA overnight. Adipose tissue was paraffin embedded by Barts Cancer Institute Pathology services and tissue was sectioned at 5μm thickness before mounting on slides. Paraffin wax was removed as follows: **1.** 2x 5-minute washes in histoclear (National Diagnostics, **cat.** NAT1334), **2.** 2x 5-minute washes in 100% ethanol and **3.** 1x 2-minute wash in distilled water. Slides were washed on the rocker for 5 minutes in Tris-buffered saline (TBS).

Antigen retrieval was carried out for 45 minutes at 95°C in 10mM citrate buffer (pH6). Slides were washed in TBS as described prior to being immersed in 0.1% Triton X-100 (Sigma-Aldrich, **cat.** T8787-250ML) for 10 minutes and then they were washed a further 3x in TBS. One drop of blocking solution (Dako, **cat.** X0909) was added to each slide and they were blocked for 30 minutes. Blocking solution was removed by washing slides in TBS.

UCP-1 antibody [1:100] (Abcam, **cat.** Ab209483) was added to each slide except the streptavidin only control, which had one drop of antibody diluent on it (DAKO, **cat.** SO809). Slides were incubated at 4°C overnight. Slides were washed 3x in TBS. Polyclonal Swine Anti-Rabbit Immunoglobulins/HRP [1:100] (DAKO, **cat.** P0217) was added to all slides except the streptavidin only control, which had one drop of antibody diluent on it. The slides were incubated in the dark at room temperature for 1 hour and then washed 3x in TBS. Streptavidin Alexa Fluor 488 conjugate (Invitrogen, **cat.** S32354) was added to all slides and slides were incubated in the dark at room temperature for 30 minutes. Slides were washed 3x in TBS.

Slides were mounted with 1x drop of Flouroshield™ with DAPI (Sigma, **cat**. F6057-20ML) and a coverslip. Slides were imaged at 60x zoom on the EVOS FL microscope.

4.2.8 Whole Blood Cellularity

Cardiac puncture was performed as previously described. Whole blood was aliquoted and sent to MRC Harwell for full blood count analysis (total blood leukocytes and the %s of lymphocytes, neutrophils, monocytes, basophils and eosinophils) on the Advia 2120 haematology analyser.

4.2.9 *E.coli* Induced Sepsis

E.coli induced sepsis was carried out as previously described. In brief, male mice were weighed before and after sepsis to monitor weight loss. Sepsis was induced with $1x10^7$ CFU *E.coli* serotype 06:K2:H1 [ATCC®19138™] and after 6 hours mice were sacrificed. Plasma and PLF were cultured overnight and CFU/ml were calculated.

4.2.10 Cytokines

Plasma was diluted using ELISA/ELISASPOT diluent (1X) at 1:10 and 1:50 dilution for IL-6 and 1:100 for TNF-α. IL-6 (Invitrogen, **cat.** 88-7064-77) and TNF-α (Invitrogen, **cat.** 88-7234-77) were quantified in plasma by ELISA as previously described.

4.2.11 Statistics

Significance was tested using the statistical analysis specified in each figure legend on GraphPad Prism 8 (GraphPad Software Inc, USA).

4.3 Results

Environmental temperature, specifically reduced temperature, is well documented to affect metabolic and immunological parameters[346,353]. Since mice are normally social creatures who huddle together for warmth it was hypothesised that SI mice might have increased thermogenesis as they have no littermates to huddle with, thus causing them to eat more to produce the energy needed to keep warm[251,337]. This hypothesis was tested here by giving some of the SI mice an artificial nest to use in order to stay warm, if they so desire.

4.3.1 Weight Gain and Nutritional Intake

To determine whether the increase in food intake despite lower weight gain across the study was the result of increased thermogenesis due to an inability to huddle, weight gain and nutritional intake was reassessed with some SI mice having an artificial nest to try and help them keep warm. There were no significant differences in weight gain across the three housing groups (**Figure 4.4a**). Food intake over the 2-week period was significantly higher in SI mice compared to SH mice, whilst food intake was significantly lower between male SI + Nest mice compared to male SI mice (**Figure 4.4b**). There was no significant difference in water consumption across the housing groups, although there was a trend towards male SI mice and SI + Nest mice having increased water intake compared to SH male mice during the 2-week period (**Figure 4.4b**).

Female SH mice showed a trend towards gaining more weight over the course of the study compared to SI mice and SI + Nest mice (**Figure 4.5a**). Food intake in female SH mice showed a trend towards being lower compared to SI mice and SI + Nest mice (**Figure 4.5b**). Water intake in female SH mice showed a trend towards being lower compared to SI mice and SI + Nest mice (**Figure 4.5b**).

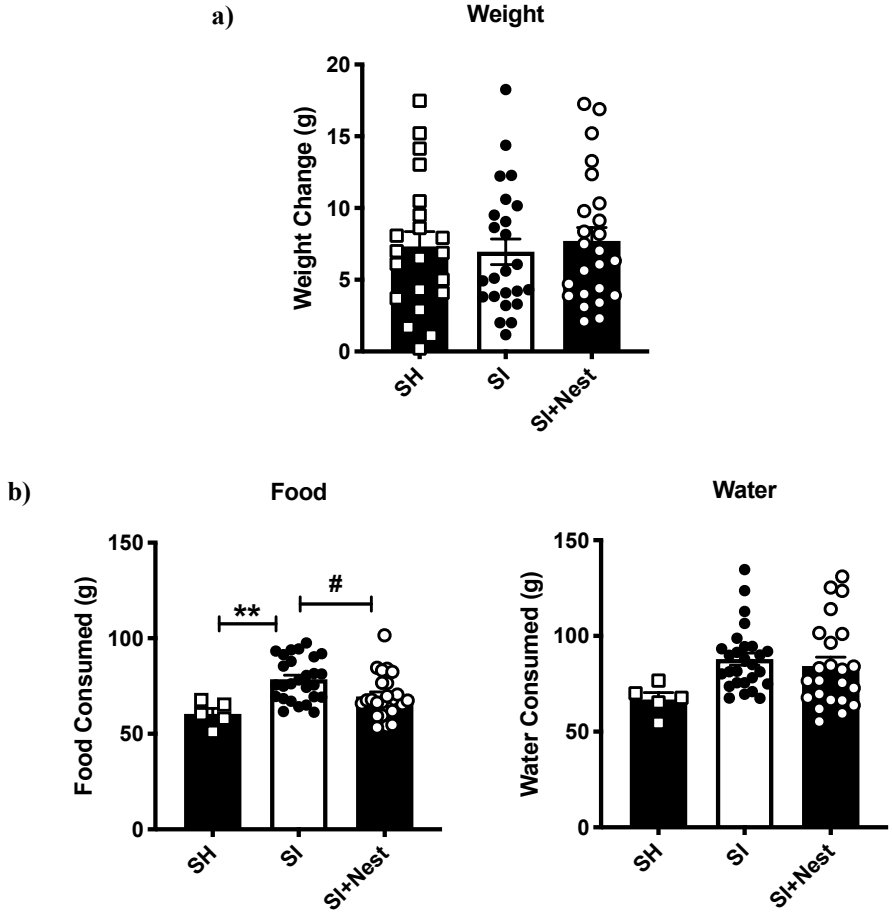

Figure 4.4: Weight and Nutritional Intake - Males. The following parameters were assessed: **a)** weight change and **b)** food and water intake over the period of 2 weeks of social housing or social isolation ± nest. Each bar shows mean ± SEM of n=22-27 mice from 4 separate experiments with each symbol representing n=1 mouse for weight or n=1 cage for food and water intake. Significance was determined when #$p<0.05$ and **$p<0.01$ was gained using a one-way ANOVA with Tukey's post-hoc analysis.

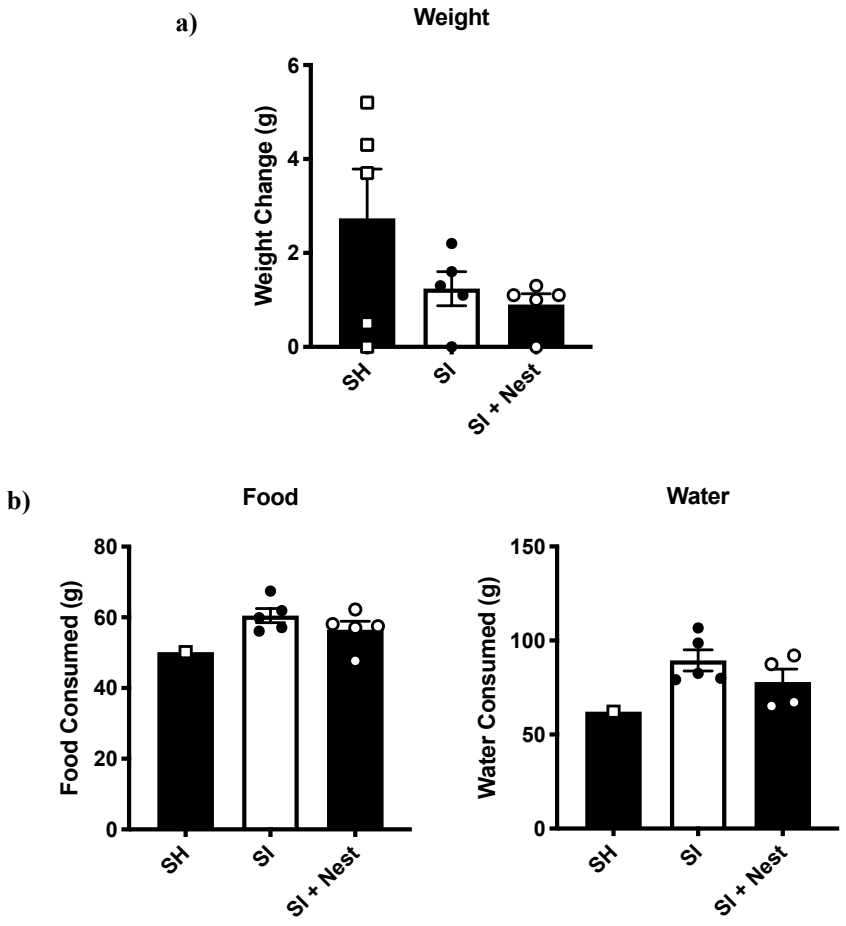

Figure 4.5: Weight and Nutritional Intake - Females. The following parameters were assessed: **a)** weight change, **b)** food and water intake over the period of 2 weeks of social housing or social isolation ± nest. Each bar shows mean ± SEM of n=4-5 mice with each symbol representing n=1 mouse for weight at 14 days or n=1 cage for food and water intake. Significance was determined when $p<0.05$ was gained using an unpaired parametric T-test between SI and SI + Nest for food and water intake and for weight a one-way ANOVA with Tukey's post-hoc analysis.

4.3.2 Plasma Leptin

In male mice, plasma leptin was measured to investigate whether satiety in SI mice was affected by the presence of an artificial nest. Plasma leptin concentration was similar between SH and SI mice (**Figure 4.6**). SH mice had a significantly higher plasma leptin concentration compared to SI mice that were given an artificial nest (**Figure 4.6**). The SI mice had significantly higher plasma leptin concentration compared to those SI mice given an artificial nest (**Figure 4.6**).

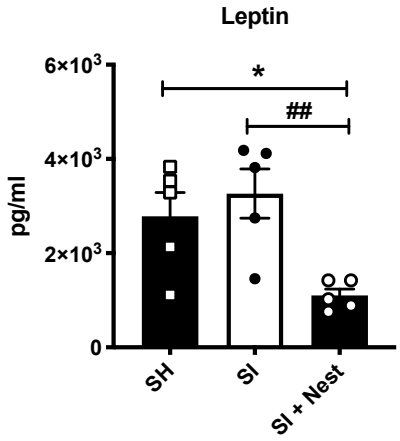

Figure 4.6: Plasma Leptin Levels. Plasma leptin levels were quantified *via* ELISA after 2 weeks of social housing or social isolation ± nest. Values are expressed as mean ± SEM of 5 mice per housing group with each symbol being representative of a single mouse. Significance was determined by use of a one-way ANOVA and post-hoc analysis using Tukey's multiple comparisons test, where * $p<0.05$ and ## $p<0.01$.

4.3.3 Tail Temperature

Tail temperature was monitored every 2-3 days over the study using an infrared thermometer to assess whether there were any differences in tail temperature between SH and SI mice that might account for the increased food intake in SI mice, and whether the presence of an artificial nest would increase tail temperature in social isolation. Throughout the study, there were no significant differences in tail temperature on any one day across all three housing groups in male mice (**Figure 4.7**). Similarly, in female mice there were no significant differences in tail temperature on any one day across the housing groups (**Figure 4.8a**). In male mice, the average tail temperature across the study for all groups was similar (**Figure 4.7b**). In female mice, the average tail temperature across the study for SH and SI mice showed a trend towards being higher compared to SI mice + nest **(Figure 4.8b**).

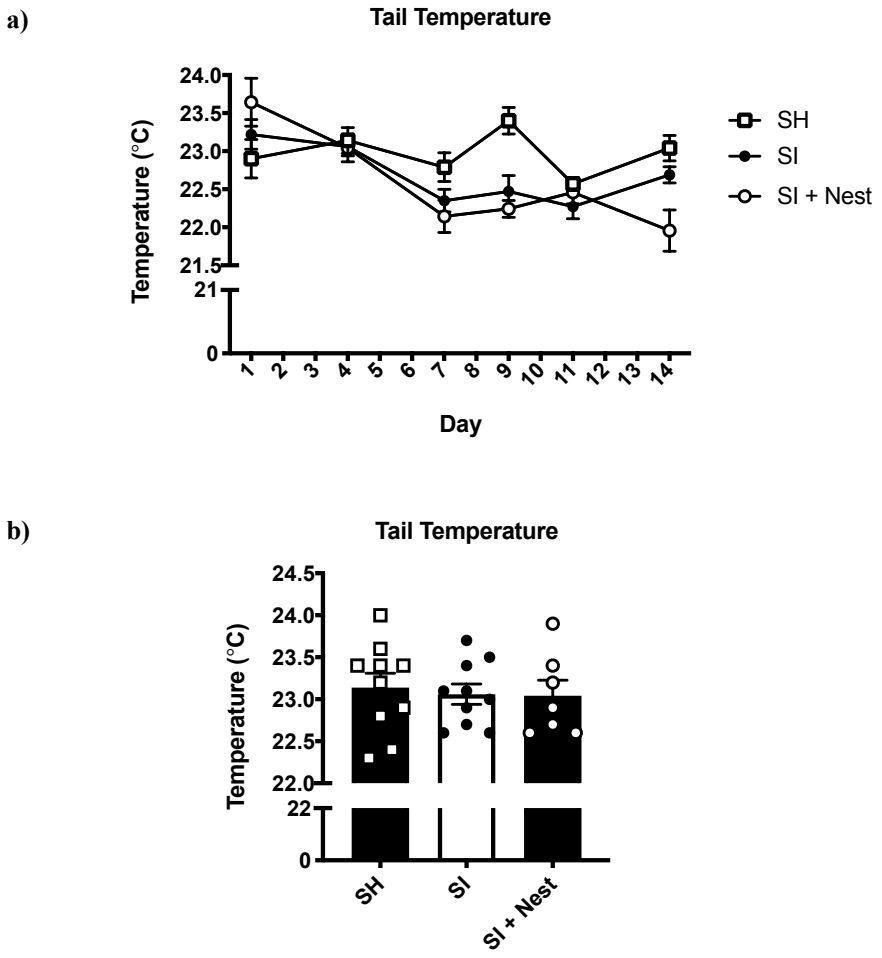

Figure 4.7: Tail Temperature in Males. a) Comparative tail temperature over time where symbols represent mean±SEM per housing group of n=7-10 mice per housing group and **b)** average tail temperature across the study for each housing group where values are expressed as mean ± SEM of n=7-10 mice per housing group and symbols represent a single mouse. Significance was assessed by use of a one-way ANOVA and post-hoc analysis using Tukey's multiple comparisons test.

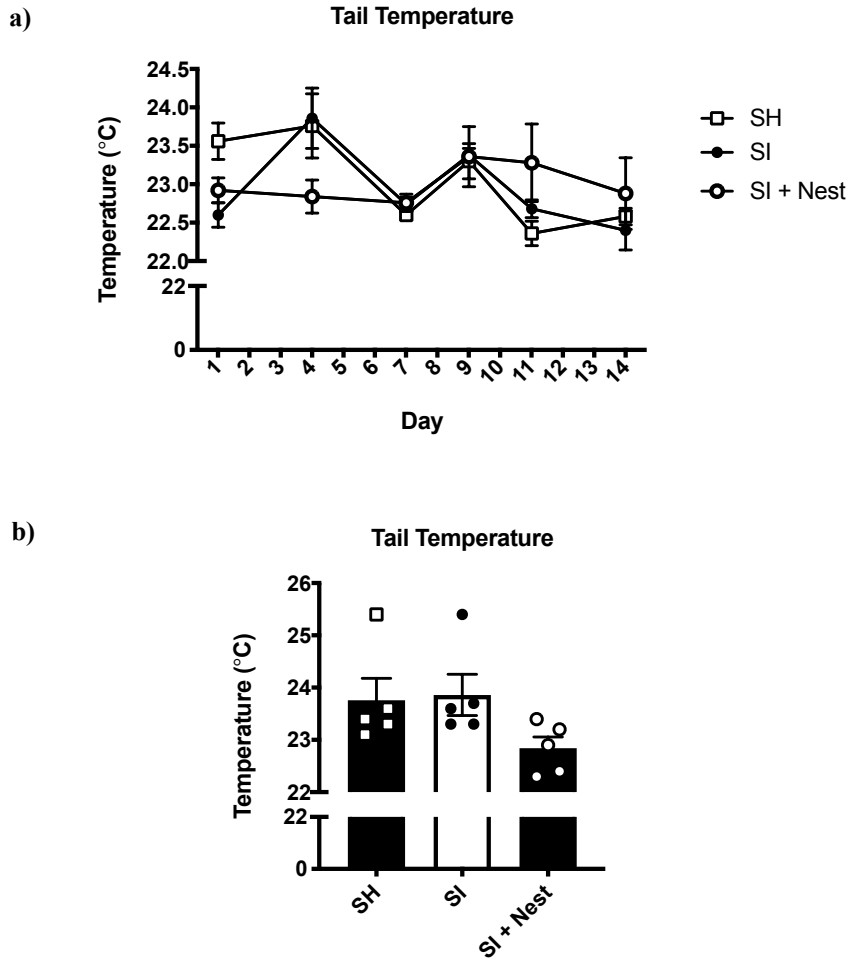

Figure 4.8: Tail Temperature in Females. a) Comparative tail temperature over time where symbols represent mean±SEM per housing group of n=5 mice per housing group and **b)** average tail temperature±SEM across the study for each housing group where n=5 mice per housing group and symbols represent a single mouse. Significance was assessed by use of a one-way ANOVA and post-hoc analysis using Tukey's multiple comparisons test.

4.3.4 Inguinal Adipose Tissue Characteristics

In male mice, there was no significant difference between adipocyte numbers between the housing groups (**Figure 4.9a**). Similarly, there was no significant difference in the adipocyte areas across the housing groups, although both SI and SI + Nest mice showed a trend towards a slightly smaller adipocyte area compared to SH mice (**Figure 4.9b**). Representative frequency of adipocyte size in 1x mouse per housing group showed that SI + nest mice and SI mice had a higher % of smaller adipocytes (<500μm^2) compared to SH mice, and that in all housing groups, as adipocyte size increases the % of adipocytes decreases (**Figure 4.9c**). Representative H & E stained images show that SH mice have less adipocytes present, which are larger in size compared to SI mice and SI + Nest, which have more adipocytes present but are smaller in size (**Figure 4.10**).

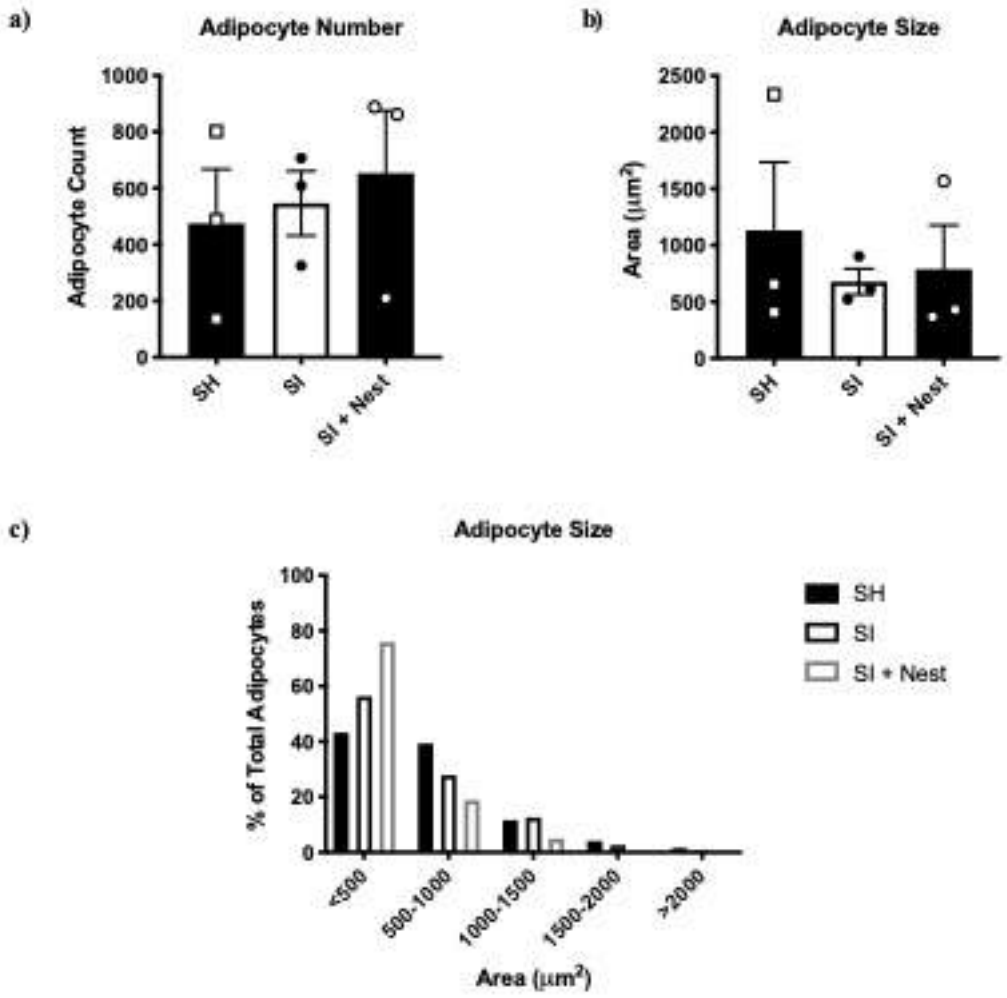

Figure 4.9: Inguinal Adipose Tissue Characteristics. Inguinal adipose tissue was stained with H & E and imaged at 20x. In the inguinal adipose tissue, the following was assessed: **a)** number of adipocytes present and **b)** adipocyte size and **c)** representative % of total adipocytes for each adipocyte size range with n=1 mouse per housing group. For adipocyte number and size, data is shown as the mean ±SEM with n=3 mice per housing group and each symbol is representative of 1x individual male mouse. Significance was assessed for adipocyte number and size by use of a one-way ANOVA and post-hoc analysis using Tukey's multiple comparisons test.

a)

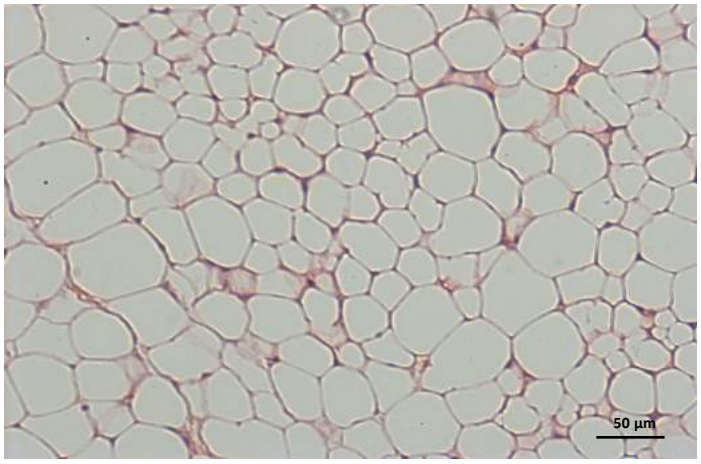

SH
Adipocytes: 147

b)

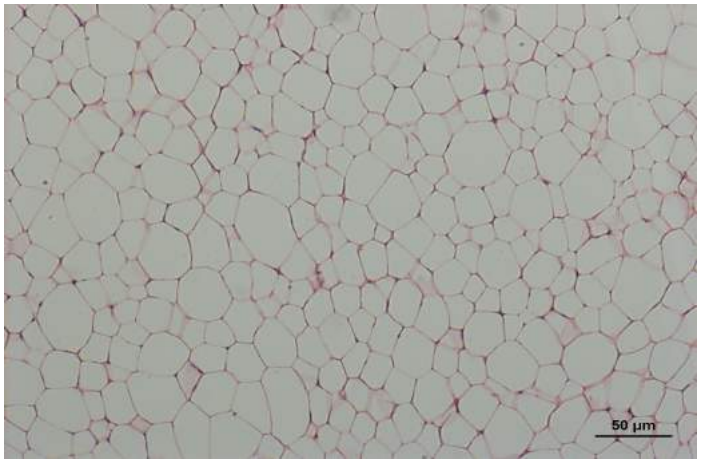

SI
Adipocytes: 202

c)

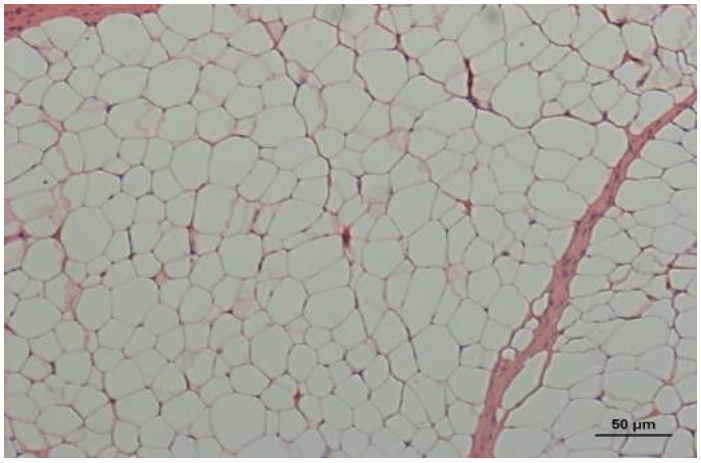

SI + Nest
Adipocytes: 262

Figure 4.10: Representative Inguinal Adipose Tissue Images. Representative images of H & E stained inguinal adipose tissue at 20x magnification from male **a)** SH, **b)** SI and SI + Nest mice. Images are representative of n=3 mice per housing group. Scale bars are representative of 50µm.

4.3.5 UCP-1 in WAT

Immunohistochemical staining for UCP-1 in WAT from male SH and SI mice demonstrated that UCP-1 was not expressed either in SH or SI mice (**Figure 4.11**). UCP-1 could however, be detected in BAT (**Figure 4.11**).

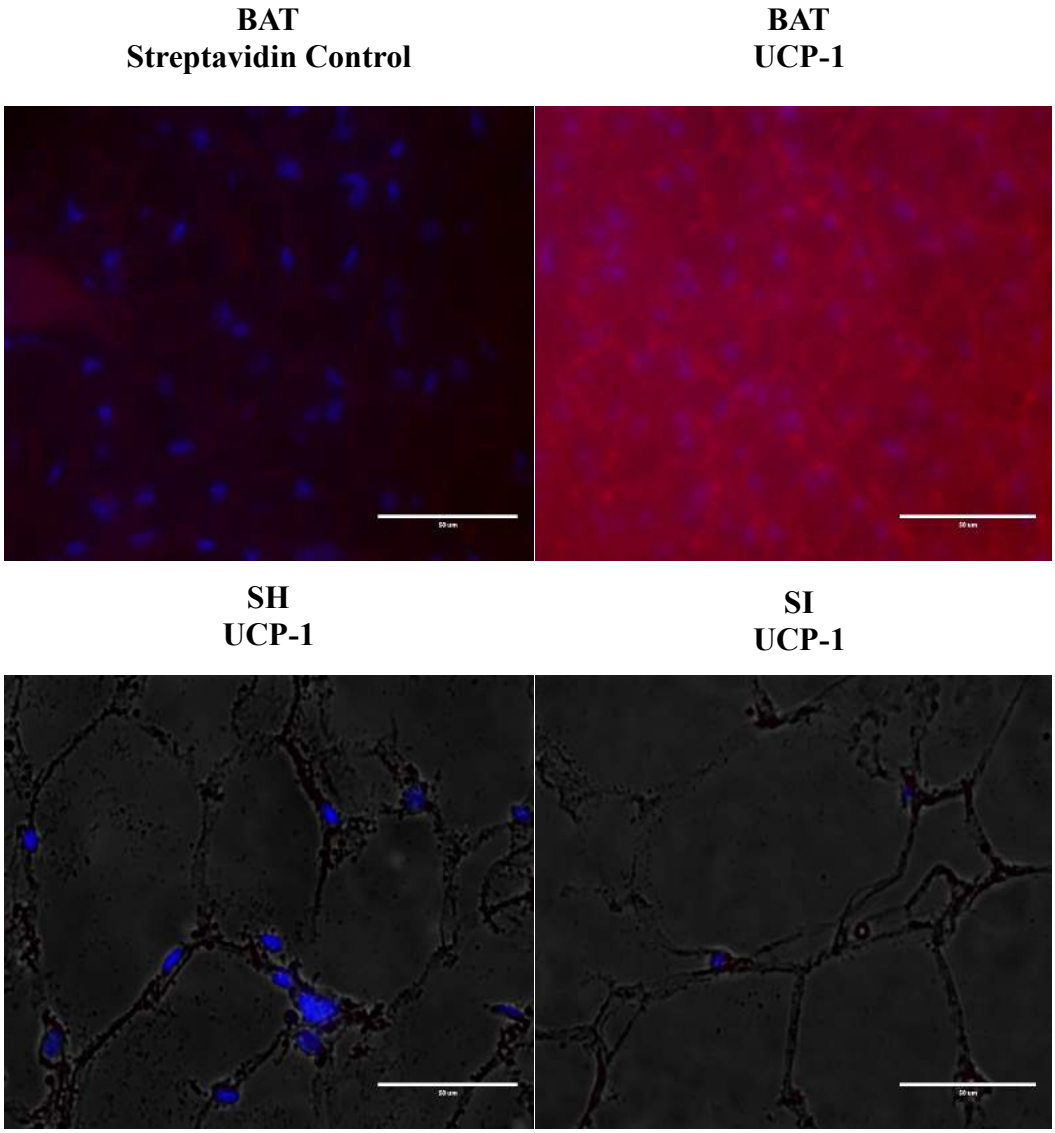

Figure 4.11: Representative UCP-1 Stained in White Adipose Tissue Images. The top panel shows representative images of BAT with streptavidin and DAPI, streptavidin only control, (left) and BAT stained with UCP-1 and DAPI, positive control, (right). The bottom panel shows representative brightfield images of UCP-1 and DAPI stained WAT in SH mice (left) and SI mice (right). Images are representative of n=3-4 mice. Scale bars represent 50µm and all images were taken at 60x zoom. UCP-1: red and DAPI: blue.

4.3.6 Peripheral Blood Counts

Since food intake was partially reversed by the presence of an artificial nest in male SI mice, basal immune cell profile was tested to determine whether the changes seen during social isolation could also be potentially caused by changes in thermogenesis. Basal immune cell profile was assessed in whole blood after 2 weeks of social isolation or social housing. Total leukocyte numbers were similar between SH and SI mice whilst there was a trend towards lower leukocyte counts in SI + Nest mice compared to the other housing groups (**Figure 4.12a**). The number of lymphocytes showed a trend towards being higher in SH mice than SI mice and SI+Nest mice, which had similar numbers of lymphocytes (**Figure 4.12b**). Monocytes and neutrophil counts were found to be similar across all housing groups (**Figure 4.12c-d**). Basophil numbers showed a trend towards being higher in SH mice compared to SI and SI + Nest Mice (**Figure 4.12e**). Across the housing groups there was no significant differences in the number of eosinophils present. (**Figure 4.12f**).

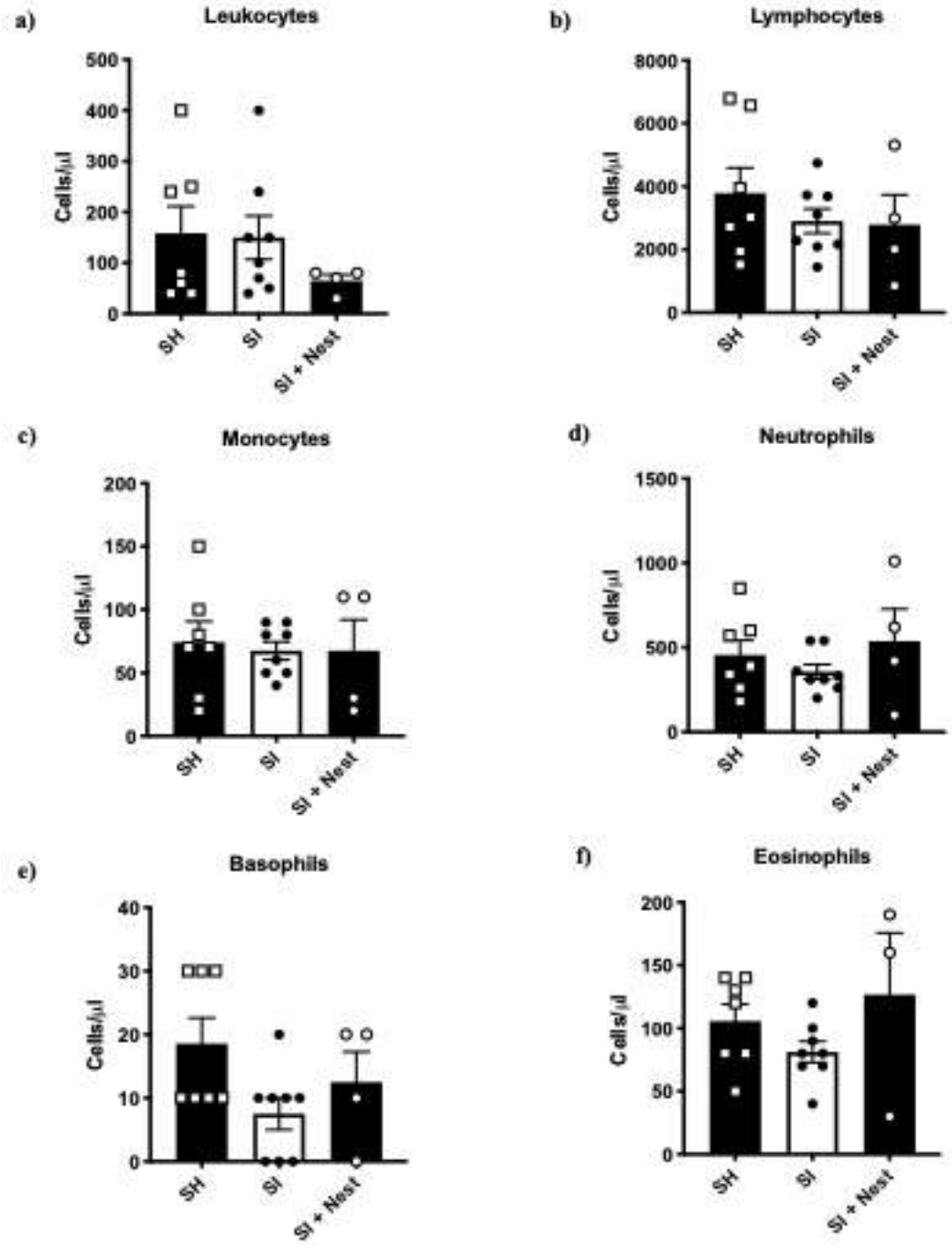

Figure 4.12: Basal Whole Blood Cellularity - Male. Basal immune cell response was assessed after 2 weeks of social isolation±nest or social housing: **a)** total leukocyte count**, b)** lymphocyte count, **c)** monocyte count, **d)** neutrophil count, **e)** basophil count and **f)** eosinophil count. Each bar shows mean ± SEM of n=4-8 mice with each symbol representing a single mouse. Significance was assessed by use of a one-way ANOVA and post-hoc analysis using Tukey's multiple comparisons test.

4.3.7 Temperature and the Environment During Sepsis

Since the presence of an artificial nest during social isolation could partially reverse increased food intake, SI mice were given an artificial nest and challenged with sepsis to elucidate whether the environment or social isolation itself was causing the beneficial changes during sepsis.

Weight loss over the 6-hour period of sepsis was measured as an objective indication of how sick the mice were. In male mice, there was a trend towards SH mice losing more weight over the 6-hour period than SI and SI + Nest mice (**Figure 4.13a**). Overnight incubation of blood and PLF on LB agar plates allowed CFU/ml to be calculated giving an indication of bacterial load. Male mice exhibited a trend towards SH mice having higher bacterial loads systemically, blood, and locally, PLF compared to SI mice and SI + Nest mice (**Figure 4.13b**). SI + Nest mice had a trend towards increased bacteria load in blood compared to SI mice (**Figure 4.13b**). There was a positive trend between increasing weight loss and higher bacteria CFU/ml in blood and PLF across all the groups (**Figure 4.13c**).

IL-6 and TNF-α concentrations were measured in plasma *via* ELISA at 6 hours after the induction of sepsis, to give an indication of systemic inflammation. TNF-α concentrations were similar in the plasma 6 hours post-sepsis across all housing groups (**Figure 4.14a**). IL-6 levels showed a trend towards being slightly lower in SI mice than in SH mice and SI + Nest mice (**Figure 4.14b**).

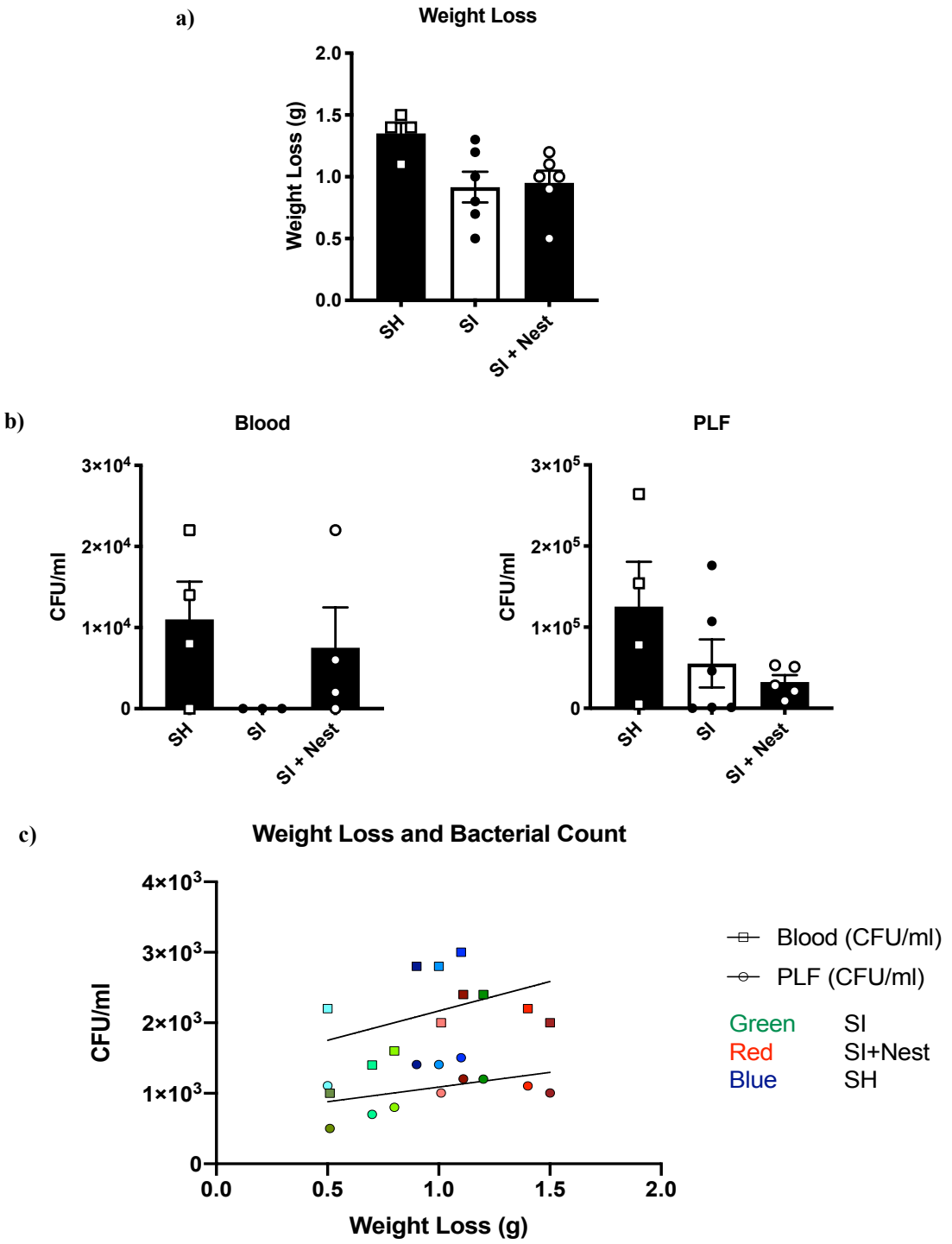

Figure 4.13: Sepsis Severity. Sepsis severity was assessed in male mice as follows: **a)** sepsis induced weight loss and **b)** bacterial clearance in blood (left) and PLF (right) after 24 hours of culture where each bar shows mean ± SEM of n=3-6 mice and each symbol representing a single mouse. Significance was assessed by use of a one-way ANOVA and post-hoc analysis using Tukey's multiple comparisons test. **c)** correlation between weight loss and bacterial count in blood and PLF where each colour shade represents a single mouse. Mice were excluded if their agar plates were too confluent to count.

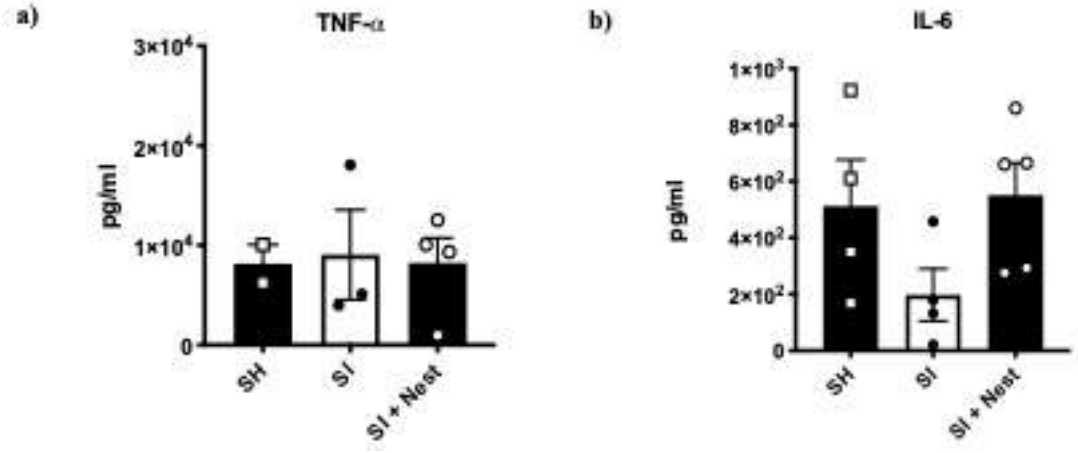

Figure 4.14: Plasma Cytokines. a) TNF-α and **b)** IL-6 were measured in plasma at 6 hours post-induction of sepsis in male mice. Data shown as mean ± SEM where n=2-6 mice per housing group and each symbol represents an individual mouse. Significance was assessed for IL-6 by use of a one-way ANOVA and post-hoc analysis using Tukey's multiple comparisons test.

4.4 Discussion

Small animals such as mice have a high surface area to body mass ratio, meaning they have a greater predisposition to losing heat to the environment, which potentially could be exacerbated in SI mice due to the lack of huddling with littermates. It was therefore proposed that SI mice might have to increase thermogenesis *via* increased food intake, as huddling can increase metabolic efficiency by 40–65%[251,337]. To this end, this chapter aimed to investigate whether thermogenesis was altered during social isolation and whether the presence of an artificial nest, to theoretically provide the option for warmth, could reverse the effects seen in nutritional intake and immune systems parameters as a result of social isolation.

Initially, weight and nutritional intake were assessed in the SI + Nest group compared to SI and SH mice to see if the presence of an artificial nest could reverse the changes in weight and nutritional intake that were demonstrated earlier in SI mice, by theoretically increasing the temperature. In male mice, weight gain across the study was similar across all groups, whilst weight gain showed a trend towards being lower in female SI and SI +Nest housing groups compared to SH females. Interestingly, female mice have been shown to be have enhanced BAT thermogenesis and be warmer overall in the absence of littermates compared to males, which might partially account for why the presence of an artificial nest does not increase weight gain over the 2 week period[251]. To confirm the results seen in female mice with regards to weight and nutritional intake in the presence of artificial nests during social isolation, larger scale studies would have to be done with around 10 mice per housing group. Food intake was partially reversed in the male SI + Nest mice but not in female SI + Nest, thus suggesting that females can better modulate their temperature in cold.

Since leptin is thought to be pyrexic in nature and is capable of increasing body temperature in a manner independent of thermogenesis, a feat that is accompanied by reducing heat loss, plasma leptin levels were measured[354]. As mentioned previously, plasma leptin levels increase with increased food intake as a preventative mechanism to avoid excessive eating[355]. Plasma leptin levels were significantly reduced in SI + Nest compared to both SI and SH mice. Since the majority of studies investigating the effects of both acute and long-term periods of cold showed that leptin levels decrease, it would be expected that leptin levels would partially return back to that of SH mice if temperature was playing a role[259–261]. However, it could be argued that the presence of an artificial nest during social isolation is enriching the environment, which could explain the lower plasma leptin concentration despite no change in food intake as environmental enrichment has been shown to decrease leptin levels[356].

Whilst in **Chapter 2**, leptin concentrations showed a trend towards being lower in SI mice compared to SH mice the trend seen in this chapter shows a very slight trend towards the opposite with regards to leptin concentrations. One reason why such a disparity might be seen between the results, is that the mice might have consumed food at different times prior to the collection of the blood. This would mean that the mice that had consumed food closer to the time of blood collection would have higher leptin concentrations than those that had consumed food at a longer time before collection[357]. In order to minimise this where possible, blood was collected first thing in the morning, but without fasting the mice it is impossible to completely rule out the possibility that the time of last food intake could be affecting plasma leptin concentrations[358].

In order to address the possibility that SI mice may be cold, tail temperature was measured using an infrared thermometer. This method was chosen as it required

minimum handling of the mice and preventing the need for surgery. However, no significant changes in tail temperature across the housing groups were seen in both male and female mice over the study. It is possible that small changes in temperature could be missed by this method, as measuring tail temperature has been shown to be more variable than that seen by the insertion of a rectal probe[359]. This suggests that by increasing food consumption to allow for increased thermogenesis, SI mice can maintain their body temperature in the absence of huddling.

In inguinal adipose tissue, whilst there were no changes in adipocyte number between the groups, there was a trend towards smaller sized adipocytes in the adipose tissue collected from SI mice compared to SH mice, thus confirming the findings shown in VAT. Interestingly, SI + Nest mice had a higher % of smaller adipocytes (<500μm^2) in comparison to the other housing groups, thus illustrating an effect of the presence of the artificial nest. The presence of smaller adipocytes in SI + Nest mice is in concordance with the decreased concentration of plasma leptin, as there is a positive correlation between increased WAT mass and its associated adipocyte hypertrophy and leptin secretion[360].

A key characteristic of browning of the adipose tissue, which commonly occurs in response to prolonged cold exposure, is high numbers of small sized adipocytes containing high numbers of mitochondria[260,361]. It has been suggested that CD-1 mice that had nesting material, thus providing increased thermal capacity, consequently have increased UCP-1 expression, a marker of browning of adipose tissue[362]. However, the absence of UCP-1 in WAT would suggest that this is not the case in this study. It would be pertinent to also assess UCP-1 in SI+Nest mice to gain an understanding of whether browning of the adipose tissue occurs in these mice. Additionally, to confirm an absence

of browning of the adipose tissue, it would be essential to look at a variety of different adipose tissue depots, as browning more readily occurs in subcutaneous adipose tissue than in VAT[363]. One reason why no change in UCP-1 is potentially seen, is that leptin is thought to be able to increase temperature in a manner independent of BAT[354]. This again suggests that SI mice can increase their thermogenic capacity *via* increased food consumption.

Whole blood profile was assessed as changes in temperature are thought to alter whole blood counts[364]. It is unsurprising that the presence of an artificial nest in SI mice did not alter the whole blood profile, since initial studies comparing SH mice and SI mice revealed no significant changes in the total number of leukocytes present and the relative % of leukocyte subtypes present.

There is evidence that as temperatures increase towards thermoneutral temperatures in both humans and mice, mobilisation of monocytes in the blood is reduced, which could prove important during infection, and for that reason the *E.coli* sepsis model was carried out in SI+ Nest mice[343]. The presence of an artificial nest during social isolation was not able to reverse decreased weight loss during the live *E.coli* model of sepsis as characteristic of SI mice. Interestingly, the data tentatively suggests that the presence of an artificial nest partially reverses enhanced bacterial clearance in the blood but not in the PLF of SI mice during sepsis. It has been reported that reduced monocyte mobilisation occurs as a result of increasing temperature, which would have implications on bacteria clearance[343]. It is therefore possible that the presence of an artificial nest might provide enough warmth independently of the increased thermogenesis seen in SI mice to maintain body temperature, and thus reduce monocyte mobilisation, explaining the partial increase in bacteria load in the blood. As bacterial clearance is only partially

reversed in blood and not in PLF, this suggests that social isolation does not indiscriminately exert its effects on the immune system.

Cytokine release from immune cells is known to be altered by temperature, thus cytokine concentrations were assessed in plasma post sepsis[365,366]. IL-6 concentrations in SI + Nest mice were reversed back to similar levels as those seen in SH mice, suggesting that increased thermogenesis might account for the blunted IL-6 response seen in SI mice. Due to issues with TNF-α detection, only a few plasma samples were analysed, which might account for why TNF-α levels in SI+Nest mice were not reversed back to that seen in SH mice, as is seen for IL-6. LPS stimulated human monocytes and macrophages have a blunted IL-6 and TNF-α response when kept in suboptimal temperatures, with the response returning to normal as temperature increases to thermoneutrality[365]. Cold temperatures lead to increased thermogenesis to maintain body temperature, thus it is not clear whether at the physiological level temperature or increased thermogenesis causes the blunted cytokine response[261]. If SI mice increase thermogenesis to maintain their body temperature, increased thermogenesis and not temperature might account for the blunted cytokine response seen in that group. When SI mice have access to a nest, this could potentially reduce the need for increased thermogenesis by helping to conserve heat, which might explain the reversal of plasma IL-6 concentration back to similar concentrations seen in SH mice. As the data indicate that SI mice maintain a similar body temperature to the other housing groups through increased thermogenesis, it is likely that the blunted cytokine response is the result of differences in thermogenesis not temperature. Higher *n* numbers are needed to confirm the results discussed here.

It is not surprising that there is a positive correlation between increased weight loss during sepsis and higher bacteria counts, both in the blood and PLF. Unfortunately, as

basal whole blood cellularity was carried out in a separate set of mice to those that got sepsis, it is impossible to see if there is any direct correlation between the numbers and types of leukocytes present, bacterial load and weight loss during sepsis. Food and water intake were not monitored throughout the 6-hour period, which would have provided an indication of sepsis severity and likelihood of survival. This is because reduced food intake, or anorexia, has been shown to be protective during bacterial infection, thus it would have been interesting to measure food intake across the 6-hour period and plasma glucose concentration, as those mice that consumed more food and thus had higher glucose levels would be less likely to survive[116].

In conclusion, there were no differences in tail temperature across the housing groups, suggesting SI mice can maintain their temperature by increasing their food intake. This was further confirmed, as in male SI+Nest mice food intake was partially reversed to a level more similar to that seen in SH mice, suggesting that SI mice increase their food intake to maintain body temperature. Furthermore, the absence of UCP-1 expression and similar adipocyte characteristics suggested that browning of the adipose tissue had not occurred, indicating an absence of temperature difference between SI and SH mice. There was an absence of any differences in the whole blood profile and weight loss during sepsis in SI+Nest mice compared to the other housing groups. The presence of an artificial nest during social isolation partially reverted the enhanced bacterial clearance in the blood but not in the PLF, suggesting that increased thermogenesis might partially play a role in systemic enhanced bacterial clearance. Taken together, these results suggest that increased food intake in SI mice is necessary to provide the extra energy needed to maintain body temperature, whilst changes in thermogenesis do not have such a profound effect on the immune system during social isolation.

Chapter 5
Social Isolation and Atherosclerosis

5.1 Introduction

Atherosclerosis is an inflammatory disease affecting both the large and medium-sized arteries, that is characterised by the presence of endothelial dysfunction and cholesterol, lipid and cell deposition, leading to the formation of atherosclerotic plaque[71]. If left untreated, this eventually results in gradual occlusion of the vessel and reduced blood flow (**Figure 5.1**). Rupture of atherosclerotic plaque leads to occlusion of the blood vessel and either MI or stroke[48].

There is increasing evidence to suggest a link between social status and CVD, but what remains elusive is the molecular mechanisms underlying this link[367–370]. Loneliness has been associated with an increased risk of heart disease, as it has been shown to be associated with larger increases in SBP over a 4 year period[118,120,371]. Additionally, loneliness has been shown to increase basal total peripheral resistance and lower cardiac output[368]. In cynomolgus monkeys, those monkeys who were socially dominant in an unstable population where there were threats to their status, were found to have increased atherosclerotic plaque in the coronary artery[369]. Social deprivation was found to be associated with increased scores for carotid plaque and intima-media thickness, after accounting for traditional risk factors in a Scottish based population[367]. Similarly, those individuals who were classed as having both a low social economic status, both in childhood and adulthood, were found to have higher scores for intima-media thickness and carotid plaque[372]. Interestingly, a recent UK Biobank cohort study investigating social isolation and loneliness as risk factors for MI and stroke, found that 85% of the respective 1.4 and 1.5-fold increased risk of incident MI and stroke could be attributed

to traditional cardiovascular risk factors e.g. smoking and obesity[370]. Whilst the English Longitudinal Study on Aging identified an increased risk of incident MI and stroke with loneliness, independent of traditional risk factors, it found no correlation between social isolation and either incident MI or stroke[176]. Therefore, it is unsurprising that the American Heart Association has highlighted in their 2020 Impact Goal that they felt the biggest area for improvement in the reduction of CVD was in health behaviours which are closely linked to mental health[54].

ApoE$^{-/-}$ mice are a commonly used model of atherosclerosis. Apolipoprotein E (ApoE) is essential for the formation of lipoproteins, which allow cholesterol to be transported around the blood[373]. Since ApoE is a ligand for the LDLR, its absence means that chylomicrons and very low density lipoprotein (VLDL) remnants cannot be taken up into the hepatocytes, where they would otherwise be cleared, thus resulting in their accumulation in the blood[374]. Therefore, *ApoE*$^{-/-}$ mice are hypercholesterolemic, with cholesterol levels at 400-500mg/dL on a standard chow diet, and this allows for the spontaneous development of plaque in these mice[375]. The American Heart Association classifies atherosclerotic lesions into different stages as follows: **(I)** lesion with foam cells (**II)** fatty streak with foam cell layers (**III**) extracellular lipid pool (**IV)** atheroma with a confluent extracellular lipid core (**V**) presence of fibroatheroma (**VI**) complex plaque with surface defect, haemorrhage, or thrombus[376,377]. The timings needed for the development of atherosclerotic burden on standard and Western diet in the *ApoE*$^{-/-}$ model are summarised in **Table 7**[378].

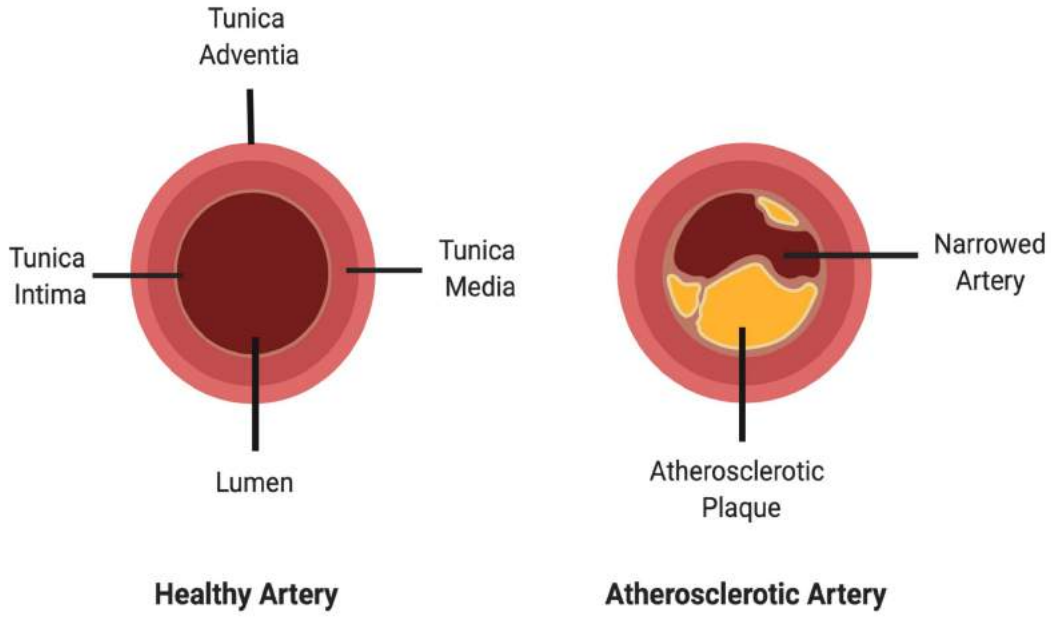

Figure 5.1: Comparison of the Healthy and Atherosclerotic Arteries. In the healthy artery blood can flow through in an undisturbed manner. In contrast, in the atherosclerotic artery, there is reduced space for the blood to flow through due to an increase in intima-medial thickness as a result of atherosclerotic plaque build-up. Image created on Biorender.

Table 7: Time Scale for Atherosclerosis Lesion Scores in *ApoE*$^{-/-}$ Mice.

	I	II	III	IV	V	VI
Standard Diet	1-2 months	4-5 months	7-9 months	8-11 months	>10 months	N/A
Western Diet	4-6 weeks	8-10 weeks	12-14 weeks	14-16 weeks	18-20 weeks	N/A

5.1.1 Chapter Aims

This chapter had the following objectives:

1. To determine both the basal effects of social isolation and *ApoE* gene deletion on weight and nutritional intake on standard chow, and whether sex can affect these parameters;
2. To explore the effect of social isolation and *ApoE* deletion on biochemical markers of organ function;
3. To investigate whether social isolation and the Western diet alters weight and nutritional intake;
4. To establish whether social isolation and the Western diet affects the adipose tissue morphology;
5. To examine whether social isolation affects total cholesterol levels, lipid profile and glucose in plasma, in mice fed standard chow and Western diet;
6. To investigate whether atherosclerotic plaque within the aortic sinus is affected by social isolation;
7. To determine if the characteristics of the atherosclerotic plaque within the aortic sinus are affected by social isolation;
8. To confirm that the unique transcriptional fingerprint of social isolation demonstrated in CD-1 mice, can also be seen in *ApoE*$^{-/-}$ mice.

5.2 Methods

5.2.1 Animal Husbandry

All animals were housed in individually ventilated enclosures with food and water being provided *ad libitum* with a 12-hour light-dark cycle. All experiments undertaken were approved and performed according to the guidelines of the Ethical Committee for the Use of Animals, Bart's and The London School of Medicine and Dentistry and the Home Office Regulations Act 1986 (Prof. D'Acquisto, PPL. 70/8714).

5.2.2 Modelling Social Isolation

Cages for social isolation and social housing were set up as described for CD-1 mice. In order to model the effect of social isolation on atherosclerosis, male and female C57BL/6 *ApoE*$^{-/-}$ mice were used and were bred in house, in trios. C57BL/6, wild type (WT), mice were bought from Charles River Ltd and given 1 week to acclimatise. All studies lasted 1 month, 4 weeks, as this was the longest period of time allowed on the project license.

Effect of *ApoE* Deletion During Social Isolation

To assess the basal effect of *ApoE* gene deletion, male and female WT mice and *ApoE*$^{-/-}$ mice at 1 month of age underwent social isolation for a period of 4 weeks, as at this time point atherosclerosis is at the very early stages with only small lesions and foam cells being present (**Figure 5.2**)[378]. *ApoE*$^{-/-}$ mice were randomly assigned to either social isolation or social housing for a period of 4 weeks, which would be akin to a person losing their long-term partner, and thus socially isolating him or herself whilst they come to terms with their loss. Mice were fed standard chow.

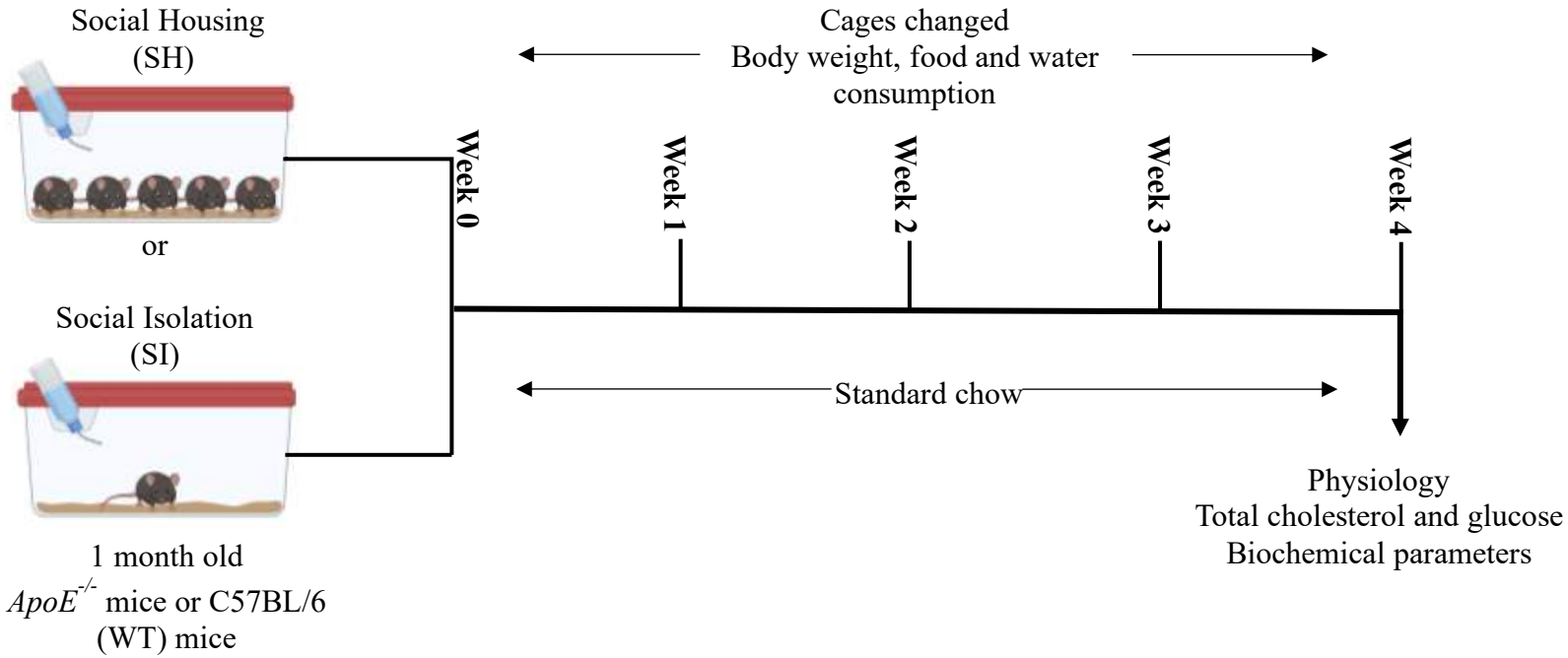

Figure 5.2: ApoE Deletion and Social Isolation Overview – Standard chow. *ApoE*$^{-/-}$ mice at 1 month of age were randomly assigned to either social housing (5x mice per cage) or social isolation (1x mouse per cage) for a period of 4 weeks, during which time the mice were fed standard chow (9.0% fat, 21.8% protein and 0.74% carbohydrate). Throughout the study, cages were changed on a weekly basis, at which time the mice were weighed. Food and water consumption were monitored every 2-3 days. After 4 weeks, mice were sacrificed and three main parameters were assessed: physiology of the mice, total cholesterol and glucose and biochemical parameters. Image created with Biorender.

Basal *ApoE*$^{-/-}$ Study – Standard Chow

In basal *ApoE*$^{-/-}$ studies, 3 month old mice were given standard diet for the 4 week period of social isolation or social housing, as this is the stage where extracellular lipid pools and formation of atheroma are beginning to occur in the ascending aorta (**Figure 5.3**)[378].

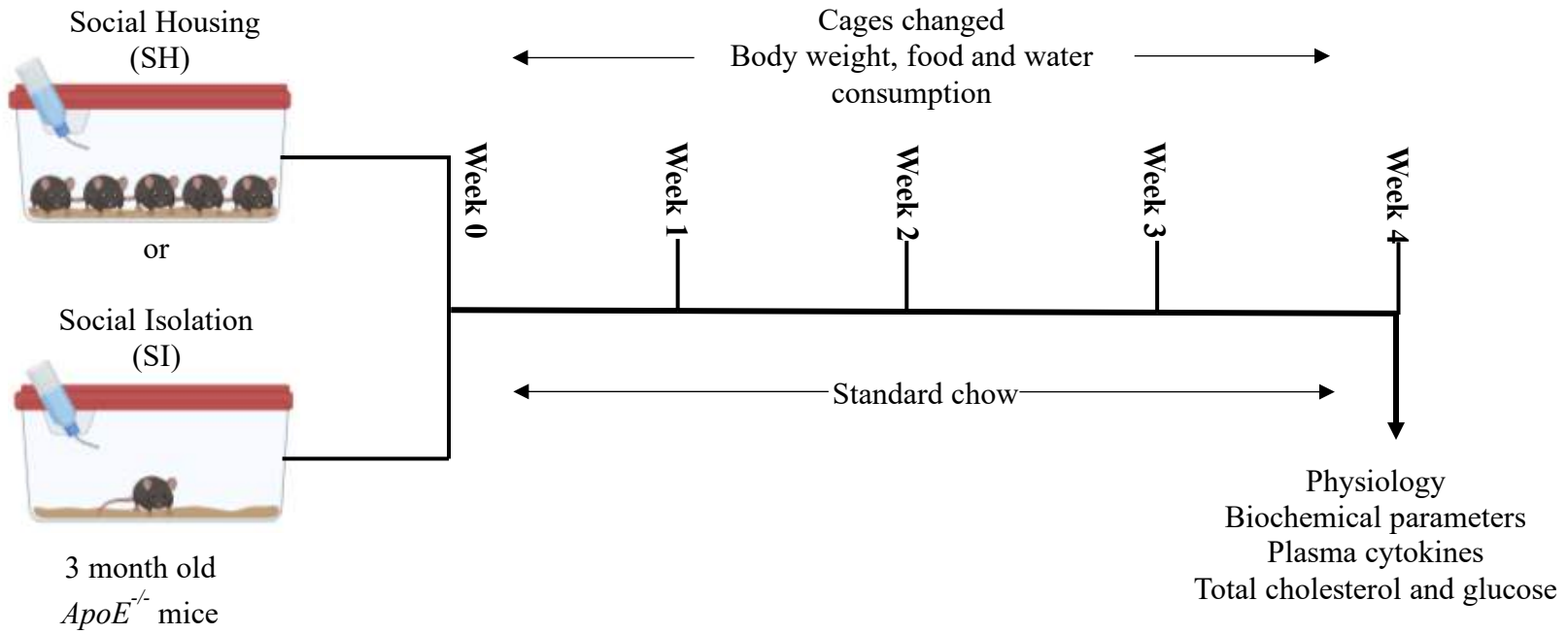

Figure 5.3: Atherosclerosis Overview – Standard chow. *ApoE*$^{-/-}$ mice at 3 months of age were randomly assigned to either social housing (5x mice per cage) or social isolation (1x mouse per cage) for a period of 4 weeks, during which time the mice were fed standard chow. Throughout the study, cages were changed on a weekly basis, at which time the mice were weighed. Food and water consumption were monitored every 2-3 days. After 4 weeks, mice were sacrificed, and four main parameters were assessed: physiology of the mice, biochemical parameters, plasma cytokines and total cholesterol and glucose. Image created with Biorender.

Basal *ApoE*$^{-/-}$ Study - Western Diet

Female mice were fed the Western diet for 4 weeks at 1 month of age in order to get an indication of the combined effect of the Western diet and social isolation at baseline.

Atherosclerosis Development Study – Western Diet

For studies looking at the development of atherosclerosis, the Western diet was given for 4 weeks at 6 months of age in male *ApoE*$^{-/-}$ mice, as at the end of the study the mice would be 7 months old which is where advanced atherosclerosis occurs (**Figure 5.4**)[378]. After the 4-week period of social isolation or social housing mice were sacrificed by a CO_2 overdose in a CO_2 chamber.

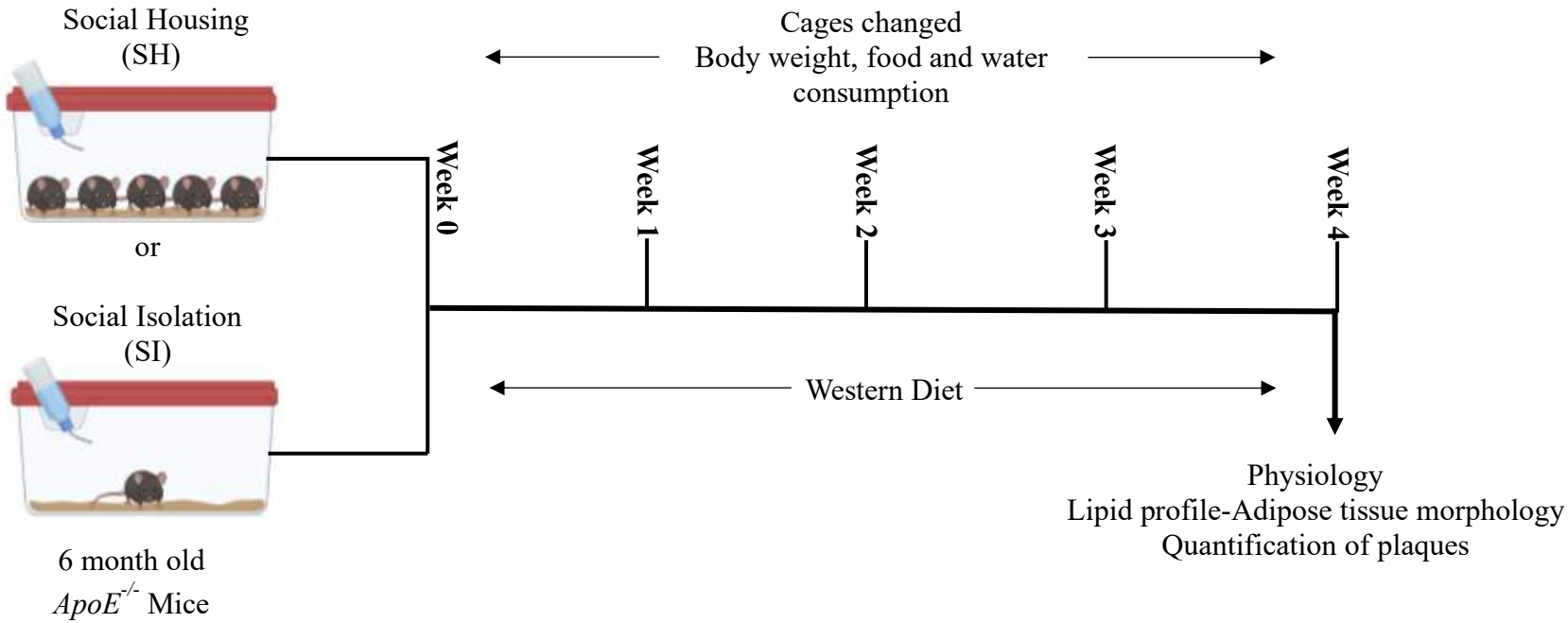

Figure 5.4: Atherosclerosis Study Overview – Western Diet. *ApoE*$^{-/-}$ mice at 6 months of age were randomly assigned to either social housing (5x mice per cage) or social isolation (1x mouse per cage) for 4 weeks, during which time the mice were fed the Western Diet (21.4% fat, 17.5% protein and 50% carbohydrate). Throughout the study cages, were changed on a weekly basis, at which time the mice were weighed. Food and water consumption were monitored every 2-3 days. After 4 weeks, mice were sacrificed, and the following parameters were assessed: physiology of the mice, lipid profile and adipose tissue morphology and atherosclerotic burden in the aortic sinus. Image created with Biorender.

5.2.3 Western Diet

ApoE$^{-/-}$ mice were placed on the Western diet (21.4% fat, 17.5% protein and 50% carbohydrate [SDS Diets, **cat.** 829100] at 6 months of age for the 4 weeks period of social isolation or social housing.

5.2.4 Weight Gain and Nutritional Intake

During the period of social housing or social isolation food and water was monitored and replenished as needed every 2-3 days. Mice were weighed once a week during cage changing to assess weight gain over the study.

5.2.5 Cardiac Puncture

After 4 weeks mice were anesthetised in a chamber using isoflurane, and cardiac puncture was carried out as previously described. Mice were sacrificed by CO_2 asphyxiation in a CO_2 chamber.

5.2.6 Plasma Leptin

Plasma was isolated from whole blood collected at the end of the social isolation period, by centrifuging samples for 5 minutes at 10,000 *g*. Leptin was measured as described previously by a murine leptin ELISA kit (Thermofisher, **cat.** KMC2281).

5.2.7 Total Cholesterol and Cholesterol Subtypes and Glucose

Total cholesterol, triglycerides, HDL, LDL and glucose concentrations were quantified in plasma using a Beckman Coulter AU680 clinical chemistry analyser at MRC Harwell.

5.2.8 Biochemical Parameters

Plasma was isolated as previously described. Plasma AST, ALT and creatinine were quantified using a Beckman Coulter AU680 clinical chemistry analyser at MRC Harwell.

5.2.9 Plasma Cytokines

Plasma was isolated as previously described and one aliquot was sent to Labospace Ltd Milan for determination of TNF-α, IL-6 and IFN-γ concentrations by use of multiplex.

5.2.10 Visceral Adipose Tissue

VAT was weighed and placed in 4% PFA overnight, before being H&E stained as previously described. The number of adipocytes and their individual areas were measured in Image J as previously stated.

5.2.11 Quantification of Atherosclerotic Plaque in the Aortic Sinus

Post sacrifice, the chest cavity was opened up and a small hole was cut in the right atrium of the heart. Using a 10ml syringe with a 25G needle, cold PBS was flushed through the left ventricle to remove any remaining blood. Once the heart was removed, it was weighed prior to being put into 4% PFA.

The heart was stored in 4% PFA prior to being cut using a scalpel blade in a parallel manner across the plane of the atria. The top section of the heart was frozen in optimal cutting temperature (OCT) (VWR Chemicals, **cat.** 00411243) mounting solution and stored at -80°C until sectioning, whilst the lower section of the heart was discarded to aid access to the aortic sinus. The OCT block was mounted on the cryostat with the aortic side of the block facing the pedestal and sectioned at 30µm until the heart becomes visible. A section was checked under the microscope to allow the anatomical position of the heart to be determined and the position of the block to be altered as required. Further 30µm sections of the heart were cut until the left and the right atria could be seen under the microscope, thus suggesting that the aortic sinus was near. Once the valve cusps were clearly visible under the microscope the sections were cut at 12µm, with every other

section being mounted onto slides until all of the valve cusps had disappeared, usually around 20-24 sections later. Slides were stored at -80°C.

0.5g of Oil Red O (Sigma, **cat.** O0625-25g) powder was dissolved in 100ml of isopropanol in a water bath to make a stock solution. The Oil Red O stock solution was passed through a 0.45μm filter. 30ml of Oil Red O stock solution was added to 20ml of distilled water to create the Oil Red O working solution. The slides were fixed in formalin and were placed in distilled water for 10 minutes. Slides were then rinsed with 60% isopropanol before being stained with Oil Red O working solution for 15 minutes. After, 15 minutes the slides are rinsed as described previously. The nuclei were stained by dipping the slides 5 times into haematoxylin (Sigma, **cat.** H3136-25g) and then the slides were rinsed in distilled water. Slides were then mounted and imaged using an EVOS XL Core microscope (10x). Plaques were quantified using Image J software.

5.2.12 Measuring Necrosis in the Atherosclerotic Plaque

Necrosis causes swelling of the cytoplasm, plasma membrane damage and the release of the cytoplasmic content including MMPs and DAMPS thus promoting the degradation of the fibrous plaque and contributing to an already proinflammatory environment[379]. Necrotic cells contribute to the necrotic core, which is a known risk factor for atherosclerotic plaque rupture[380].

Using Image J, areas of the atherosclerotic plaque that had not been stained with either Oil Red O or haematoxylin, were measured as these areas are considered to be necrotic[381]. Necrosis was assessed for each of the 15x distances from the aortic sinus in each mouse and the area was calculated as a % of the total plaque area for each section. The average % of necrosis was calculated and plotted for each mouse.

5.2.13 Picro-Sirius Red Staining of Atherosclerotic Plaque

Aortic sinuses were stained using Pico-Sirius Red stain kit (Abcam, **cat.** ab150681) according to the manufacturer's instructions. In brief, an adequate volume of Picro-Sirius Red Solution was added to each aortic sinus section, and slides were incubated for 60 minutes. Slides were then briefly rinsed 2x in acetic acid solution, before being rinsed in 100% ethanol. In order to dehydrate the sections, they were washed with 2 changes of 100% ethanol for 2 minutes each. Entellan® (Sigma-Aldrich, **cat.** 107600500) was used to mount slides. Sections were imaged at 4x magnification on a Nikon Eclipse TE300 microscope. The amount of collagen present was quantified by measuring the intensity of the red stain within the atherosclerotic plaque using Image J.

5.2.14 Peritoneal Macrophages

$CD11b^+$ $F4/80^+$ macrophages were identified as previously described. In brief, samples were centrifuged for 5 minutes at 264 *g* and the pelleted leukocytes were resuspended in 200µl of residual volume. Cells were then blocked and stained with 50µl of Anti-Mouse CD11b FITC (eBioscience) and Anti-Mouse F4/80 PE (eBioscience) in FACS buffer for 30 minutes at 4°C. Cells were fixed in 4% PFA and were acquired on a LSRFortessa flow cytometer (Becton Dickson). Analysis was carried out using FlowJo 8.0 software (Tree Star).

5.2.15 Validation of Microarray Genes

Whole blood was stored in RNeasy Protect Animal Blood Tubes and RNA was extracted using the RNeasy Protect Animal Blood Kit as previously described. cDNA was extracted and RT-PCR was carried out to measure gene expression of *cd55*, *cd52*, *bach2* and *xaf1*, as previously described. Genes of interest were normalised to the housekeeping

gene *GAPDH* and analysed using the $\Delta\Delta C_T$ method of analysis to calculate the fold change.

5.2.16 Statistics

Significance was tested using the statistical analysis specified in each figure legend on GraphPad Prism 8 (GraphPad Software Inc, USA).

5.3 Results

5.3.1 Effect of *ApoE* Gene Deletion on Nutritional Intake

In order to investigate the effect of *ApoE* deletion on weight gain and nutritional intake, SI C57BL/6 (WT) mice were compared to age-matched SI *ApoE*$^{-/-}$ mice fed standard chow. Throughout the duration of the study, SI *ApoE*$^{-/-}$ male mice gained significantly more weight than SI male WT mice (**Figure 5.5a**). During this time SI male *ApoE*$^{-/-}$ mice ate significantly more food than SI male WT mice (**Figure 5.5b**). Similarly, water intake was significantly increased in SI *ApoE*$^{-/-}$ male than SI male WT mice (**Figure 5.5b**). Over the 4-week period of social isolation, female SI *ApoE*$^{-/-}$ mice put on significantly more weight than female SI WT mice (**Figure 5.6a**). During this time SI female *ApoE*$^{-/-}$ mice ate significantly more food than SI female WT mice (**Figure 5.6b**). Similarly, water intake was significantly increased in SI female *ApoE*$^{-/-}$ mice than SI female WT mice (**Figure 5.6b**).

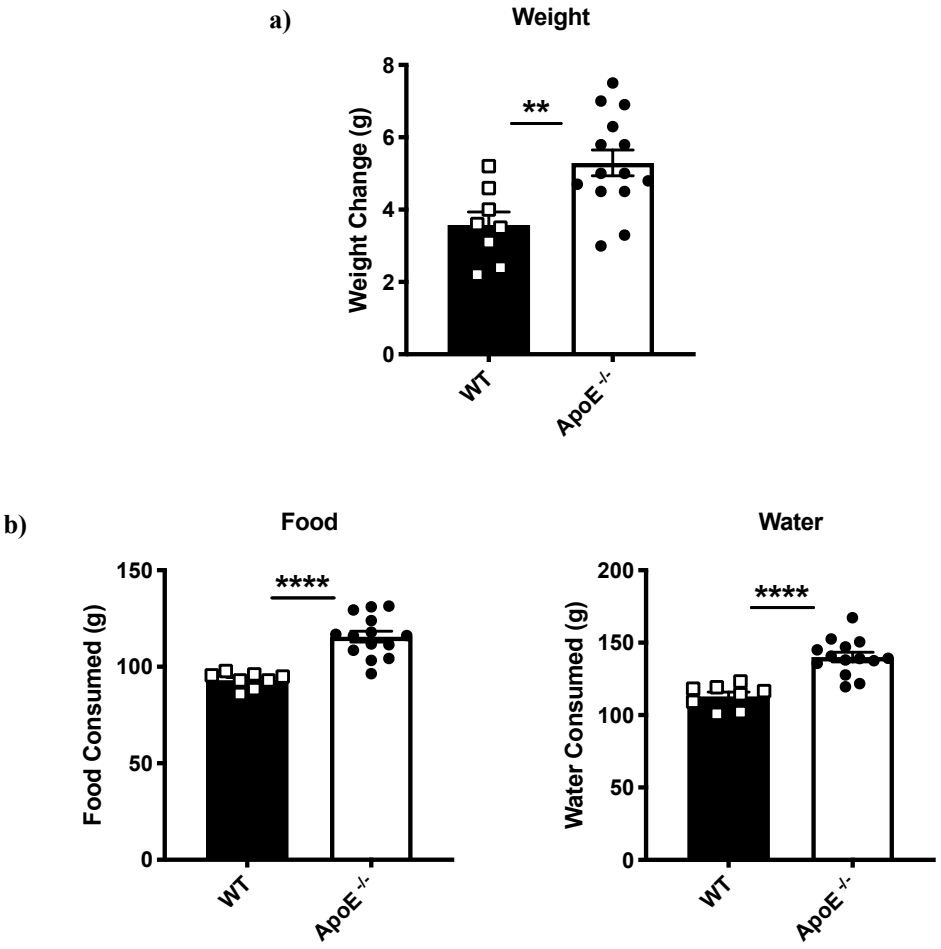

Figure 5.5: Weight Gain and Nutritional Intake – SI Males. The following parameters were assessed: **a)** weight change, **b)** food and water intake over the period of 4 weeks of social isolation. Each bar shows mean ± SEM of n=8-14 mice with each symbol representing an individual mouse. **p<0.01 and ****p<0.00001, where significance was determined using an unpaired parametric T-test.

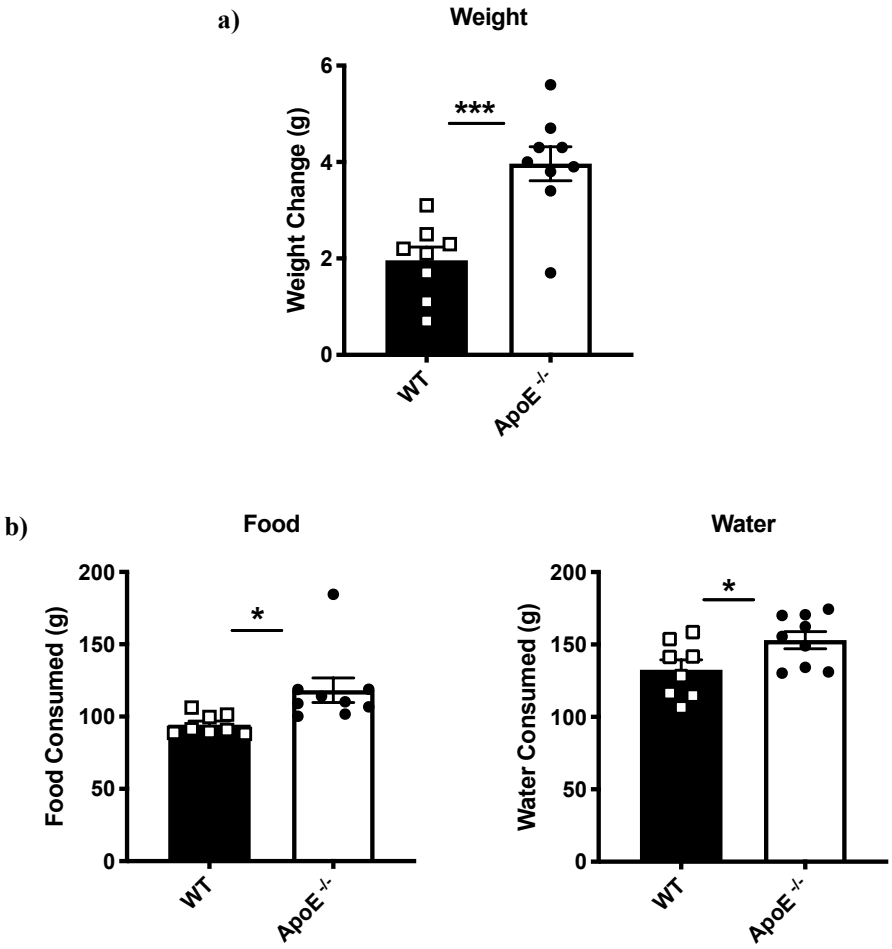

Figure 5.6: Weight Gain and Nutritional Intake – SI Females. The following parameters were assessed: **a)** weight change, **b)** food and water intake over the period of 4 weeks of social isolation. Each bar shows mean ± SEM of n=8-9 mice with each symbol representing n=1 mouse. *p<0.05 and ***p<0.005, where significance was determined using an unpaired parametric T-test.

5.3.2 Effect of *ApoE* Gene Deletion on Plasma Total Cholesterol and Glucose

Plasma total cholesterol and glucose concentration was assessed both in SI WT and SI *ApoE*$^{-/-}$ mice fed standard chow, in order to determine whether the deletion of *ApoE* gene during social isolation would affect these parameters. SI male *ApoE*$^{-/-}$ mice had significantly higher levels of total cholesterol in their plasma compared to SI WT mice (**Figure 5.7a**). Plasma glucose concentration was at similar levels between male SI WT and SI *ApoE*$^{-/-}$ mice (**Figure 5.7b**). In a similar manner to male SI mice, female SI *ApoE*$^{-/-}$ mice had significantly higher levels of total cholesterol in their plasma compared to SI WT mice (**Figure 5.8a**). Plasma glucose concentration was significantly lower in SI *ApoE*$^{-/-}$ mice compared to SI WT mice (**Figure 5.8b**).

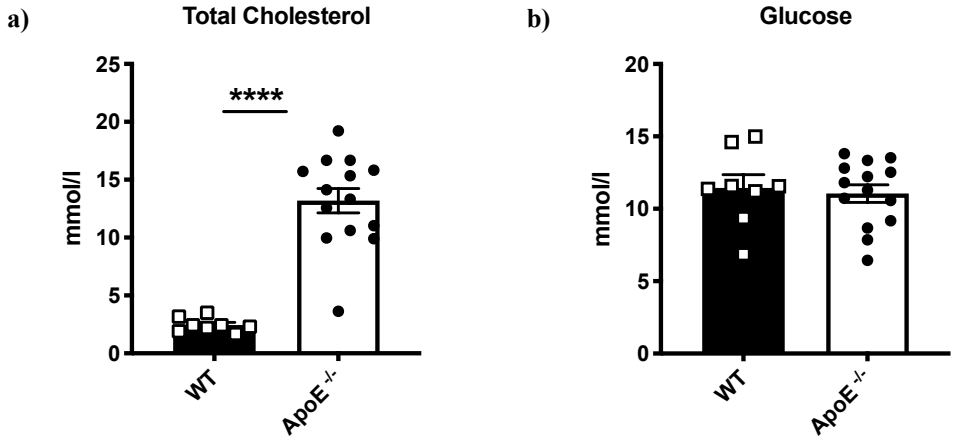

Figure 5.7: Total Cholesterol and Glucose Concentration – SI Males. The following concentrations were assessed in plasma: **a)** total cholesterol and **b)** glucose after 4 weeks of social isolation. Data shown as mean ± SEM, where each symbol represents a single mouse with n=8-14 mice per housing group. **** $p<0.0001$ as assessed by an unpaired parametric T-test.

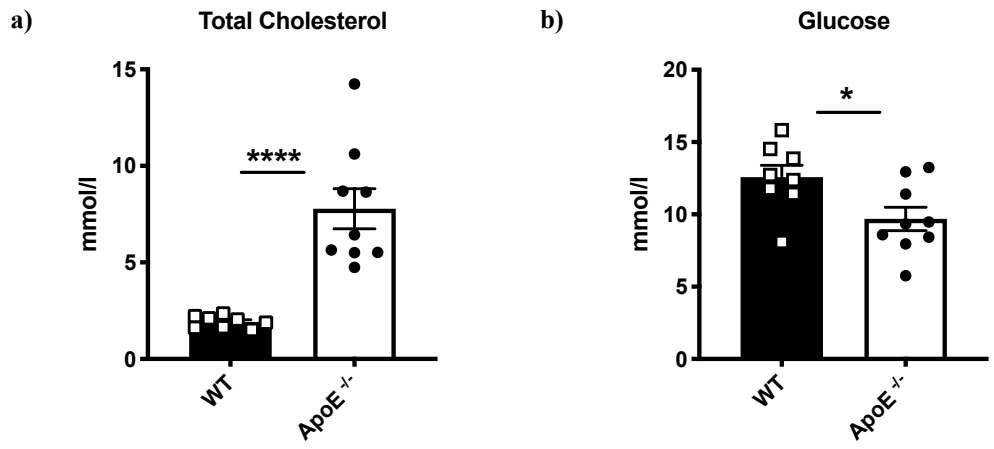

Figure 5.8: Total Cholesterol and Glucose Concentration – SI Females. The following concentrations were assessed in plasma: **a)** total cholesterol and **b)** glucose after 4 weeks of social isolation. Data shown as mean per housing group ± SEM, where n=8-9 mice per group and each symbol represents a single mouse. * $p<0.05$ and **** $p<0.0001$ as assessed by an unpaired parametric T-test.

5.3.3 Effect of *ApoE* Gene Deletion on Biochemical Parameters

Biochemical parameters including markers of liver and kidney function were also assessed as an indication of systemic inflammation, as inflammation drives atherosclerosis. To assess the effect of *ApoE* gene deletion on plasma AST, ALT and creatinine levels, they were measured in SI WT and SI *ApoE*$^{-/-}$ mice fed standard chow. There were no differences in AST or ALT levels between SI *ApoE*$^{-/-}$ mice and SI WT mice (**Figure 5.9a**). Creatinine levels in plasma were significantly lower in male SI *ApoE*$^{-/-}$ mice compared to male SI WT mice (**Figure 5.9b**). Plasma AST was found to have similar concentrations between female SI WT and female SI *ApoE*$^{-/-}$ mice (**Figure 5.10a**). ALT levels are not reported for female mice due to concentrations being below the limit of detection for the assay in most mice. Creatinine concentrations were significantly lower in SI *ApoE*$^{-/-}$ mice compared to SI WT mice (**Figure 5.10b**).

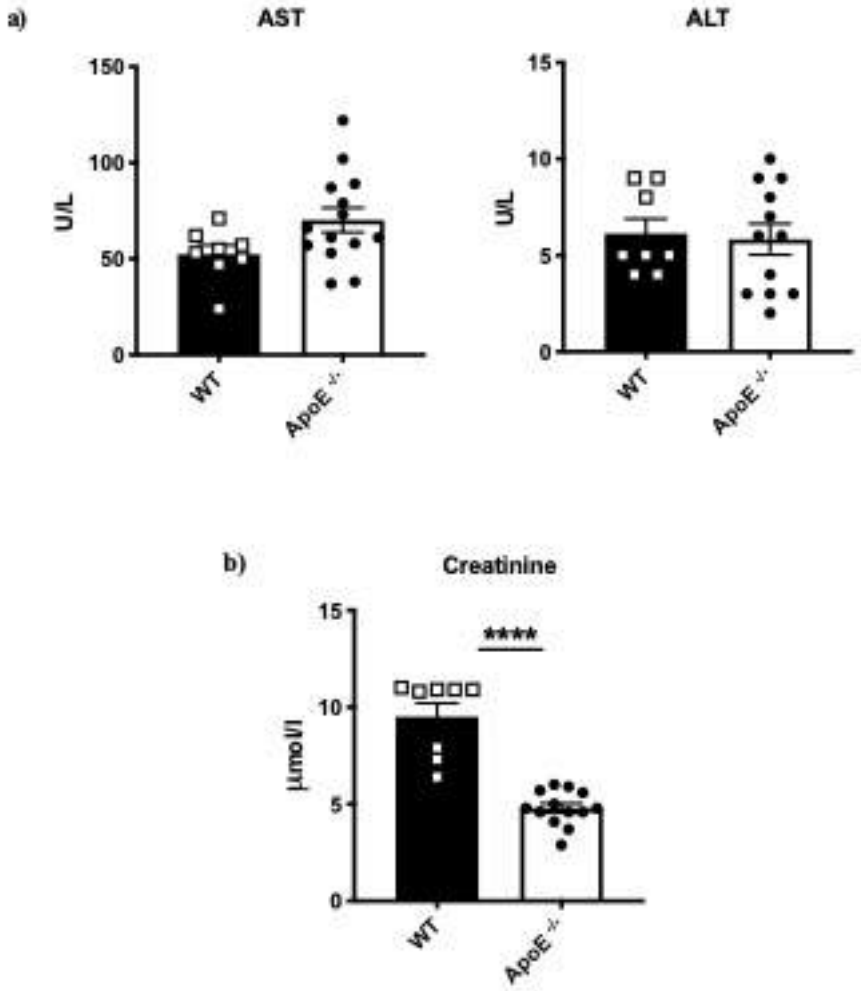

Figure 5.9: Biochemical Markers of Liver and Kidney Function – SI Males. The following biochemical parameters were analysed in plasma for **a)** liver function, AST and ALT, and **b)** kidney function**,** creatinine. Data shown as mean ± SEM, where n=8-14 mice per group and each symbol represents a single mouse. **** $p<0.0001$ as assessed by an unpaired parametric T-test.

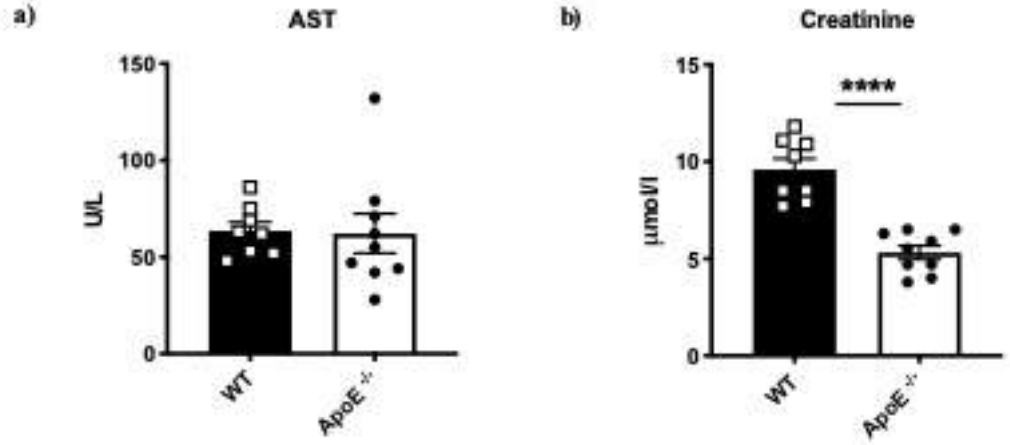

Figure 5.10: Biochemical Markers of Liver and Kidney Function – SI Females. The following biochemical parameters were analysed in plasma for **a)** liver function, AST and **b)** kidney function**,** creatinine. Data shown as mean ± SEM, where n=8-9 mice per group and each symbol represents a single mouse. **** $p<0.0001$ as assessed by an unpaired parametric T-test.

5.3.4 Effect of *ApoE* Gene Deletion on Plasma Cytokine Levels

Basal inflammation was assessed by measuring TNF-α, IL-6 and IFN-γ concentrations in plasma. However, TNF-α, IL-6 and IFN-γ concentrations were too low to be detected from both male and female SI *ApoE*$^{-/-}$ mice and SI WT mice by the multiplex assay, thus the data is not shown.

5.3.5 Weight Gain and Nutritional Intake – *ApoE*$^{-/-}$ Mice Fed Standard Chow

Weight and nutritional intake were assessed over the course of the study to give an indication of any physiological changes that may potentially affect the susceptibility of the mice to the development of atherosclerosis. The weight change observed over the 4-week period of social isolation was not significantly different in SI male *ApoE*$^{-/-}$ mice, but there was a trend towards SI male *ApoE*$^{-/-}$ mice gaining less weight than SH male *ApoE*$^{-/-}$ mice (**Figure 5.11a**). Food and water intake showed a trend towards being increased in male SI *ApoE*$^{-/-}$ mice compared to male SH *ApoE*$^{-/-}$ mice (**Figure 5.11b**). Weight change observed over the 4-week period of social isolation showed that SI female *ApoE*$^{-/-}$ mice put on slightly less weight than SH female *ApoE*$^{-/-}$ mice (**Figure 5.12a**). Food and water intake were increased respectively in female SI *ApoE*$^{-/-}$ mice compared to female *ApoE*$^{-/-}$ SH mice (**Figure 5.12b**).

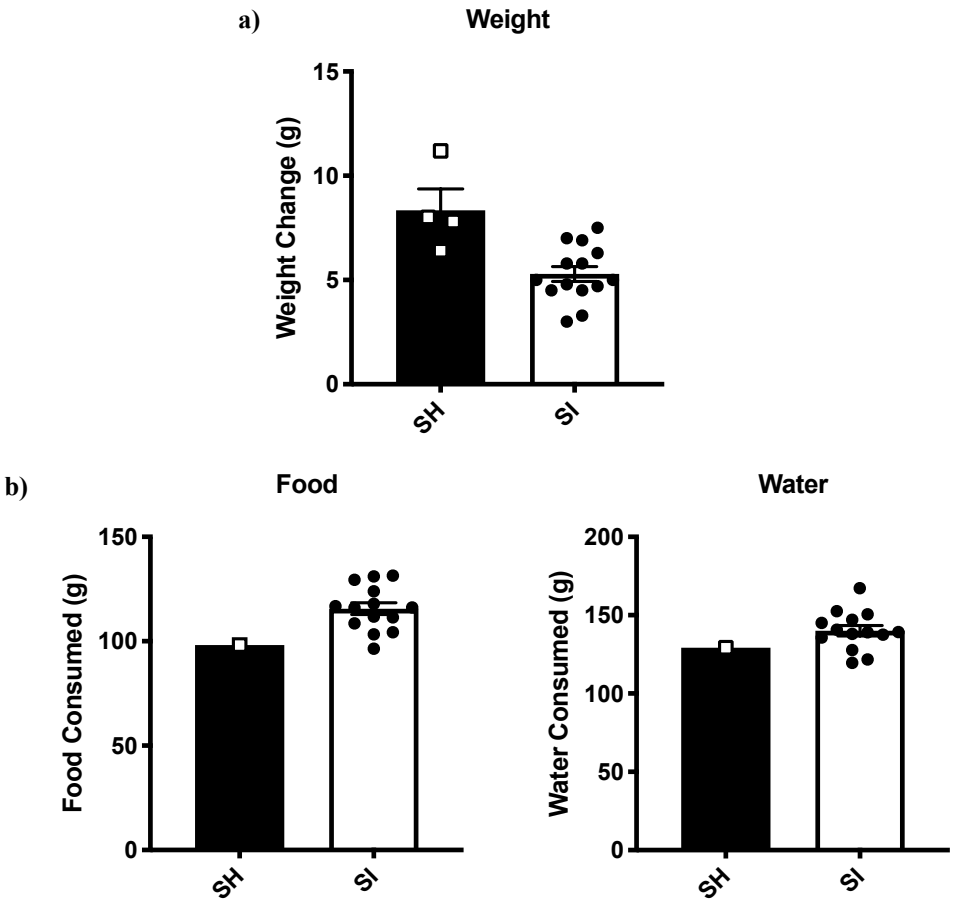

Figure 5.11: Weight and Nutritional Intake - Standard Chow *ApoE*$^{-/-}$ Males. The following parameters were assessed: **a)** weight change, **b)** food and water intake over the 4 weeks of social isolation or social housing. Each bar shows mean ± SEM of n=4-14 mice with each symbol representing n=1 mouse for weight or n=1 cage for food and water intake. Significance was determined by an unpaired parametric T-test where $p<0.05$.

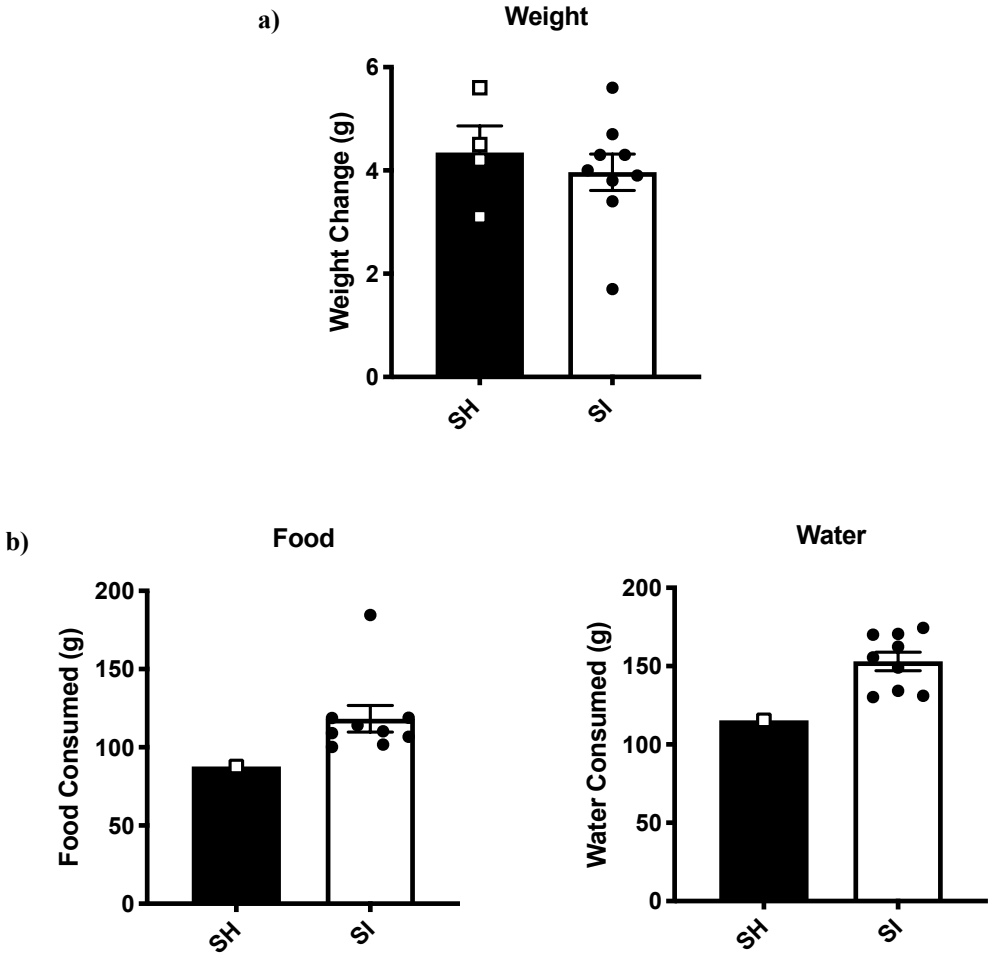

Figure 5.12: Weight and Nutritional Intake - Standard Chow *ApoE*$^{-/-}$ Females. The following parameters were assessed: **a)** weight change, **b)** food and water intake over the 4 weeks of social isolation or social housing. Each bar shows mean ± SEM of n=4-8 mice with each symbol representing n=1 mouse for weight or n=1 cage for food and water intake. Significance was assessed by an unpaired parametric T-test where $p<0.05$.

5.3.6 Plasma Leptin – Standard Chow

The satiety hormone, leptin, was measured in plasma to assess whether changes in its concentration could account for the changes in food intake seen on standard chow during social isolation. There was significantly higher plasma leptin in SI mice compared to SH *ApoE*$^{-/-}$ mice fed on standard diet (**Figure 5.13**).

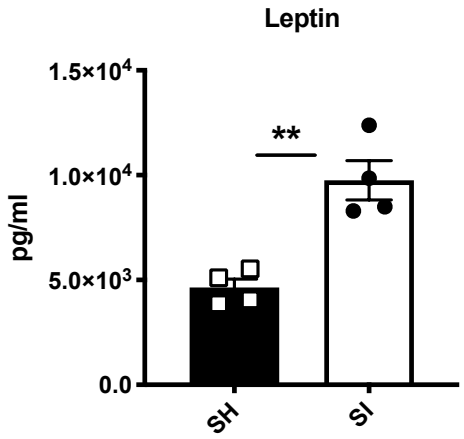

Figure 5.13: Plasma Leptin Levels – Male *ApoE*$^{-/-}$ Standard Diet. Plasma leptin levels were quantified after 4 weeks of social isolation or social housing *via* ELISA in male *ApoE*$^{-/-}$ mice fed standard diet. Values are expressed as mean ± SEM of 4 mice per housing group with each symbol being representative of a single mouse. **p<0.001 as determined using an unpaired parametric T-test.

5.3.7 Biochemical Parameters - *ApoE*$^{-/-}$ Mice Fed Standard Chow

Biomarkers of liver and kidney function were assessed in SH and SI *ApoE*$^{-/-}$ mice fed standard chow, as an indication of systemic inflammation. For liver function, AST and ALT concentrations were assessed in plasma from both male and female SH and SI *ApoE*$^{-/-}$ mice fed standard chow. Plasma AST concentration in male *ApoE*$^{-/-}$ mice fed standard chow showed a trend towards being slightly lower in male SI mice compared to SH *ApoE*$^{-/-}$ mice (**Figure 5.14**). However, plasma ALT concentration in SH mice was too low to be detected in 50% of the male *ApoE*$^{-/-}$ mice used in this study, and for that reason the data is not shown. This was also the case for plasma creatinine concentration, a marker of kidney function, and for that reason the data is not shown. In female *ApoE*$^{-/-}$ mice, plasma AST concentration was significantly lower in SI mice compared to SH mice (**Figure 5.15a**). Since a substantial number, 77%, of female SI *ApoE*$^{-/-}$ mice had plasma ALT concentrations below the range of detection, the data is not shown. Creatinine concentration in plasma showed a trend towards being lower in female SI *ApoE*$^{-/-}$ mice compared to SH female *ApoE*$^{-/-}$ mice (**Figure 5.15b**).

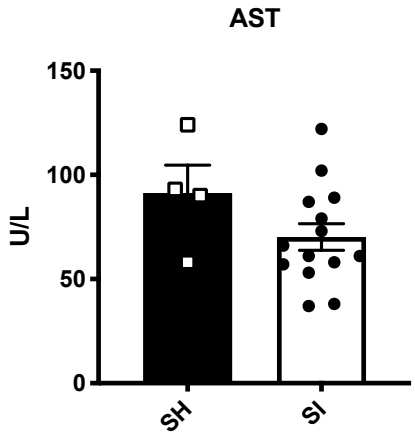

Figure 5.14: Biochemical Marker of Liver Function– Male *ApoE*$^{-/-}$ Mice. Liver function was assessed by measuring AST concentration in plasma. Data shown as mean ± SEM, where n=4-14 mice per housing group and each symbol represents a single mouse. Significance was assessed by an unpaired parametric T-test where $p<0.05$.

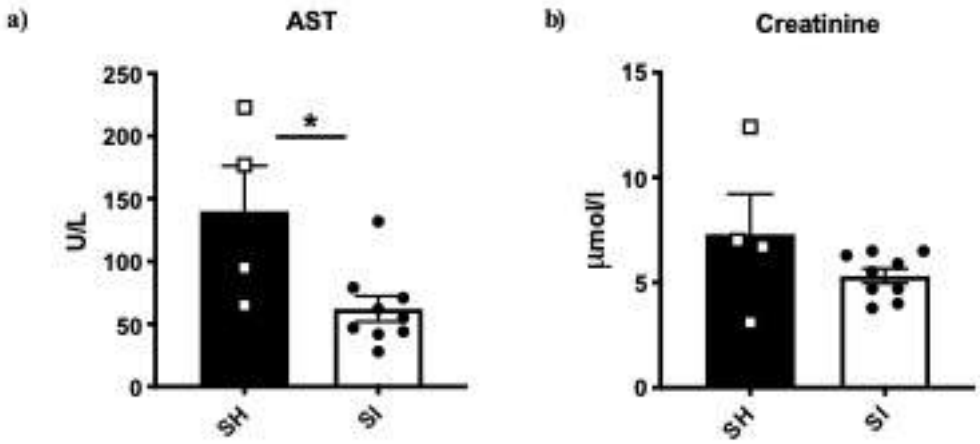

Figure 5.15: Liver and Kidney Function Bicohemistry – Female *ApoE*$^{-/-}$ Mice. The following biochemical parameters were analysed in plasma for **a)** liver function, AST, and **b)** kidney function**,** creatinine. Data shown as mean ± SEM where each symbol represents a single mouse and n=4-9 mice per housing group. *p<0.05 as assessed by an unpaired parametric T-test.

5.3.8 Plasma Cytokines - *ApoE*$^{-/-}$ Mice Fed Standard Chow

In order to assess basal inflammation, TNF-α, IL-6 and IFN-γ concentrations were measured in plasma. However, in basal plasma from both male and female *ApoE*$^{-/-}$ mice and in both housing groups, TNF-α, IL-6 and IFN-γ concentrations were too low to be detected by the multiplex assay, thus data is not shown.

5.3.9 Plasma Total Cholesterol and Glucose - *ApoE*$^{-/-}$ Mice Fed Standard Chow

Quantification of cholesterol, lipid profiling and glucose levels was carried out as cholesterol levels, and the levels of cholesterol subtypes present, affect the progression of atherosclerosis, whilst high glucose levels promote inflammation exacerbating this disease. After the duration of the study the total cholesterol concentration in plasma was significantly higher in male SI mice as opposed to male SH *ApoE*$^{-/-}$ mice (**Figure 5.16a**). Plasma glucose concentrations were slightly higher in male SI *ApoE*$^{-/-}$ mice as opposed to male SH *ApoE*$^{-/-}$ mice (**Figure 5.16b**). After 4 weeks of either social isolation or housing, the total cholesterol in plasma was similar in SI and SH female *ApoE*$^{-/-}$ mice (**Figure 5.17a**). Plasma glucose concentrations were similar between SI and SH female *ApoE*$^{-/-}$ mice (**Figure 5.17b**).

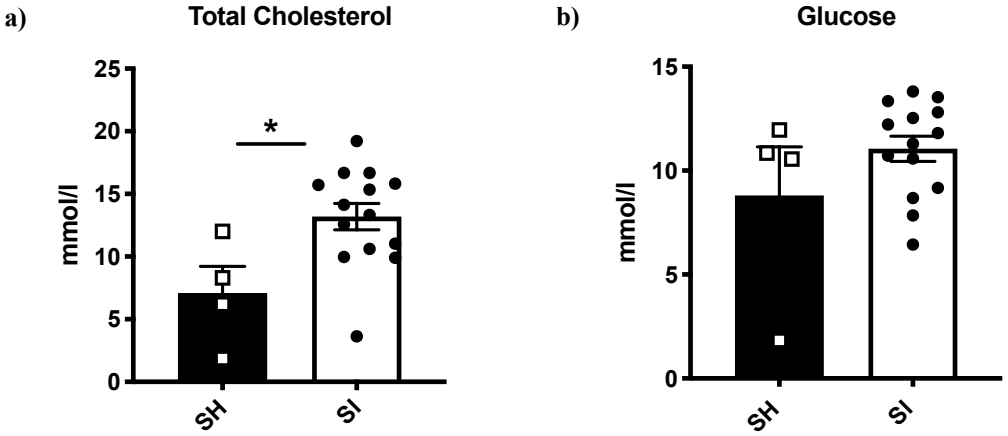

Figure 5.16: Total Cholesterol and Glucose – Male *ApoE*$^{-/-}$ Mice. The following were assessed in plasma: **a)** total cholesterol and **b)** glucose concentrations were measured in SH and SI male *ApoE*$^{-/-}$ mice. Data shown as mean ± SEM, where n=4-14 mice per housing group with each symbol represents a single mouse. * $p<0.05$ as determined by an unpaired parametric T-test.

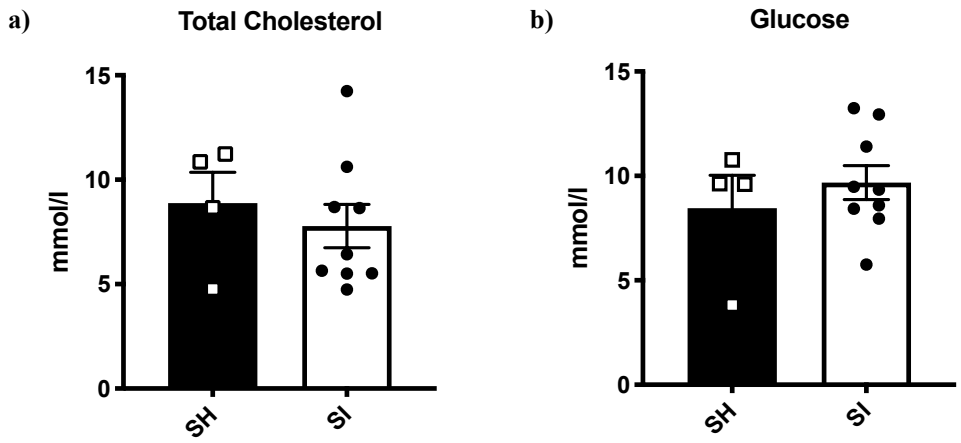

Figure 5.17: Total Cholesterol and Glucose – Female *ApoE*$^{-/-}$ Mice. The following were assessed in plasma: **a)** total cholesterol and **b)** glucose concentrations. Data shown as mean ± SEM, where n=4-9 mice per housing group and each symbol represents a single mouse. Significance was assessed by an unpaired parametric T-test where $p<0.05$.

5.3.10 Weight Change and Nutritional Intake in *ApoE*$^{-/-}$ Mice Fed Western Diet

Weight change and nutritional intake were assessed to see if a change in diet from standard to Western, would alter any of the physiological changes associated with social isolation, and whether these changes were sex dependent. Throughout the study male SI mice showed a trend towards putting on less weight than SH mice (**Figure 5.18a**). Male mice consumed similar amounts of food over the duration of the study, regardless of their housing group (**Figure 5.18b**). There was no significant difference in the water intake of male mice (**Figure 5.18b**). Female SH mice showed a trend towards losing weight across the study compared to the female SI mice, which showed almost no change in weight (**Figure 5.19a**). There was a trend towards an increase in food intake and water consumption in female SI mice compared to female SH mice (**Figure 5.19b**).

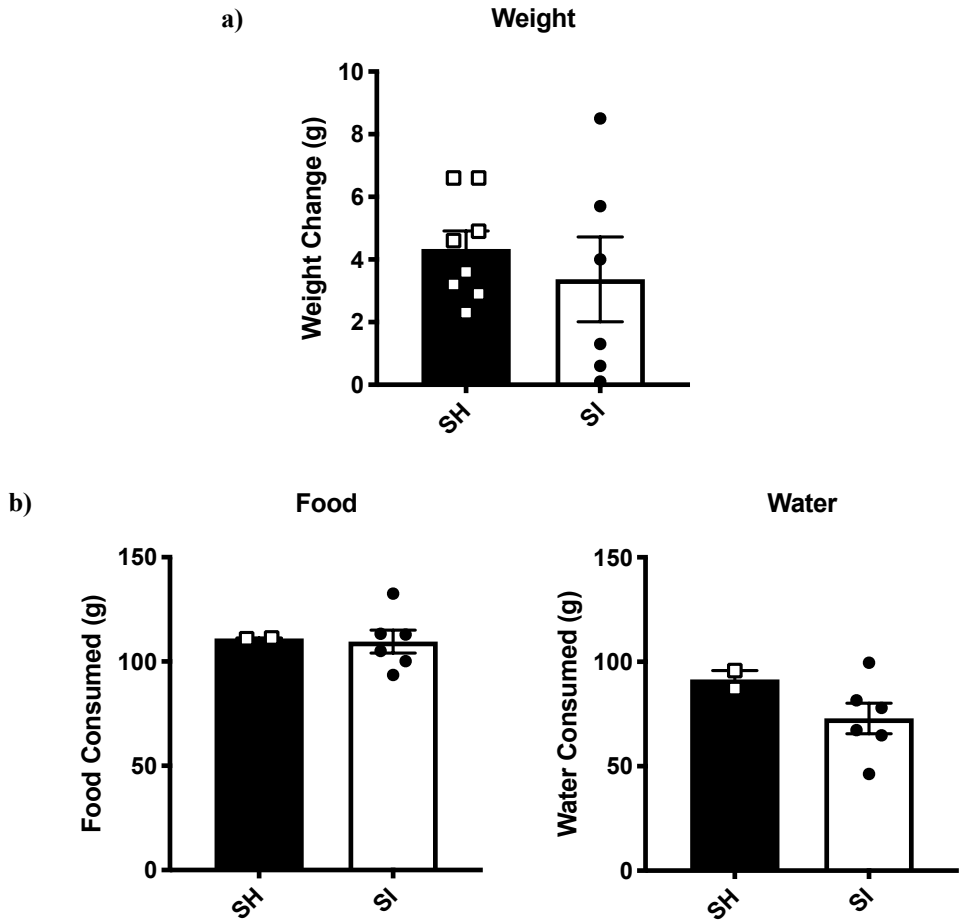

Figure 5.18: Weight Gain and Nutritional Intake on Western Diet – Males. The following parameters were assessed: **a)** weight change, **b)** food and water intake after 4 weeks of social housing or social isolation. Each bar shows mean ± SEM of n=6-8 mice, with each symbol representing n=1 cage. Significance was assessed by an unpaired parametric T-test where $p<0.05$.

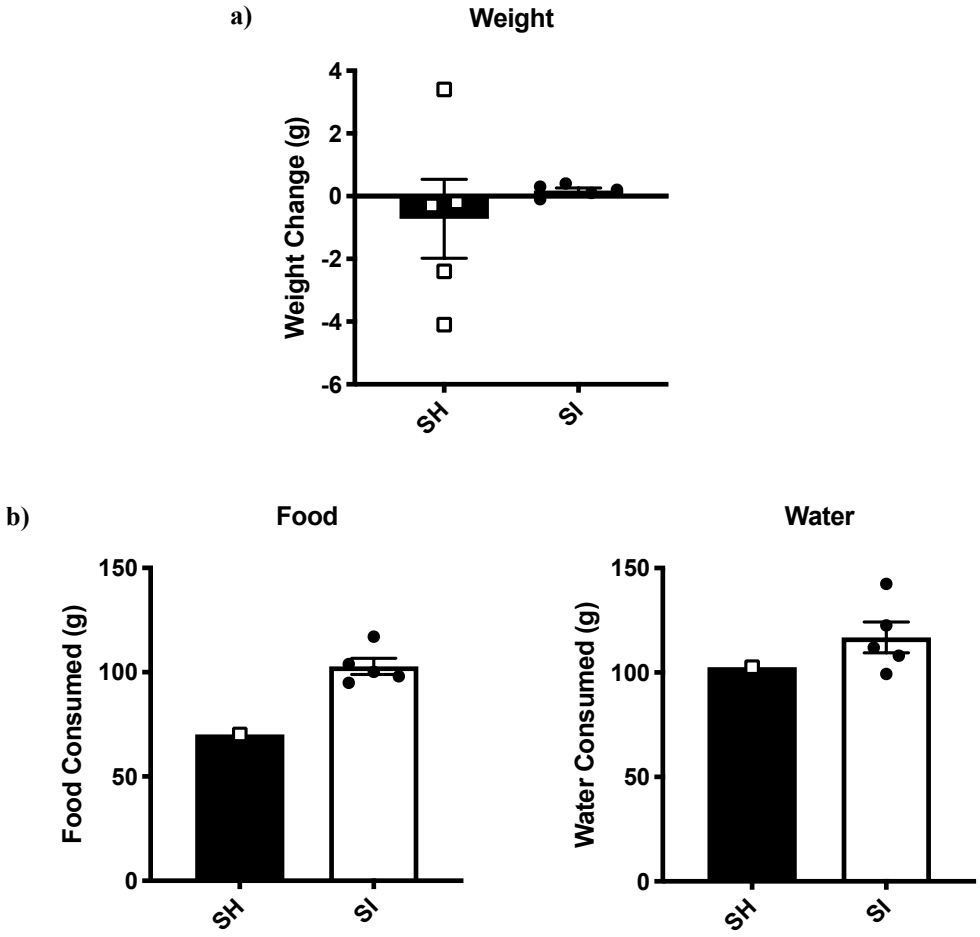

Figure 5.19: Weight Gain and Nutritional Intake on Western Diet – Females. The following parameters were assessed: **a)** weight change, **b)** food and water intake over a period of 2 weeks of social housing or social isolation. Each bar shows mean ± SEM of n=4-5 mice, with each symbol representing n=1 cage. Significance was assessed for weight change using an unpaired parametric T-test where $p<0.05$.

5.3.11 Plasma Leptin – Western Diet

The satiety hormone, leptin, was measured in plasma to assess whether changes in its concentration could account for the differences in food intake between standard chow and Western diet seen during social isolation. There was significantly lower plasma leptin in SI mice compared to SH mice fed on Western diet (**Figure 5.20**).

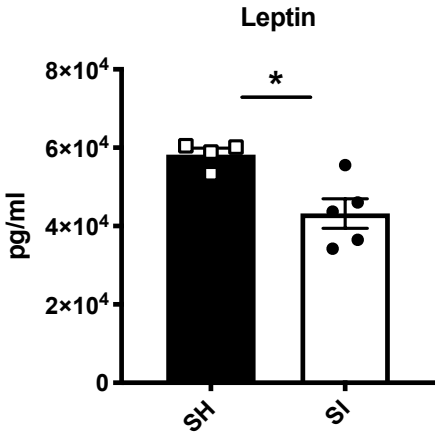

Figure 5.20: Plasma Leptin Levels on Western Diet – Males. Plasma leptin levels were quantified after 4 weeks of social isolation or social housing *via* ELISA in male *ApoE*$^{-/-}$ mice fed the Western diet. Values are expressed as mean ± SEM of 4-5 mice per housing group, with each symbol being representative of a single mouse. *$p<0.05$ as determined by use of an unpaired parametric T-test.

5.3.12 Comparison of Calorie Intake on Western and Standard Diet

In order to assess whether total calorie intake in SI *ApoE*$^{-/-}$ mice was similar between diets, calorie intake was calculated. SH *ApoE*$^{-/-}$ mice's calorie intake on Western diet showed a trend towards being higher compared to SH *ApoE*$^{-/-}$ mice on the standard diet (**Figure 5.21**). In contrast, SI *ApoE*$^{-/-}$ mice showed a trend towards consuming less calories on the Western diet compared to on standard diet (**Figure 5.21**).

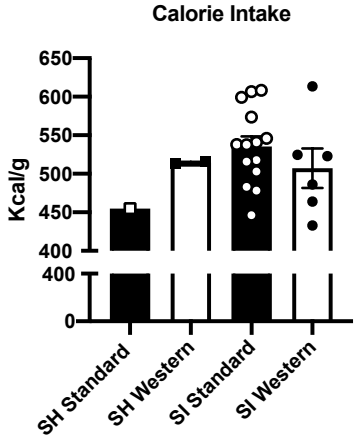

Figure 5.21: Comparison of Calorie Intake Between Diets – Males. Calorie intake was calculated from food intake on standard and Western diet. Values are expressed as mean ± SEM of 5-14 mice per housing group, with each symbol being representative of a one cage.

5.3.13 Visceral Adipose Tissue Characteristics

VAT was collected from male *ApoE*$^{-/-}$ mice after 1 month of social isolation and Western diet to assess whether differences in the morphology of adipocytes were present, which would be indicative of changes in thermogenesis. Representative H & E stained VAT images subjectively revealed differences in the area and number of adipocytes present, whereby SI mice had an increased number of smaller adipocytes and more of them, compared to SH mice (**Figure 5.22**). The VAT was weighed, and the % of body weight was calculated. VAT showed a trend towards accounting for a lower % of body weight in SI mice compared to in SH mice (**Figure 5.23a**). VAT underwent H & E staining to allow for the number of adipocytes to be counted and for their size to be determined, as this can give an indication of whether VAT dysfunctions were seen. There was a significant increase in the number of adipocytes present in the VAT from SI mice compared to SH mice (**Figure 5.23b**). There was a significant difference in adipocyte size between SI and SH mice, whereby adipocytes from SI mice had a smaller adipocyte area compared to those of SH VAT (**Figure 5.23b**).

a) **SH Adipocyte Count= 19**

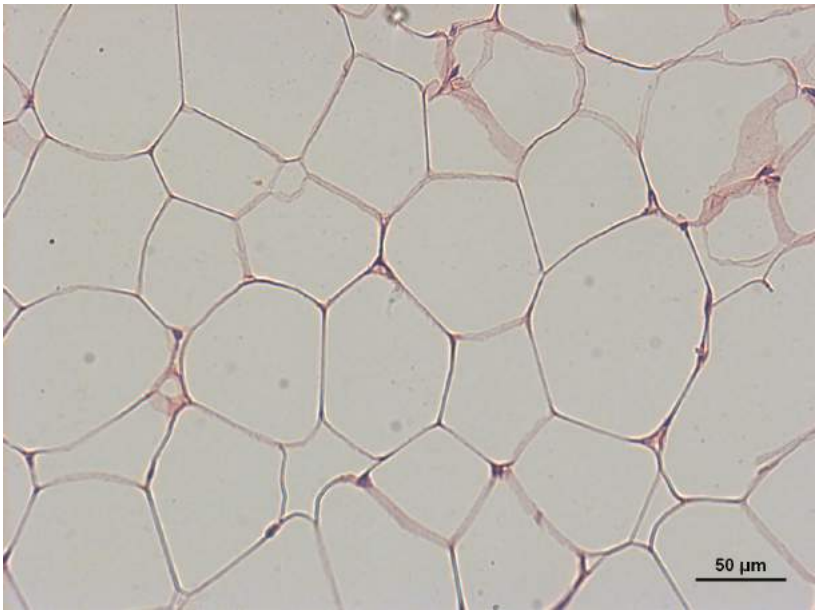

b) **SI Adipocyte Count**= 31

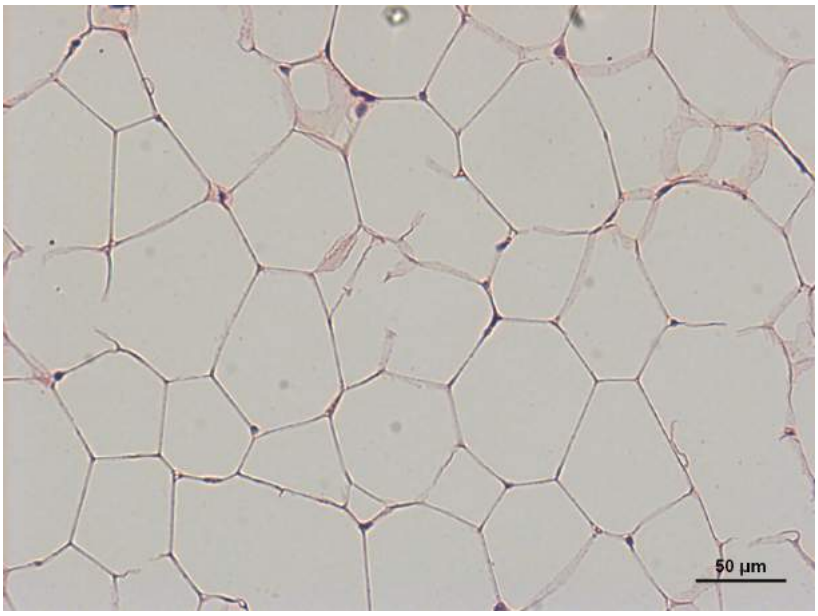

Figure 5.22: Representative VAT H & E Images – Males Western Diet. Representative images of H & E stained VAT at 20x magnification from **a)** SH and **b)** SI *ApoE*$^{-/-}$ mice. Scale bars are representative of 50µm.

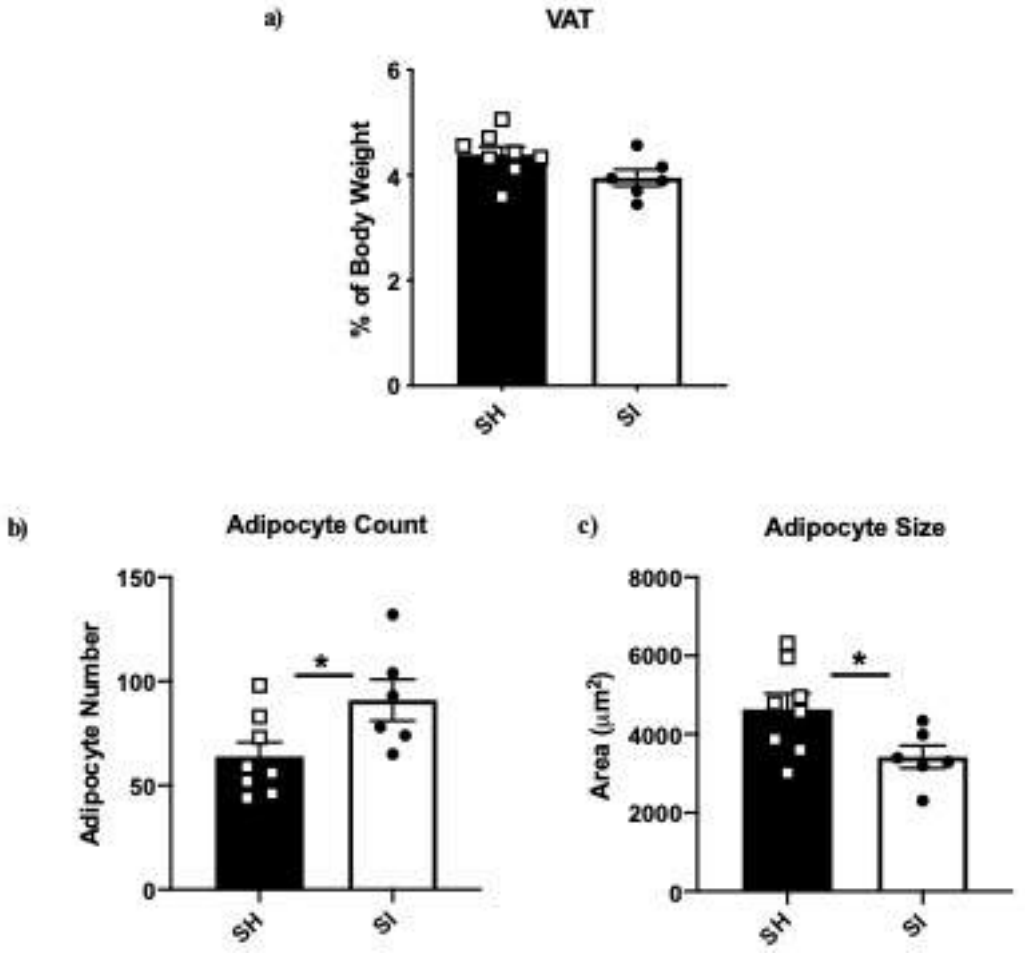

Figure 5.23: VAT Characteristics – Males Western Diet. VAT was characterised as follows: **a)** weight as a % of body weight, **b**) numbers of adipocytes and **c**) adipocyte area. Data are expressed as mean ± SEM, where n=6-8 mice per housing group, with symbols representing an individual mouse. *p<0.05 as determined by use of an unpaired parametric T-test.

5.3.14 Total Cholesterol, Cholesterol Subtypes and Glucose – Western Diet

Quantification of glucose, total cholesterol and its subtypes (triglycerides, HDL and LDL) were assessed in plasma in *ApoE*$^{-/-}$ mice fed the Western diet to give an indication of whether any changes in cholesterol or glucose would be seen between the housing groups, that might contribute to the progression and development of atherosclerosis.

Although there were no significant changes in the total cholesterol concentration between housing groups, male SI mice had a trend towards a lower concentration compared to male SH mice (**Figure 5.24a**). Plasma concentration of triglycerides was at similar levels in male mice from both housing groups (**Figure 5.24b**). HDL concentrations were slightly lower in male SI mice compared to male SH mice (**Figure 5.24c**). Unfortunately, due to lipaemia, plasma LDL and glucose concentrations could not be measured accurately in plasma (data not shown).

In female mice fed the Western diet, total cholesterol concentration in plasma was similar between the housing groups (**Figure 5.25a**). Similarly, in female mice fed the western diet, triglyceride concentrations were similar between SH mice and SI mice (**Figure 5.25b**). Plasma HDL concentrations were again similar between females SH and SI mice (**Figure 5.25c**). LDL concentrations in plasma showed a trend towards being slightly lower in female SI mice, than in SH mice (**Figure 5.25d**).

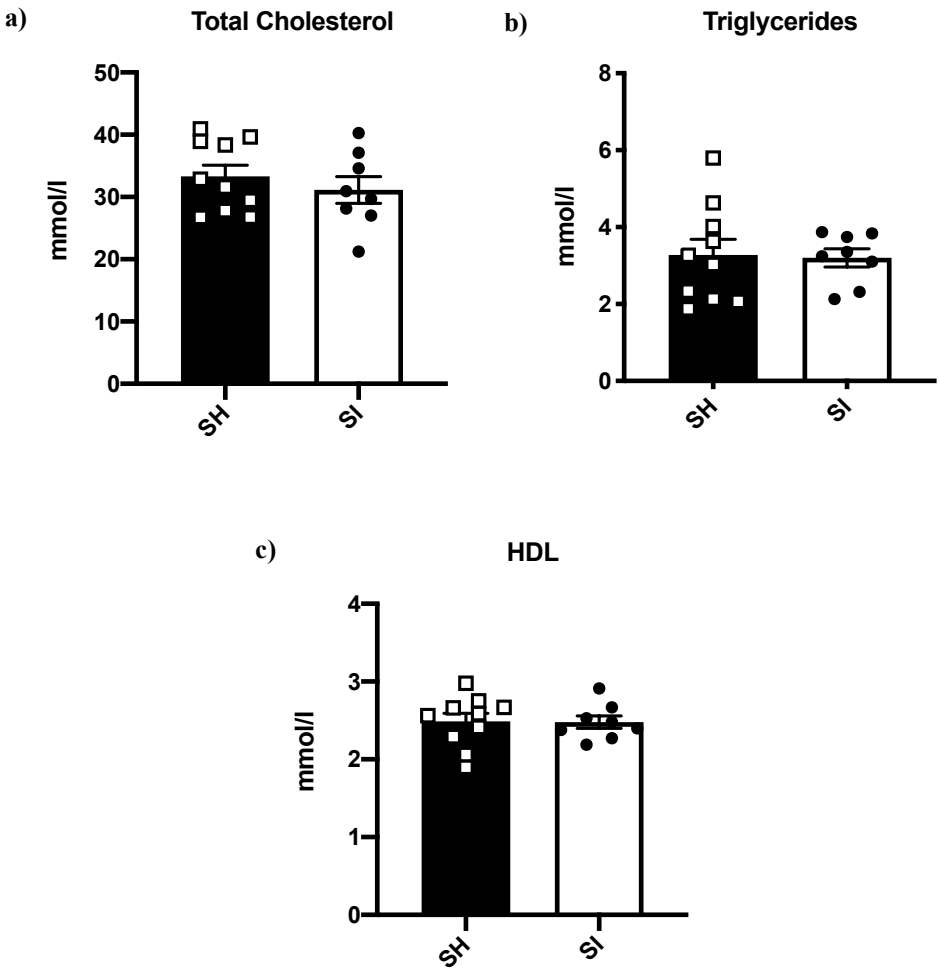

Figure 5.24: Total Cholesterol and Lipid Profile – Male Western Diet. Plasma from male *ApoE*$^{-/-}$ mice had the following assessed: **a)** total cholesterol, **b)** triglycerides and **c)** HDL concentrations. Data shown as mean ± SEM with n=5-8 mice per housing group, where each symbol represents a single mouse. Significance was assessed by an unpaired parametric T-test where $p<0.05$.

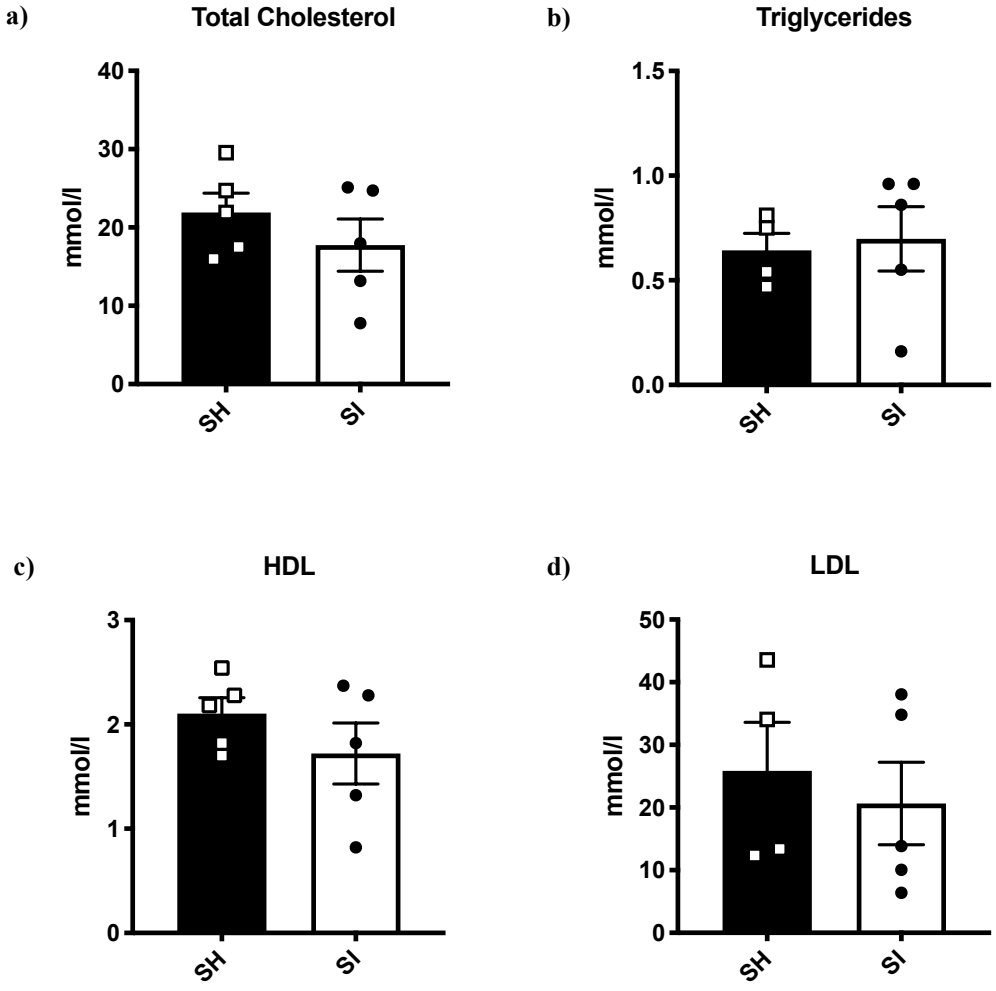

Figure 5.25: Total Cholesterol and Lipid Profile – Females Western Diet. Plasma from male *ApoE*$^{-/-}$ mice had the following assessed: **a)** total cholesterol, **b)** triglycerides, **c)** HDL and **d)** LDL concentrations. Data shown as mean ± SEM where n=4-5 mice, with each symbol representing a single mouse. Significance was assessed by an unpaired parametric T-test where $p<0.05$.

5.3.15 Atherosclerotic Plaque Burden in Aortic Sinus

Atherosclerotic plaque was quantified using Oil Red O staining in the aortic sinus after 4 weeks of social isolation or social housing in *ApoE*$^{-/-}$ mice fed the Western diet, to determine whether some of the increased risk of heart disease seen could be attributed to increased atherosclerotic burden. There were no differences in atherosclerotic plaque area throughout the aortic sinus (**Figure 5.26a**). The mean plaque area in the aortic sinus was similar between housing groups (**Figure 5.26b**). Representative images of atherosclerotic plaques showed larger areas of plaque in SI mice compared to SH mice (**Figure 5.27**).

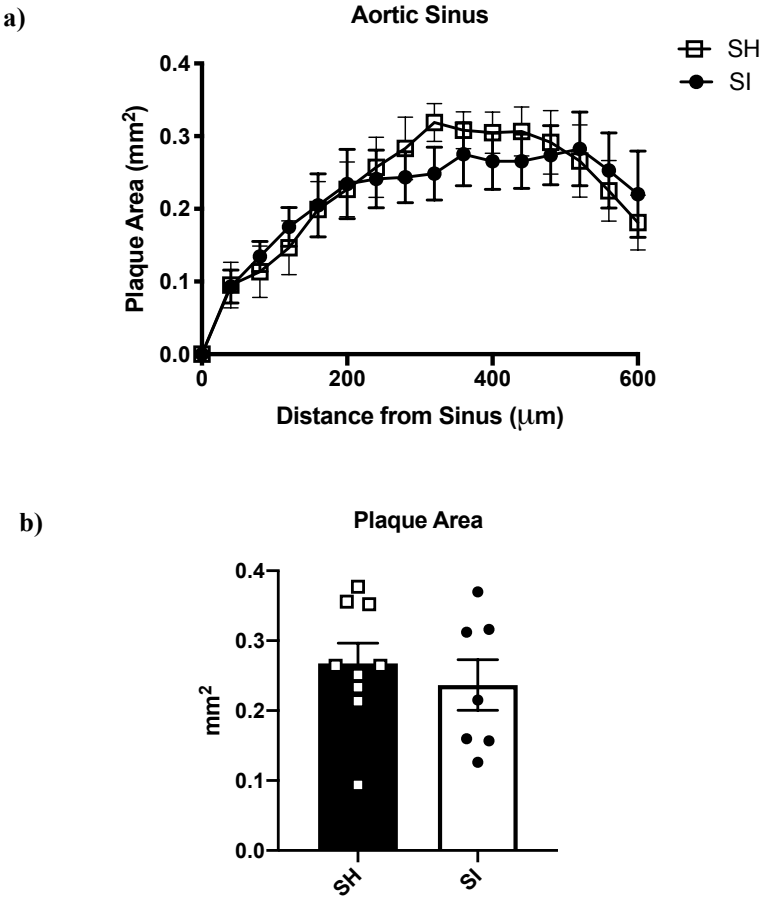

Figure 5.26: Atherosclerotic Plaque in Aortic Sinus. Atherosclerotic plaque area was quantified from the aortic root through the aortic sinus with the following shown **a)** mean atherosclerotic plaque area ± SEM across serial 40μm sections from the start of the aortic valves (0μm) through the aortic root. Significance was assessed using a one-way ANOVA. **b)** mean whole atherosclerotic plaque area between 80μm and 560μm from the sinus. Data shown as mean ± SEM, where each symbol represents a single mouse where n=7-8 mice per housing group. Significance was assessed by an unpaired parametric T-test where $p<0.05$.

a) **Social Housing**

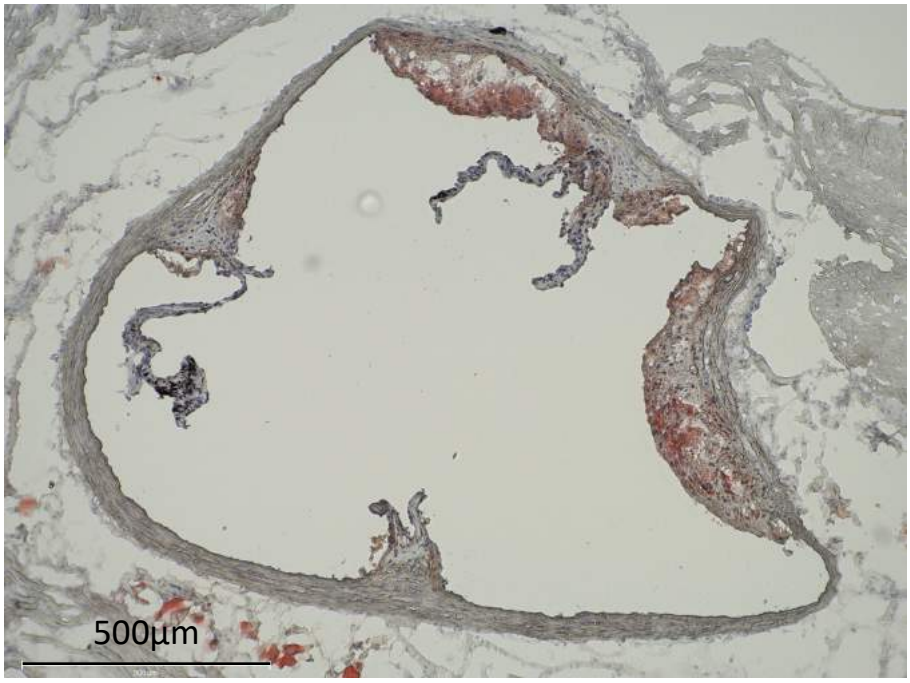

b) **Social Isolation**

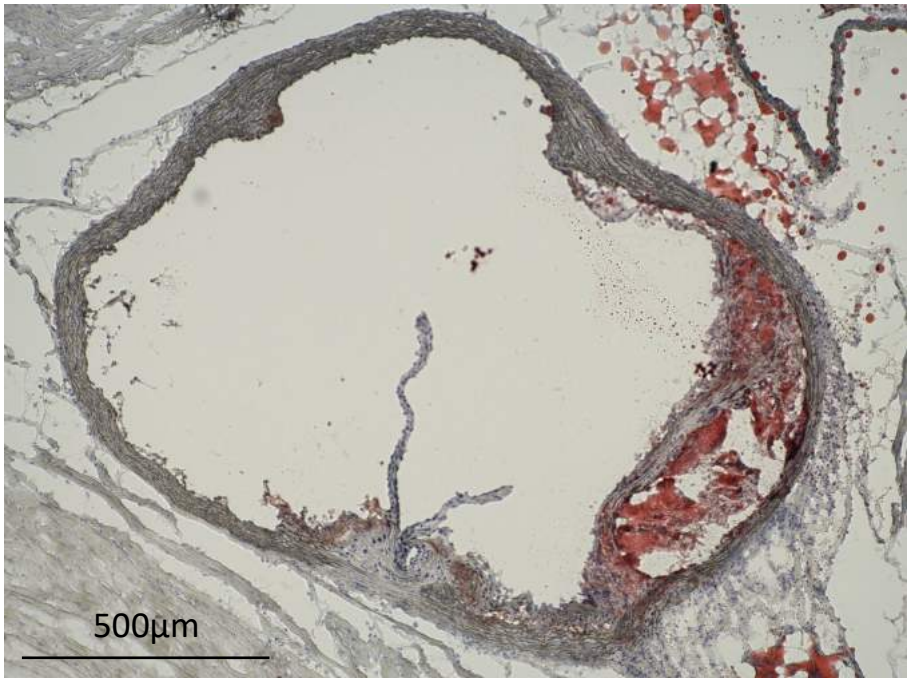

Figure 5.27: Representative Images of Atherosclerotic Plaque in Aortic Sinus. Representative images of Oil Red O staining for the identification of atherosclerotic plaque in the aortic sinus (10x) in **a)** SH and **b)** SI mice. Scale bars are representative of 500µm.

5.3.16 Atherosclerotic Plaque Stability

Despite SI and lonely people being found to have increased risk of cardiovascular events, there was no difference in atherosclerotic burden[176,178,370]. Therefore, the stability of the plaque was assessed by measuring the % of necrosis and analysing the collagen content. The % of necrosis within the aortic sinuses of SI mice was significantly higher in comparison to SH mice (**Figure 5.28**). Representative images of the necrosis within the atherosclerotic plaques seen in each of the housing groups are circled (**Figure 5.29**).

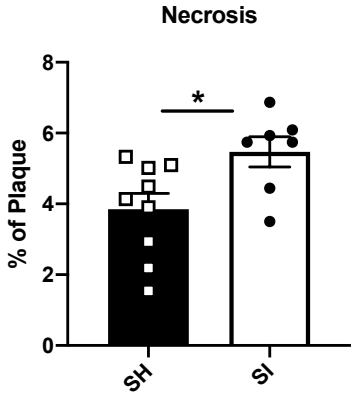

Figure 5.28: Necrosis in Atherosclerotic Plaque. The % of atherosclerotic plaque within the aortic sinus of each housing group is shown. Data is shown as the mean ± SEM where n=7-9 mice per housing group, and each symbol is representative of a single mouse. Significance was assessed using an unpaired parametric T-test where * $p<0.05$.

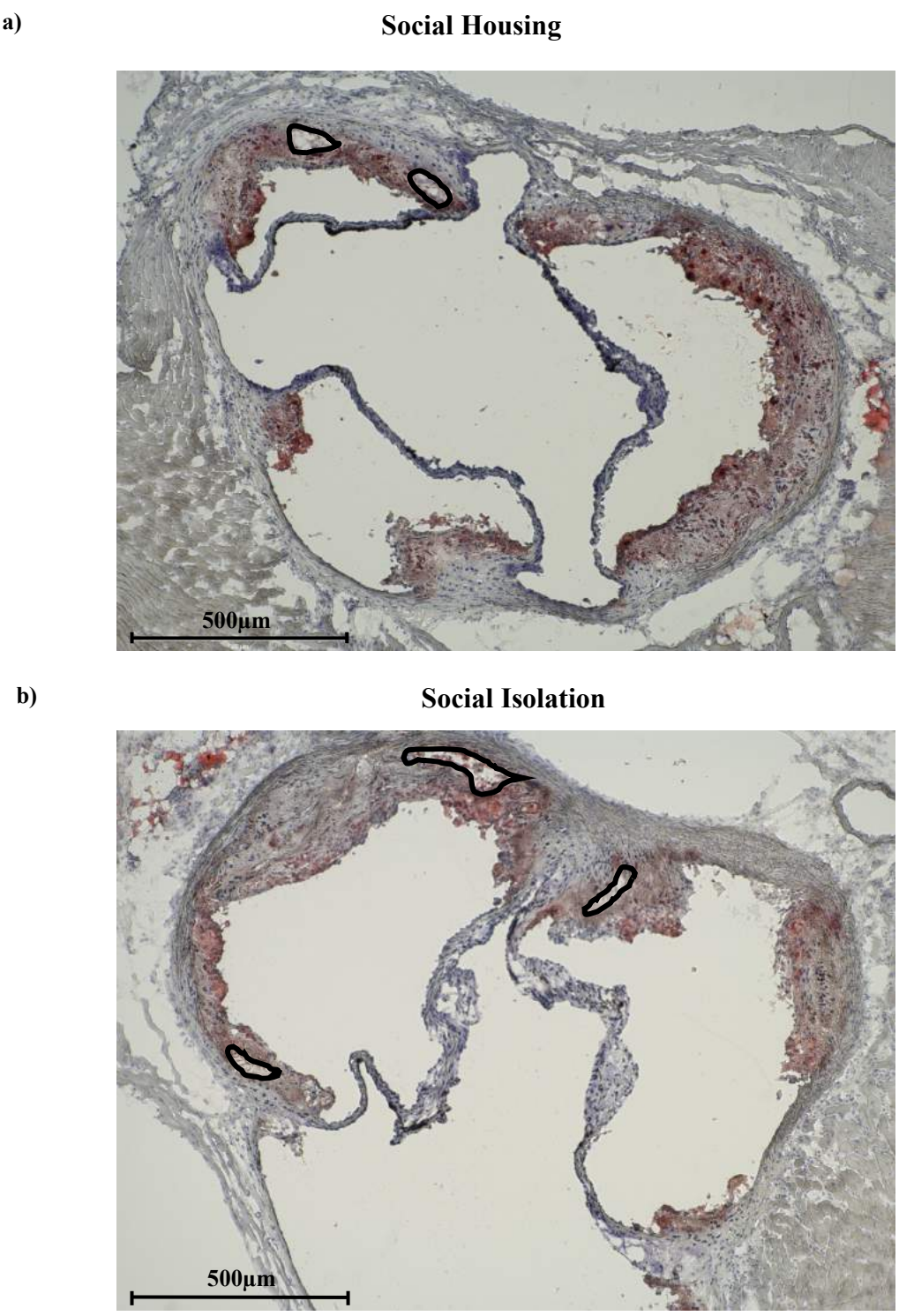

Figure 5.29: Representative Images of Necrosis in Atherosclerotic Plaque. Representative images of necrosis, circled areas, within the atherosclerotic plaque in the aortic sinus stained by Oil Red O at (10x) in **a)** SH and **b)** SI mice. Scale bars are representative of 500µm.

Another one of the main determinants of atherosclerotic plaque stability, is the quantity of collagen present within the plaque[382]. There was a similar intensity of the Pico-Sirius Red stain in the atherosclerotic plaque within the aortic sinus between the two housing groups (**Figure 5.30**). Representative images of the collagen within the atherosclerotic plaques seen in each of the housing groups show no differences in collagen content (**Figure 5.31**).

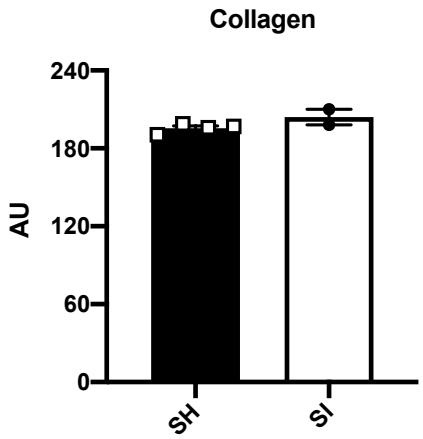

Figure 5.30: Collagen Content in Atherosclerotic Plaque. The intensity of the Pico-Sirius Red stain for collagen was measured using Image J. Data is shown as mean ± SEM where n=2-4 mice per housing group, and each symbol is representative of a single mouse.

a) **Social Housing**

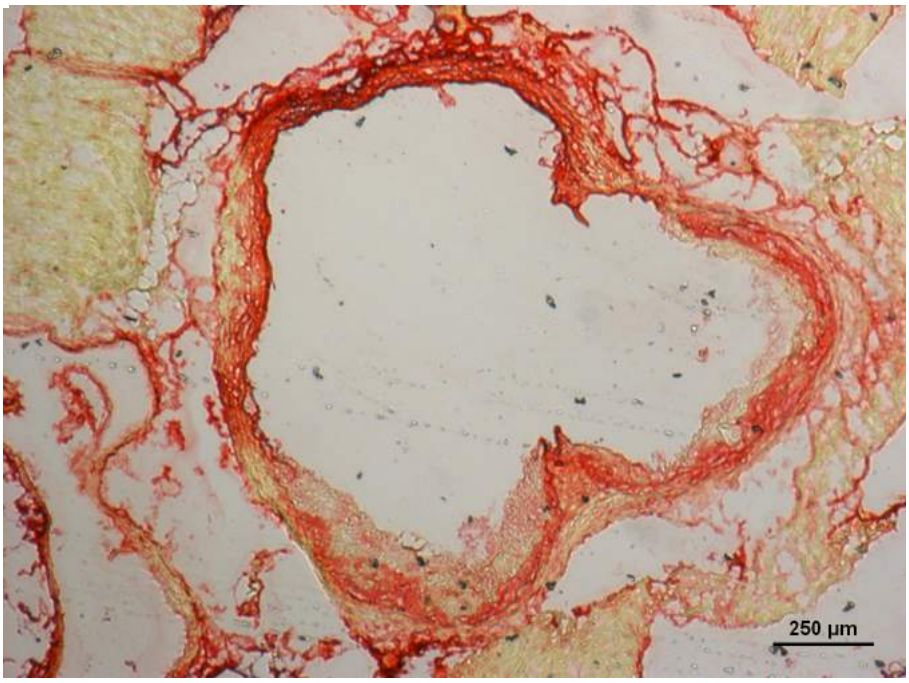

b) **Social Isolation**

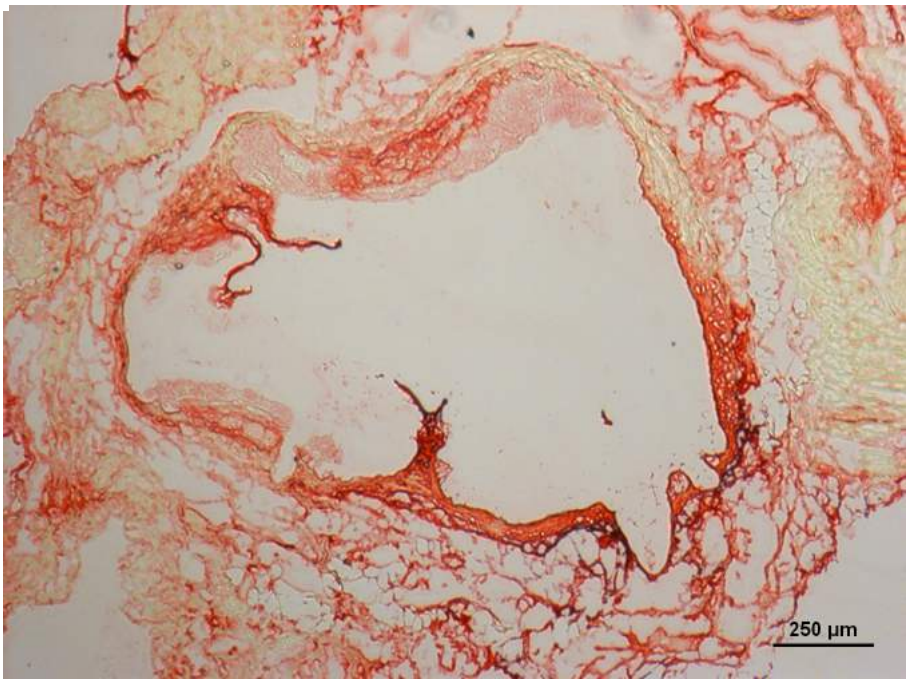

Figure 5.31: Representative Collagen Images Within Atherosclerotic Plaque. Representative images of Pico-Sirius Red staining (4x) for the identification of atherosclerotic plaque at 440-480µm into the aortic sinus in **a)** SH and **b)** SI mice. Scale bars are representative of 250µm.

5.3.17 Heart Weight

After 4 weeks of social isolation or social housing hearts were weighed as an indication of whether fibrosis of the heart tissue might be occurring. There was a trend towards SI hearts accounting for a higher % overall body weight compared to SH hearts (**Figure 5.32**).

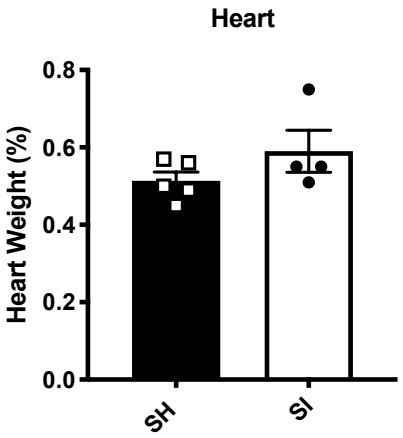

Figure 5.32: Heart Weight. After 4 weeks of social isolation or social housing, hearts from *ApoE*$^{-/-}$ mice were weighed and the % of overall body weight was calculated. Data is shown as the mean ± SEM where n=4-5 mice per housing group, and each symbol is representative of a single mouse. Significance was assessed using an unpaired parametric T-test where $p<0.05$.

5.3.18 Resident Peritoneal Macrophages – Western Diet

F4/80^{+} macrophages were quantified in the PLF of the *ApoE*$^{-/-}$ mice fed the Western diet. LPMs showed a trend towards accounting for a larger % of all the cells found in the PLF compared to SH mice (**Figure 5.33a**). There were no significant differences in CD11b mean fluorescence intensity (MFI) (**Figure 5.33b**).

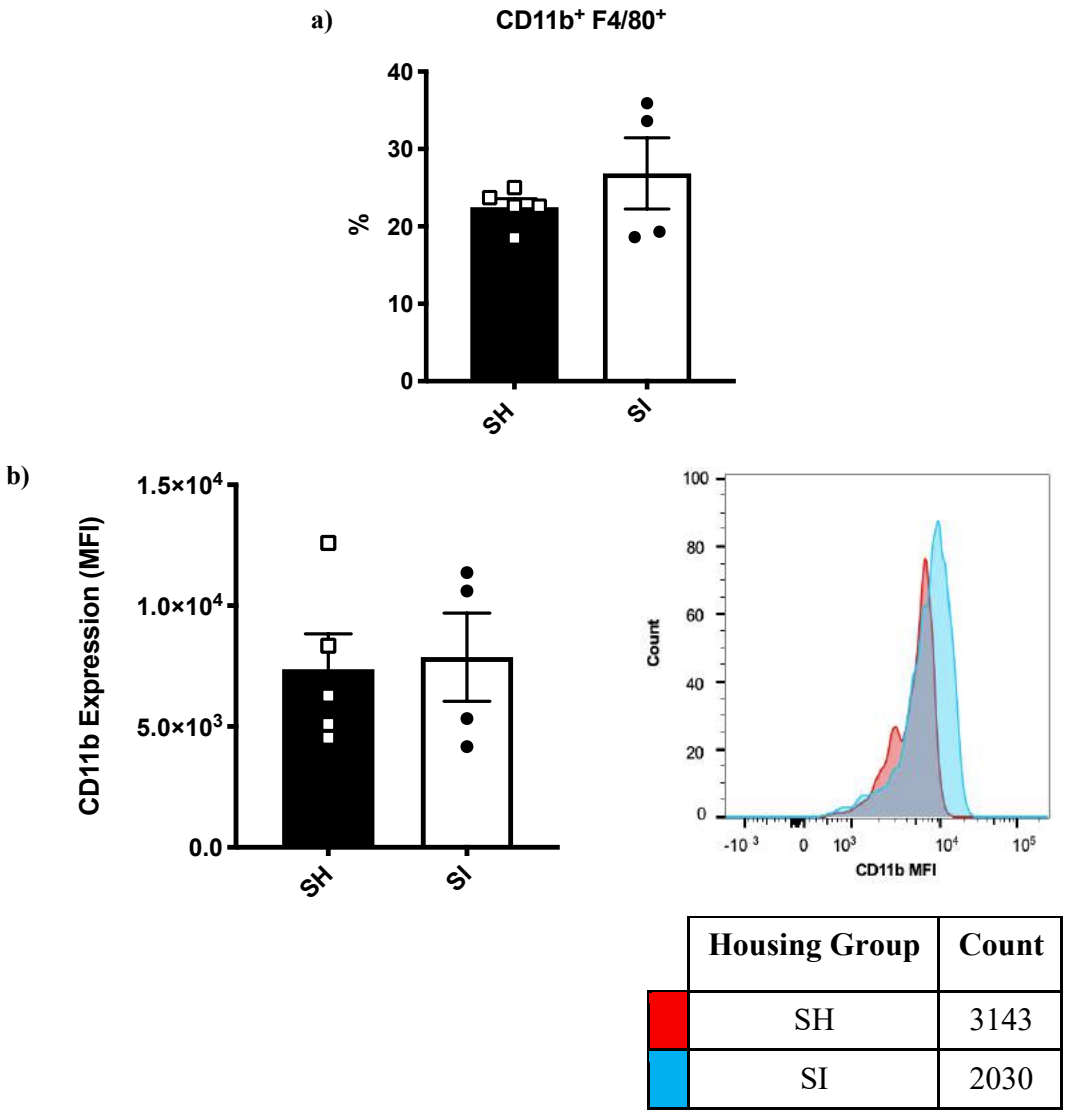

Figure 5.33: Peritoneal CD11b^{+} F4/80^{+} Macrophages. In the PLF the following was assessed: **a)** % of CD11b^{+} F4/80^{+} peritoneal cells and **b)** CD11b MFI. Representative histogram is shown for MFI. Bars are representative of the mean ± SEM per housing group where n=4-5 mice per group, and symbols represent a single mouse. Significance was assessed using an unpaired parametric T-test where $p<0.05$.

5.3.19 Confirmation of Microarray Genes – *ApoE*$^{-/-}$ Mice

The microarray genes were confirmed at a gene level in whole blood using RT-PCR to ensure they were true biomarkers of social isolation, and to confirm that they were strain independent. *Cd55*, *cd52*, *xaf1* and *bach2* showed a trend towards being upregulated in SI mice compared to SH mice **(Figure 5.34**).

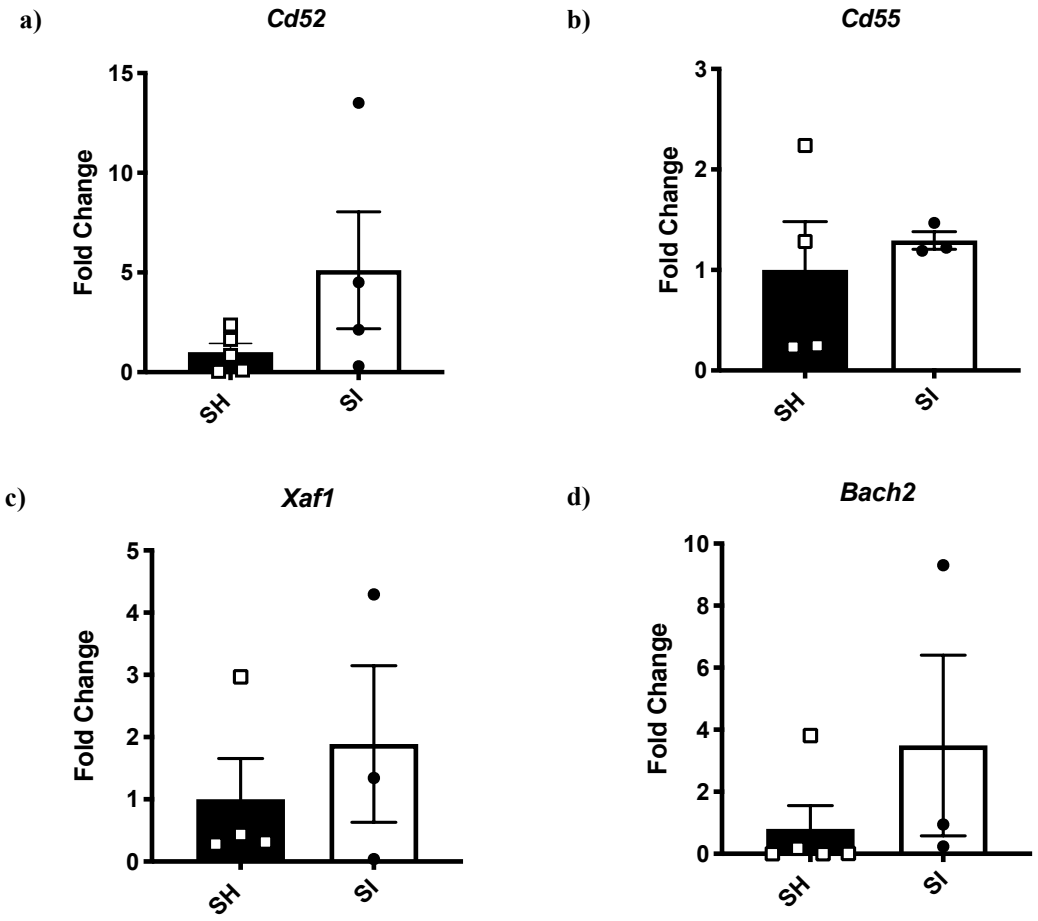

Figure 5.34: Confirmation of Microarray Genes in Whole Blood - *ApoE*$^{-/-}$ Mice. mRNA levels were assessed *via* RT-PCR for genes that were identified in the whole blood as being potentially associated with social isolation. Fold increase was calculated for the following genes: **a)** *cd52*, **b)** *cd55*, **c)** *xaf1* and **d)** *bach2*. Data are representative of the average fold change of the gene expression normalised to *GAPDH* in each housing group, where n=3-5 mice per group. Significance was assessed using an unpaired T test where $p<0.05$.

5.4 Discussion

This chapter aimed to better understand whether social isolation contributes to the development of atherosclerotic plaque, and the potential mechanisms that might play a role in the pathogenesis of this disease. It was shown that deletion of the *ApoE* gene during social isolation influences weight, nutritional intake and biochemical markers of inflammation. The Western diet reversed the effects of social isolation on weight and nutritional intake. This study showed that social isolation does not affect atherosclerotic burden but increases necrosis within the atherosclerotic plaque. It was confirmed that there is a trend towards increased gene expression of the microarray genes *bach2*, *cd52*, *xaf1*, *cd55*.

Initially, to elucidate the effect of *ApoE* deletion on nutritional intake and weight gain during social isolation, SI *ApoE*$^{-/-}$ mice were compared to SI WT mice both fed standard diet. Deletion of *ApoE* led to increased weight gain and increased food and water intake across the study, in a manner independent of the sex of the mice. Older *ApoE*$^{-/-}$ mice than the ones used in this study have been reported in the literature as exhibiting increased food intake compared to C57BL/6 mice after 12 months of age[383]. This suggests that the effects of social isolation on nutritional intake and weight gain can be exacerbated by *ApoE* deletion.

As ApoE is an apolipoprotein, and is able to bind cholesterol and is involved in the transport of it around the blood for eventual clearance, it is not surprising that when the *ApoE* gene is knocked out, that SI *ApoE*$^{-/-}$ mice have higher total cholesterol than SI WT mice[373]. Normal cholesterol concentrations in *ApoE*$^{-/-}$ mice fed standard chow are thought to be around 22.2 mmol/l, which is higher than the ~13.18 mmol/l seen in the mice used in this study, but this could be due to the relatively young age of the mice used, 3 months,

as hypercholesteremia becomes more pronounced with age[375]. Deletion of the *ApoE* gene did not affect plasma glucose concentrations in SI male mice compared to SI male WT mice, whilst SI female *ApoE*$^{-/-}$ mice had lower plasma glucose concentrations compared to SI female WT mice. The literature indicates that male *ApoE*$^{-/-}$ mice at 3 months of age fed standard chow for 7 weeks have higher fasting plasma glucose concentrations compared to C57BL/6 controls. Interestingly, the fasting plasma glucose concentrations of the C57BL/6 mice used in their study are markedly lower than the plasma glucose concentrations seen in the SI C57BL/6 mice used for comparison to SI male *ApoE*$^{-/-}$ mice[384]. Since the mice used to compare the effect of the *ApoE* gene on plasma glucose concentration were not fasted, this might account for the absence of a difference between the SI strains used in this study.

In a similar manner to experiments investigating weight gain and nutritional intake in CD-1 mice, SI *ApoE*$^{-/-}$ mice on standard chow were found to have a trend towards increased food intake, whilst not gaining as much weight compared to SH *ApoE*$^{-/-}$ male mice. Interestingly, this effect is ablated on the Western diet. As mentioned previously, the increased food intake without weight gain on standard chow is most likely accounted for by the fact that mice get up to 65% of their warmth by huddling, and by being singly housed this source of warmth is not available to SI mice, meaning they have to expend more energy to keep warm (**Figure 5.35**)[251]. It is possible that since the Western Diet is highly calorific, that it provides enough energy to maintain body temperature without the need for increased food intake. This hypothesis was confirmed since when calorie intake was assessed, a similar number of calories were consumed regardless of diet in SI mice, but not in SH mice who had increased calorie consumption on the Western diet, suggesting that SH mice might have leptin resistance. This suggests it is the number of

calories consumed not their nutritional value that determines weight gain a finding that has also been shown in humans during weight loss[385].

Leptin concentration in plasma was higher in SI *ApoE*$^{-/-}$ mice on standard chow compared to those SH *ApoE*$^{-/-}$ mice, but was lower in SI *ApoE*$^{-/-}$ mice on the Western diet suggesting that the effects of social isolation on leptin can be blunted by Western diet. Similar to what was seen with regards to leptin concentration in SI *ApoE*$^{-/-}$ mice, social isolation has been associated in men, but not women with increased serum leptin concentration, with the effect being exacerbated by depressive symptoms[386]. Despite VAT accounting for a similar % of body weight in both housing groups the characteristics of VAT were markedly different between the groups, whereby SI mice had higher numbers of smaller adipocytes present. Both mice and humans eating the Western diet often become leptin resistant, meaning that despite high concentrations of leptin, increased food intake and thus increased weight gain are not inhibited[387,388]. There is evidence to suggest that the mRNA of leptin receptor long form (Lepr-b) becomes downregulated whilst inhibitors of Lepr-b such as suppressor of cytokine signaling-3 (SOCS3), are upregulated in the adipocytes, leading to constitutive storage of triglycerides and thus increased hypertrophy of adipocytes in WAT[389]. Thus, it is possible since leptin levels were significantly lower in SI mice and adipocyte size was significantly smaller, that SI mice have increased Lepr-b and thus exhibit, to some degree, protection against leptin resistance, which would also explain why SI mice on Western diet no longer consume more food as seen in SI mice on standard chow.

In order to assess inflammation at baseline plasma cytokine concentrations and biochemical markers of inflammation were measured. Since plasma cytokines were consistently too low to measure accurately, this suggests that basal inflammation is very

low. In female mice fed standard chow, plasma AST concentration was significantly lower in SI mice compared to SH *ApoE*$^{-/-}$ mice, whilst in males the plasma AST concentration was similar between the housing groups, suggesting a sex difference. In fact, differences in AST concentrations have been reported between male and female C57BL/6J mice, the background strain of the *ApoE*$^{-/-}$ mice used in this study, with females tending to have higher AST and ALT concentrations in serum than male[390]. Deletion of the *ApoE* gene did not exacerbate plasma AST concentration in either male or female SI mice, nor plasma ALT concentrations in male SI mice compared to age-matched SI WT mice[390]. Similarly to the results seen in male *ApoE*$^{-/-}$ mice in this study, social isolation for a period of 13 weeks has been shown to have no effect on either AST or ALT plasma concentrations in male C57BL/6J mice[391]. Interestingly, when SI *ApoE*$^{-/-}$ mice were compared to SI WT mice fed standard chow plasma creatinine concentrations were significantly lower in the *ApoE*$^{-/-}$ mice, regardless of sex. A small-scale study comparing WT and *ApoE*$^{-/-}$ mice in standard housing, found that the deletion of the *ApoE* gene did not affect serum creatinine concentrations[392]. This suggests that the difference in plasma creatinine concentration seen is the result of the social isolation as opposed to deletion of the *ApoE* gene. In female *ApoE*$^{-/-}$ mice fed standard chow, there was no difference in plasma creatinine concentrations between SI and SH mice. This finding is in concordance with the absence of a difference in creatinine levels in SI and socially integrated heart failure patients, who were involved in the "Waiting for a new heart study"[393].

On standard chow, it was demonstrated that SI male *ApoE*$^{-/-}$ mice had increased plasma concentrations of total cholesterol. In contrast social isolation and the Western diet did not alter total cholesterol levels or lipid profile in plasma. There are only a few studies investigating the effect of social isolation as opposed to loneliness in humans or animal

models, but the majority of existing data suggests that there is no link between social isolation and total cholesterol levels[394–397]. However, one study in *ApoE*$^{-/-}$ mice found that there was an increase in plasma lipids during 20 weeks of social isolation[398]. One possible reason for the similar total cholesterol concentrations between the housing groups upon the Western diet, could be the result of the male SI mice having a similar food intake to SH mice, as opposed to SI mice having a higher food intake on standard chow compared to SH mice. Plasma glucose concentration in both males and females under the aforementioned conditions were similar between both housing groups, both with and without the Western diet. Similar findings were seen in social isolation in rats[399]. However, higher levels of social inclusion in humans has been shown to be associated with lower predicted blood glucose and LDL, whilst having no effect on HDL concentrations[264].

Lipaemia refers to turbidity that occurs in samples due to high levels of lipoprotein particles and consumption of high fat diets, such as the Western diet, can cause it to occur[400–402]. The presence of lipaemia is well-known to interfere with assay reliability, particularly for those assays that rely on photometric techniques, including the Beckman Coulter AU680 Chemistry Analyzer and ELISA, which was used for total cholesterol and lipid profiling of plasma and for the determination of plasma glucose levels[400,403–406]. Lipaemic samples have high levels of lipoprotein particles that absorb light, with the amount of light being inversely proportional to the wavelength. Since the plasma samples from those mice fed the Western diet were highly lipemic, the results of the aforementioned tests should be interpreted with caution. It is for this reason plasma LDL and glucose levels are not shown as the samples were above the cut-off level of lipaemia for being reliable[405,406]. Plasma cytokines were not measured, as their concentration would be measured by ELISA, a photometric technique, and it was likely that there

would be interference by the lipaemic status of the samples rendering any results gained unreliable[404]. In order, to avoid lipaemic samples, mice would have to undergo fasting prior to sacrifice, which arguably could be seen as a source of stress and thus a potential confounding factor[270,407].

Quantification of the atherosclerotic plaque did not reveal any differences in atherosclerotic plaque burden in the sinuses from SI mice compared to SH mice. A small scale study carried out in *ApoE*$^{-/-}$ mice subjected to social isolation for 20 weeks, found increased atherosclerotic plaque burden within the intima artery but not in the thoracic artery[398]. This suggests that the effect of social isolation on atherosclerotic burden might be area dependent, which is one possible reason why no differences were seen in atherosclerotic burden. Similarly increased atherosclerotic burden was demonstrated in female cynomolgus monkeys and in Watanabe heritable hyperlipidemic rabbits[408,409]. The difference in the effect of social isolation on atherosclerotic plaque is most likely attributed to the length of social isolation, which for the studies done in this chapter were 4 weeks compared to the 20 weeks of social isolation used in the majority of the aforementioned studies.

Since there were no significant differences in atherosclerotic burden within the aortic sinus, plaque stability was assessed, as both loneliness and social isolation are associated with increased risk of MI and stroke, which is often caused by rupture of the atherosclerotic plaque[178,370]. It was demonstrated that social isolation increased the % of necrosis within the atherosclerotic plaque, which potentially suggests that social isolation could increase the risk of atherosclerotic plaque rupture by increasing the size of the necrotic core[410,411]. Interestingly, necrosis occurs as a result of insufficient ability of macrophages to undergo phagocytosis of apoptotic cells, with this inability to effectively

clear apoptotic cells being potentially linked to oxidative stress[412]. The accumulation of apoptotic cells within the atherosclerotic plaque is associated with changes in inflammatory indices, with it being reported to cause an increase in IFN-γ production from the atherosclerotic plaque and the spleen, as well as a decrease in IL-10 production from the spleen, resulting in enhanced necrosis and promotion of the development of atherosclerosis[413]. Given that *bach2* and *xaf1*, genes involved in the promotion of apoptosis, were significantly upregulated in the whole blood of SI mice it is not inconceivable that SI mice might have enhanced apoptosis, which would in turn lead to greater necrosis. It is worth noting that *bach2* has been found to be elevated in PAD so there is potential for it to be involved in atherosclerosis[308]. Higher BMI and thus weight are associated with increased risk of plaque rupture, yet it is the SI mice who weigh less who that have heightened levels of necrosis, a key risk factor for rupture of the plaque[414]. As necrosis is extremely pro-inflammatory, it suggests that it is a heightened immune response, rather than metabolic changes, that drive the documented increased risk of acute coronary artery events including MI[370,379].

Plaque instability is characterised by low collagen content and large necrotic cores[379,415]. *ApoE*$^{-/-}$ mice fed the Western diet form fibrous caps and significant necrotic cores within their atherosclerotic plaques at 18-20 weeks of continuous on the Western diet, or greater than 10 months on standard chow[378]. Therefore, the absence of high levels of collagen deposition in the mice used in this study is not surprising, as they were fed the Western diet for 1 month at 6 months of age. To this end, the absence of a fibrous cap meant collagen deposition could not be calculated as a % of the area of the atherosclerotic plaque within the sinus, but was tentatively determined instead by the intensity of the red of the Pico-Sirius Red stain within the plaque area. Due to the small number of aortic sinus samples available to stain with Pico-Sirius Red, it is impossible to get a clear

indication of any differences in collagen present, but the data thus far suggests there is very little if any difference in collagen within the plaques of SI *ApoE*$^{-/-}$ mice[416]. Similarly, it is important to note that the difference in % of necrosis between the groups whilst significant is relatively small, 1.6%, but has the potential to become more pronounced over time and to have more translational value. The atherosclerotic plaques seen in *ApoE*$^{-/-}$ mice do not tend to rupture without intervention, thus it is not clear what % of the plaque would have to be necrotic in this model to cause the plaque to rupture. In humans, the necrotic core accounts for about 15-23% of the plaque in 75% of ruptured atherosclerotic plaques, which is a much higher % than the averages seen in this study[379,417].

Studies have shown that cardiac hypertrophy is seen in *ApoE*$^{-/-}$ mice as they age and is exacerbated by the Western diet. The main causes of cardiac hypertrophy in these mice are arterial stiffness and hypertension[418]. The heart to body weight ratio is commonly used to assess cardiac hypertrophy in mice[419]. In this study, preliminary results show that SI mice have a slightly higher heart to body weight ratio, suggesting that they might have increased cardiac hypertrophy. As loneliness in humans has been shown to increase both blood pressure and risk of CVD, it is perhaps surprising that preliminary data suggest that there are no significant differences between SI *ApoE*$^{-/-}$ and SH *ApoE*$^{-/-}$ mice, as both of these factors lead to exacerbated cardiac hypertrophy[178,371].

Similarly to what was demonstrated in CD-1 mice subjected to *E.coli* induced sepsis, SI *ApoE*$^{-/-}$ mice had a trend towards a higher % of CD11b^{+} F4/80^{+} cells, LPMs, in the peritoneal cavity compared to SH *ApoE*$^{-/-}$ mice. LPMs have been shown to be heavily involved in clearing apoptotic cells and tissue repair, which is interesting since a lot of the upregulated differentially expressed genes in SI mice in the microarray also promote

apoptosis, suggesting SI mice might be able to promote apoptosis as opposed to necrosis[420]. Peritoneal macrophages from mice fed high fat diet have been shown to have enhanced phagocytosis, suggesting that having higher numbers of LPMs might be beneficial in inducing low grade inflammation, which is key for the development of atherosclerotic plaque[416].

In order to confirm the validity of the genes (*cd52*, *cd55*, *xaf1* and *bach2*) identified as being upregulated in CD-1 mice by both microarray and RT-PCR in *ApoE*$^{-/-}$ mice, these genes were tested in whole blood from *ApoE*$^{-/-}$ mice fed the Western diet to elucidate whether the results were strain and diet dependent. There was a trend towards upregulation of *cd52*, *cd55*, *xaf1* and *bach2* gene expression in SI mice compared to SH mice. Possible reasons for the absence of significant changes in the gene expression of *cd52*, *cd55*, *xaf1* and *bach2* in whole blood, such as those seen in CD-1 mice, could possibly be due either to the strain of mice or the change in diet from standard chow in CD-1 mice to Western diet in *ApoE*$^{-/-}$ mice. In order, to address whether the change in diet could attribute for the variability of the data, the genes of interest would have to be tested in *ApoE*$^{-/-}$ mice fed standard chow.

In summary, comparison of SI WT mice to SI *ApoE*$^{-/-}$ mice revealed that *ApoE*$^{-/-}$ mice gained more weight over the study, as a result of increased food intake and higher total cholesterol, accompanied by a decrease in creatinine concentration in plasma. It was demonstrated that on standard chow SI mice have increased food intake despite not gaining as much weight, an effect that can be overcome by the calorific Western diet. Additionally, it was shown that VAT had increased numbers of smaller sized adipocytes. Taken together, these results are indicative of increased energy expenditure, probably as a requirement for keeping warm. Furthermore, atherosclerotic plaque size was found to

be similar between housing groups, as was total cholesterol and lipid profile. SI mice had a higher % of necrosis in their atherosclerotic plaques, suggesting that they would be more prone to rupture. However, it was shown that SI mice had a trend towards increased LPMs. All the genes tested from the microarray showed a trend towards being upregulated in SI mice compared to SH mice suggesting, a unique transcriptional fingerprint in the whole blood during social isolation. In conclusion, since both housing groups have similar atherosclerotic burden with a higher % of necrosis seen in SI atherosclerotic plaques, this highlights the importance of the role of the immune system in atherosclerotic disease development.

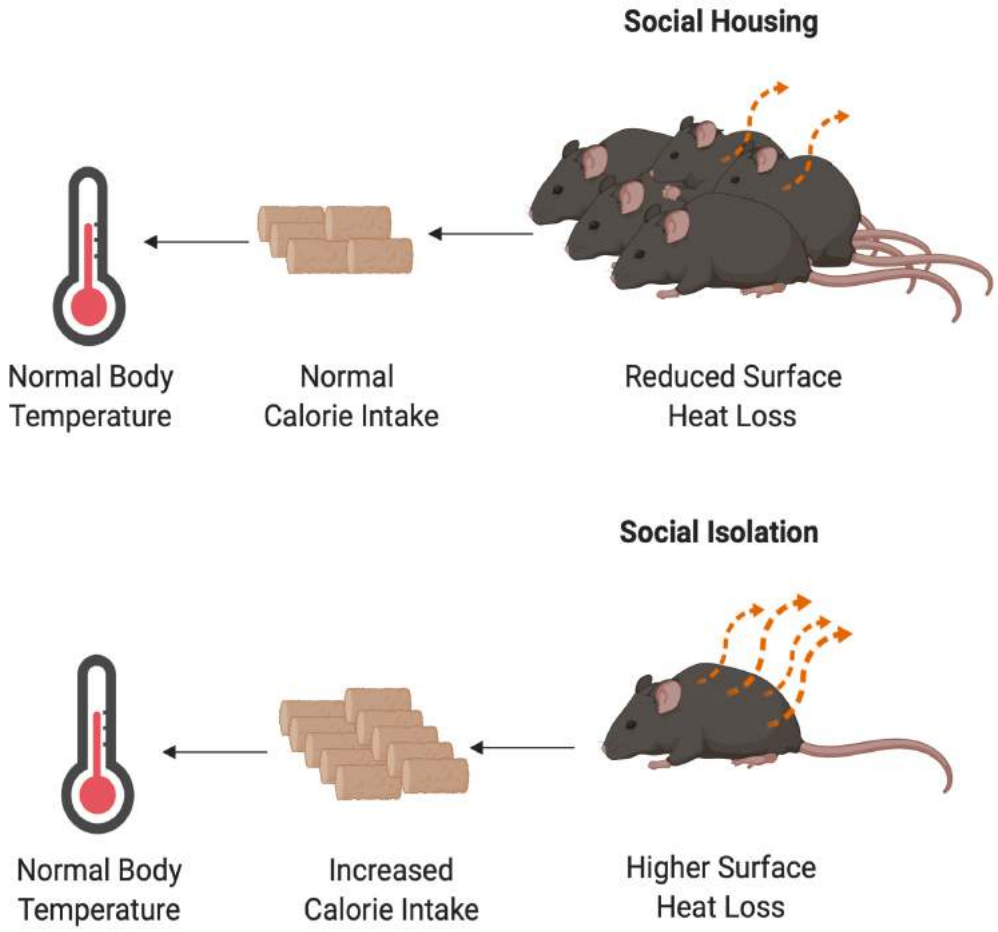

Figure 5.35: Role of Huddling in Thermogenesis. Mice that huddle together such as SH mice have a lower surface:volume ratio, and thus have reduced heat loss. This means SH mice do not have to increase their calorie intake in order to maintain their body temperature. In contrast, SI mice that cannot huddle together for warmth have a higher surface:volume ratio, and thus have increased heat loss. As SI mice lose more heat to their surroundings, they have to increase their calorie intake in order to maintain their body temperature.

Chapter 6
General Discussion

6.1 General Discussion

Social isolation and loneliness are becoming increasingly prevalent, with it being estimated that around 5% of adults in England 'often' or 'always' feel lonely, according to the Jo Cox Commission on Loneliness[160]. However, this figure is probably highly underestimated since there is a stigma surrounding admitting feeling lonely[421]. This increase in the prevalence of loneliness has important implications to the economy, as loneliness is estimated to cost the UK £2.5 billion per year[160]. Since social isolation is thought to be as dangerous as smoking 15 cigarettes per day, it is unsurprising that both loneliness and social isolation are risk factors for premature mortality and a number of inflammatory diseases, including atherosclerosis[147,152,166,177,370]. Therefore, there is a need to better understand the molecular mechanisms which confer such an increased risk of premature mortality.

It is important to note that the use of experimental animal models, including mice, to model social isolation is a very simplified but useful tool. It allows elucidation of the molecular and transcriptional changes caused by social isolation, and the subsequent impact on the physiology of the organism in the model. Humans are inherently complex both in terms of their behavior and personality. For example, some people enjoy solace as opposed to company, which might affect the impact of social isolation on the body. It is known, as mentioned previously that poor social connections result in increased prevalence of risk behaviours, such as increased alcohol consumption, sedentary lifestyle and smoking, as well as poor medical adherence. All of which contribute to some extent to the increased risk of chronic inflammatory disease, and thus premature mortality seen

in this population of people[120]. These changes in behavior are not easily modelled in mice. It is not clear how much of an effect and thus how important such effects are in this increased risk, as there is disparity in the literature about whether or not social isolation and loneliness are independent risk factors for disease, or whether changes in health behaviours are responsible[178,370,422]. Additionally, the studies carried out are over relatively short time frames, 2-4 weeks, compared to those seen in humans who might face social isolation over periods of years, with this being particularly relevant for those suffering from debilitating diseases such as RA[423]. However, it is important to note that as mice only live 2 years, a period of 2-4 weeks of social isolation is thought to be the equivalent of ~1.6-3.1 human years, thus our models are the equivalent of a relatively long period of social isolation, such as that seen in humans who have chronic debilitating diseases such as RA, or mental illnesses such as depression[148,424,425].

There is some uncertainty amongst the scientific community as to whether mice have personalities. Humans have complex personalities, which affect how they act and the choices they make every day[426]. This is an important aspect to consider as some individuals are more introverted, like to be alone more, whilst others are more extroverted and like to be surrounded by people[427]. At a basic level the behavioural traits exploration, activity and boldness have been demonstrated to differ between different mice and remain consistent over time within the same mouse[428]. Recently, it has been demonstrated in mice that there appears to be four different identity domains, with each domain being akin to different 'personalities', that were found to be stable over time regardless of the social environment. Personalities were determined by the frequency of the following behaviours in their everyday life: **1**. approach other mice, **2.** be approached by other mice, **3.** chase other mice, **4.** escape from other mice, **5.** contact duration, **6**. time alone outside, **7.** time outside, **8.** mean speed, **9**. food and water habits, **10.** distance , **11.**

location preference, **12.** predictability and **13.** entry into the elevated area. The identity domains were shown to result in transcriptomic variance within the brain[429]. There are considered to be two main characteristics of personality traits seen in humans. Personality traits refer to a continuous gradient of individual differences seen in humans, and these characteristics remain relatively stable over time[426]. Therefore, it could be argued that mice display some degree of personality, not too dissimilar to that seen in humans. Additionally, sociability was a factor that was found to differ between the four identity domains demonstrated in mice, and this was on a spectrum similar to what is seen in humans[427].

In humans, feeling lonely or having poor social connections can induce a complex set of behavioural changes, including engagement in risky behaviours, such as increased alcohol consumption and poor dietary choices, which often lead to anxiety and depression, all of which have been associated with increased risk of metabolic dysfunctions[120]. The combination of behavioural changes that occur as a result of social isolation are not easily modelled in mice, but the effect of consumption of high fat food compared to a normal diet during social isolation, is modelled by use of the Western diet and standard chow respectively. This simple change of diet allows for the effects of social isolation and diet, on nutritional intake and immunology of the mice to be elucidated. In fact, it might be the combination of behavioural changes that are not easily modelled in mice, which might partially account for the absence of any difference in atherosclerotic burden between the two housing groups. The period of social isolation used in this study was relatively short and since atherosclerosis is a chronic disease that progresses over time, it is possible that longer periods of social isolation might show a more profound effect in atherosclerotic burden. Necrosis is an immune driven process that occurs as a result of insufficient ability of macrophages to undergo phagocytosis of apoptotic cells,

suggesting that changes in the immune system as a result of social isolation might play more a role in atherosclerosis development[379].

As social isolation and loneliness can cause depressive and anxiogenic behaviours in humans, it is important to understand whether such behavioural changes can be seen in mice during social isolation, and thus test the validity of this model[430–433]. There is some degree of discrepancy with regards to whether social isolation induces depressive and anxiogenic behaviours in mice post-weaning (**Table 8**). However, the majority of studies suggest that social isolation in mice results in increased depressive and anxiogenic behaviours, which is in agreement with what is characterised in lonely and SI people[430–436]. It is possible that the use of different behavioural tests for anxiety or depression can render different results, as can be seen in the study carried out by Võikar *et al* (2004), where they demonstrated decreased anxiety on the elevated plus maze, but increased anxiety in both the dark light test and novelty-induced feeding suppression test[436]. Both the age of the mice and the duration of social isolation differ throughout the studies, making it harder to get a clear picture of whether social isolation is modelled accurately in mice.

It is also important to note that the majority of the studies in **Table 8** were carried out using the C57BL/6J strain, meaning there is a possibility of a strain effect, although when DBA/2 and C57BL/6J were compared in the same study, no differences in the main behavioural findings were seen between strains[436]. Furthermore, only 2x studies addressed the effect of social isolation on behaviour in female mice[435,437]. There is some debate surrounding whether the stage a female mouse is in within the oestrous cycle, can influence the results of behavioural tests. In CD-1 mice, no effect of the oestrous cycle was found on the open field test, and this was also true in C57BL/6J females[438,439].

However, female BALB/c mice were found to have differing results in the open field, startle reflex and tail suspension test, depending on the stage of the oestrous cycle. These remained consistent in C57BL/6J females irrespective of the stage of the oestrous cycle [439]. Therefore, it is likely the effect of the oestrous cycle is strain dependent and it is unclear whether social isolation itself causes any true behavioural effects.

Social hierarchy is an aspect that is not considered in this thesis. yet it is present in most animal societies and refers to an organisational scheme that is in place to determine access to resources, whereby group members are either considered to be dominant or to be subordinate[440]. Mice housed with other mice are known to exhibit social hierarchy. Socially dominant mice are more likely to win conflicts, exhibit agonistic behaviours, have first access to food, mark their territory with urine and have a prominent role in the grooming of other mice within the social hierarchy[441].

It is likely that social hierarchy would occur in the SH mice used throughout this thesis, although it is important to note that all SH mice were weaned together to minimise fighting and its associated social stress. Whilst it is impossible to know whether social hierarchy is influencing food intake of each mouse in SH cages, as food is measured for the whole cage rather than on an individual mouse basis, it is likely that those individuals who are more dominant would exhibit increased food intake. However, weight change throughout the studies consistently shows a distribution that might suggest dominance ranking, whereby the SH mice that gain the most weight have access to food first and eat more, whilst those who are lower ranked gain less weight due to later access to food later meaning they probably eat less[441].

One way to test such a hypothesis would be to carry out social hierarchy testing of the SH mice by use of either the test tube test or the food competition test[440,442]. Briefly, the

test tube test involves two mice entering a narrow tube at opposite ends and meeting in the middle. The mouse that retreats out of the tube is considered to be a subordinate, and the mouse that remains in the tube is considered to be the dominate mouse[440]. The food competition test is where mice are fasted for 12 hours and two mice are given a highly appetitive piece of food e.g. a vanilla cookie, and the mouse that wins the food is considered to be the dominant out of the two mice[442]. For both tests, the procedure is then repeated so that each mouse competes against the other mice in the cage, with increased wins correlating with increased social rank[440,442]. These tests would help to establish the individual ranks of the mice and these could be compared to weight gain to determine whether social hierarchy influences this factor.

It has also been demonstrated that social hierarchy can affect how well the immune system responds to infection. Plasma corticosterone levels were found to be lowest in lower ranked mice and to increase as dominance increases, with the highest levels seen in the most dominant members who are probably subjected to enhanced social stress mice[442]. In healthy mice there were no differences in the immune secretion of IL-10, IL-4, IFN-**γ** and IL-2 from the splenocytes of both dominant and subordinate mice[443]. However, social hierarchy has been shown to affect how the immune system responds to infection, whereby 21 days after a challenge with purified tuberculin, IFN-**γ** and IL-10 production from spleen cells was higher in higher ranked mice compared to lower ranked mice. In contrast, cytokine production after LPS stimulation was unaffected by social rank, as was bacterial growth[442]. This suggests that whilst there is some variation in the concentrations of cytokines in PLF and plasma in SH mice challenged with LPS, it is mostly not accounted for by differences in social rank. However, there is an almost linear distribution of individual mice with regards to weight loss, CFU/ml of bacteria in blood and PLF and plasma cytokine concentrations that occurs in SH mice during *E.coli*

induced sepsis. This could indicate an effect of social hierarchy. Since dominant mice have been shown to be more resistant to tumoral, parasitic and viral challenges compared to lower ranked mice within the social hierarchy, it would be expected that those mice with the lowest bacterial counts and weight loss after the *E.coli* challenge would be the dominant mice, whilst those with greater weight loss and bacterial counts would have lower ranks within the social hierarchy [444–446]. A similar distribution in individual mouse values for weight loss occurs in poly(I:C) septic SH mice to that seen in SH mice with *E.coli* induced sepsis, thus suggesting social rank might have a role in disease severity. Interestingly, the percentage of neutrophils and macrophages does not appear to be affected by social hierarchy as the individual values for each mouse forms a cluster with the rest of the SH group. Again, to have a better understanding of how social hierarchy affects the immune system in the SH mice used in this thesis, the test tube test or the food competition test would need to be carried out to determine the social rank of each individual mouse[440,442].

Sexual dimorphism has been documented with regards to the immune response[327,447]. Yet it is estimated that less that 10% of immunological studies included female mice [448]. Similarly, despite evidence showing that women have double the risk of being diagnosed with anxiety or depression than men, less than 45% of animal studies used females when investigating these diseases, and this is particularly important in preclinical drug trails since 8 of the prescription drugs withdrawn by the food and drug administration during the period of 1997-2000, where found to have greater adverse effects in woman than men[449–453]. Traditionally, the main reason female mice are not commonly used is because of a concern that the oestrous cycle would affect the variability of results[451]. However, there is evidence to show that a range of biomedical parameters including pain, behaviour (strain-dependent) and food intake have demonstrated a similar level of variability in

results carried out in female mice across the oestrous cycle, to those seen in male mice [438,439,454–456]. For the majority of studies, where possible, experiments have been carried out in both males and females to try to account for any differences caused as a result of sexual dimorphism in the immune response. With regards to atherosclerosis, female *ApoE*$^{-/-}$ mice spontaneously have smaller atherosclerotic lesions compared to males, and that is also true on atherogenic diets[457,458]. The evidence for such differences in lesion size are thought to be accounted for by oestrogen playing an atheroprotective role in female mice[457–459]. Since the mice could only be placed in social isolation and on the Western diet for a 4-week period due to restrictions on the Home Office Project License, the decision was made to only use male mice. Therefore, the findings with regards to no difference in lesion size, most likely would only hold true in the male population, particularly as premenopausal female humans, like mice, are thought to benefit from protection against CVD[460–462].

A key finding was that in a similar manner to loneliness which induces a unique transcriptional fingerprint expression known as the CTRA in whole blood, it was demonstrated for the first time that just 2 weeks of social isolation was enough to generate a unique transcriptional fingerprint in the blood, with 36 genes being differentially expressed[325]. Additionally, in genome wide analysis studies, loci have been identified both for loneliness and social interaction, suggesting that our findings are likely to translate over into humans[196]. This unique transcriptional fingerprint, once validated in humans, has the potential to act as a biomarker for social isolation, and could potentially identify those individuals who are at increased risk of chronic inflammatory diseases as a result of social isolation but due to stigma, do not want to admit they feel this way. For example, in the Loneliness experiment, when the word ‘loneliness’ was not used, 30% of respondents moved from the ‘never’ feeling lonely to the ‘sometimes’ feeling lonely

category, suggesting a reluctance to admit feeling lonely. This reluctance to admit to loneliness was most prevalent in women rather than men, and decreased with increasing age[463]. If such individuals can be identified, preventative measures including pharmaceuticals could be used as well, as social interventions to potentially attenuate the increased risk of chronic disease seen in this population.

Interestingly, just 2 weeks of social isolation was found to profoundly alter the immune system, suggesting that even short periods of time might lead to clinically relevant changes in the immune response to infection. It was demonstrated at a molecular level that peritoneal macrophages have altered TLR signaling, that is primed for bacterial infections at the expense of viral infections. This was then confirmed using the viral mimic, poly (I:C), to induce viral sepsis and LPS and live *E.coli* to induce bacterial sepsis. Social isolation enhanced bacterial clearance in the live *E.coli* model of sepsis, and the mice were less sick than those mice in social housing. Both housing groups responded to poly (I:C) induced sepsis with a similar response. The social ecology theory of the immune system, states that this favoritism towards clearance of bacterial infections at the expense of a viral infection is probably an evolutionary response. Those people who are more socially integrated are more likely to get a viral infection than a bacterial infection, as they are most commonly spread from person to person, whilst the opposite is true of a person who is alone[464]. Lonely individuals also have a change in gene expression, including upregulation of IL-1β and IL-6 and downregulation of type I interferon genes, resulting in a gene expression profile that favours an immune response tailored to bacterial infections, as opposed to viral response[175]. Similarly, emerging evidence suggests that lonely people report more severe symptoms when challenged with rhinovirus, and lonely individuals have higher titers of Epstein-Barr virus

antibodies[188,465]. This shows that the models used in this thesis translate reasonably well into humans.

As described previously, sepsis has a proinflammatory and an anti-inflammatory phase[466]. The main issue with the *E.coli* model of sepsis is that it is carried out only over a 6-hour period and thus is only a model of the proinflammatory stage of sepsis[467]. However, during the anti-inflammatory phase, viruses such as herpes simplex are reactivated, and social isolation no longer confers a benefit[44]. Thus, it is possible that in the anti-inflammatory stage of sepsis, SI may have an equal or higher mortality rate than those individuals with larger social network sizes[153,325]. Our research would suggest that in the anti-inflammatory stage, equal mortality would occur, as social isolation did not appear to be beneficial after a poly (I:C) challenge.

The LPS model, as well as other TLR mimic models such as poly(I:C), are simple and very reproducible models, but are acute in nature. The main disadvantage of the LPS and poly (I:C) models as discussed in **Chapter 3**, is that they are both TLR mimics thus they cannot test the functional effects of the immune system e.g. phagocytosis, which in contrast is the main advantage of the *E.coli* model of sepsis (**Figure 3.2**). Aside from this the hemodynamic response differs compared to that seen in humans, and is considered to be highly dose dependent[468,469].

Another aspect that should be considered, particularly with regards to the bacterial models of sepsis, is that only one type of bacteria, *E.coli*, was injected to induce sepsis. In the clinical setting, whilst one type of bacteria might predominate, often multiple types of bacteria will lead to the induction of sepsis, thus our model of sepsis is perhaps a simplified one, but confers the benefit of no requirement for surgery[470]. The gold standard model of murine bacterial sepsis is known as the CLP model, and it addresses the need

for microbial diversity to be modelled without the need for high bacterial loads at one time. Sepsis in humans is normally the result of a septic focal point that over time, gradually builds up to a high bacterial load[468]. In brief, the CLP model is carried out by ligating the cecum directly below the ileocecal valve, which causes proinflammatory necrotic tissue to form. A needle is then used to perforate the cecum, allowing faecal material to leak into the peritoneal cavity and thus sepsis is induced[471]. Aside from the previously mentioned advantages conferred by the CLP model, it more closely models human sepsis progression in terms of hemodynamic and metabolic phases, as well as having both the hyper- and hypoinflammatory phases. Additionally, it has the advantage of a prolonged and lower cytokine release, which better mimics the human response and this is contrast to the high and rapid increase in cytokines seen in the LPS and poly (I:C) models[468]. Therefore, for the aforementioned reasons, the CLP model would have been ideally used as it mimics the human response to bacterial sepsis more closely. However, the CLP model is not perfect, as sepsis severity is dependent on the percentage of cecum that is ligated and thus the amount of necrosis that is induced[468,471].

Social isolation was shown to induce changes in the microbiota after just 2 weeks, and these differences in the phyla of bacteria seen between SI and SH mice give an indication of the potential changes that occur as a result of social isolation. However, for these findings to be more translationally viable, longer-term studies would need to be carried out to establish whether changes in the microbiota are long-lived, or if further changes occur over time. It is not clear how other behavioural factors that can occur as a result of social isolation, such as poor diet and sedentary lifestyle would influence the changes seen during social isolation, but most likely they would exacerbate the dysbiosis seen and contribute to making it even more proinflammatory[472–475]. To further complicate matters a lot of the diseases including diabetes and hypertension that are more common

in SI people, and even some of their treatments such as statins, are known to influence microbiota[476–478].

Whilst changes in the abundance of microbiota phyla is demonstrated in SI mice compared to SH mice and is useful for partially understanding the mechanisms underlying increased risk of chronic diseases, it is important to note that the changes in the abundance of certain phyla, and their potential associations with disease are based primarily on correlative studies, as opposed to single bacteria transfer studies into GFM[93]. Thus, it is not clear how the individual phylum shifts in the microbiota seen in SI mice would influence their risk of developing diseases, such as depression and RA. However, it would probably be more translationally relevant to measure small molecule production. For example, in SI mice compared to SH mice, a lower % of the firmicute phyla is seen in the faecal boli which is thought to be correlated with depression, thus it would be interesting to measure the small molecules butyrate, propionate and acetate as they have been implicated in depressive symptoms[90,288,479–481].

An issue with the atherosclerosis studies in particular, is that the mice were only SI for 4 weeks which is the equivalent of ~1.6-3.1 human years[424]. However, atherosclerosis builds up over decades so to truly understand the translational value of the findings much longer periods of social isolation would be needed, ideally with different time point studies being carried out to establish whether social isolation can accelerate the progression of the disease and the overall disease burden in the long-term[482]. Whilst SI mice appear to have increased necrosis in their atherosclerotic plaques a major flaw of all murine models of atherosclerosis is that atherosclerotic plaque rupture does not spontaneously occur, thus it is difficult to know whether differences in necrosis might lead to the higher incidence of cardiovascular events seen in the human population[417].

Despite the *ApoE*$^{-/-}$ model of atherosclerosis being a very commonly used model, it has some limitations that need to be considered[483]. Whilst mutations in *ApoE* are seen in humans, causing them to have hypercholesteremia, they are incredibly rare and even when present, the levels of plasma cholesterol (~300mg/DL - standard diet and ~1000mg/DL – Western diet) are not as high as that seen in the *ApoE*$^{-/-}$ mouse (400-500mg/DL)[483,484]. High levels of plasma cholesterol in people without FH are ≥240mg/DL, which is considerably lower than the plasma cholesterol concentrations seen in the *ApoE*$^{-/-}$ mouse[485]. Another aspect to consider, is that the majority of plasma cholesterol in *ApoE*$^{-/-}$ mice is carried by VLDL and chylomicrons particles, whereas it is mainly transported by LDL in humans[483]. Despite the differences in plasma cholesterol between the *ApoE*$^{-/-}$ mouse model and the majority of humans, this model is favoured as the lesion distribution is considered to be very similar to that of humans, where atherosclerotic plaques predominantly occur in the aortic root, carotid artery and aortic branches[483]. Thus, it is likely that the no difference in atherosclerotic plaque would also hold true in humans.

In conclusion, social isolation profoundly alters the physiology of mice to one that suggests enhanced thermogenesis is taking place. It was demonstrated that social isolation induced a unique transcriptional fingerprint in whole blood, that has the potential, given further validation, to be used as a marker of social isolation. The immune system is altered during social isolation to one that is primed towards bacterial infections, which was demonstrated by enhanced bacterial clearance during *E.coli* induced sepsis, whilst social isolation was neither beneficial or detrimental during viral infections. Social isolation did not appear to exacerbate atherosclerotic burden but did increase necrosis, suggesting that the plaques might be more prone to rupture. On the Western diet, it appears that social isolation might be protective against leptin resistance. This thesis has

demonstrated for the first time that even short periods of social isolation can have profound transcriptional, physiological and immunological effects upon the body. This has implications clinically, as if those people who meet the diagnostic criteria for social isolation can be identified sooner, preventative treatments can be put in place to potentially stop the development or exacerbation of chronic inflammatory diseases.

Table 8: Summary of Behavioural Phenotypes in SI Mice.

Study	Strain (Sex)	Age (Weeks)	Period of Social Isolation (Weeks)	Behavioural Tests	Results
Social Isolation Stress Induces Anxious-Depressive-Like Behavior and Alterations of Neuroplasticity-Related Genes in Adult Male Mice[434].	C57BL/6J (Male)	9	5	Open field test and tail suspension test	Higher locomotor activity and decreased time spent in open field. Reduced distance on open arms and higher immobility time in the tail suspension test. **Increased anxiety and depression**
Effect of post-weaning isolation on anxiety- and depressive-like behaviors of C57BL/6J mice[437]. ox	C57BL/6J (Male and Female)	3	5	Open field test and forced swim test	In both sexes, decreased time spent in open field and less distance travelled in the open field test. Females had decreased immobile time in the forced swim test whilst no difference in males. **Increased anxiety in both sexes and decreased depression in females**
HINT1 is involved in the behavioral abnormalities induced by social isolation rearing[486].	C57BL/6J (Male)	3	4	Open field test, forced swim test and elevated plus maze	No difference in locomotion on the open field test. Increased immobility on the forced swim test. No difference in duration spent or number of entries on the open arms. **Increased depression and no difference in anxiety**
The lonely mouse: Verification of a separation-induced model of	C57BL/6J (Female)	8	16	Light/dark box, forced swim test, tail suspension	Fewer transitions in the light/dark box. Increased immobility in the forced swim test. Increased bouts of immobility in the tail suspension test.

depression in female mice[435].				test, acoustic startle test	Lower startle response in the acoustic startle response test. **Increased depression and anxiety**
Long-term individual housing in C57BL/6J and DBA/2 mice: assessment of behavioral consequences[436].	C57BL/6J (Male) DBA/2 (Male)	4	7	Elevated plus maze, light/dark box, Y-maze, novelty-induced feeding suppression test and the forced swim test	**Note:** results given are seen in both strains. Entered open arms faster, had higher % of open arm entries, longer time in open arms and reduced latency to start grooming in the elevated plus maze. Higher spontaneous locomotor activity. Increased latency to enter central area, reduced number of central entries and increased faecal boli numbers in the light/dark box. Reduced habituation, longer latency to start grooming and shorter grooming period in the Y-maze. Number of approaches and latency to start eating in the novelty-induced feeding suppression test. Lower % immobility in the forced swim test. **Unclear anxiety (reduced=elevated plus maze but increased =** light**/dark box and novelty-induced feeding suppression test) and decreased depression**

6.2 Future Perspectives

An aspect that remains unanswered is whether the unique transcriptional fingerprint demonstrated in SI murine whole blood could be used as a biomarker of social isolation in humans. Initially, studies would need to be carried out to confirm the genes of interest at a protein level, using techniques such as Western blotting and flow cytometry. Confirmation of the genes found for social isolation would require a cohort of healthy people matching the diagnostic criteria for social isolation. Finding such a cohort might be difficult, since most of the people who would fit that criteria are likely to be elderly and suffer from chronic diseases which often require the use of anti-inflammatory drugs. Most of the genes found to be upregulated in whole blood during social isolation are associated with inflammation and apoptosis, which increase with age, which would be a confounding factor[487].

In order to confirm that SI mice can maintain their body temperature by increased calorie consumption to provide energy for increased thermogenesis, it would be pertinent to determine temperature using a more accurate and sensitive method to avoid small but potentially significant changes in temperature being missed. Ideally, the core temperature of the mouse would be assessed *via* the use of radiotelemetry probes to allow monitoring of the temperature of the mice over a prolonged period, and to minimise intervariablity between readings. However, the implantation of radiotelemetry probes requires the mice to undergo major surgery which in itself will cause stress on the mouse, and thus would be a confounding factor in the study[488]. Additionally, the thermal properties such as the level of insulation could be assessed for the artificial nest and bedding using thermal imaging to assess whether an increase in temperature can reverse the phenotype induced by social isolation[362]. In humans, changes in temperature as a result of social isolation could easily be reversed by increasing temperature by use of central heating or wrapping

up warm, thus it is not clear what, if any, effect temperature changes might have on the physiology of humans. Nonetheless it would be interesting to compare body temperature of SI people to those who have larger social networks to try and answer this question. Social exclusion has been shown to lower skin temperature, so it would be expected that social isolation would have a similar effect[489]. However, changes in temperature might not be seen as increased calorie intake as a result of increased food intake in SI mice might provide them with enough energy to maintain body temperature. Ideally, metabolism would be monitored in metabolic cages but the need to singly house mice makes it difficult to fairly compare SH mice with SI mice[490]. Additionally, there is evidence that metabolic cages can induce stress, which would be a confounding factor[331,332,490].

Another area that requires further investigation is whether or not social isolation is protective against leptin resistance in *ApoE*$^{-/-}$ mice on the Western diet, as SI mice had lower plasma leptin concentrations compared to SH mice. One possible way to assess this hypothesis would be to give both SH and SI *ApoE*$^{-/-}$ mice fed the Western diet, daily i.p. injections of leptin after the 4-week period for a further week to see whether suppression of food intake and weight gain in either of the two housing groups occurs. If SH mice do in fact have leptin resistance, their food intake would remain largely unchanged. Leptin mainly acts on the arcuate nucleus (ARC) in the hypothalamus to reduce energy uptake by suppressing the release of neuropeptide Y (NPY) and agouti-related peptide (AgRP), appetite stimulating hormones. Therefore, mRNA levels of NPY and AgRP should be assessed in the ARC, as a further way of determining whether leptin resistance is present[491]. SOCS3 is known to inhibit leptin signalling and it has been shown that mRNA of SOCS3 in the ARC is upregulated during leptin resistance[492]. This

suggests that SOCS3 should also be investigated in the ARC as a further indication of whether leptin resistance is present in SH mice.

There is increasing evidence to suggest that anxiety levels increase the progression of atherosclerosis, thus it would be particularly pertinent to carry out behavioural testing of the *ApoE*$^{-/-}$ mice in both housing groups particularly as there is a debate surrounding whether or not *ApoE*$^{-/-}$ mice have increased anxiety[493]. Some studies have found that *ApoE*$^{-/-}$ mice have increased anxiety as measured by increased time on the open arms of the elevated plus maze, whilst other studies have reported the opposite[494,495]. Additionally, one study has found that *ApoE*$^{-/-}$ mice have an increased startle response indicating increased anxiety[494]. Despite, the debate surrounding whether or not the *ApoE*$^{-/-}$ mice might suffer from increased anxiety, this model was used as opposed to the *LDLR*$^{-/-}$, another leading atherosclerosis model, because there is more literature exploring the behavioral phenotype of *ApoE*$^{-/-}$ mice, as it is also being investigated as a model for Alzheimer's disease[496]. It should be noted that *LDLR*$^{-/-}$ mice have been shown by use of sucrose preference test, splash test, and tail suspension test to exhibit depressive like behaviour compared to WT mice, and depression is also known to be a risk factor for heart disease[497–499]. The known literature for both models is summarised in **Table 9**. Therefore, ideally both the previous models of atherosclerosis would be tested to see which model has the least behavioural abnormalities that might confound the effect of social isolation on the development of atherosclerosis.

One of the main questions that remains unanswered is whether longer periods of social isolation would exacerbate atherosclerotic plaque. Ideally, the *ApoE*$^{-/-}$ mice would be placed in social isolation for at least 20 weeks whilst being fed the Western diet, as there is evidence to suggest that mice that are singly housed for 20 weeks have exacerbated

atherosclerosis in the innominate artery but not in the thoracic artery[398]. After 20 weeks *ApoE*$^{-/-}$ mice fed the Western diet are known to have fully developed atherosclerosis in the ascending aorta, thus studies lasting 20 weeks would be ideal to elucidate the effect of longer periods of social isolation[378]. It would also be pertinent to do a time point study to assess whether social isolation induces atherosclerosis at an earlier time point.

A possibility that has not been fully explored is whether social isolation affects plaque stability as opposed to atherosclerotic burden, which could account for the increased risk of MI as a result of social isolation and loneliness. Longer-term studies would be needed to elucidate any changes in plaque stability, as this would allow much larger atherosclerotic plaques to form. Assessment of plaque stability could be investigated initially by using Pico-Sirius red staining for collagen in a larger number of samples, and if changes were identified, MMP levels would also have to be assessed[415]. As changes were seen in necrosis, it would also be worth using the TUNEL stain for apoptosis on the atherosclerotic plaque as apoptosis, particularly of vascular smooth muscle cells is known to affect plaque vulnerability[500,501]. It would be also worth assessing galectin-3 by immunohistochemistry of the aortic sinuses in order to determine the macrophage content within the atherosclerotic plaque[502]. Since recent evidence suggests that neutrophil infiltration and release of histone H4 from their NETs promotes lytic cell death, and is positively correlated with atherosclerotic plaque vulnerability, it would be interesting to determine this by immunohistochemistry for $Ly6G^{+}$, neutrophil marker, and histone H4[503].

One area not explored within the studies carried out is the effect of social isolation on adaptive immunity. In fact, within this field this area has largely remained unexplored. Social isolation in a murine model of breast cancer was found to result in a decrease in

the number of $CD8^+$ T cells in the spleen and activated T cells[504]. Similarly, early life social isolation has been shown to decrease the ratio of helper to suppressor T cells in rhesus monkeys[505]. However, in a small study in humans subjected to solitary confinement, no differences in either T cell type, number or proliferation were detected[506]. As T cells interact with macrophages to allow recognition of oXLDL during atherosclerosis associated with social isolation, it would be interesting to explore how social isolation alters the adaptive immune system[13].

Table 9: Summary of Behavioural Phenotype in *ApoE*$^{-/-}$ and *LDLR*$^{-/-}$ Mice.

Study	Strain	Age (months)	Diet	Behavioural Test	Results
'apoE Isoforms and Measures of Anxiety in Probable AD Patients and Apoe$^{-/-}$ Mice'[494]	*ApoE*$^{-/-}$	6-8	Standard	Acoustic startle response and the elevated plus maze	Higher acoustic startle response; decreased time spent in open arms, reduced distance on open arms and decreased time spent going over edge of open arms. **Increased anxiety**
'Differences in Anxiety-Related Behavior between Apolipoprotein E-deficient C57BL/6 and Wild Type C57BL/6 Mice'[495]	*ApoE*$^{-/-}$	2-3	Standard	Elevated Plus Maze	Decreased anxiety on elevated plus maze – increased time in open arms with females visited open arms more often. **Decreased anxiety**
'Is there an association between hypercholesterolemia and depression? Behavioural evidence from the LDLr(-/-) mouse experimental model'[497]	*LDLR*$^{-/-}$	3	Standard	Sucrose preference test, splash test and tail suspension test	Lower sucrose preference; decreased grooming time in splash test and increased immobility in the tail suspension test. **Increased depression**
'Increased locomotor activity in mice lacking the low-density lipoprotein receptor'[507]	*LDLR*$^{-/-}$	3	Standard and high fat	Open field test, light/dark test and elevated plus maze	No difference in any of the tests or diet. **No anxiety phenotype**

Bibliography

1. Rittirsch D, Flierl MA, Ward PA. Harmful molecular mechanisms in sepsis. Nat Rev Immunol. 2008;8(10):776–87.
2. Vestweber D. How leukocytes cross the vascular endothelium. Nat Rev Immunol. 2015;15(11):692–704.
3. Sumagin R, Prizant H, Lomakina E, Waugh RE, Sarelius IH. LFA-1 and Mac-1 define characteristically different intralumenal crawling and emigration patterns for monocytes and neutrophils in situ. J Immunol. 2010;185(11):7057–66.
4. Golan SM, Thomas FWL, Bajmoczi SK, Shaw RM, Froio DEL, Yang JR, et al. Endothelial cell cortactin coordinates intercellular adhesion molecule-1 clustering and actin cytoskeleton remodeling during polymorphonuclear leukocyte adhesion and transmigration. J Immunol Ref. 2006;177(9):6440–9.
5. Muller WA. The role of PECAM-1 (CD31) in leukocyte emigration: studies in vitro and in vivo. J Leukoc Biol. 1995;57(4):523–8.
6. Nourshargh S, Alon R. Leukocyte Migration into Inflamed Tissues. Vol. 41, Immunity. 2014. p. 694–707.
7. Cai H, Harrison DG. Endothelial dysfunction in cardiovascular diseases: the role of oxidant stress. Circ Res. 2000;87(10):840–4.
8. Keaney JF, Vita JA. Atherosclerosis, oxidative stress, and antioxidant protection in endothelium-derived relaxing factor action. Prog Cardiovasc Dis. 1995;38(2):129–54.
9. Fichtlscherer S, Rosenberger G, Walter DH, Breuer S, Dimmeler S, Zeiher AM. Elevated C-reactive protein levels and impaired endothelial vasoreactivity in patients with coronary artery disease. Circulation. 2000;102(9):1000–6.
10. Haynes WG, Strachan FE, Webb DJ. Endothelin ET $_A$ and ET $_B$ Receptors Cause Vasoconstriction of Human Resistance and Capacitance Vessels In Vivo. Circulation. 1995;92(3):357–63.
11. Royall JA, Berkow RL, Beckman JS, Cunningham MK, Matalon S, Freeman BA. Tumor necrosis factor and interleukin 1 alpha increase vascular endothelial permeability. Am J Physiol Cell Mol Physiol. 1989;257(6):L399–410.
12. Rubio-Guerra AF, Vargas-Robles H, Serrano AM, Lozano-Nuevo JJ, Escalante-Acosta BA. Correlation between the levels of circulating adhesion molecules and

atherosclerosis in type-2 diabetic normotensive patients: Circulating adhesion molecules and atherosclerosis. Cell Adh Migr. 2009;34:369–72.

13. Mallat Z, Taleb S, Ait-Oufella H, Tedgui A. The role of adaptive T cell immunity in atherosclerosis. J Lipid Res. 2009;50 Suppl(Suppl):S364–S369.
14. Peiser L, Gordon S. The function of scavenger receptorsexpressed by macrophages and their rolein the regulation of inflammation. Microbes Infect. 2001;3(2):149–59.
15. Singer M, Deutschman CS, Seymour CW, Shankar-Hari M, Annane D, Bauer M, et al. The Third International Consensus Definitions for Sepsis and Septic Shock (Sepsis-3). JAMA. 2016;315(8):801–10.
16. The UK Sepsis Trust. WHAT IS SEPSIS? - UK Sepsis Trust [Internet].
17. Opal SM, Dellinger RP, Vincent J-L, Masur H, Angus DC. The next generation of sepsis clinical trial designs: what is next after the demise of recombinant human activated protein C? Crit Care Med. 2014;42(7):1714–21.
18. Vincent J-L, Rello J, Marshall J, Silva E, Anzueto A, Martin CD, et al. International study of the prevalence and outcomes of infection in intensive care units. JAMA. 2009;302(21):2323–9.
19. Vincent J-L, Sakr Y, Sprung CL, Ranieri VM, Reinhart K, Gerlach H, et al. Sepsis in European intensive care units: results of the SOAP study. Crit Care Med. 2006;34(2):344–53.
20. Angus DC, Linde-Zwirble WT, Lidicker J, Clermont G, Carcillo J, Pinsky MR. Epidemiology of severe sepsis in the United States: analysis of incidence, outcome, and associated costs of care. Crit Care Med. 2001;29(7):1303–10.
21. Martin GS, Mannino DM, Eaton S, Moss M. The Epidemiology of Sepsis in the United States from 1979 through 2000. N Engl J Med. 2003;348(16):1546–54.
22. Adrie C, Azoulay E, Francais A, Clec'h C, Darques L, Schwebel C, et al. Influence of gender on the outcome of severe sepsis: a reappraisal. Chest. 2007;132(6):1786–93.
23. Sakr Y, Elia C, Mascia L, Barberis B, Cardellino S, Livigni S, et al. The influence of gender on the epidemiology of and outcome from severe sepsis. Crit Care. 2013;17(2):R50.
24. Mayr FB, Yende S, Linde-Zwirble WT, Peck-Palmer OM, Barnato AE, Weissfeld LA, et al. Infection rate and acute organ dysfunction risk as explanations for racial differences in severe sepsis. JAMA. 2010;303(24):2495–

503.

25. Lorenz E, Mira JP, Frees KL, Schwartz DA. Relevance of Mutations in the TLR4 Receptor in Patients With Gram-Negative Septic Shock. Arch Intern Med. 2002;162(9):1028–32.
26. Majetschak M, Flohé S, Obertacke U, Schröder J, Staubach K, Nast-Kolb D, et al. Relation of a TNF gene polymorphism to severe sepsis in trauma patients. Ann Surg. 1999;230(2):207–14.
27. Stüber F, Petersen M, Bokelmann F, Schade U. A genomic polymorphism within the tumor necrosis factor locus influences plasma tumor necrosis factor-alpha concentrations and outcome of patients with severe sepsis. Crit Care Med. 1996;24(3):381–4.
28. Hotchkiss RS, Monneret G, Payen D. Sepsis-induced immunosuppression: from cellular dysfunctions to immunotherapy. Nat Rev Immunol. 2013;13(12):862–74.
29. Akira S, Takeda K. Toll-like receptor signalling. Nat Rev Immunol. 2004;4(7):499–511.
30. Kawai T, Takeuchi O, Fujita T, Inoue J, Mühlradt PF, Sato S, et al. Lipopolysaccharide stimulates the MyD88-independent pathway and results in activation of IFN-regulatory factor 3 and the expression of a subset of lipopolysaccharide-inducible genes. J Immunol. 2001;167(10):5887–94.
31. Tian B, Nowak DE, Brasier AR. A TNF-induced gene expression program under oscillatory NF-kappaB control. BMC Genomics. 2005;6(137).
32. Copeland S, Warren HS, Lowry SF, Calvano SE, Remick D. Acute inflammatory response to endotoxin in mice and humans. Clin Diagn Lab Immunol. 2005;12(1):60–7.
33. Varma TK, Lin CY, Toliver-Kinsky TE, Sherwood ER. Endotoxin-induced gamma interferon production: contributing cell types and key regulatory factors. Clin Diagn Lab Immunol. 2002;9(3):530–43.
34. Tressel SL, Kaneider NC, Kasuda S, Foley C, Koukos G, Austin K, et al. A matrix metalloprotease-PAR1 system regulates vascular integrity, systemic inflammation and death in sepsis. EMBO Mol Med. 2011;3(7):370–84.
35. Pawlinski R, Pedersen B, Schabbauer G, Tencati M, Holscher T, Boisvert W, et al. Role of tissue factor and protease-activated receptors in a mouse model of endotoxemia. Blood. 2003;103(4):1342–7.

36. Gould TJ, Vu TT, Swystun LL, Dwivedi DJ, Mai SHC, Weitz JI, et al. Neutrophil Extracellular Traps Promote Thrombin Generation Through Platelet-Dependent and Platelet-Independent Mechanisms. Arterioscler Thromb Vasc Biol. 2014;34(9):1977–84.
37. Czaikoski PG, Mota JMSC, Nascimento DC, Sônego F, Castanheira FV e S, Melo PH, et al. Neutrophil Extracellular Traps Induce Organ Damage during Experimental and Clinical Sepsis. Efron PA, editor. PLoS One. 2016;11(2):e0148142.
38. Cabioglu N, Bilgic S, Deniz G, Aktas E, Seyhun Y, Turna A, et al. Decreased cytokine expression in peripheral blood leukocytes of patients with severe sepsis. Arch Surg. 2002;137(9):1037–43.
39. Hotchkiss RS, Swanson PE, Freeman BD, Tinsley KW, Cobb JP, Matuschak GM, et al. Apoptotic cell death in patients with sepsis, shock, and multiple organ dysfunction. Crit Care Med. 1999;27(7):1230–51.
40. Hotchkiss RS, Tinsley KW, Swanson PE, Schmieg RE, Hui JJ, Chang KC, et al. Sepsis-induced apoptosis causes progressive profound depletion of B and CD4+ T lymphocytes in humans. J Immunol. 2001;166(11):6952–63.
41. Monneret Julien Bohe G, Bienvenu J, Lepape A, Fabienne Venet WS, Pachot A, Debard A-L, et al. Ligand-Dependent Mechanism Survival through a Fas/Fas Lipopolysaccharide-Induced Monocyte Lymphocytes Inhibit Regulatory T + CD25 + Human CD4 Human CD4 ⁄ CD25 ⁄ Regulatory T Lymphocytes Inhibit Lipopolysaccharide-Induced Monocyte Survival through a Fas/Fas Ligand-Dependent Mechanism 1. J Immunol J Immunol. 2006;177(177):6540–7.
42. Poehlmann H, Schefold JC, Zuckermann-Becker H, Volk H-D, Meisel C. Phenotype changes and impaired function of dendritic cell subsets in patients with sepsis: a prospective observational analysis. Crit Care. 2009;13(4):R119.
43. Weiterer S, Uhle F, Lichtenstern C, Siegler BH, Bhuju S, Jarek M, et al. Sepsis induces specific changes in histone modification patterns in human monocytes. PLoS One. 2015;10(3):e0121748.
44. Walton AH, Muenzer JT, Rasche D, Boomer JS, Sato B, Brownstein BH, et al. Reactivation of multiple viruses in patients with sepsis. PLoS One. 2014;9(2):e98819.
45. Drewry AM, Samra N, Skrupky LP, Fuller BM, Compton SM, Hotchkiss RS. Persistent lymphopenia after diagnosis of sepsis predicts mortality. Shock.

2014;42(5):383–91.

46. Yende S, D'Angelo G, Kellum J a., Weissfeld L, Fine J, Welch RD, et al. Inflammatory Markers at Hospital Discharge Predict Subsequent Mortality after Pneumonia and Sepsis. Am J Respir Crit Care Med. 2008;177(11):1242–7.
47. WHO. Cardiovascular diseases (CVDs) [Internet]. WHO. World Health Organization; 2017.
48. Libby P. Inflammation in atherosclerosis. Nature. 2002;420(6917):868–74.
49. George J, Rapsomaniki E, Pujades-Rodriguez M, Shah AD, Denaxas S, Herrett E, et al. How Does cardiovascular disease first present in women and men? Incidence of 12 cardiovascular diseases in a contemporary cohort of 1,937,360 people. Circulation. 2015;132(14):1320–8.
50. Nordestgaard BG, Chapman MJ, Humphries SE, Ginsberg HN, Masana L, Descamps OS, et al. Familial hypercholesterolaemia is underdiagnosed and undertreated in the general population: guidance for clinicians to prevent coronary heart disease: Consensus Statement of the European Atherosclerosis Society. Eur Heart J. 2013;34(45):3478–90.
51. Krogh HW, Mundal L, Holven KB, Retterstøl K. Patients with familial hypercholesterolaemia are characterized by presence of cardiovascular disease at the time of death. Eur Heart J. 2016;37(17):1398–405.
52. Haveman-Nies A, De Groot LPGM, Burema J, Amorim Cruz JA, Osler M, Van Staveren WA. Dietary quality and lifestyle factors in relation to 10-year mortality in older Europeans: The SENECA Study. Am J Epidemiol. 2002;156(10):962–8.
53. Coulter A. Lifestyles and social class: implications for primary care. J R Coll Gen Pract. 1987;37(305):533–6.
54. American Heart Association. American Heart Association 2020 Impact Goal [Internet]. 2013.
55. World Health Organisation. A global brief on HYPERTENSION [Internet]. 2013.
56. Manson JE, Hu FB, Rich-Edwards JW, Colditz GA, Stampfer MJ, Willett WC, et al. A Prospective Study of Walking as Compared with Vigorous Exercise in the Prevention of Coronary Heart Disease in Women. N Engl J Med. 1999;341(9):650–8.
57. Warren TY, Barry V, Hooker SP, Sui X, Church TS, Blair SN. Sedentary

behaviors increase risk of cardiovascular disease mortality in men. Med Sci Sports Exerc. 2010;42(5):879–85.

58. Hubert HB, Feinleib M, McNamara PM, Castelli WP. Obesity as an independent risk factor for cardiovascular disease: a 26-year follow-up of participants in the Framingham Heart Study. Circulation. 1983;67(5):968–77.
59. Guallar-Castillón P, Rodríguez-Artalejo F, Tormo MJ, Sánchez MJ, Rodríguez L, Quirós JR, et al. Major dietary patterns and risk of coronary heart disease in middle-aged persons from a Mediterranean country: The EPIC-Spain cohort study. Nutr Metab Cardiovasc Dis. 2012;22(3):192–9.
60. Chen Z, Peto R, Collins R, MacMahon S, Lu J, Li W. Serum cholesterol concentration and coronary heart disease in population with low cholesterol concentrations. BMJ. 1991;303(6797):276–82.
61. United States. Public Health Service. Office of the Surgeon General., United States. Office on Smoking and Health. The health consequences of smoking : a report of the Surgeon General. U.S. Dept. of Health and Human Services, Public Health Service, Office of the Surgeon General; 2004. 941 p.
62. Park C, Guallar E, Linton JA, Lee D-C, Jang Y, Son DK, et al. Fasting Glucose Level and the Risk of Incident Atherosclerotic Cardiovascular Diseases. Diabetes Care. 2013;36(7):1988–93.
63. Haffner SM, Lehto S, Rönnemaa T, Pyörälä K, Laakso M. Mortality from Coronary Heart Disease in Subjects with Type 2 Diabetes and in Nondiabetic Subjects with and without Prior Myocardial Infarction. N Engl J Med. 1998;339(4):229–34.
64. Zhang C. The role of inflammatory cytokines in endothelial dysfunction. Basic Res Cardiol. 2008;103(5):398–406.
65. Vink A, Schoneveld AH, van der Meer JJ, van Middelaar BJ, Sluijter JPG, Smeets MB, et al. In vivo evidence for a role of toll-like receptor 4 in the development of intimal lesions. Circulation. 2002;106(15):1985–90.
66. Carnevale R, Nocella C, Petrozza V, Cammisotto V, Pacini L, Sorrentino V, et al. Localization of lipopolysaccharide from Escherichia Coli into human atherosclerotic plaque. Sci Rep. 2018;8(1):3598.
67. Hurt E, Bondjers G, Camejo G. Interaction of LDL with human arterial proteoglycans stimulates its uptake by human monocyte-derived macrophages. J Lipid Res. 1990;31(3):443–54.

68. Lusis AJ. Atherosclerosis. Nature. 2000;407(6801):233–41.
69. Martorell J, Santomá P, Kolandaivelu K, Kolachalama VB, Melgar-Lesmes P, Molins JJ, et al. Extent of flow recirculation governs expression of atherosclerotic and thrombotic biomarkers in arterial bifurcations. Cardiovasc Res. 2014;103(1):37–46.
70. Sprague AH, Khalil RA. Inflammatory cytokines in vascular dysfunction and vascular disease. Biochem Pharmacol. 2009;78(6):539–52.
71. Hansson GK, Libby P. The immune response in atherosclerosis: a double-edged sword. Nat Rev Immunol. 2006;6(7):508–19.
72. Grundtman C, Kreutmayer SB, Almanzar G, Wick MC, Wick G. Heat shock protein 60 and immune inflammatory responses in atherosclerosis. Arterioscler Thromb Vasc Biol. 2011;31(5):960–8.
73. Tabas I, García-Cardeña G, Owens GK. Recent insights into the cellular biology of atherosclerosis. J Cell Biol. 2015;209(1):13–22.
74. Luttun A, Lutgens E, Manderveld A, Maris K, Collen D, Carmeliet P, et al. Loss of Matrix Metalloproteinase-9 or Matrix Metalloproteinase-12 Protects Apolipoprotein E-Deficient Mice Against Atherosclerotic Media Destruction but Differentially Affects Plaque Growth. Circulation. 2004;109(11):1408–14.
75. Loftus IM, Naylor AR, Goodall S, Crowther M, Jones L, Bell PR, et al. Increased matrix metalloproteinase-9 activity in unstable carotid plaques. A potential role in acute plaque disruption. Stroke. 2000;31(1):40–7.
76. Sukhova GK, Schönbeck U, Rabkin E, Schoen FJ, Poole AR, Billinghurst RC, et al. Evidence for increased collagenolysis by interstitial collagenases-1 and -3 in vulnerable human atheromatous plaques. Circulation. 1999;99(19):2503–9.
77. Sekirov I, Russell SL, Antunes LCM, Finlay BB. Gut microbiota in health and disease. Physiol Rev. 2010;90(3):859–904.
78. Kamada N, Seo S-U, Chen GY, Núñez G. Role of the gut microbiota in immunity and inflammatory disease. Nat Rev Immunol. 2013;13(5):321–35.
79. Kennedy EA, King KY, Baldridge MT. Mouse Microbiota Models: Comparing Germ-Free Mice and Antibiotics Treatment as Tools for Modifying Gut Bacteria. Front Physiol. 2018;9:1534.
80. Khosravi A, Yáñez A, Price JG, Chow A, Merad M, Goodridge HS, et al. Gut microbiota promote hematopoiesis to control bacterial infection. Cell Host Microbe. 2014;15:374–81.

81. Abramas GD, Bauer H, Sprinz H. Influence of the normal flora on mucosal morphology and cellular renewal in the ileum. A comparison of germ-free and conventional mice. Lab Invest. 1963;12:355–64.
82. Johansson MEV, Phillipson M, Petersson J, Velcich A, Holm L, Hansson GC. The inner of the two Muc2 mucin-dependent mucus layers in colon is devoid of bacteria. Proc Natl Acad Sci U S A. 2008;105(39):15064–9.
83. De Vadder F, Grasset E, Holm LM, Karsenty G, Macpherson AJ, Olofsson LE, et al. Gut microbiota regulates maturation of the adult enteric nervous system via enteric serotonin networks. Proc Natl Acad Sci U S A. 2018;115(25):6458–63.
84. Ganal SC, Sanos SL, Kallfass C, Oberle K, Johner C, Kirschning C, et al. Priming of Natural Killer Cells by Nonmucosal Mononuclear Phagocytes Requires Instructive Signals from Commensal Microbiota. Immunity. 2012;37(1):171–86.
85. Keighley MR, Arabi Y, Dimock F, Burdon DW, Allan RN, Alexander-Williams J. Influence of inflammatory bowel disease on intestinal microflora. Gut. 1978;19(12):1099–104.
86. Putignani L, Del Chierico F, Vernocchi P, Cicala M, Cucchiara S, Dallapiccola B, et al. Gut Microbiota Dysbiosis as Risk and Premorbid Factors of IBD and IBS Along the Childhood–Adulthood Transition. Inflamm Bowel Dis. 2016;22(2):487–504.
87. Turnbaugh PJ, Hamady M, Yatsunenko T, Cantarel BL, Duncan A, Ley RE, et al. A core gut microbiome in obese and lean twins. Nature. 2009;457(7228):480–4.
88. Lambeth SM, Carson T, Lowe J, Ramaraj T, Leff JW, Luo L, et al. Composition, Diversity and Abundance of Gut Microbiome in Prediabetes and Type 2 Diabetes. J diabetes Obes. 2015;2(3):1–7.
89. Brandsma E, Kloosterhuis NJ, Koster M, Dekker DC, Gijbels MJJ, van der Velden S, et al. A Proinflammatory Gut Microbiota Increases Systemic Inflammation and Accelerates Atherosclerosis. Circ Res. 2019;124(1):94–100.
90. Jiang H, Ling Z, Zhang Y, Mao H, Ma Z, Yin Y, et al. Altered fecal microbiota composition in patients with major depressive disorder. Brain Behav Immun. 2015;48:186-194.
91. Jiang H, Zhang X, Yu Z, Zhang Z, Deng M, Zhao J, et al. Altered gut microbiota profile in patients with generalized anxiety disorder. J Psychiatr Res.

2018;104:130–6.

92. Pyndt Jørgensen B, Hansen JT, Krych L, Larsen C, Klein AB, Nielsen DS, et al. A Possible Link between Food and Mood: Dietary Impact on Gut Microbiota and Behavior in BALB/c Mice. Bereswill S, editor. PLoS One. 2014;9(8):e103398.
93. Fischbach MA. Microbiome: Focus on causation and mechanism HHS Public Access. Cell. 2018;174(4):785–90.
94. Zhu W, Gregory JC, Org E, Buffa JA, Gupta N, Wang Z, et al. Gut Microbial Metabolite TMAO Enhances Platelet Hyperreactivity and Thrombosis Risk. Cell. 2016;165(1):111–24.
95. Gregory JC, Buffa JA, Org E, Wang Z, Levison BS, Zhu W, et al. Transmission of atherosclerosis susceptibility with gut microbial transplantation. J Biol Chem. 2015;290(9):5647–60.
96. Gronbach K, Flade I, Holst O, Lindner B, Ruscheweyh HJ, Wittmann A, et al. Endotoxicity of Lipopolysaccharide as a Determinant of T-Cell−Mediated Colitis Induction in Mice. Gastroenterology. 2014;146(3):765–75.
97. Wang H, Wei C-X, Min L, Zhu L-Y. Good or bad: gut bacteria in human health and diseases. Biotechnol Biotechnol Equip. 2018;32(5):1075–80.
98. Anderson CJ, Kendall MM. Salmonella enterica Serovar Typhimurium Strategies for Host Adaptation. Front Microbiol. 2017;8:1983.
99. Rao S, Schieber AMP, O'Connor CP, Leblanc M, Michel D, Ayres JS. Pathogen-Mediated Inhibition of Anorexia Promotes Host Survival and Transmission. Cell. 2017;168(3):503-516.e12.
100. Lu J, Synowiec S, Lu L, Yu Y, Bretherick T, Takada S, et al. Microbiota influence the development of the brain and behaviors in C57BL/6J mice. Skoulakis EMC, editor. PLoS One. 2018;13(8):e0201829.
101. Klarer M, Arnold M, Günther L, Winter C, Langhans W, Meyer U. Gut vagal afferents differentially modulate innate anxiety and learned fear. J Neurosci. 2014;34(21):7067–76.
102. Bravo JA, Forsythe P, Chew M V., Escaravage E, Savignac HM, Dinan TG, et al. Ingestion of Lactobacillus strain regulates emotional behavior and central GABA receptor expression in a mouse via the vagus nerve. Proc Natl Acad Sci. 2011;108(38):16050–5.
103. Vanuytsel T, Van Wanrooy S, Vanheel H, Vanormelingen C, Verschueren S,

Houben E, et al. Psychological stress and corticotropin-releasing hormone increase intestinal permeability in humans by a mast cell-dependent mechanism. Gut. 2014;63:1293–9.

104. Keita å. v., Söderholm JD, Ericson A -c. Stress-induced barrier disruption of rat follicle-associated epithelium involves corticotropin-releasing hormone, acetylcholine, substance P, and mast cells. Neurogastroenterol Motil. 2010;22(7):770-e222.
105. Velin AK, Ericson A-C, Braaf Y, Wallon C, Söderholm JD. Increased antigen and bacterial uptake in follicle associated epithelium induced by chronic psychological stress in rats. Gut. 2004;53(4):494–500.
106. Maes M, Kubera M, Leunis J-C, Berk M. Increased IgA and IgM responses against gut commensals in chronic depression: Further evidence for increased bacterial translocation or leaky gut. J Affect Disord. 2012;141(1):55–62.
107. Lin H V., Frassetto A, Kowalik Jr EJ, Nawrocki AR, Lu MM, Kosinski JR, et al. Butyrate and Propionate Protect against Diet-Induced Obesity and Regulate Gut Hormones via Free Fatty Acid Receptor 3-Independent Mechanisms. Brennan L, editor. PLoS One. 2012;7(4):e35240.
108. Jeong M-Y, Jang H-M, Kim D-H. High-fat diet causes psychiatric disorders in mice by increasing Proteobacteria population. Neurosci Lett. 2019;698:51–7.
109. Yirmiya R, Rimmerman N, Reshef R. Depression as a Microglial Disease. 2015;
110. Ihara K, Yoshida H, Jones PB, Hashizume M, Suzuki Y, Ishijima H, et al. Serum BDNF levels before and after the development of mood disorders: a case–control study in a population cohort. Transl Psychiatry. 2016;6(4):e782–e782.
111. Koo JW, Russo SJ, Ferguson D, Nestler EJ, Duman RS. Nuclear factor- B is a critical mediator of stress-impaired neurogenesis and depressive behavior. Proc Natl Acad Sci. 2010;107(6):2669–74.
112. Dantzer R, O'Connor JC, Freund GG, Johnson RW, Kelley KW. From inflammation to sickness and depression: when the immune system subjugates the brain. Nat Rev Neurosci. 2008;9(1):46–56.
113. Dantzer R. Cytokine, sickness behavior, and depression. Immunol Allergy Clin North Am. 2009;29(2):247–64.
114. van Dam A-M, Brouns M, Louisse S, Berkenbosch F. Appearance of interleukin-1 in macrophages and in ramified microglia in the brain of endotoxin-treated rats: a pathway for the induction of non-specific symptoms of

sickness? Brain Res. 1992;588(2):291–6.

115. Knoll JG, Krasnow SM, Marks DL. Interleukin-1β signaling in fenestrated capillaries is sufficient to trigger sickness responses in mice. J Neuroinflammation. 2017;14(1):219.
116. Wang A, Huen SC, Luan HH, Yu S, Zhang C, Gallezot J-D, et al. Opposing Effects of Fasting Metabolism on Tissue Tolerance in Bacterial and Viral Inflammation. Cell. 2016;166(6):1512-1525.e12.
117. Carney RM, Blumenthal JA, Stein PK, Watkins L, Catellier D, Berkman LF, et al. Depression, Heart Rate Variability, and Acute Myocardial Infarction. Circulation. 2001;104(17):2024–8.
118. Valtorta NK, Kanaan M, Gilbody S, Ronzi S, Hanratty B. Loneliness and social isolation as risk factors for coronary heart disease and stroke: systematic review and meta-analysis of longitudinal observational studies. Heart. 2016;102(13):1009–16.
119. Steptoe A, Shankar A, Demakakos P, Wardle J. Social isolation, loneliness, and all-cause mortality in older men and women. Proc Natl Acad Sci U S A. 2013;110(15):5797–801.
120. Holt-Lunstad J, Smith TB. Loneliness and social isolation as risk factors for CVD: implications for evidence-based patient care and scientific inquiry. Heart. 2016;102(13):978–90.
121. Moeller AH, Foerster S, Wilson ML, Pusey AE, Hahn BH, Ochman H. Social behavior shapes the chimpanzee pan-microbiome. Sci Adv. 2016;2(1):e1500997.
122. Raulo A, Ruokolainen L, Lane A, Amato K, Knight R, Leigh S, et al. Social behaviour and gut microbiota in red-bellied lemurs (*Eulemur rubriventer*): In search of the role of immunity in the evolution of sociality. Dussutour A, editor. J Anim Ecol. 2018;87(2):388–99.
123. Tung J, Barreiro LB, Burns MB, Grenier J-C, Lynch J, Grieneisen LE, et al. Social networks predict gut microbiome composition in wild baboons. Elife. 2015;4.
124. Dill-McFarland KA, Tang Z-Z, Kemis JH, Kerby RL, Chen G, Palloni A, et al. Close social relationships correlate with human gut microbiota composition. Sci Rep. 2019;9(1):703.
125. Dunphy-Doherty F, O'Mahony SM, Peterson VL, O'Sullivan O, Crispie F, Cotter PD, et al. Post-weaning social isolation of rats leads to long-term

disruption of the gut microbiota-immune-brain axis. Brain Behav Immun. 2018;68:261–73.

126. Sgritta M, Dooling SW, Buffington SA, Momin EN, Francis MB, Britton RA, et al. Mechanisms Underlying Microbial-Mediated Changes in Social Behavior in Mouse Models of Autism Spectrum Disorder. Neuron. 2019;101(2):246-259.e6.
127. Frost TF, Wilson HG. Effects of locus of control and A-B personality type on job satisfaction within the health care field. Psychol Rep. 1983;53:399–405.
128. Denollet J. Personality and risk of cancer in men with coronary heart disease. Psychol Med. 1998;28:991–8.
129. Denollet J. DS14: Standard assessment of negative affectivity, social inhibition, and type D personality. Psychosom Med. 2005;67:89–97.
130. Kupper N, Gidron Y, Winter J, Denollet J. Association Between Type D Personality, Depression, and Oxidative Stress in Patients With Chronic Heart Failure. Psychosom Med. 2009;71(9):973–80.
131. Boehm JK, Williams DR, Rimm EB, Ryff C, Kubzansky LD. Association between optimism and serum antioxidants in the midlife in the United States study. Psychosom Med. 2013;75(1):2–10.
132. Lim S-A, Cheong K-J. Regular Yoga Practice Improves Antioxidant Status, Immune Function, and Stress Hormone Releases in Young Healthy People: A Randomized, Double-Blind, Controlled Pilot Study. J Altern Complement Med. 2015;21(9):530–8.
133. Kim D-H, Moon Y-S, Kim H-S, Jung J-S, Park H-M, Suh H-W, et al. Effect of Zen Meditation on serum nitric oxide activity and lipid peroxidation. Prog Neuro-Psychopharmacology Biol Psychiatry. 2005;29(2):327–31.
134. Hegde S V, Adhikari P, Kotian S, Pinto VJ, D'Souza S, D'Souza V. Effect of 3-month yoga on oxidative stress in type 2 diabetes with or without complications: a controlled clinical trial. Diabetes Care. 2011;34(10):2208–10.
135. Najjar S, Pearlman DM, Alper K, Najjar A, Devinsky O. Neuroinflammation and psychiatric illness. J Neuroinflammation. 2013;10(43).
136. Howren MB, Lamkin DM, Suls J. Associations of Depression With C-Reactive Protein, IL-1, and IL-6: A Meta-Analysis. Psychosom Med. 2009;71(2):171–86.
137. Tuglu C, Kara SH, Caliyurt O, Vardar E, Abay E. Increased serum tumor necrosis factor-alpha levels and treatment response in major depressive disorder. Psychopharmacology (Berl). 2003;170(4):429–33.

138. Baek S-E, Lee G-J, Rhee C-K, Rho D-Y, Kim D-H, Huh S, et al. Decreased Total Antioxidant Activity in Major Depressive Disorder Patients Non-Responsive to Antidepressant Treatment. Psychiatry Investig. 2016;13(2):222–6.
139. Kim Y-K, Paik J-W, Lee S-W, Yoon D, Han C, Lee B-H. Increased plasma nitric oxide level associated with suicide attempt in depressive patients. Prog Neuro-Psychopharmacology Biol Psychiatry. 2006;30(6):1091–6.
140. Lee B-H, Lee S-W, Yoon D, Lee H-J, Yang J-C, Shim S-H, et al. Increased plasma nitric oxide metabolites in suicide attempters. Neuropsychobiology. 2006;53(3):127–32.
141. Sommershof A, Aichinger H, Engler H, Adenauer H, Catani C, Boneberg E-M, et al. Substantial reduction of naïve and regulatory T cells following traumatic stress. Brain Behav Immun. 2009;23(8):1117–24.
142. von Känel R, Hepp U, Kraemer B, Traber R, Keel M, Mica L, et al. Evidence for low-grade systemic proinflammatory activity in patients with posttraumatic stress disorder. J Psychiatr Res. 2007;41(9):744–52.
143. Zhou J, Nagarkatti P, Zhong Y, Ginsberg JP, Singh NP, Zhang J, et al. Dysregulation in microRNA expression is associated with alterations in immune functions in combat veterans with post-traumatic stress disorder. PLoS One. 2014;9(4):e94075.
144. Arranz L, Guayerbas N, Fuente MD la. Impairment of several immune functions in anxious women. J Psychosom Res. 2007;62(1):1–8.
145. Chan A, Raman P, Ma S, Malhotra R. Loneliness and all-cause mortality in community-dwelling elderly Singaporeans. Demogr Res. 2015;32:1361–82.
146. Holt-Lunstad J, Smith TB, Layton JB. Social Relationships and Mortality Risk: A Meta-analytic Review. Brayne C, editor. PLoS Med. 2010;7(7):e1000316.
147. Wilson RS, Krueger KR, Arnold SE, Schneider JA, Kelly JF, Barnes LL, et al. Loneliness and Risk of Alzheimer Disease. Arch Gen Psychiatry. 2007;64(2):234–40.
148. Ge L, Yap CW, Ong R, Heng BH. Social isolation, loneliness and their relationships with depressive symptoms: A population-based study. PLoS One. 2017;12(8):e0182145.
149. Gan Y, Gong Y, Tong X, Sun H, Cong Y, Dong X, et al. Depression and the risk of coronary heart disease: a meta-analysis of prospective cohort studies. BMC Psychiatry. 2014;14(371).

150. Perissinotto CM, Stijacic Cenzer I, Covinsky KE. Loneliness in older persons: A predictor of functional decline and death. Arch Intern Med. 2012;172(14):1078–83.
151. Richard A, Rohrmann S, Vandeleur CL, Schmid M, Barth J, Eichholzer M. Loneliness is adversely associated with physical and mental health and lifestyle factors: Results from a Swiss national survey. PLoS One. 2017;12(7):1–18.
152. Whisman MA. Loneliness and the metabolic syndrome in a population-based sample of middle-aged and older adults. Heal Psychol. 2010;29(5):550–4.
153. Snyder-Mackler N, Sanz J, Kohn JN, Brinkworth JF, Morrow S, Shaver AO, et al. Social status alters immune regulation and response to infection in macaques. Science (80-). 2016;354(6315):1041–5.
154. Sztainberg Y, Chen A. An environmental enrichment model for mice. Nat Protoc. 2010;5(9):1535–9.
155. Brod S, Gobbetti T, Gittens B, Ono M, Perretti M, D'Acquisto F. The impact of environmental enrichment on the murine inflammatory immune response. JCI Insight. 2017;2(7):e90723.
156. Pusic KM, Pusic AD, Kraig RP. Environmental Enrichment Stimulates Immune Cell Secretion of Exosomes that Promote CNS Myelination and May Regulate Inflammation. Cell Mol Neurobiol. 2016;36(3):313–25.
157. Xu H, Gelyana E, Rajsombath M, Yang T, Li S, Selkoe D. Environmental Enrichment Potently Prevents Microglia-Mediated Neuroinflammation by Human Amyloid β-Protein Oligomers. J Neurosci. 2016;36(35):9041–56.
158. Cole SW, Hawkley LC, Arevalo JM, Sung CY, Rose RM, Cacioppo JT, et al. Social regulation of gene expression in human leukocytes. Genome Biol. 2007;8(9).
159. Cole SW, Capitanio JP, Chun K, Arevalo JMG, Ma J, Cacioppo JT. Myeloid differentiation architecture of leukocyte transcriptome dynamics in perceived social isolation. Proc Natl Acad Sci. 2015;112(49):15142–7.
160. Jo Cox Comission. Combatting loneliness one conversation at a time a call to action [Internet]. 2017.
161. EU. Loneliness-an unequally shared burden in Europe* Policy Context The prevalence of loneliness in Europe [Internet]. 2018.
162. Australian Psychology Society. Australian Loneliness Report - A survey exploring the loneliness levels of Australians and the impact on their health and

wellbeing [Internet]. 2018.

163. New Zealand Government M of SD. The Social Report 2016 Te pūrongo oranga tangata [Internet]. 2016.
164. Lee EE, Depp C, Palmer BW, Glorioso D, Daly R, Liu J, et al. High prevalence and adverse health effects of loneliness in community-dwelling adults across the lifespan: role of wisdom as a protective factor. 2018;
165. Dijulio B, Hamel L, Muñana C, Brodie M. Loneliness and Social Isolation in the United States, the United Kingdom, and Japan: An International Survey [Internet]. 2018.
166. Holt-Lunstad J, Smith TB, Baker M, Harris T, Stephenson D. Loneliness and Social Isolation as Risk Factors for Mortality: A Meta-Analytic Review. Perspect Psychol Sci. 2015;10(2):227–37.
167. Hammond C. BBC Radio 4 - The Anatomy of Loneliness - Who feels lonely? The results of the world's largest loneliness study [Internet]. 2018.
168. Ferreira-Alves J, Magalhães P, Viola L, Simoes R. Loneliness in middle and old age: Demographics, perceived health, and social satisfaction as predictors. Arch Gerontol Geriatr. 2014;59(3):613–23.
169. Savikko N, Routasalo P, Tilvis RS, Strandberg TE, Pitkälä KH. Predictors and subjective causes of loneliness in an aged population. Arch Gerontol Geriatr. 2005;41(3):223–33.
170. Routasalo PE, Savikko N, Tilvis RS, Strandberg TE, Pitkälä KH. Social contacts and their relationship to loneliness among aged people - A population-based study. Gerontology. 2006;52(3):181–7.
171. Chalise HN, Kai I, Saito T. Social Support and its Correlation with Loneliness: A Cross-Cultural Study of Nepalese Older Adults. Int J Aging Hum Dev. 2010;71(2):115–36.
172. Russell D, Peplau LA, Cutrona CE. The revised UCLA Loneliness Scale: Concurrent and discriminant validity evidence. J Pers Soc Psychol. 1980;39(3):472–80.
173. Oshagan H, Allen RL. Three Loneliness Scales: An Assessment of Their Measurement Properties. J Pers Assess. 1992;59(2):390–409.
174. Zavaleta D, Samuel K, Mills CT. Measures of Social Isolation. Soc Indic Res. 2017;131(1):367–91.
175. Cole SW, Levine ME, Arevalo JMG, Ma J, Weir DR, Crimmins EM, et al.

Loneliness, eudaimonia, and the human conserved transcriptional response to adversity. Psychoneuroendocrinology. 2015;62:11–7.

176. Valtorta NK, Kanaan M, Gilbody S, Hanratty B. Loneliness, social isolation and risk of cardiovascular disease in the English Longitudinal Study of Ageing. Eur J Prev Cardiol. 2018;0(00):1–10.
177. Brinkhues S, Dukers-Muijrers NHTM, Hoebe CJPA, van der Kallen CJH, Dagnelie PC, Koster A, et al. Socially isolated individuals are more prone to have newly diagnosed and prevalent type 2 diabetes mellitus - the Maastricht study –. BMC Public Health. 2017;17(1):955.
178. Valtorta NK, Kanaan M, Gilbody S, Ronzi S, Hanratty B. Loneliness and social isolation as risk factors for coronary heart disease and stroke: systematic review and meta-analysis of longitudinal observational studies. Heart. 2016;102(13):1009–16.
179. Sun M, Choi EY, Magee DJ, Stets CW, During MJ, Lin E-JD, et al. Metabolic Effects of Social Isolation in Adult C57BL/6 Mice. Int Sch Res Not. 2014;2014:1–9.
180. Jaremka LM, Fagundes CP, Peng J, Belury MA, Andridge RR, Malarkey WB, et al. Loneliness predicts postprandial ghrelin and hunger in women. Horm Behav. 2015;70:57–63.
181. Ein-Dor T, Coan JA, Reizer A, Gross EB, Dahan D, Wegener MA, et al. Sugarcoated isolation: evidence that social avoidance is linked to higher basal glucose levels and higher consumption of glucose. Front Psychol. 2015;6:492.
182. Sun M, Choi EY, Magee DJ, Stets CW, During MJ, Lin E-JD, et al. Metabolic Effects of Social Isolation in Adult C57BL/6 Mice. Int Sch Res Not. 2014;2014:1–9.
183. Schiavone S, Camerino GM, Mhillaj E, Zotti M, Colaianna M, De Giorgi A, et al. Visceral Fat Dysfunctions in the Rat Social Isolation Model of Psychosis. Front Pharmacol. 2017;8:787.
184. Hackett RA, Hamer M, Endrighi R, Brydon L, Steptoe A. Loneliness and stress-related inflammatory and neuroendocrine responses in older men and women. Psychoneuroendocrinology. 2012;37:1801–9.
185. Corsi-Zuelli F, Fachim HA, Loureiro CM, Shuhama R, Bertozi G, Joca SRL, et al. Prolonged Periods of Social Isolation From Weaning Reduce the Anti-inflammatory Cytokine IL-10 in Blood and Brain. Front Neurosci.

2019;12:1011.

186. Dixon D, Cruess S, Kilbourn K, Klimas N, Fletcher MA, Ironson G, et al. Social Support Mediates Loneliness and Human Herpesvirus Type 6 (HHV-6) Antibody Titers. J Appl Soc Psychol. 2001;31(6):1111–32.
187. Yang YC, McClintock MK, Kozloski M, Li T. Social isolation and adult mortality: the role of chronic inflammation and sex differences. J Health Soc Behav. 2013;54(2):183–203.
188. Glaser R, Kiecolt-Glaser JK, Speicher CE, Holliday JE. Stress, loneliness, and changes in herpesvirus latency. J Behav Med. 1985;8(3):249–60.
189. Pressman SD, Cohen S, Miller GE, Barkin A, Rabin BS, Treanor JJ. Loneliness, Social Network Size, and Immune Response to Influenza Vaccination in College Freshmen. Heal Psychol. 2005;24(3):297–306.
190. Bervoets L, Van Hoorenbeeck K, Kortleven I, Van Noten C, Hens N, Vael C, et al. Differences in gut microbiota composition between obese and lean children: A cross-sectional study. Gut Pathog. 2013;5(1).
191. Valles-Colomer M, Falony G, Darzi Y, Tigchelaar EF, Wang J, Tito RY, et al. The neuroactive potential of the human gut microbiota in quality of life and depression. Nat Microbiol. 2019;1.
192. Taylor AM, Thompson S V., Edwards CG, Musaad SMA, Khan NA, Holscher HD. Associations among diet, the gastrointestinal microbiota, and negative emotional states in adults. Nutr Neurosci. 2019;1–10.
193. Hemmings SMJ, Malan-Müller S, van den Heuvel LL, Demmitt BA, Stanislawski MA, Smith DG, et al. The Microbiome in Posttraumatic Stress Disorder and Trauma-Exposed Controls. Psychosom Med. 2017;79(8):936–46.
194. Le Chatelier E, Nielsen T, Qin J, Prifti E, Hildebrand F, Falony G, et al. Richness of human gut microbiome correlates with metabolic markers. Nature. 2013;500(7464):541–6.
195. Brod S, Gobbetti T, Gittens B, Ono M, Perretti M, D'Acquisto F. The impact of environmental enrichment on the murine inflammatory immune response. JCI insight. 2017;2(7):e90723.
196. Day FR, Ong KK, Perry JRB. Elucidating the genetic basis of social interaction and isolation. Nat Commun. 2018;9(1):2457.
197. Liu J, Dietz K, DeLoyht JM, Pedre X, Kelkar D, Kaur J, et al. Impaired adult myelination in the prefrontal cortex of socially isolated mice. Nat Neurosci.

2012;15(12):1621–3.

198. Takahashi T, Shimizu K, Shimazaki K, Toda H, Nibuya M. Environmental enrichment enhances autophagy signaling in the rat hippocampus. Brain Res. 2014;1592:113–23.
199. Lozupone C, Knight R. UniFrac: A new phylogenetic method for comparing microbial communities. Appl Environ Microbiol. 2005;71:8228–35.
200. Oksanen J, Blanchet FG, Roeland K, Pierre L, Simpson G, Peter S, et al. vegan-package: Community Ecology Package: Ordination, Diversity and... in vegan: Community Ecology Package [Internet].
201. Culhane AC, Thioulouse J, Perrière G, Higgins DG. MADE4: An R package for multivariate analysis of gene expression data. Bioinformatics. 2005;21.
202. Bai XH, Fischer S, Keshavjee S, Liu M. Heparin interference with reverse transcriptase polymerase chain reaction of RNA extracted from lungs after ischemia-reperfusion. Transpl Int. 2000;13(2):146–50.
203. Panduro A, Rivera-Iñiguez I, Sepulveda-Villegas M, Roman S. Genes, emotions and gut microbiota: The next frontier for the gastroenterologist. World J Gastroenterol. 2017;23(17):3030–42.
204. Kelsen JR, Wu GD. The gut microbiota, environment and diseases of modern society. Gut Microbes. 2012;3(4):374–82.
205. Wagner J, Damaschke N, Yang B, Truong M, Guenther C, McCormick J, et al. Overexpression of the novel senescence marker β-galactosidase (GLB1) in prostate cancer predicts reduced PSA recurrence. PLoS One. 2015;10(4).
206. Liu J, Miwa T, Hilliard B, Chen Y, Lambris JD, Wells AD, et al. The complement inhibitory protein DAF (CD55) suppresses T cell immunity in vivo. J Exp Med. 2005;201(4):567–77.
207. Wang Y, Li Y, Dalle Lucca SL, Simovic M, Tsokos GC, Dalle Lucca JJ, et al. Decay accelerating factor (CD55) protects neuronal cells from chemical hypoxia-induced injury. J Neuroinflammation. 2010;7(1):24.
208. Oh SJ, Kim JH, Chung DH. NOD2-mediated suppression of CD55 on neutrophils enhances C5a generation during polymicrobial sepsis. PLoS Pathog. 2013;9(5):e1003351.
209. Subramanian Vignesh K, Landero Figueroa JA, Porollo A, Divanovic S, Caruso JA, Deepe GS. IL-4 Induces Metallothionein 3- and SLC30A4-Dependent Increase in Intracellular Zn 2+ that Promotes Pathogen Persistence in

Macrophages. Cell Rep. 2016;16(12):3232–46.

210. Yoshimura S, Gerondopoulos A, Linford A, Rigden DJ, Barr FA. Family-wide characterization of the DENN domain Rab GDP-GTP exchange factors. J Cell Biol. 2010;191(2):367–81.
211. Wang Y, Ledet RJ, Imberg-Kazdan K, Logan SK, Garabedian MJ. Dynein axonemal heavy chain 8 promotes androgen receptor activity and associates with prostate cancer progression. Oncotarget. 2016;7(31):49268–80.
212. Söhle J, Machuy N, Smailbegovic E, Holtzmann U, Grönniger E, Wenck H, et al. Identification of New Genes Involved in Human Adipogenesis and Fat Storage. PLoS One. 2012;7(2).
213. Li Y, Iglehart JD, Richardson AL, Wang ZC. The amplified cancer gene LAPTM4B promotes tumor growth and tolerance to stress through the induction of autophagy. Autophagy. 2012;8(2):273–4.
214. Yang H, Zhai G, Ji X, Xiong F, Su J, McNutt MA. Correlation of LAPTM4B polymorphisms with gallbladder carcinoma susceptibility in Chinese patients. Med Oncol. 2012;29(4):2809–13.
215. Liu Y, Zhang Q-Y, Qian N, Zhou R-L. Relationship between LAPTM4B gene polymorphism and susceptibility of gastric cancer. Ann Oncol. 2007;18(2):311–6.
216. Xu Y, Liu Y, Zhou R, Meng F, Gao Y, Yang S, et al. LAPTM4B polymorphisms is associated with ovarian cancer susceptibility and its prognosis. Jpn J Clin Oncol. 2012;42(5):413–9.
217. Li X, Kong X, Chen X, Zhang N, Jiang L, Ma T, et al. LAPTM4B allele *2 is associated with breast cancer susceptibility and prognosis. PLoS One. 2012;7(9):e44916.
218. Blom T, Li S, Dichlberger A, Bäck N, Kim YA, Loizides-Mangold U, et al. LAPTM4B facilitates late endosomal ceramide export to control cell death pathways. Nat Chem Biol. 2015;11(10):799–806.
219. Milkereit R, Persaud A, Vanoaica L, Guetg A, Verrey F, Rotin D. LAPTM4b recruits the LAT1-4F2hc Leu transporter to lysosomes and promotes mTORC1 activation. Nat Commun. 2015;6(1).
220. Ma J, Chen C, Barth AS, Cheadle C, Guan X, Gao L. Lysosome and cytoskeleton pathways are robustly enriched in the blood of septic patients: A meta-analysis of transcriptomic data. Vol. 2015, Mediators of Inflammation.

2015.

221. Sanders AR, Göring HHH, Duan J, Drigalenko EI, Moy W, Freda J, et al. Transcriptome study of differential expression in schizophrenia. Hum Mol Genet. 2013;22(24):5001–14.
222. Qi R, Gu J, Zhang Z, Yang K, Li B, Fan J, et al. Potent antitumor efficacy of XAF1 delivered by conditionally replicative adenovirus vector via caspase-independent apoptosis. Cancer Gene Ther. 2007;14(1):82–90.
223. Lee M-G, Han J, Jeong S-I, Her N-G, Lee J-H, Ha T-K, et al. XAF1 directs apoptotic switch of p53 signaling through activation of HIPK2 and ZNF313. Proc Natl Acad Sci U S A. 2014;111(43):15532–7.
224. Choo Z, Lin Koh RY, Wallis K, Wei Koh TJ, Kuick CH, Sobrado V, et al. XAF1 promotes neuroblastoma tumor suppression and is required for KIF1B-B-mediated apoptosis. Oncotarget. 2016;7(23):34229–39.
225. Xia Y, Novak R, Lewis J, Duckett CS, Phillips AC. Xaf1 can cooperate with TNFα in the induction of apoptosis, independently of interaction with XIAP. Mol Cell Biochem. 2006;286(1–2):67–76.
226. Rao SP, Sancho J, Campos-Rivera J, Boutin PM, Severy PB, Weeden T, et al. Human peripheral blood mononuclear cells exhibit heterogeneous CD52 expression levels and show differential sensitivity to alemtuzumab mediated cytolysis. PLoS One. 2012;7(6).
227. Poh K-W, Yeo J-F, Stohler CS, Ong W-Y. Comprehensive Gene Expression Profiling in the Prefrontal Cortex Links Immune Activation and Neutrophil Infiltration to Antinociception. J Neurosci. 2012;32(1):35–45.
228. Roychoudhuri R, Clever D, Li P, Wakabayashi Y, Quinn KM, Klebanoff CA, et al. BACH2 regulates CD8 + T cell differentiation by controlling access of AP-1 factors to enhancers. Nat Immunol. 2016;17(7):851–60.
229. Muto A, Ochiai K, Kimura Y, Itoh-Nakadai A, Calame KL, Ikebe D, et al. Bach2 represses plasma cell gene regulatory network in B cells to promote antibody class switch. EMBO J. 2010;29(23):4048–61.
230. Chen Z, Pittman EF, Romaguera J, Fayad L, Wang M, Neelapu SS, et al. Nuclear Translocation of B-Cell-Specific Transcription Factor, BACH2, Modulates ROS Mediated Cytotoxic Responses in Mantle Cell Lymphoma. PLoS One. 2013;8(8).
231. NCBI. Igkv10-96 immunoglobulin kappa variable 10-96 [Mus musculus (house

mouse)] [Internet].

232. Yang Y, Cao J, Shi Y. Identification and characterization of a gene encoding human LPGAT1, an endoplasmic reticulum-associated lysophosphatidylglycerol acyltransferase. J Biol Chem. 2004;279(53):55866–74.
233. Baier LJ, Traurig MT, Orczewska JI, Ortiz DJ, Bian L, Marinelarena AM, et al. Evidence for a role of LPGAT1 in influencing BMI and percent body fat in Native Americans. Obesity. 2013;21(1):193–202.
234. Lemaitre RN, Tanaka T, Tang W, Manichaikul A, Foy M, Kabagambe EK, et al. Genetic loci associated with plasma phospholipid N-3 fatty acids: A Meta-Analysis of Genome-Wide association studies from the charge consortium. PLoS Genet. 2011;7(7).
235. Ma C, Wang N, Detre C, Wang G, O'Keeffe M, Terhorst C. Receptor signaling lymphocyte-activation molecule family 1 (Slamf1) regulates membrane fusion and NADPH oxidase 2 (NOX2) activity by recruiting a Beclin-1/Vps34/ultraviolet radiation resistance-associated gene (UVRAG) complex. J Biol Chem. 2012;287(22):18359–65.
236. Gomi H, Mori K, Itohara S, Izumi T. Rab27b Is Expressed in a Wide Range of Exocytic Cells and Involved in the Delivery of Secretory Granules Near the Plasma Membrane. Mol Biol Cell. 2007;18(11):4377–86.
237. Singh RK, Furze RC, Birrell MA, Rankin SM, Hume AN, Seabra MC. A role for Rab27 in neutrophil chemotaxis and lung recruitment. BMC Cell Biol. 2014;15(39).
238. Ejlerskov P, Christensen DP, Beyaie D, Burritt JB, Paclet M-H, Gorlach A, et al. NADPH oxidase is internalized by clathrin-coated pits and localizes to a Rab27A/B GTPase-regulated secretory compartment in activated macrophages. J Biol Chem. 2012;287(7):4835–52.
239. Kurata M, Hirata M, Watabe S, Miyake M, Takahashi SY, Yamamoto Y. Expression, purification, and inhibitory activities of mouse cytotoxic T-lymphocyte antigen-2alpha. Protein Expr Purif. 2003;32(1):119–25.
240. Denizot F, Brunet J-F, Roustan P, Harper K, Suzan M, Luciani M-F, et al. Novel structures CTLA-2α and CTLA-2β expressed in mouse activated T cells and mast cells and homologous to cysteine proteinase proregions. Eur J Immunol. 1989;19(4):631–5.
241. Chen Z, Lund R, Aittokallio T, Kosonen M, Nevalainen O, Lahesmaa R.

Identification of novel IL-4/Stat6-regulated genes in T lymphocytes. J Immunol. 2003;171(7):3627–35.

242. Stankiewicz AM, Goscik J, Majewska A, Swiergiel AH, Juszczak GR. The Effect of Acute and Chronic Social Stress on the Hippocampal Transcriptome in Mice. PLoS One. 2015;10(11):e0142195.
243. Shi TT, Li G, Xiao HT. The Role of RhoJ in Endothelial Cell Biology and Tumor Pathology. Biomed Res Int. 2016;39(6):1606–11.
244. Renauer P, Coit P, Jeffries MA, Merrill JT, McCune WJ, Maksimowicz-McKinnon K, et al. DNA methylation patterns in naïve CD4+ T cells identify epigenetic susceptibility loci for malar rash and discoid rash in systemic lupus erythematosus. Lupus Sci Med. 2015;2(1).
245. Salas-Vidal E, Meijer AH, Cheng X, Spaink HP. Genomic annotation and expression analysis of the zebrafish Rho small GTPase family during development and bacterial infection. Genomics. 2005;86(1):25–37.
246. OMIM. * 616318 GLYCEROPHOSPHODIESTER PHOSPHODIESTERASE DOMAIN-CONTAINING PROTEIN 3; GDPD3 [Internet].
247. Kaji T, Hijikata A, Ishige A, Kitami T, Watanabe T, Ohara O, et al. CD4 memory T cells develop and acquire functional competence by sequential cognate interactions and stepwise gene regulation. Int Immunol. 2016;28(6):267–82.
248. Nonogaki K, Nozue K, Oka Y. Social Isolation Affects the Development of Obesity and Type 2 Diabetes in Mice. Endocrinology. 2007;148(10):4658–66.
249. Sun M, Choi EY, Magee DJ, Stets CW, During MJ, Lin E-JD. Metabolic Effects of Social Isolation in Adult C57BL/6 Mice. Int Sch Res Not. 2014;2014:1–9.
250. Bartolomucci A, Palanza P, Sacerdote P, Ceresini G, Chirieleison A, Panerai AE, et al. Individual housing induces altered immuno-endocrine responses to psychological stress in male mice. Psychoneuroendocrinology. 2003;28(4):540–58.
251. Harshaw C, Culligan JJ, Alberts JR. Sex differences in thermogenesis structure behavior and contact within huddles of infant mice. PLoS One. 2014;9(1):e87405.
252. Campbell LAD, Tkaczynski PJ, Lehmann J, Mouna M, Majolo B. Social thermoregulation as a potential mechanism linking sociality and fitness: Barbary macaques with more social partners form larger huddles. Sci Rep. 2018;8(6074).

253. Hess SE, Rohr S, Dufour BD, Gaskill BN, Pajor EA, Garner JP. Home improvement: C57BL/6J mice given more naturalistic nesting materials build better nests. J Am Assoc Lab Anim Sci. 2008;47(6):25–31.
254. Gordon CJ. Effect of cage bedding on temperature regulation and metabolism of group-housed female mice. Comp Med. 2004;54(1):63–8.
255. Klok MD, Jakobsdottir S, Drent ML. The role of leptin and ghrelin in the regulation of food intake and body weight in humans: a review. Obes Rev. 2007;8(1):21–34.
256. Maffei M, Halaas J, Ravussin E, Pratley RE, Lee GH, Zhang Y, et al. Leptin levels in human and rodent: measurement of plasma leptin and ob RNA in obese and weight-reduced subjects. Nat Med. 1995;1(11):1155–61.
257. Jaremka LM, Belury MA, Andridge RR, Malarkey WB, Glaser R, Christian L, et al. Interpersonal stressors predict ghrelin and leptin levels in women. Psychoneuroendocrinology. 2014;48:178–88.
258. Iio W, Takagi H, Ogawa Y, Tsukahara T, Chohnan S, Toyoda A. Effects of chronic social defeat stress on peripheral leptin and its hypothalamic actions. BMC Neurosci. 2014;15.
259. Ricci MR, Fried SK, Mittleman KD. Acute cold exposure decreases plasma leptin in women. Metabolism. 2000;49(4):421–3.
260. Ravussin Y, Xiao C, Gavrilova O, Reitman ML. Effect of Intermittent Cold Exposure on Brown Fat Activation, Obesity, and Energy Homeostasis in Mice. Aguila MB, editor. PLoS One. 2014;9(1):e85876.
261. Zhu W long, Jia T, Lian X, Wang Z kun. Effects of cold acclimation on body mass, serum leptin level, energy metabolism and thermognesis in Eothenomys miletus in Hengduan Mountains region. J Therm Biol. 2010;35(1):41–6.
262. Ye L, Wu J, Cohen P, Kazak L, Khandekar MJ, Jedrychowski MP, et al. Fat cells directly sense temperature to activate thermogenesis. Proc Natl Acad Sci. 2013;110(30):12480–5.
263. Hilakivi LA, Ota M, Lister RG. Effect of isolation on brain monoamines and the behavior of mice in tests of exploration, locomotion, anxiety and behavioral “despair”. Pharmacol Biochem Behav. 1989;33(2):371–4.
264. Floyd K, Veksler AE, McEwan B, Hesse C, Boren JP, Dinsmore DR, et al. Social Inclusion Predicts Lower Blood Glucose and Low-Density Lipoproteins in Healthy Adults. Health Commun. 2017;32(8):1039–42.

265. van der Kooij MA, Jene T, Treccani G, Miederer I, Hasch A, Voelxen N, et al. Chronic social stress-induced hyperglycemia in mice couples individual stress susceptibility to impaired spatial memory. Proc Natl Acad Sci U S A. 2018;115(43):E10187–96.
266. Denroche HC, Huynh FK, Kieffer TJ. The role of leptin in glucose homeostasis. J Diabetes Investig. 2012;3(2):115–29.
267. Zhang Y, Proenca R, Maffei M, Barone M, Leopold L, Friedman JM. Positional cloning of the mouse obese gene and its human homologue. Nature. 1994;372(6505):425–32.
268. Ellacott KLJ, Morton GJ, Woods SC, Tso P, Schwartz MW. Assessment of Feeding Behavior in Laboratory Mice. Cell Metab. 2010;12(1):10–7.
269. Kurokawa M, Akino K, Kanda K. A new apparatus for studying feeding and drinking in the mouse. Physiol Behav. 2000;70(1–2):105–12.
270. Jensen TL, Kiersgaard MK, Sørensen DB, Mikkelsen LF. Fasting of mice: a review. Lab Anim. 2013;47(4):225–40.
271. Mühlbauer E, Gross E, Labucay K, Wolgast S, Peschke E. Loss of melatonin signalling and its impact on circadian rhythms in mouse organs regulating blood glucose. Eur J Pharmacol. 2009;606(1–3):61–71.
272. Nowell NW. Circadian rhythm of glucose tolerance in laboratory mice. Diabetologia. 1970;6:488–92.
273. Pratt DS, Kaplan MM. Evaluation of Abnormal Liver-Enzyme Results in Asymptomatic Patients. N Engl J Med. 2000;342(17):1266–71.
274. Liu X, Shen Y, Wang H, Ge Q, Fei A, Pan S. Prognostic Significance of Neutrophil-to-Lymphocyte Ratio in Patients with Sepsis: A Prospective Observational Study. Mediators Inflamm. 2016;2016.
275. Naess A, Nilssen SS, Mo R, Eide GE, Sjursen H. Role of neutrophil to lymphocyte and monocyte to lymphocyte ratios in the diagnosis of bacterial infection in patients with fever. Infection. 2017;45(3):299–307.
276. Kim S, Eliot M, Koestler DC, Wu W-C, Kelsey KT. Association of Neutrophil-to-Lymphocyte Ratio With Mortality and Cardiovascular Disease in the Jackson Heart Study and Modification by the Duffy Antigen Variant. JAMA Cardiol. 2018;3(6):455.
277. Ma J, Kuzman J, Ray A, Lawson BO, Khong B, Xuan S, et al. Neutrophil-to-lymphocyte Ratio (NLR) as a predictor for recurrence in patients with stage III

melanoma. Sci Rep. 2018;8(1):4044.

278. Cole SW. Social regulation of leukocyte homeostasis: the role of glucocorticoid sensitivity. Brain Behav Immun. 2008;22(7):1049–55.
279. Ushach I, Zlotnik A. Biological role of granulocyte macrophage colony-stimulating factor (GM-CSF) and macrophage colony-stimulating factor (M-CSF) on cells of the myeloid lineage. J Leukoc Biol. 2016;100(3):481–9.
280. Parajuli B, Sonobe Y, Kawanokuchi J, Doi Y, Noda M, Takeuchi H, et al. GM-CSF increases LPS-induced production of proinflammatory mediators via upregulation of TLR4 and CD14 in murine microglia. J Neuroinflammation. 2012;9(1):268.
281. Fischer HG, Frosch S, Reske K, Reske-Kunz AB. Granulocyte-macrophage colony-stimulating factor activates macrophages derived from bone marrow cultures to synthesis of MHC class II molecules and to augmented antigen presentation function. J Immunol. 1988;141(11):3882–8.
282. Cook AD, Turner AL, Braine EL, Pobjoy J, Lenzo JC, Hamilton JA. Regulation of systemic and local myeloid cell subpopulations by bone marrow cell-derived granulocyte-macrophage colony-stimulating factor in experimental inflammatory arthritis. Arthritis Rheum. 2011;63(8):2340–51.
283. Zhu S-N, Chen M, Jongstra-Bilen J, Cybulsky MI. GM-CSF regulates intimal cell proliferation in nascent atherosclerotic lesions. J Exp Med. 2009;206(10):2141–9.
284. Meisel C, Schefold JC, Pschowski R, Baumann T, Hetzger K, Gregor J, et al. Granulocyte-macrophage colony-stimulating factor to reverse sepsis-associated immunosuppression: A double-blind, randomized, placebo-controlled multicenter trial. Am J Respir Crit Care Med. 2009;180(7):640–8.
285. Presneill JJ, Harris T, Stewart AG, Cade JF, Wilson JW. A randomized phase II trial of granulocyte-macrophage colony-stimulating factor therapy in severe sepsis with respiratory dysfunction. Am J Respir Crit Care Med. 2002;166(2):138–43.
286. Rosenbloom AJ, Linden PK, Dorrance A, Penkosky N, Cohen-Melamed MH, Pinsky MR. Effect of granulocyte-monocyte colony-stimulating factor therapy on leukocyte function and clearance of serious infection in nonneutropenic patients. Chest. 2005;127(6):2139–50.
287. Jianguo L, Xueyang J, Cui W, Changxin W, Xuemei Q. Altered gut metabolome

contributes to depression-like behaviors in rats exposed to chronic unpredictable mild stress. Transl Psychiatry. 2019;9(1):40.

288. Huang Y, Shi X, Li Z, Shen Y, Shi X, Wang L, et al. Possible association of Firmicutes in the gut microbiota of patients with major depressive disorder. Neuropsychiatr Dis Treat. 2018;Volume 14:3329–37.
289. Koliada A, Syzenko G, Moseiko V, Budovska L, Puchkov K, Perederiy V, et al. Association between body mass index and Firmicutes/Bacteroidetes ratio in an adult Ukrainian population. BMC Microbiol. 2017;17(1).
290. Ismail NA, Ragab SH, ElBaky AA, Shoeib ARS, Alhosary Y, Fekry D. Frequency of Firmicutes and Bacteroidetes in gut microbiota in obese and normal weight Egyptian children and adults. Arch Med Sci. 2011;7(3):501–7.
291. Duncan SH, Lobley GE, Holtrop G, Ince J, Johnstone a M, Louis P, et al. Human colonic microbiota associated with diet, obesity and weight loss. Int J Obes (Lond). 2008;32(11):1720–4.
292. Larsen N, Vogensen FK, Van Den Berg FWJ, Nielsen DS, Andreasen AS, Pedersen BK, et al. Gut microbiota in human adults with type 2 diabetes differs from non-diabetic adults. PLoS One. 2010;5(2).
293. Zhang C, Zhang M, Pang X, Zhao Y, Wang L, Zhao L. Structural resilience of the gut microbiota in adult mice under high-fat dietary perturbations. ISME J. 2012;6(10):1848–57.
294. Lukaschek K, Baumert J, Kruse J, Meisinger C, Ladwig KH. Sex differences in the association of social network satisfaction and the risk for type 2 diabetes. BMC Public Health. 2017;17(379).
295. Yang C, Qu Y, Fujita Y, Ren Q, Ma M, Dong C, et al. Possible role of the gut microbiota-brain axis in the antidepressant effects of (R)-ketamine in a social defeat stress model. Transl Psychiatry. 2017;7(12).
296. Chen J, Wright K, Davis JM, Jeraldo P, Marietta E V., Murray J, et al. An expansion of rare lineage intestinal microbes characterizes rheumatoid arthritis. Genome Med. 2016;8(1):43.
297. Tedjo DI, Smolinska A, Savelkoul PH, Masclee AA, Van Schooten FJ, Pierik MJ, et al. The fecal microbiota as a biomarker for disease activity in Crohn's disease. Sci Rep. 2016;6(35216).
298. Kuehbacher T, Rehman A, Lepage P, Hellmig S, F??lsch UR, Schreiber S, et al. Intestinal TM7 bacterial phylogenies in active inflammatory bowel disease. J

Med Microbiol. 2008;57:1569–76.

299. Brinig MM, Lepp PW, Ouverney CC, Armitage GC, Relman DA. Prevalence of bacteria of division TM7 in human subgingival plaque and their association with disease. Appl Environ Microbiol. 2003;69:1687–94.
300. Rey FE, Gonzalez MD, Cheng J, Wu M, Ahern PP, Gordon JI. Metabolic niche of a prominent sulfate-reducing human gut bacterium. Proc Natl Acad Sci. 2013;110(33):13582–7.
301. Ebino KY, Yoshinaga K, Saito TR, Takahashi KW. A simple method for prevention of coprophagy in the mouse. Lab Anim. 1988;22(1):1–4.
302. Nersesian P V., Han H-R, Yenokyan G, Blumenthal RS, Nolan MT, Hladek MD, et al. Loneliness in middle age and biomarkers of systemic inflammation: Findings from Midlife in the United States. Soc Sci Med. 2018;209:174–81.
303. Jaremka LM, Fagundes CP, Peng J, Bennett JM, Glaser R, Malarkey WB, et al. Loneliness promotes inflammation during acute stress. Psychol Sci. 2013;24(7):1089–97.
304. Wang Y, Li Y, Dalle Lucca SL, Simovic M, Tsokos GC, Dalle Lucca JJ. Decay accelerating factor (CD55) protects neuronal cells from chemical hypoxia-induced injury. J Neuroinflammation. 2010;7(24).
305. Lewis RD, Perry MJ, Guschina IA, Jackson CL, Morgan BP, Hughes TR. CD55 deficiency protects against atherosclerosis in ApoE-deficient mice via C3a modulation of lipid metabolism. Am J Pathol. 2011;179(4):1601–7.
306. Rashidi M, Bandala-Sanchez E, Lawlor KE, Zhang Y, Neale AM, Vijayaraj SL, et al. CD52 inhibits Toll-like receptor activation of NF-κB and triggers apoptosis to suppress inflammation. Cell Death Differ. 2017;25:392–405.
307. Rock KL, Kono H. The inflammatory response to cell death. Annu Rev Pathol. 2008;3:99–126.
308. Masud R, Shameer K, Dhar A, Ding K, Kullo IJ. Gene expression profiling of peripheral blood mononuclear cells in the setting of peripheral arterial disease. J Clin Bioinforma. 2012;2(1).
309. Muto A, Tashiro S, Tsuchiya H, Kume A, Kanno M, Ito E, et al. Activation of Maf/AP-1 repressor Bach2 by oxidative stress promotes apoptosis and its interaction with promyelocytic leukemia nuclear bodies. J Biol Chem. 2002;277(23):20724–33.
310. Cazalis M-A, Lepape A, Venet F, Frager F, Mougin B, Vallin H, et al. Early and

dynamic changes in gene expression in septic shock patients: a genome-wide approach. Intensive Care Med Exp. 2014;2(20).

311. Winkleby MA, Jatulis DE, Frank E, Fortmann SP. Socioeconomic status and health: how education, income, and occupation contribute to risk factors for cardiovascular disease. Am J Public Health. 1992;82(6):816–20.
312. Oestergaard LB, Schmiegelow MD, Bruun NE, Skov RL, Petersen A, Andersen PS, et al. The associations between socioeconomic status and risk of Staphylococcus aureus bacteremia and subsequent endocarditis – a Danish nationwide cohort study. BMC Infect Dis. 2017;17(1):589.
313. Schnegelsberg A, Mackenhauer J, Nibro HL, Dreyer P, Koch K, Kirkegaard H. Impact of socioeconomic status on mortality and unplanned readmission in septic intensive care unit patients. Acta Anaesthesiol Scand. 2016;60(4):465–75.
314. Ojard C, Donnelly JP, Safford MM, Griffin R, Wang HE. Psychosocial Stress as a Risk Factor for Sepsis: A Population-Based Cohort Study. Psychosom Med. 2015;77(1):93–100.
315. Moore JX, Donnelly JP, Griffin R, Howard G, Safford MM, Wang HE. Defining Sepsis Mortality Clusters in the United States. Crit Care Med. 2016;44(7):1380–7.
316. Rush B, Wiskar K, Celi LA, Walley KR, Russell JA, McDermid RC, et al. Association of Household Income Level and In-Hospital Mortality in Patients With Sepsis: A Nationwide Retrospective Cohort Analysis. J Intensive Care Med. 2018;33(10):551–6.
317. Hsieh LS, Wen JH, Miyares L, Lombroso PJ, Bordey A. Outbred CD1 mice are as suitable as inbred C57BL/6J mice in performing social tasks. Neurosci Lett. 2017;637:142–7.
318. Ando H, Takamura T, Ota T, Nagai Y, Kobayashi K. Cerivastatin improves survival of mice with lipopolysaccharide-induced sepsis. J Pharmacol Exp Ther. 2000;294(3):1043–6.
319. Xu J, Tong L, Yao J, Guo Z, Lui KY, Hu X, et al. Association of Sex with Clinical Outcome in Critically Ill Sepsis Patients. SHOCK. 2018;1.
320. Sakr Y, Elia C, Mascia L, Barberis B, Cardellino S, Livigni S, et al. The influence of gender on the epidemiology of and outcome from severe sepsis. Crit Care. 2013;17(2):R50.
321. Nachtigall I, Tafelski S, Rothbart A, Kaufner L, Schmidt M, Tamarkin A, et al.

Gender-related outcome difference is related to course of sepsis on mixed ICUs: a prospective, observational clinical study. Crit Care. 2011;15(3):R151.

322. Nasir N, Jamil B, Siddiqui S, Talat N, Khan FA, Hussain R. Mortality in Sepsis and its relationship with Gender. Pakistan J Med Sci. 2015;31(5):1201.
323. Wichmann MW, Inthorn D, Andress H-J, Schildberg FW. Incidence and mortality of severe sepsis in surgical intensive care patients: the influence of patient gender on disease process and outcome. Intensive Care Med. 2000;26(2):167–72.
324. Dalli J, Chiang N, Serhan CN. Elucidation of novel 13-series resolvins that increase with atorvastatin and clear infections. Nat Med. 2015;21(9):1071–5.
325. Cole SW, Hawkley LC, Arevalo JM, Sung CY, Rose RM, Cacioppo JT. Social regulation of gene expression in human leukocytes. Genome Biol. 2007;8(9).
326. Cunningham C, Campion S, Teeling J, Felton L, Perry VH. The sickness behaviour and CNS inflammatory mediator profile induced by systemic challenge of mice with synthetic double-stranded RNA (poly I:C). Brain Behav Immun. 2007;21(4):490–502.
327. Oertelt-Prigione S. The influence of sex and gender on the immune response. Autoimmun Rev. 2012;11(6–7):A479–85.
328. Shrum B, Anantha R V, Xu SX, Donnelly M, Haeryfar S, McCormick JK, et al. A robust scoring system to evaluate sepsis severity in an animal model. BMC Res Notes. 2014;7(1):233.
329. Granger JI, Ratti P-L, Datta SC, Raymond RM, Opp MR. Sepsis-induced morbidity in mice: Effects on body temperature, body weight, cage activity, social behavior and cytokines in brain. Psychoneuroendocrinology. 2013;38(7):1047–57.
330. van Schaik SM, Abbas AK. Role of T cells in a murine model of Escherichia coli sepsis. Eur J Immunol. 2007;37(11):3101–10.
331. Gil MC, Aguirre JA, Lemoine AP, Segura ET, Barontini M, Armando I. Influence of age on stress responses to metabolic cage housing in rats. Cell Mol Neurobiol. 1999;19(5):625–33.
332. Sahin Z, Solak H, Koc A, Ozen Koca R, Ozkurkculer A, Cakan P, et al. Long-term metabolic cage housing increases anxiety/depression-related behaviours in adult male rats. Arch Physiol Biochem. 2019;125(2):122–7.
333. Pyter LM, Yang L, McKenzie C, da Rocha JM, Carter CS, Cheng B, et al.

Contrasting mechanisms by which social isolation and restraint impair healing in male mice. Stress. 2014;17(3):256–65.

334. Cain DW, O'Koren EG, Kan MJ, Womble M, Sempowski GD, Hopper K, et al. Identification of a tissue-specific, C/EBPβ-dependent pathway of differentiation for murine peritoneal macrophages. J Immunol. 2013;191(9):4665–75.
335. Ghosn EEB, Cassado AA, Govoni GR, Fukuhara T, Yang Y, Monack DM, et al. Two physically, functionally, and developmentally distinct peritoneal macrophage subsets. Proc Natl Acad Sci U S A. 2010;107(6):2568–73.
336. Henderson RB, Hobbs JAR, Mathies M, Hogg N, Sinickas V, Gall JA, et al. Rapid recruitment of inflammatory monocytes is independent of neutrophil migration. Blood. 2003;102(1):328–35.
337. Deem JD, Muta K, Ogimoto K, Nelson JT, Velasco KR, Kaiyala KJ, et al. Leptin regulation of core body temperature involves mechanisms independent of the thyroid axis. Am J Physiol Metab. 2018;315(4):E552–64.
338. Nadal A, Quesada I, Tudurí E, Nogueiras R, Alonso-Magdalena P. Endocrine-disrupting chemicals and the regulation of energy balance. Nat Rev Endocrinol. 2017;13(9):536–46.
339. Sanchez-Gurmaches J, Hung C-M, Guertin DA. Emerging Complexities in Adipocyte Origins and Identity. Trends Cell Biol. 2016;26(5):313–26.
340. Cypess AM, Lehman S, Williams G, Tal I, Rodman D, Goldfine AB, et al. Identification and Importance of Brown Adipose Tissue in Adult Humans. N Engl J Med. 2009;360(15):1509–17.
341. Giles DA, Ramkhelawon B, Donelan EM, Stankiewicz TE, Hutchison SB, Mukherjee R, et al. Modulation of ambient temperature promotes inflammation and initiates atherosclerosis in wild type C57BL/6 mice. Mol Metab. 2016;5(11):1121–30.
342. Tian XY, Ganeshan K, Hong C, Nguyen KD, Qiu Y, Kim J, et al. Thermoneutral Housing Accelerates Metabolic Inflammation to Potentiate Atherosclerosis but Not Insulin Resistance. Cell Metab. 2016;23(1):165–78.
343. Williams JW, Elvington A, Ivanov S, Kessler S, Luehmann H, Baba O, et al. Thermoneutrality but Not UCP1 Deficiency Suppresses Monocyte Mobilization Into Blood. Circ Res. 2017;121(6):662–76.
344. Kokolus KM, Spangler HM, Povinelli BJ, Farren MR, Lee KP, Repasky EA. Stressful Presentations: Mild Cold Stress in Laboratory Mice Influences

Phenotype of Dendritic Cells in Naïve and Tumor-Bearing Mice. Front Immunol. 2014;5.

345. Cao L, Choi EY, Liu X, Martin A, Wang C, Xu X, et al. White to Brown Fat Phenotypic Switch Induced by Genetic and Environmental Activation of a Hypothalamic-Adipocyte Axis. Cell Metab. 2011;14(3):324–38.
346. van Marken Lichtenbelt WD, Vanhommerig JW, Smulders NM, Drossaerts JMAFL, Kemerink GJ, Bouvy ND, et al. Cold-Activated Brown Adipose Tissue in Healthy Men. N Engl J Med. 2009;360(15):1500–8.
347. Cohen P, Spiegelman BM. Brown and Beige Fat: Molecular Parts of a Thermogenic Machine. Diabetes. 2015;64(7):2346–51.
348. Harms M, Seale P. Brown and beige fat: development, function and therapeutic potential. Nat Med. 2013;19(10):1252–63.
349. Dong M, Yang X, Lim S, Cao Z, Honek J, Lu H, et al. Cold exposure promotes atherosclerotic plaque growth and instability via UCP1-dependent lipolysis. Cell Metab. 2013;18(1):118–29.
350. Petruzzelli M, Schweiger M, Schreiber R, Campos-Olivas R, Tsoli M, Allen J, et al. A Switch from White to Brown Fat Increases Energy Expenditure in Cancer-Associated Cachexia. Cell Metab. 2014;20(3):433–47.
351. Das SK, Eder S, Schauer S, Diwoky C, Temmel H, Guertl B, et al. Adipose Triglyceride Lipase Contributes to Cancer-Associated Cachexia. Science (80-). 2011;333(6039):233–8.
352. Paschos GK, Tang SY, Theken KN, Li X, Verginadis I, Lekkas D, et al. Cold-Induced Browning of Inguinal White Adipose Tissue Is Independent of Adipose Tissue Cyclooxygenase-2. Cell Rep. 2018;24(4):809–14.
353. Cichoń M, Chadzińska M, Ksiazek A, Konarzewski M. Delayed effects of cold stress on immune response in laboratory mice. Proc Biol Sci. 2002;269(1499):1493–7.
354. Fischer AW, Hoefig CS, Abreu-Vieira G, de Jong JMA, Petrovic N, Mittag J, et al. Leptin Raises Defended Body Temperature without Activating Thermogenesis. Cell Rep. 2016;14(7):1621–31.
355. Patel BK, Koenig JI, Kaplan LM, Hooi SC. Increase in plasma leptin and Lep mRNA concentrations by food intake is dependent on insulin. Metabolism. 1998;47(5):603–7.
356. Mainardi M, Scabia G, Vottari T, Santini F, Pinchera A, Maffei L, et al. A

sensitive period for environmental regulation of eating behavior and leptin sensitivity. Proc Natl Acad Sci U S A. 2010;107(38):16673–8.

357. Weigle DS, Duell PB, Connor WE, Steiner RA, Soules MR, Kuijper JL. Effect of Fasting, Refeeding, and Dietary Fat Restriction on Plasma Leptin Levels. J Clin Endocrinol Metab. 1997;82(2):561–5.
358. Burnett LC, Skowronski AA, Rausch R, LeDuc CA, Leibel RL. Determination of the half-life of circulating leptin in the mouse. Int J Obes (Lond). 2017;41(3):355–9.
359. Saegusa Y, Tabata H. Usefulness of infrared thermometry in determining body temperature in mice. J Vet Med Sci. 2003;65(12):1365–7.
360. Couillard C, Mauriège P, Imbeault P, Prud'homme D, Nadeau A, Tremblay A, et al. Hyperleptinemia is more closely associated with adipose cell hypertrophy than with adipose tissue hyperplasia. Int J Obes Relat Metab Disord. 2000;24(6):782–8.
361. Wu J, Cohen P, Spiegelman BM. Adaptive thermogenesis in adipocytes: Is beige the new brown? Genes Dev. 2013;27(3):234–50.
362. Gaskill BN, Gordon CJ, Pajor EA, Lucas JR, Davis JK, Garner JP. Impact of nesting material on mouse body temperature and physiology. Physiol Behav. 2013;110–111:87–95.
363. Hui X, Gu P, Zhang J, Nie T, Pan Y, Wu D, et al. Adiponectin Enhances Cold-Induced Browning of Subcutaneous Adipose Tissue via Promoting M2 Macrophage Proliferation. Cell Metab. 2015;22(2):279–90.
364. Brenner IKM, Castellani JW, Gabaree C, Young AJ, Zamecnik J, Shephard RJ, et al. Immune changes in humans during cold exposure: effects of prior heating and exercise. J Appl Physiol. 1999;87(2):699–710.
365. Fairchild KD, Viscardi RM, Hester L, Singh IS, Hasday JD. Effects of Hypothermia and Hyperthermia on Cytokine Production by Cultured Human Mononuclear Phagocytes from Adults and Newborns. J Interf Cytokine Res. 2000;20(12):1049–55.
366. Kirkley JE, Thompson BJ, Coon JS. Temperature Alters Lipopolysaccharide-Induced Cytokine Secretion by RAW 264.7 Cells. Scand J Immunol. 2003;58(1):51–8.
367. Deans KA, Bezlyak V, Ford I, Batty GD, Burns H, Cavanagh J, et al. Differences in atherosclerosis according to area level socioeconomic deprivation:

cross sectional, population based study. BMJ. 2009;339(b4170).

368. Hawkley LC, Burleson MH, Berntson GG, Cacioppo JT. Loneliness in everyday life: cardiovascular activity, psychosocial context, and health behaviors. J Pers Soc Psychol. 2003;85(1):105–20.
369. Kaplan, J. R., Manuck, S. B., Clarkson, T. B., Lusso, F. M. & Taub, D. M. Snuck SB. Social status, environment, and atherosclerosis in cynomolgus monkeys. Arteriosclerosis. 1982;2(5):359–68.
370. Hakulinen C, Pulkki-Råback L, Virtanen M, Jokela M, Kivimäki M, Elovainio M. Social isolation and loneliness as risk factors for myocardial infarction, stroke and mortality: UK Biobank cohort study of 479 054 men and women. Heart. 2018;0:1–7.
371. Hawkley LC, Thisted RA, Masi CM, Cacioppo JT. Loneliness predicts increased blood pressure: 5-year cross-lagged analyses in middle-aged and older adults. Psychol Aging. 2010;25(1):132–41.
372. Nash SD, Cruickshanks KJ, Klein R, Klein BEK, Nieto FJ, Ryff CD, et al. Socioeconomic status and subclinical atherosclerosis in older adults. Prev Med (Baltim). 2011;52(3–4):208–12.
373. Getz GS, Reardon CA. Animal models of atherosclerosis. Arterioscler Thromb Vasc Biol. 2012;32(5):1104–15.
374. Getz GS, Reardon CA. Do the Apoe−/− and Ldlr−/- Mice Yield the Same Insight on Atherogenesis? Arterioscler Thromb Vasc Biol. 2016;36(9):1734–41.
375. Reddick RL, Zhang SH, Maeda N. Atherosclerosis in mice lacking apo E. Evaluation of lesional development and progression. Arterioscler Thromb Vasc Biol. 1994;14(1):141–7.
376. Stary HC, Chandler AB, Dinsmore RE, Fuster V, Glagov S, Insull W, et al. A Definition of Advanced Types of Atherosclerotic Lesions and a Histological Classification of Atherosclerosis. Circulation. 1995;92(5):1355–74.
377. Li T, Li X, Zhao X, Zhou W, Cai Z, Yang L, et al. Classification of human coronary atherosclerotic plaques using ex vivo high-resolution multicontrast-weighted MRI compared with histopathology. Am J Roentgenol. 2012;
378. Whitman SC. A practical approach to using mice in atherosclerosis research. Clin Biochem Rev. 2004;25(1):81–93.
379. Martinet W, Schrijvers DM, De Meyer GRY. Necrotic cell death in atherosclerosis. Basic Res Cardiol. 2011;106(5):749–60.

380. Stefanadis C, Antoniou C-K, Tsiachris D, Pietri P. Coronary Atherosclerotic Vulnerable Plaque: Current Perspectives. J Am Heart Assoc. 2017;6(3).
381. Gonzalez L, MacDonald ME, Deng YD, Trigatti BL. Hyperglycemia Aggravates Diet-Induced Coronary Artery Disease and Myocardial Infarction in SR-B1-Knockout/ApoE-Hypomorphic Mice. Front Physiol. 2018;9:1398.
382. Plenz GA., Deng MC, Robenek H, Völker W. Vascular collagens: spotlight on the role of type VIII collagen in atherogenesis. Atherosclerosis. 2003;166(1):1–11.
383. Raber J, Akana SF, Bhatnagar S, Dallman MF, Wong D, Mucke L. Hypothalamic–Pituitary–Adrenal Dysfunction inApoe −/− Mice: Possible Role in Behavioral and Metabolic Alterations. J Neurosci. 2000;20(5).
384. Schierwagen R, Maybüchen L, Zimmer S, Hittatiya K, Bäck C, Klein S, et al. Seven weeks of Western diet in apolipoprotein-E-deficient mice induce metabolic syndrome and non-alcoholic steatohepatitis with liver fibrosis. Sci Rep. 2015;5(1):12931.
385. Sacks FM, Bray GA, Carey VJ, Smith SR, Ryan DH, Anton SD, et al. Comparison of weight-loss diets with different compositions of fat, protein, and carbohydrates. N Engl J Med. 2009;360(9):859–73.
386. Häfner S, Zierer A, Emeny RT, Thorand B, Herder C, Koenig W, et al. Social isolation and depressed mood are associated with elevated serum leptin levels in men but not in women. Psychoneuroendocrinology. 2011;36(2):200–9.
387. Frederich RC, Hamann A, Anderson S, Löllmann B, Lowell BB, Flier JS. Leptin levels reflect body lipid content in mice: evidence for diet-induced resistance to leptin action. Nat Med. 1995;1(12):1311–4.
388. Considine R V., Sinha MK, Heiman ML, Kriauciunas A, Stephens TW, Nyce MR, et al. Serum Immunoreactive-Leptin Concentrations in Normal-Weight and Obese Humans. N Engl J Med. 1996;334(5):292–5.
389. Wang M-Y, Orci L, Ravazzola M, Unger RH. Fat storage in adipocytes requires inactivation of leptin's paracrine activity: implications for treatment of human obesity. Proc Natl Acad Sci U S A. 2005;102(50):18011–6.
390. Zhou X, Hansson GK. Effect of Sex and Age on Serum Biochemical Reference Ranges in C57BL/6J Mice. Comp Med. 2004;54(2):176–8.
391. Sakakibara H, Suzuki A, Kobayashi A, Motoyama K, Matsui A, Sayama K, et al. Social isolation stress induces hepatic hypertrophy in C57BL/6J mice. J Toxicol

Sci. 2012;37(5):1071–6.

392. Chen G, Paka L, Kako Y, Singhal P, Duan W, Pillarisetti S. A protective role for kidney apolipoprotein E. Regulation of mesangial cell proliferation and matrix expansion. J Biol Chem. 2001;276(52):49142–7.
393. Spaderna H, Mendell NR, Zahn D, Wang Y, Kahn J, Smits JMA, et al. Social isolation and depression predict 12-month outcomes in the “waiting for a new heart study". J Heart Lung Transplant. 2010;29(3):247–54.
394. Grant N, Hamer M, Steptoe A. Social Isolation and Stress-related Cardiovascular, Lipid, and Cortisol Responses. Ann Behav Med. 2009;37(1):29–37.
395. Shankar A, Mcmunn A, Banks J, Steptoe A. Loneliness, Social Isolation, and Behavioral and Biological Health Indicators in Older Adults. 2011;
396. Peuler JD, Scotti M-AL, Phelps LE, McNeal N, Grippo AJ. Chronic social isolation in the prairie vole induces endothelial dysfunction: implications for depression and cardiovascular disease. Physiol Behav. 2012;106(4):476–84.
397. Pérez C, Canal JR, Domínguez E, Campillo JE, Guillén M, Torres MD. Individual housing influences certain biochemical parameters in the rat. Lab Anim. 1997;31(4):357–61.
398. Bernberg E, Andersson IJ, Gan L, Naylor AS, Johansson ME, Bergström G. Effects of social isolation and environmental enrichment on atherosclerosis in ApoE −/− mice. Stress. 2008;11(5):381–9.
399. Izadi MS, Radahmadi M, Ghasemi M, Rayatpour A. Effects of Isolation and Social Subchronic Stresses on Food Intake and Levels of Leptin, Ghrelin, and Glucose in Male Rats. Adv Biomed Res. 2018;7:118.
400. Farrell CJL, Carter AC. Serum indices: managing assay interference [Internet]. Vol. 53, Annals of Clinical Biochemistry. 2016. p. 527–38.
401. Sanders TAB. Dietary fat and postprandial lipids. Curr Atheroscler Rep. 2003;5(6):445–51.
402. Cohen JC, Noakes TD, Benade AJ. Serum triglyceride responses to fatty meals: effects of meal fat content. Am J Clin Nutr. 1988;47(5):825–7.
403. Beckman Coulter. Cholesterol [Internet]. 2015.
404. Nikolac N. Lipemia: causes, interference mechanisms, detection and management. Biochem medica. 2014;24(1):57–67.
405. Beckman Coulter. LDL-CHOLESTEROL [Internet]. 2009.

406. Beckman Coulter. Glucose [Internet]. 2009.
407. Champy M, Selloum M, Piard L, Zeitler V, Caradec C, Chambon P, et al. Mouse functional genomics requires standardization of mouse handling and housing conditions. Mamm Genome. 2004;15(10):768–83.
408. Shively CA, Clarkson TB, Kaplan JR. Social deprivation and coronary artery atherosclerosis in female cynomolgus monkeys. Atherosclerosis. 1989;77(1):69–76.
409. McCabe PM, Gonzales JA, Zaias J, Szeto A, Kumar M, Herron AJ, et al. Social Environment Influences the Progression of Atherosclerosis in the Watanabe Heritable Hyperlipidemic Rabbit. Circulation. 2002;105(3):354–9.
410. Laimoud M, Faris F, Elghawaby H. Coronary Atherosclerotic Plaque Vulnerability Rather than Stenosis Predisposes to Non-ST Elevation Acute Coronary Syndromes. Cardiol Res Pract. 2019;2019:1–7.
411. Nakamura T, Kubo N, Funayama H, Sugawara Y, Ako J, Momomura S. Plaque Characteristics of the Coronary Segment Proximal to the Culprit Lesion in Stable and Unstable Patients. Clin Cardiol. 2009;32(8):E9–12.
412. Schrijvers DM, De Meyer GRY, Kockx MM, Herman AG, Martinet W. Phagocytosis of Apoptotic Cells by Macrophages Is Impaired in Atherosclerosis. Arterioscler Thromb Vasc Biol. 2005;25(6):1256–61.
413. Ait-Oufella H, Kinugawa K, Zoll J, Simon T, Boddaert J, Heeneman S, et al. Lactadherin Deficiency Leads to Apoptotic Cell Accumulation and Accelerated Atherosclerosis in Mice. Circulation. 2007;115(16):2168–77.
414. Kang S-J, Mintz GS, Witzenbichler B, Metzger DC, Rinaldi MJ, Duffy PL, et al. Effect of Obesity on Coronary Atherosclerosis and Outcomes of Percutaneous Coronary Intervention. Circ Cardiovasc Interv. 2015;8(1).
415. Newby AC. Metalloproteinases and vulnerable atherosclerotic plaques. Trends Cardiovasc Med. 2007;17(8):253–8.
416. Santos EW, de Oliveira DC, Hastreiter A, Beltran JS de O, Rogero MM, Fock RA, et al. High-fat diet or low-protein diet changes peritoneal macrophages function in mice. Nutrire. 2016;41(1):6.
417. Johnson JL, Jackson CL. Atherosclerotic plaque rupture in the apolipoprotein E knockout mouse. Atherosclerosis. 2001;
418. Vasquez EC, Peotta VA, Gava AL, Pereira TMC, Meyrelles SS. Cardiac and vascular phenotypes in the apolipoprotein E-deficient mouse. J Biomed Sci.

2012;19(1).

419. Sowah D, Brown BF, Quon A, Alvarez B V., Casey JR. Resistance to cardiomyocyte hypertrophy in ae3-/- mice, deficient in the AE3 Cl-/HCO3- exchanger. BMC Cardiovasc Disord. 2014;14.
420. Wang J, Kubes P. A Reservoir of Mature Cavity Macrophages that Can Rapidly Invade Visceral Organs to Affect Tissue Repair. 2016;
421. Lau S, Gruen GE. The Social Stigma of Loneliness: Effect of Target Person's and Perceiver's Sex. Personal Soc Psychol Bull. 1992;18(2):182–9.
422. Thurston RC, Kubzansky LD. Women, Loneliness, and Incident Coronary Heart Disease. Psychosom Med. 2009;71(8):836.
423. El-Mansoury TM, Taal E, Abdel-Nasser AM, Riemsma RP, Mahfouz R, Mahmoud JA, et al. Loneliness among women with rheumatoid arthritis: a cross-cultural study in the Netherlands and Egypt. Clin Rheumatol. 2008;27(9):1109–18.
424. Dutta S, Sengupta P. Men and mice: Relating their ages. Life Sci. 2016;152:244–8.
425. Wilburn J, McKenna SP, Twiss J, Rouse M, Korkosz M, Jancovic R, et al. Further international adaptation and validation of the Rheumatoid Arthritis Quality of Life (RAQoL) questionnaire. Rheumatol Int. 2015;35(4):669–75.
426. Mount MK, Barrick MR, M. SS, Rounds J. Higher-order Dimensions Of The Big Five Personality Traits And The Big Six Vocational Interest Types. Pers Psychol. 2005;58(2):447–78.
427. Lei X, Yang T, Wu T. Functional neuroimaging of extraversion-introversion. Neurosci Bull. 2015;(6):663–75.
428. Schuster AC, Carl T, Foerster K. Repeatability and consistency of individual behaviour in juvenile and adult Eurasian harvest mice. Sci Nat. 2017;104(3–4):10.
429. Forkosh O, Karamihalev S, Roeh S, Alon U, Anpilov S, Touma C, et al. Identity domains capture individual differences from across the behavioral repertoire. Nat Neurosci. 2019;22(12):2023–8.
430. Matthews T, Danese A, Wertz J, Odgers CL, Ambler A, Moffitt TE, et al. Social isolation, loneliness and depression in young adulthood: a behavioural genetic analysis. Soc Psychiatry Psychiatr Epidemiol. 2016;51(3):339–48.
431. Domènech-Abella J, Mundó J, Haro JM, Rubio-Valera M. Anxiety, depression,

loneliness and social network in the elderly: Longitudinal associations from The Irish Longitudinal Study on Ageing (TILDA). J Affect Disord. 2019;246:82–8.

432. Alpass FM, Neville S. Loneliness, health and depression in older males. Aging Ment Health. 2003;7(3):212–6.
433. Beutel ME, Klein EM, Brähler E, Reiner I, Jünger C, Michal M, et al. Loneliness in the general population: prevalence, determinants and relations to mental health. BMC Psychiatry. 2017;17(1):97.
434. Ieraci A, Mallei A, Popoli M. Social Isolation Stress Induces Anxious-Depressive-Like Behavior and Alterations of Neuroplasticity-Related Genes in Adult Male Mice. Neural Plast. 2015;2016.
435. Martin AL, Brown RE. The lonely mouse: Verification of a separation-induced model of depression in female mice. Behav Brain Res. 2010;207(1):196–207.
436. Võikar V, Polus A, Vasar E, Rauvala H. Long-term individual housing in C57BL/6J and DBA/2 mice: assessment of behavioral consequences. Genes, Brain Behav. 2004;4(4):240–52.
437. Huang Q, Zhou Y, Liu L-Y. Effect of post-weaning isolation on anxiety- and depressive-like behaviors of C57BL/6J mice. Exp Brain Res. 2017;235(9):2893–9.
438. Palanza P, Gioiosa L, Parmigiani S. Social stress in mice: Gender differences and effects of estrous cycle and social dominance. Physiol Behav. 2001;73(3):411–20.
439. Meziane H, Ouagazzal AM, Aubert L, Wietrzych M, Krezel W. Estrous cycle effects on behavior of C57BL/6J and BALB/cByJ female mice: Implications for phenotyping strategies. Genes, Brain Behav. 2007;6(2):192–200.
440. Fan Z, Zhu H, Zhou T, Wang S, Wu Y, Hu H. Using the tube test to measure social hierarchy in mice. Nat Protoc. 2019;14:819–31.
441. Wang F, Kessels HW, Hu H. The mouse that roared: neural mechanisms of social hierarchy. Trends Neurosci. 2014;37(11):674–82.
442. Merlot E, Moze E, Bartolomucci A, Dantzer R, Neveu PJ. The rank assessed in a food competition test influences subsequent reactivity to immune and social challenges in mice. Brain Behav Immun. 2004;18(5):468–75.
443. Bartolomucci A, Palanza P, Gaspani L, Limiroli E, Panerai AE, Ceresini G, et al. Social status in mice: behavioral, endocrine and immune changes are context dependent. Physiol Behav. 2001;73(3):401–10.

444. Ebbesen P, Villadsen JA, Villadsen HD, Heller KE. Effect of subordinance, lack of social hierarchy, and restricted feeding on murine survival and virus leukemia. Exp Gerontol. 1991;26(5):479–86.
445. Grimm MS, Emerman JT, Weinberg J. Effects of social housing condition and behavior on growth of the Shionogi mouse mammary carcinoma. Physiol Behav. 1996;59(4–5):633–42.
446. Schuster JP, Schaub GA. Experimental Chagas disease: the influence of sex and psychoneuroimmunological factors. Parasitol Res. 2001;87(12):994–1000.
447. Klein SL, Flanagan KL. Sex differences in immune responses. Nat Rev Immunol. 2016;16(10):626–38.
448. Beery AK, Zucker I. Sex bias in neuroscience and biomedical research. Neurosci Biobehav Rev. 2011;35(3):565–72.
449. Watson KT, Roberts NM, Saunders MR. Factors Associated with Anxiety and Depression among African American and White Women. ISRN Psychiatry. 2012;2012:1–8.
450. Howell HB, Brawman-Mintzer O, Monnier J, Yonkers KA. Generalized Anxiety Disorder in Women. Psychiatr Clin North Am. 2001;24(1):165–78.
451. Zucker I, Beery AK. Males still dominate animal studies. Nature. 2010;465(7299):690–690.
452. Lee SK. Sex as an important biological variable in biomedical research. BMB Rep. 2018;51(4):167–73.
453. Noble RE. Depression in women. Metabolism. 2005;54(5 Suppl 1):49–52.
454. Mogil JS, Chanda ML. The case for the inclusion of female subjects in basic science studies of pain. Pain. 2005;117(1):1–5.
455. Smarr B, Rowland NE, Zucker I. Male and female mice show equal variability in food intake across 4-day spans that encompass estrous cycles. Mintz EM, editor. PLoS One. 2019;14(7):e0218935.
456. Prendergast BJ, Onishi KG, Zucker I. Female mice liberated for inclusion in neuroscience and biomedical research. Neurosci Biobehav Rev. 2014;40:1–5.
457. Zhang G, Li C, Zhu N, Chen Y, Yu Q, Liu E, et al. Sex differences in the formation of atherosclerosis lesion in apoE-/-mice and the effect of 17β-estrodiol on protein S-nitrosylation. Biomed Pharmacother. 2018;99:1014–21.
458. Chiba T, Ikeda M, Umegaki K, Tomita T. Estrogen-dependent activation of neutral cholesterol ester hydrolase underlying gender difference of atherogenesis

in apoE−/− mice. Atherosclerosis. 2011;219(2):545–51.

459. Bourassa PA, Milos PM, Gaynor BJ, Breslow JL, Aiello RJ. Estrogen reduces atherosclerotic lesion development in apolipoprotein E-deficient mice. Proc Natl Acad Sci U S A. 1996;93(19):10022–7.
460. Kannel WB, HJORTLAND MC, McNAMARA PM, GORDON T. Menopause and Risk of Cardiovascular Disease. Ann Intern Med. 1976;85(4):447.
461. Bittner V. Menopause, Age, and Cardiovascular Risk. J Am Coll Cardiol. 2009;54(25):2374–5.
462. Coylewright M, Reckelhoff JF, Ouyang P. Menopause and Hypertension: an age-old debate. Hypertension. 2008;51(4):952–9.
463. Qualter P. The BBC Loneliness Experiment - School of Environment, Education and Development - The University of Manchester [Internet].
464. Irwin MR, Cole SW. Reciprocal regulation of the neural and innate immune systems. Nat Rev Immunol. 2011;11(9):625–32.
465. LeRoy AS, Murdock KW, Jaremka LM, Loya A, Fagundes CP. Loneliness Predicts Self-reported Cold Symptoms after a Viral Challenge. Health Psychol. 2017;36(5):512.
466. Chaudhry H, Zhou J, Zhong Y, Ali MM, McGuire F, Nagarkatti PS, et al. Role of cytokines as a double-edged sword in sepsis. In Vivo. 2013;27(6):669–84.
467. Seemann S, Zohles F, Lupp A. Comprehensive comparison of three different animal models for systemic inflammation. J Biomed Sci. 2017;24(1):60.
468. Dejager L, Pinheiro I, Dejonckheere E, Libert C. Cecal ligation and puncture: the gold standard model for polymicrobial sepsis? Trends Microbiol. 2011;19(4):198–208.
469. Brognara F, Castania JA, Dias DPM, Kanashiro A, Salgado HC. Time Course of Hemodynamic Responses to Different Doses of Lipopolysaccharide in Unanesthetized Male Rats. Front Physiol. 2019;10:771.
470. Angus DC, van der Poll T. Severe sepsis and septic shock. N Engl J Med. 2013;369(9):840–51.
471. Rittirsch D, Huber-Lang MS, Flierl MA, Ward PA. Immunodesign of experimental sepsis by cecal ligation and puncture. Nat Protoc. 2009;4(1):31–6.
472. Martinez-Medina M, Denizot J, Dreux N, Robin F, Billard E, Bonnet R, et al. Western diet induces dysbiosis with increased e coli in CEABAC10 mice, alters host barrier function favouring AIEC colonisation. Gut. 2014;63(1):116–24.

473. Bressa C, Bailén-Andrino M, Pérez-Santiago J, González-Soltero R, Pérez M, Montalvo-Lominchar MG, et al. Differences in gut microbiota profile between women with active lifestyle and sedentary women. Dasgupta S, editor. PLoS One. 2017;12(2):e0171352.
474. He Y, Wu W, Wu S, Zheng H-M, Li P, Sheng H-F, et al. Linking gut microbiota, metabolic syndrome and economic status based on a population-level analysis. Microbiome. 2018;6(1):172.
475. Qamar N, Castano D, Patt C, Chu T, Cottrell J, Chang SL. Meta-analysis of alcohol induced gut dysbiosis and the resulting behavioral impact. Behav Brain Res. 2019;376:112196.
476. Yang T, Santisteban MM, Rodriguez V, Li E, Ahmari N, Carvajal JM, et al. Gut Dysbiosis is Linked to Hypertension. Hypertension. 2015;65(6):1331–40.
477. Caparrós-Martín JA, Lareu RR, Ramsay JP, Peplies J, Reen FJ, Headlam HA, et al. Statin therapy causes gut dysbiosis in mice through a PXR-dependent mechanism. Microbiome. 2017;5(1):95.
478. Sato J, Kanazawa A, Ikeda F, Yoshihara T, Goto H, Abe H, et al. Gut dysbiosis and detection of "Live gut bacteria" in blood of Japanese patients with type 2 diabetes. Diabetes Care. 2014;37(8):2343–50.
479. van de Wouw M, Boehme M, Lyte JM, Wiley N, Strain C, O'Sullivan O, et al. Short-chain fatty acids: microbial metabolites that alleviate stress-induced brain-gut axis alterations. J Physiol. 2018;596(20):4923–44.
480. Skonieczna-Żydecka K, Grochans E, Maciejewska D, Szkup M, Schneider-Matyka D, Jurczak A, et al. Faecal Short Chain Fatty Acids Profile is Changed in Polish Depressive Women. Nutrients. 2018;10(12).
481. Chen J-J, Zhou C-J, Liu Z, Fu Y-Y, Zheng P, Yang D-Y, et al. Divergent Urinary Metabolic Phenotypes between Major Depressive Disorder and Bipolar Disorder Identified by a Combined GC-MS and NMR Spectroscopic Metabonomic Approach. J Proteome Res. 2015;14(8):3382–9.
482. Mushenkova N V, Summerhill VI, Silaeva YY, Deykin A V, Orekhov AN. Modelling of atherosclerosis in genetically modified animals. Am J Transl Res. 2019;11(8):4614–33.
483. Oppi S, Lüscher TF, Stein S. Mouse Models for Atherosclerosis Research—Which Is My Line? Front Cardiovasc Med. 2019;6:46.
484. Lohse P, Brewer B, Meng MS, Skarlatos SI, Larosa JC. Familial apolipoprotein

E deficiency and type Ill hyperlipoproteinemia due to a premature stop codon in the apolipoprotein E gene. Natl Institutes Heal. 1992;10.

485. NIH. High Blood Cholesterol ATP III Guidelines At-A-Glance Quick Desk Reference [Internet]. 2001.
486. Dang Y, Liu P, Ma R, Chu Z, Liu Y, Wang J, et al. HINT1 is involved in the behavioral abnormalities induced by social isolation rearing. Neurosci Lett. 2015;607:40–5.
487. Franceschi C, Garagnani P, Parini P, Giuliani C, Santoro A. Inflammaging: a new immune–metabolic viewpoint for age-related diseases. Nat Rev Endocrinol. 2018;14(10):576–90.
488. Newsom DM, Bolgos GL, Colby L, Nemzek JA. Comparison of Body Surface Temperature Measurement and Conventional Methods for Measuring Temperature in the Mouse. Contemp Top Lab Anim Sci. 2004;43(5):13–8.
489. IJzerman H, Gallucci M, Pouw WTJL, Weiβgerber SC, Van Doesum NJ, Williams KD. Cold-blooded loneliness: Social exclusion leads to lower skin temperatures. Acta Psychol (Amst). 2012;140(3):283–8.
490. Kalliokoski O, Jacobsen KR, Darusman HS, Henriksen T, Weimann A, Poulsen HE, et al. Mice do not habituate to metabolism cage housing--a three week study of male BALB/c mice. PLoS One. 2013;8(3):e58460.
491. Meakin PJ, Jalicy SM, Montagut G, Allsop DJP, Cavellini DL, Irvine SW, et al. Bace1-dependent amyloid processing regulates hypothalamic leptin sensitivity in obese mice. Sci Rep. 2018;8(1):55.
492. Münzberg H, Flier JS, Bjørbæk C. Region-Specific Leptin Resistance within the Hypothalamus of Diet-Induced Obese Mice. Endocrinology. 2004;145(11):4880–9.
493. Paterniti S, Zureik M, Ducimetière P, Touboul P-J, Fève J-M, Alpérovitch A. Sustained Anxiety and 4-Year Progression of Carotid Atherosclerosis. Arterioscler Thromb Vasc Biol. 2001;21(1):136–41.
494. Robertson J, Curley J, Kaye J, Quinn J, Pfankuch T, Raber J, et al. apoE isoforms and measures of anxiety in probable AD patients and Apoe-/- mice. Neurobiol Aging. 2005;26(5):637–43.
495. Mclachlan CS, Yi C, Soh X. Differences in Anxiety-Related Behavior Between Apolipoprotein E-Deficient C57BL/6 and Wild Type C57BL/6 Mice. Physiol Res. 2005;54:701–4.

496. Avdesh A, Wong P, Martins RN, Martin-Iverson MT. Memory Function in a Mouse Genetic Model of Alzheimer's Disease. J Alzheimer's Dis. 2011;25(3):433–44.
497. Engel DF, de Oliveira J, Lopes JB, Santos DB, Moreira ELG, Farina M, et al. Is there an association between hypercholesterolemia and depression? Behavioral evidence from the LDLr−/− mouse experimental model. Behav Brain Res. 2016;311:31–8.
498. Hippisley-Cox J, Fielding K, Pringle M. Depression as a risk factor for ischaemic heart disease in men: population based case-control study. BMJ. 1998;316(7146):1714–9.
499. Whang W, Kubzansky LD, Kawachi I, Rexrode KM, Kroenke CH, Glynn RJ, et al. Depression and Risk of Sudden Cardiac Death and Coronary Heart Disease in Women. J Am Coll Cardiol. 2009;53(11):950–8.
500. Clarke M, Bennett M. The Emerging Role of Vascular Smooth Muscle Cell Apoptosis in Atherosclerosis and Plaque Stability. Am J Nephrol. 2006;26(6):531–5.
501. Hutter R, Valdiviezo C, Sauter B V., Savontaus M, Chereshnev I, Carrick FE, et al. Caspase-3 and Tissue Factor Expression in Lipid-Rich Plaque Macrophages. Circulation. 2004;109(16):2001–8.
502. Nachtigal M, Al-Assaad Z, Mayer EP, Kim K, Monsigny M. Galectin-3 expression in human atherosclerotic lesions. Am J Pathol. 1998;152(5):1199–208.
503. Silvestre-Roig C, Braster Q, Wichapong K, Lee EY, Teulon JM, Berrebeh N, et al. Externalized histone H4 orchestrates chronic inflammation by inducing lytic cell death. Nature. 2019;569(7755):236–40.
504. Budiu RA, Vlad AM, Nazario L, Bathula C, Cooper KL, Edmed J, et al. Restraint and Social Isolation Stressors Differentially Regulate Adaptive Immunity and Tumor Angiogenesis in a Breast Cancer Mouse Model. Cancer Clin Oncol. 2016;6(1):12.
505. Lewis MH, Gluck JP, Petitto JM, Hensley LL, Ozer H. Early social deprivation in nonhuman primates: long-term effects on survival and cell-mediated immunity. Biol Psychiatry. 2000;47(2):119–26.
506. Schmitt DA, Peres C, Sonnenfeld G, Tkackzuk J, Arquier M, Mauco G, et al. Immune Responses in Humans after 60 Days of Confinement. Brain Behav

Immun. 1995;9(1):70–7.

507. Elder GA, Ragnauth A, Dorr N, Franciosi S, Schmeidler J, Haroutunian V, et al. Increased locomotor activity in mice lacking the low-density lipoprotein receptor. Behav Brain Res. 2008;191(2):256–65.